frontiers

RESEARCH TOPICS

MICROBIAL ENZYMES THAT OXIDIZE HYDROCARBONS

Topic Editors
Rachel N. Austin and Amy V. Callaghan

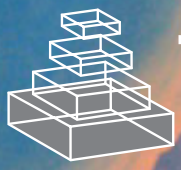

frontiers in MICROBIOLOGY

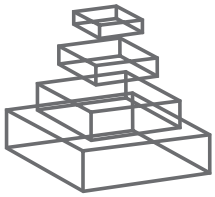

frontiers

Cover image provided by Ibbl sarl, Lausanne CH

ISSN 1664-8714
ISBN 978-2-88919-187-1
DOI 10.3389/978-2-88919-187-1

ABOUT FRONTIERS

Frontiers is more than just an open-access publisher of scholarly articles: it is a pioneering approach to the world of academia, radically improving the way scholarly research is managed. The grand vision of Frontiers is a world where all people have an equal opportunity to seek, share and generate knowledge. Frontiers provides immediate and permanent online open access to all its publications, but this alone is not enough to realize our grand goals.

FRONTIERS JOURNAL SERIES

The Frontiers Journal Series is a multi-tier and interdisciplinary set of open-access, online journals, promising a paradigm shift from the current review, selection and dissemination processes in academic publishing.
All Frontiers journals are driven by researchers for researchers; therefore, they constitute a service to the scholarly community. At the same time, the Frontiers Journal Series operates on a revolutionary invention, the tiered publishing system, initially addressing specific communities of scholars, and gradually climbing up to broader public understanding, thus serving the interests of the lay society, too.

DEDICATION TO QUALITY

Each Frontiers article is a landmark of the highest quality, thanks to genuinely collaborative interactions between authors and review editors, who include some of the world's best academicians. Research must be certified by peers before entering a stream of knowledge that may eventually reach the public - and shape society; therefore, Frontiers only applies the most rigorous and unbiased reviews.
Frontiers revolutionizes research publishing by freely delivering the most outstanding research, evaluated with no bias from both the academic and social point of view.
By applying the most advanced information technologies, Frontiers is catapulting scholarly publishing into a new generation.

WHAT ARE FRONTIERS RESEARCH TOPICS?

Frontiers Research Topics are very popular trademarks of the Frontiers Journals Series: they are collections of at least ten articles, all centered on a particular subject. With their unique mix of varied contributions from Original Research to Review Articles, Frontiers Research Topics unify the most influential researchers, the latest key findings and historical advances in a hot research area!
Find out more on how to host your own Frontiers Research Topic or contribute to one as an author by contacting the Frontiers Editorial Office: researchtopics@frontiersin.org

MICROBIAL ENZYMES THAT OXIDIZE HYDROCARBONS

Topic Editors:
Rachel N. Austin, Bates College, USA
Amy V. Callaghan, University of Oklahoma, USA

Microbial enzymes oxidize most of the hydrocarbons that enter the environment each year. Both aerobic and anaerobic hydrocarbon oxidation processes occur. The aim of this Research Topic is to highlight recent advances in our knowledge of the enzymes that catalyze the oxidation of hydrocarbons and our understanding of the molecular mechanisms that they use. Welcomed in this special issue were reviews and original research on the identity, structure and mechanisms of microbial enzymes that catalyze the oxidation of hydrocarbons as well as papers that describe any aspect of the cellular biology of hydrocarbon utilization.

Table of Contents

frontiers in
MICROBIOLOGY

EDITORIAL
published: 13 November 2013
doi: 10.3389/fmicb.2013.00338

Microbial enzymes that oxidize hydrocarbons

Rachel N. Austin[1]* and Amy V. Callaghan[2]*

[1] *Department of Chemistry, Bates College, Lewiston, ME, USA*
[2] *Department of Microbiology and Plant Biology, University of Oklahoma, Norman, OK, USA*
**Correspondence: raustin@bates.edu; acallaghan@ou.edu*

Edited by:
Bradley M. Tebo, Oregon Health and Science University, USA

Keywords: alkane oxidation, anaerobic alkane oxidation, hydrocarbon metabolism, anaerobic hydrocarbon metabolism, deepwater horizon, deep sea vents

Hydrocarbons are ubiquitous compounds of both natural and anthropogenic origin. Natural sources are derived via biosynthesis reactions in bacteria, phytoplankton, plants and fungi (Ladygina et al., 2006), as well as diagenesis and catagenesis (Horsfield and Rullkotter, 1994). As a result, hydrocarbons are environmentally distributed in microbial mats (Green and Jahnke, 2010), deep subsurface oil reservoirs (Sephton and Hazen, 2013), coalbeds (Strąpoć et al., 2011), and natural oil seeps (Kvenvolden and Cooper, 2003). Hydrocarbons are energy-rich biological substrates. However, accessing this energy requires novel enzymes. The metabolic ability of microorganisms to transform hydrocarbons is not surprising given that microbes have been exposed to these compounds throughout the course of evolution. The coupling of microbial processes and hydrocarbon transformation have important implications with regard to our understanding of biogeochemical cycling, biotransformation of environmental pollutants, subsurface production and oxidation of methane, and host/pathogen relationships. This special issue highlights recent advances in our understanding of the enzymes that govern hydrocarbon transformation in both microbial and environmental systems.

From a microbe's metabolic perspective, the largest thermodynamic benefit of hydrocarbon metabolism is derived from the oxidation of hydrocarbons with molecular oxygen. Harnessing the free energy inherent in oxygen reactivity requires an organism to have evolved mechanisms of activating oxygen and processing the reactive intermediates in ways that lead to the selective oxidation of the desired substrate, without incurring indiscriminate reactions within the organism itself. To date, the mechanisms involved in aerobic hydrocarbon oxidation are well-described, and the most prevalent feature of these processes is the dual role of oxygen as a physiological requirement and as a reactant (Berthe-Corti and Fetzner, 2002; National Research Council, 2003). Several articles in this issue review these aerobic mechanisms and the requisite enzymes. Specifically, these articles address aerobic enzymes involved in alkane oxidation (Ji et al., 2013; Wang and Shao, 2013) and new insights to the characterization of the model methanotroph, *Methylosinus trichosporium* OB3b (Matsen et al., 2013; Yang et al., 2013).

In the absence of oxygen, anaerobic and facultative microorganisms use alternative electrons acceptors, such as sulfate, nitrate, iron, manganese, and carbon dioxide to oxidize hydrocarbons. The last 30 years have yielded new insights into the novel biochemistry of anaerobic microorganisms with respect to hydrocarbon activation and degradation. Several pathways have emerged as common themes among physiologically diverse microorganisms utilizing a range of hydrocarbon substrates under a myriad of terminal electron accepting conditions (Heider and Schühle, 2013). Among recent discoveries are new mechanisms and enzymes involved in anaerobic alkane oxidation. In this issue, we have included review articles by Callaghan (2013) and Agrawal and Gieg (2013) outlining the current state of knowledge regarding anaerobic methane and non-methane alkane oxidation and methods for the *in situ* detection of anaerobic alkane biodegradation.

In addition to hydrocarbon metabolism, which is widespread among microbial taxa, some microorganisms synthesize hydrocarbons, and the purpose of these biosynthesized hydrocarbons is not well-elucidated. For example, the microalga *Botryococcus braunii* can synthesize up to 75% of its dry weight in alkanes (Banerjee et al., 2002). In some organisms, the alkanes constitute protective coatings, whereas in other microbes, they may serve as a strategy to store excess energy when other required nutrients are not available for metabolism and protein synthesis. Protective coatings, however, can serve as substrates for antagonistic microorganisms, and the strategies employed to oxidize hydrocarbons on the outside of cells appear to be different than those employed to utilize hydrocarbon stores within cells. The article by Pedrini et al. (2013) provides detailed evidence for microbial oxidation of alkanes in a host/pathogen relationship.

Given the tragedy of the Deepwater Horizon oil spill, the role of microorganisms in mitigating natural and anthropogenic hydrocarbon inputs to marine and terrestrial ecosystems has been brought to the forefront of scientific inquiry. Three papers in this issue focus on microbial activity in oil-impacted environments. Porter and Young (2013) investigate the distribution and potential use of *bamA* as a biomarker for anaerobic aromatic hydrocarbon degradation in environmental samples. Kimes et al. (2013) evaluate the use of metabolite profiling coupled with metagenomics to investigate the response of sediment microbial communities to the Deepwater Horizon oil spill. Finally, Bertrand et al. (2013) elucidate the identity and mechanisms of alkane hydroxylases found in organisms isolated from deep-sea vents, an environment in which the natural release of chemosynthetic alkanes may serve as an important fuel source.

While the flux of hydrocarbons through anthropogenic combustion is much larger than the flux via microbial processing and tends to dominate the public's attention due to concerns about global climate change, the selectivity and diversity of microbial transformations of hydrocarbons remains a powerful reminder

of the unrivaled elegance of molecular evolution. The future, in which we continue to isolate novel organisms, harness significant advances in sequencing technology, and develop new environmental monitoring tools will undoubtedly unveil exciting and unexpected aspects of the fundamental roles that microbial metabolism plays in hydrocarbon transformation.

ACKNOWLEDGEMENTS

Amy V. Callaghan would like to acknowledge support from the National Science Foundation (MCB-0921265). Rachel N. Austin would like to acknowledge support from the National Institutes of Health (2R15GM072506).

REFERENCES

Agrawal, A., and Gieg, L. M. (2013). *In situ* detection of anaerobic alkane metabolites in subsurface environments. *Front. Microbiol.* 4:140. doi: 10.3389/fmicb.2013.00140

Banerjee, A., Sharma, R., Chisti, Y., and Banerjee, U. C. (2002). *Botryococcus braunii*: a renewable source of hydrocarbons and other chemicals. *Crit. Rev. Biotechnol.* 22, 245–279. doi: 10.1080/07388550290789513

Berthe-Corti, L., and Fetzner, S. (2002). Bacterial metabolism of *n*-alkanes and ammonia under oxic, suboxic and anoxic conditions. *Acta Biotechnol.* 22, 299–336. doi: 10.1002/1521-3846(200207)22:3/4<299::AID-ABIO299>3.0.CO;2-F

Bertrand, E. M., Keddis, R., Groves, J. T., Vetriani, C., and Austin, R. N. (2013). Identity and mechanisms of alkane-oxidizing metalloenzymes from deep-sea hydrothermal vents. *Front. Microbiol.* 4:109. doi: 10.3389/fmicb.2013.00109

Callaghan, A. V. (2013). Enzymes involved in the anaerobic oxidation of *n*-alkanes: from methane to long-chain paraffins. *Front. Microbiol.* 4:89. doi: 10.3389/fmicb.2013.00089

Green, S. J., and Jahnke, L. L. (2010). "Molecular investigations and experimental manipulations of microbial mats: a view to paleomicrobial ecosystems," in *Microbial Mats: Modern and Ancient Microorganisms in Stratified Systems,* eds J. Seckbach and A. Oren (Dordrecht; Heidelberg; London; New York, NY: Springer), 183–206.

Heider, J., and Schühle, K. (2013). "Anaerobic biodegradation of hydrocarbons including methane," in *The Prokaryotes,* eds E. Rosenberg, E. F. Delong, S. Lory, E. Stackebrandt, and F. Thompson (Berlin; Heidelberg: Springer-Verlag), 605–634.

Horsfield, B., and Rullkotter, J. (1994). "Diagenesis, catagenesis, and metagenesis of organic matter," in *The Petroleum System - From Source to Trap,* eds L. B. Magoon and W.G. Dow. (Tulsa, OK: American Association Of Petroleum Engineers), 189–199.

Ji, Y., Mao, G., Wang, Y., and Bartlam, M. (2013). Structural insights into diversity and *n*-alkane biodegradation mechanisms of alkane hydroxylases. *Front. Microbiol.* 4:58. doi: 10.3389/fmicb.2013.00058

Kimes, N. E., Callaghan, A. V., Aktas, D. F., Smith, W. L., Sunner, J., Golding, B. T., et al. (2013). Metagenomic analysis and metabolite profiling of deep-sea sediments from the Gulf of Mexico following the Deepwater Horizon oil spill. *Front. Microbiol.* 4:50. doi: 10.3389/fmicb.2013.00050

Kvenvolden, K. A., and Cooper, C. K. (2003). Natural seepage of crude oil into the marine environment. *Geo-Mar. Lett.* 23, 140–146. doi: 10.1007/s00367-003-0135-0

Ladygina, N., Dedyukhina, E. G., and Vainshtein, M. B. (2006). A review on microbial synthesis of hydrocarbons. *Proc. Biochem.* 41, 1001–1014. doi: 10.1016/j.procbio.2005.12.007

Matsen, J. B., Yang, S., Stein, L. Y., Beck, D., and Kalyuzhnaya, M. G. (2013). Global molecular analyses of methane metabolism in methanotrophic alphaproteobacterium, *Methylosinus trichosporium* OB3b. Part I: transcriptomic study. *Front. Microbiol.* 4:40. doi: 10.3389/fmicb.2013.00040

National Research Council. (2003). *Oil in the Sea III: Inputs, Fates, and Effects. Committee on Oil in the Sea: Inputs, Fates, and Effects*, ed F. Committee on Oil in the Sea: Inputs, And Effect Ocean Studies Board and Marine Board Divisions of Earth and Life Studies and Transportation Research Board (Washington, DC: National Academies Press).

Pedrini, N., Ortiz-Urquiza, A., Huarte-Bonnet, C., Zhang, S., and Keyhani, N. O. (2013). Targeting of insect epicuticular lipids by the entomopathogenic fungus *Beauveria bassiana*: hydrocarbon oxidation within the context of a host-pathogen interaction. *Front. Microbio.* 4:24. doi: 10.3389/fmicb.2013.00024

Porter, A. W., and Young, L. Y. (2013). The *bamA* gene for anaerobic ring fission is widely distributed in the environment. *Front. Microbiol.* 4:302. doi: 10.3389/fmicb.2013.00302

Sephton, M. A., and Hazen, R. M. (2013). On the origins of deep hydrocarbons. *Rev. Mineral. Geochem.* 75, 449–465. doi: 10.2138/rmg.2013.75.14

Strąpoć, D., Mastalerz, M., Dawson, K., Macalady, J., Callaghan, A. V., Wawrik, B., et al. (2011). Biogeochemistry of microbial coal-bed methane. *Ann. Rev. Earth Planet. Sci.* 39, 617–656. doi: 10.1146/annurev-earth-040610-133343

Wang, W., and Shao, Z. (2013). Enzymes and genes involved in aerobic alkane degradation. *Front. Microbiol.* 4:116. doi: 10.3389/fmicb.2013.00116

Yang, S., Matsen, J. B., Konopka, M., Green-Saxena, A., Clubb, J., Sadilek, M., et al. (2013). Global molecular analyses of methane metabolism in methanotrophic Alphaproteobacterium, *Methylosinus trichosporium* OB3b. Part, I. I. metabolomics and ^{13}C-labeling study. *Front. Microbiol.* 4:70. doi: 10.3389/fmicb.2013.00070

Received: 17 October 2013; accepted: 25 October 2013; published online: 13 November 2013.

*Citation: Austin RN and Callaghan AV (2013) Microbial enzymes that oxidize hydrocarbons. Front. Microbiol. **4**:338. doi: 10.3389/fmicb.2013.00338*

This article was submitted to Microbiological Chemistry, a section of the journal Frontiers in Microbiology.

frontiers in
MICROBIOLOGY

REVIEW ARTICLE
published: 28 May 2013
doi: 10.3389/fmicb.2013.00116

Enzymes and genes involved in aerobic alkane degradation

Wanpeng Wang[1,2,3] and Zongze Shao[1,2,3]*

[1] State Key Laboratory Breeding Base of Marine Genetic Resources, Xiamen, China
[2] Key Laboratory of Marine Genetic Resources, Third Institute of Oceanography, State Oceanic Administration, Xiamen, China
[3] Key Laboratory of Marine Genetic Resources of Fujian Province, Xiamen, China

Edited by:
Amy V. Callaghan, University of Oklahoma, USA

Reviewed by:
Rachel N. Austin, Bates College, USA
Xiao-lei Wu, Peking University, China

***Correspondence:**
Zongze Shao, Key Laboratory of Marine Genetic Resources, Third Institute of Oceanography, State Oceanic Administration, Daxue Road 178, Xiamen 361005, Fujian, China.
e-mail: shaozz@163.com

Alkanes are major constituents of crude oil. They are also present at low concentrations in diverse non-contaminated because many living organisms produce them as chemo-attractants or as protecting agents against water loss. Alkane degradation is a widespread phenomenon in nature. The numerous microorganisms, both prokaryotic and eukaryotic, capable of utilizing alkanes as a carbon and energy source, have been isolated and characterized. This review summarizes the current knowledge of how bacteria metabolize alkanes aerobically, with a particular emphasis on the oxidation of long-chain alkanes, including factors that are responsible for chemotaxis to alkanes, transport across cell membrane of alkanes, the regulation of alkane degradation gene and initial oxidation.

Keywords: alkane degradation, hydroxylation, monooxygenase, regulations of gene expression, chemotaxis, transporter, AlmA, LadA

INTRODUCTION

Various microorganisms, including bacteria, filamentous fungi and yeasts, can degrade alkanes (van Beilen et al., 2003; Wentzel et al., 2007; Rojo, 2009). Notably, some recently characterized bacterial species are highly specialized for hydrocarbon degradation. These species are called hydrocarbonoclastic bacteria (HCB), and they play a key role in the removal of hydrocarbons from polluted and non-polluted environments (Harayama et al., 2004; Head et al., 2006; Yakimov et al., 2007; Wang et al., 2010a,b).

Of particular importance is *Alcanivorax*, a marine bacterium that can assimilate various linear or branched alkanes but that is unable to metabolize aromatic hydrocarbons, sugars, amino acids, and most other common carbon sources (Liu and Shao, 2005; Yakimov et al., 2007; Wu et al., 2008). *Alcanivorax* bacteria are present in non-polluted seawater in low numbers; however, the number of *Alcanivorax* can increase as a result of an oil spill, and they are believed to play an important role in the natural bioremediation of oil spills worldwide (Kasai et al., 2002; Hara et al., 2003; Harayama et al., 2004; McKew et al., 2007a,b; Yakimov et al., 2007; Wang et al., 2010a,b).

More recently, other HCBs belonging to the genera *Thalassolituus* (Yakimov et al., 2004), *Oleiphilus* (Golyshin et al., 2002), *Oleispira* (Yakimov et al., 2003), *Marinobacter* (Duran, 2010), *Bacillus* and *Geobacillus* (Marchant et al., 2006; Meintanis et al., 2006; Wang et al., 2006) have also been shown to play an important role in the degradation of oil spills in marine environments (Coulon et al., 2007; McKew et al., 2007a,b; Hazen et al., 2010).

Several reviews have covered different aspects of the physiology, enzymes and pathways that are responsible for alkane degradation (van Beilen et al., 2003; van Hamme et al., 2003; Coon, 2005; van Beilen and Funhoff, 2007; Wentzel et al., 2007; Rojo, 2009; Austin and Groves, 2011). This review focuses on recent advances in alkane chemotaxis, across membrane transport and gene regulations. In addition, newly discovered enzymes that are responsible for long-chain alkane mineralization are also discussed.

CHEMOTAXIS TO LINEAR ALKANES

Chemotaxis facilitates the movement of microorganisms toward or away from chemical gradients in the environment, and this process plays a role in biodegradation by bringing cells into contact with degradation substrates (Parales and Harwood, 2002; Parales et al., 2008). Alkanes are sources of carbon and energy for many bacterial species and have been shown to function as chemo-attractants for certain microorganisms. A bacterial *Flavimonas oryzihabitans* isolate that was obtained from soil contaminated with gas oil was shown to be chemotactic to gas oil and hexadecane (Lanfranconi et al., 2003). Similarly, *Pseudomonas aeruginosa* PAO1 is chemotactic to hexadecane (Smits et al., 2003). The *tlpS* gene, which is located downstream of the alkane hydroxylase gene *alkB1* in the PAO1 genome, is predicted to encode membrane-bound methyl-accepting chemotaxis proteins (MCP) that may play a role in alkane chemotaxis (Smits et al., 2003), although no experimental evidence exists. Similarly, the gene *alkN* is predicted to encode an MCP that could be involved in alkane chemotaxis in *P. putida* GPo1 (van Beilen et al., 2001). Our recent investigation of the genome sequence of *Alcanivorax dieselolei* B-5 (Lai et al., 2012) identified the alkane chemotaxis machinery of *Alcanivorax*, which consists of eight cytoplasmic chemotaxis proteins that transmit signals from the MCP proteins to the flagellar motors (**Figure 1**). This chemotaxis machinery is similar to that of *Escherichia coli* (Parales and Ditty, 2010). However, further investigation is necessary to confirm the mechanism of alkane chemotaxis in *A. dieselolei* B-5.

n-ALKANE UPTAKE IN BACTERIA

Although the genes and proteins that enable the passage of aromatic hydrocarbons across the bacterial outer membrane have been identified (van den Berg, 2005; Mooney et al., 2006; Hearn et al., 2008, 2009), the active transport mechanisms involved in alkane uptake remain unclear. Previous reviews(Rojo, 2009) discussed the observation that direct uptake of alkane molecules from the water phase is only possible for low molecular weight alkanes,

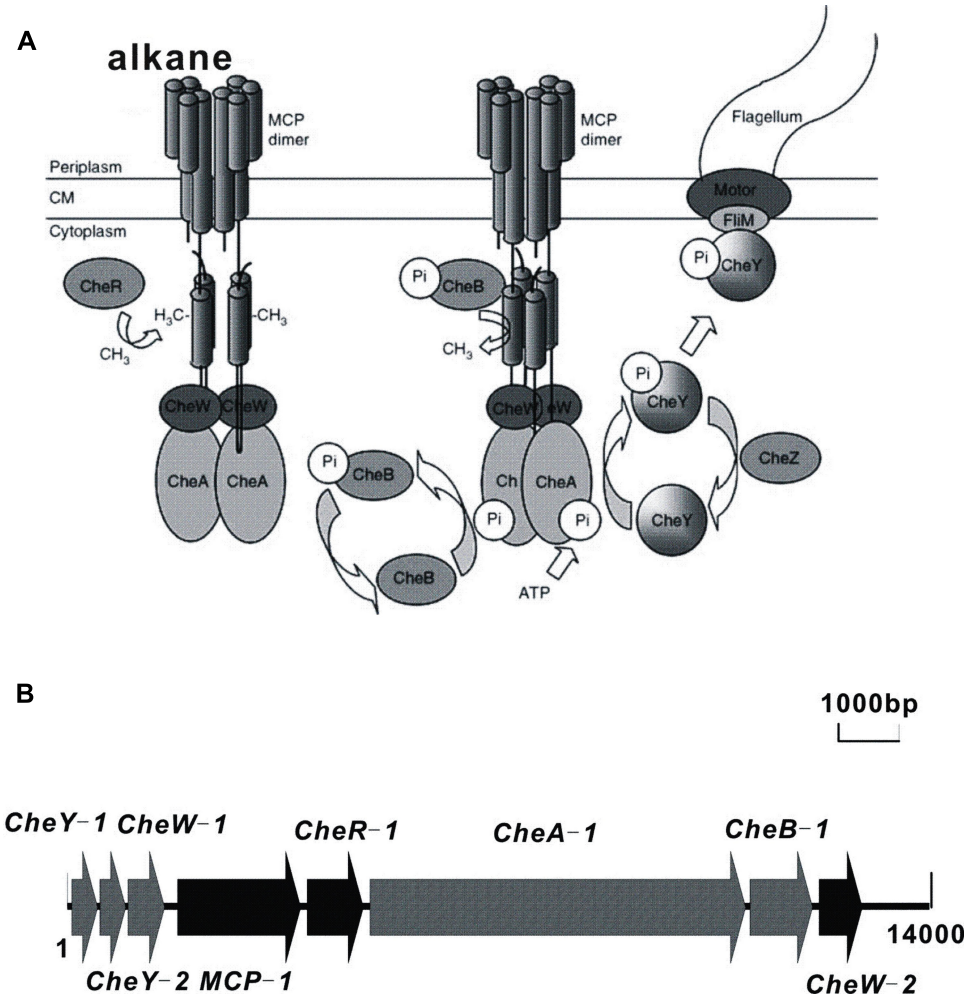

FIGURE 1 | Schematic diagram of the chemosensory signaling system of *A. dieselolei* B-5. (A) MCP dimers with associated CheW and CheA proteins are shown in the presence (left) and absence of alkane (right). Cells responding to a gradient of attractant will sense the attractant bound to the periplasmic side of the cognate MCP and will continue swimming in the favorable direction due to the inability of CheA to autophosphorylate. In the absence of CheA-P, CheY remains in the inactive unphosphorylated state, and swimming behavior remains unchanged. Cells swimming down a gradient of attractant will sense the decrease in attractant concentration due to decreased occupancy of the MCPs. Under these conditions, the MCPs undergo a conformational change that is transmitted across the cytoplasmic membrane and stimulates CheA kinase activity. CheA-P phosphorylates CheY, which in its phosphorylated state binds to the FliM protein in the flagellar motor and causes a change in the direction of flagellar rotation allowing the cell to randomly reorient and swim off in a new direction. Dephosphorylation of CheY-P is accelerated by the CheZ phosphatase. Under all conditions, the constitutive methyltransferase CheR methylates specific glutamyl residues on the cytoplasmic side of the MCP. Methylated MCPs stimulate CheA autophosphorylation, thus resetting the system such that further increases in attractant concentration can be detected. The methylesterase, CheB, becomes active when it is phosphorylated by CheA-P. CheB-P competes with CheR and removes methyl groups from the MCPs. CM, cytoplasmic membrane. **(B)** Organization of chemotaxis genes involved in alkane metabolism in *A. dieselolei* B-5. The detailed information of the ORFs of *MCP* gene cluster is presented. MCP, methyl-accepting chemotaxis protein; CheY-1, CheY-like receiver protein; CheY-2, CheY-like receiver protein; CheW-1, CheW-like protein, signal transduction protein; CheW-2, Chemotaxis protein, signal transduction protein; CheA, CheA signal transduction histidine kinase; CheB, CheB methylesterase; CheR, CheR methyltransferase.

which are sufficiently soluble to facilitate efficient transport into cells. For medium- and long-chain *n*-alkanes, microorganisms may gain access to these compounds by adhering to hydrocarbon droplets (which is facilitated by the hydrophobic cell surface) or by surfactant-facilitated access, as reviewed by Rojo (2009). Surfactants have been reported to increase the uptake and assimilation of alkanes, such as hexadecane, in liquid culture (Beal and Betts, 2000; Noordman and Janssen, 2002), but their exact role in alkane uptake is not fully understood. Bacteria that are capable of oil degradation usually produce and secrete surfactants of diverse chemical nature that allow alkane emulsification (Yakimov et al., 1998; Peng et al., 2007, 2008; Qiao and Shao, 2010; Shao, 2010). Based on our understanding of biosurfactant structure and the mechanism of outer membrane transport, we speculate that biosurfactants may be excluded from entering the cell and remain in the extracellular milieu.

In *P. putida*, *alkL* in the *alk* operon is postulated to play an important role in alkane transport into the cell (van Beilen et al.,

2004; Hearn et al., 2009). Transcriptome analysis of *A. borkumensis* Sk2 revealed that the alkane-induced gene *blc*, encoding the outer membrane lipoprotein Blc, might be involved in alkane uptake because it contains a so-called lipocalin domain (Sabirova et al., 2011). When this domain contacts organic solvents, a small hydrophobic pocket forms and catalyzes the transport of small hydrophobic molecules. More recently, our genome analysis (Lai et al., 2012) and closer examination of *A. dieselolei* B-5indicated that three outer membrane proteins that belong to the long-chain fatty acid transporter protein (FadL) family are involved in alkane transport (unpublished). The FadL homologs are present in many bacteria that are involved in the biodegradation of xenobiotics (van den Berg, 2005), which are usually hydrophobic and probably enter cells by a mechanism similar to that employed for long-chain (LC) fatty acids by FadL in *E. coli*.

DEGRADATION PATHWAYS OF *n*-ALKANES

The initial terminal hydroxylation of *n*-alkanes can be carried out by enzymes that belong to different families. Microorganisms degrading short-chain length alkanes (C_2–C_4, where the subindex indicates the number of carbon atoms of the alkane molecule) have enzymes related to methane monooxygenases (van Beilen and Funhoff, 2007). Strains degrading medium-chain length alkanes (C_5–C_{17}) frequently contain soluble cytochrome P450s and integral membrane non-heme iron monooxygenases, such as AlkB (Rojo, 2009; Austin and Groves, 2011).

Interestingly, alkane hydroxylases of long-chain length (LC-) alkanes (>C18) are unrelated to the above alkane hydroxylases as characterized recently. One such hydroxylase, AlmA, is an LC-alkane monooxygenase from *Acinetobacter*. A second hydroxylase is LadA, which is a thermophilic soluble LC-alkane monooxygenase from *Geobacillus* (Feng et al., 2007; Throne-Holst et al., 2007; Wentzel et al., 2007).

The *almA* gene, which encodes a putative monooxygenase belonging to the flavin-binding family, was identified from *Acinetobacter* sp. DSM 17874 (Throne-Holst et al., 2007; Wentzel et al., 2007). This gene encodes the first experimentally confirmed enzyme that is involved in the metabolism of LC *n*-alkanes of C_{32} and longer. We provided the first evidence that the AlmA of the genus *Alcanivorax* functions as an LC-alkane hydroxylase, and found that the gene *almA* in both *A. hongdengensis* A-11-3 and *A. dieselolei* B-5 strains expressed at high levels to facilitate the efficient degradation of LC *n*-alkanes (Liu et al., 2011; Wang and Shao, 2012a). The *almA* gene sequences were present in several bacterial genera capable of LC *n*-alkane degradation, including *Alcanivorax*, *Marinobacter*, *Acinetobacter*, and *Parvibaculum* (Wang and Shao, 2012b). In addition, similar genes are found in other genera in GenBank, such as *Oceanobacter* sp. RED65, *Ralstonia* spp., *Mycobacterium* spp., *Photorhabdus* sp., *Psychrobacter* spp., and *Nocardia farcinica* IFM10152. However, few of these genes have been functionally characterized.

A unique LC-alkane hydroxylase from the thermophilic bacterium *Geobacillus thermodenitrificans* NG80-2 has been characterized. This enzyme is called LadA and oxidizes C_{15}–C_{36} alkanes, generating the corresponding primary alcohols (Feng et al., 2007). The LadA crystal structure has been identified, revealing that LadA belongs to the bacterial luciferase family, which is two-component, flavin-dependent oxygenase (Li et al., 2008). LadA is believed to oxidize alkanes by a mechanism similar to that of other flavoprotein monooxygenases, and its ability to recognize and hydroxylate LC-alkanes most likely results from the way in which it captures the alkane(Li et al., 2008). Therefore, the hydroxylases involved in LC-alkane degradation appear to have evolved specifically, which is in contrast with other alkane monooxygenases such as AlkB and P450.

Interestingly, branched-chain alkanes are thought to be more difficult to degrade than linear alkanes (Pirnik et al., 1974). However, *Alcanivorax* bacteria efficiently degrade branched alkanes (Hara et al., 2003). In *A. borkumensis* SK2, isoprenoid hydrocarbon (phytane) strongly induces *P450* (a) and *alkB2* (Schneiker et al., 2006). In a previous report, we found that both pristane and phytane activate the expression of *alkB1* and *almA* in *A. dieselolei* B-5 (Liu et al., 2011). In *A. hongdengensis* A-11-3, we recently found that pristane selectively activates the expression of *alkB1*, *P450-3* and *almA* (Wang and Shao, 2012a). However, the metabolic pathways that mediate this activity are poorly understood, although they may involve the ω- or β-oxidation of the hydrocarbon molecule (Watkinson and Morgan, 1990).

REGULATION OF ALKANE-DEGRADATION PATHWAYS

The expression of the bacterial genes involved in alkane assimilation is tightly regulated. Alkane-responsive regulators ensure that alkane degradation genes are induced only in the presence of the appropriate hydrocarbons. Many microorganisms(Rojo, 2009; Austin and Groves, 2011) contain several sets of alkane degradation systems, each one being active on a particular kind of alkane or being expressed under specific physiological conditions. In these cases, the regulatory mechanisms should assure an appropriate differential expression of each set of enzymes. The regulators that have been characterized belong to different families, including LuxR/MalT, AraC/XylS, and other non-related families (**Table 1**).

REGULATION OF THE ALKANE DEGRADATION PATHWAY IN *Pseudomonas* spp.

Pseudomonas butanovora species oxidize C_2–C_8 *n*-alkanes into the corresponding alcohols with an alkane monooxygenase termed butane monooxygenase (BMO). BMO is a multimeric protein that is formed by the products of the *bmoXYBZDC* operon (Sluis et al., 2002). The expression of the genes encoding BMO is activated by BmoR, a δ^{54}-dependent transcriptional regulator that recognizes alcohols and aldehydes derived from the C_2–C_8 *n*-alkanes that are substrates of BMO, although BmoR does not recognize the alkanes themselves (Kurth et al., 2008).

In *P. putida* GPo1, the OCT plasmid encodes all of the genes required for the assimilation of C_3–C_{13} alkanes (van Beilen et al., 1994, 2005; Johnson and Hyman, 2006). The genes in this pathway are grouped into two clusters, *alkBFGHJKL* and *alkST* (van Beilen et al., 1994, 2001). The *alkBFGHJKL* operon is transcribed from a promoter named *PalkB*, whose expression requires the transcriptional activator AlkS and the presence of alkanes (Kok et al., 1989; Panke et al., 1999). An AlkS-dependent reporter system based on a *PalkB-luxAB* fusion showed that C_5–C_{10} alkanes are efficient activators of the AlkS regulator (Sticher et al., 1997). When alkanes become available, AlkS binds and represses *PalkS1* more efficiently

than it does in the absence of alkanes. From this binding site, AlkS activates the *PalkS2* promoter, resulting in high expression of the *alkST* genes (Canosa et al., 2000). Therefore, this pathway is controlled by a positive feedback mechanism that is driven by AlkS.

REGULATION OF THE ALKANE DEGRADATION PATHWAY IN *Alcanivorax* spp.

A gene similar to *alkS* in *P. putida* GPo1 is located upstream of *alkB1* in *A. borkumensis* SK2, and AlkS is predicted to be an alkane-responsive transcriptional activator. The expression level of AlkS in strain SK2 cells grown in hexadecane is higher than that of pyruvate-grown cells (Sabirova et al., 2006). Evidence suggests that in *A. borkumensis*, AlkS activates the expression of *alkB1*, a gene that encodes an alkane hydroxylase, in response to alkanes. However, it is unlikely that AlkS regulates the expression of *alkB2*, despite the induction of this gene in response to alkanes (van Beilen et al., 2004). Interestingly, a gene encoding a transcriptional regulator belonging to the GntR family is located immediately upstream of *alkB2*; however, its role in *alkB2* expression has not been reported. *A. borkumensis* has three genes encoding cytochrome P450 of the CYP153 family (Schneiker et al., 2006). A gene encoding a transcriptional regulator belonging to the AraC family is located close to *P450-1*, but its role in regulating the *P450-1* gene cluster has not been investigated (Schneiker et al., 2006).

In *A. hongdengensis,* a gene downstream of *alkB1* encodes a protein that is similar to TetR family transcriptional regulators (Wang and Shao, 2012a). In addition, a gene encoding a transcriptional regulator belonging to the GntR family is located just upstream of *alkB2*, although its role in the regulation of *alkB2* is not known (Wang and Shao, 2012a). Genes encoding transcriptional regulators belonging to the AraC family are located near *P450-1* and *P450-2* (Wang and Shao, 2012a). Similar to many of the genes described above, their role in the regulation of the corresponding P450 genes requires further investigation.

Three regulators that are involved in alkane degradation were identified in the *A. dieselolei* strain B-5 genome sequence, and they belong to different MerR and AraC families (**Table 1**). Regulatory genes are located upstream of *alkB1* and *P450*, and the proteins encoded by these genes are 46 and 64% similar to MerR and AraC from *P. aeruginosa* and *A. borkumensis* SK2, respectively (Liu et al., 2011). Downstream of *alkB2*, there is a gene encoding a transcriptional regulator that shares 61% similarity with AraC from *Marinobacter* sp. ELB17 (Liu et al., 2011). Therefore, *Alcanivorax* strains usually encode multiple alkane hydroxylases that are expressed under the control of different regulators encoded in the same gene cluster as the monooxygenase gene. Our lab is using strain B-5 as a model system to study how cells modulate the expression of these genes in response to different alkanes with varied chain lengths.

GLOBAL REGULATION OF THE ALKANE DEGRADATION PATHWAY

The expression of alkane degradation pathway genes is often down regulated by complex global regulatory controls that ensure that the genes are expressed only under the appropriate physiological conditions or in the absence of any preferred compounds

Table 1 | Transcriptional regulators known or presumed to control the expression of alkane degradation pathways.

Bacterium	Gene	Family	Effector	Evidence	Reference
P. putida GPo1	*alkS*	LuxR/MalT	C_6–C_{10} *n*-alkanes	Direct	Sticher et al. (1997) and Panke et al. (1999)
P. putida P1	*alkS*	LuxR/MalT	Not tested	Similarity	van Beilen et al. (2001)
A. borkumensis SK2	*alkS*	LuxR/MalT	Not tested	Similarity	Schneiker et al. (2006)
A. borkumensis SK2	*gntR*	GntR	Not tested	No	Schneiker et al. (2006)
A. borkumensis SK2	*araC*	AraC/XylS	Not tested	No	Schneiker et al. (2006)
A. borkumensis AP1	*alkS*	LuxR/MalT	Not tested	Similarity	van Beilen et al. (2004)
A.hongdengensis A-11-3	*tetR*	TetR	Not tested	Similarity	Wang and Shao (2012a)
A.hongdengensis A-11-3	*gntR*	GntR	Not tested	Similarity	Wang and Shao (2012a)
A.hongdengensis A-11-3	*araC1*	AraC/XylS	Not tested	Similarity	Wang and Shao (2012a)
A.hongdengensis A-11-3	*araC2*	AraC/XylS	Not tested	Similarity	Wang and Shao (2012a)
A. dieselolei B-5	*merR*	MerR	C_{14}–C_{26} *n*-alkanols	Similarity	Liu et al. (2011)
A. dieselolei B-5	*araC1*	AraC/XylS	C_{12}–C_{26} *n*-alkanols	Similarity	Liu et al. (2011)
A. dieselolei B-5	*araC2*	AraC/XylS	C_8–C_{16} *n*-alkanols	Similarity	Liu et al. (2011)
P. butanovora	*bmoR*	δ^{54}-Dependent	C_2–C_8 *n*-alkanols	Direct	Kurth et al. (2008)
P. aeruginosa RR1	*gntR*	GntR	C_{10}-C_{20} *n*-alkanols	Indirect	Marín et al. (2003)
Acinetobacter sp. ADP1	*alkR*	AraC/XylS	C_7-C_{18} *n*-alkanols	Direct	Ratajczak et al. (1998)
Acinetobacter sp. M1	*alkRa*	AraC/XylS	$>C_{22}$ *n*-alkanols	Indirect	Tani et al. (2001)
Acinetobacter sp. M1	*alkRb*	OruR	C_{16}–C_{22} *n*-alkanols	Indirect	Tani et al. (2001)

(Rojo, 2009). Two global regulatory networks exist. One network relies on the global regulatory protein Crc (Yuste and Rojo, 2001), while the other network receives information from cytochrome o ubiquinol oxidase (Cyo), which is a component of the electron transport chain (Dinamarca et al., 2002, 2003).

The Crc is an RNA-binding protein that interacts with the 5′ end of the *alkS* mRNA, inhibiting translation (Moreno et al., 2007). A recent study further showed that Crc inhibits the induction of the alkane degradation pathway by limiting not only the translation of their transcriptional activators but also that of genes involved in the entire alkane degradation pathway in *P. putida* (Hernández-Arranz et al., 2013). In addition, results of this study suggests that Crc follows a multi-step strategy in many cases, targeting uptake, transcription regulation, and/or the production of the associated pathways' catabolic enzymes (Hernández-Arranz et al., 2013).

However, when cells grow in a minimal salt medium containing succinate as the carbon source, the activity of Crc is low; instead, Cyo terminal oxidase play a key role in the global control that inhibits the induction of the alkane degradation genes (Yuste and Rojo, 2001; Dinamarca et al., 2003). Cyo is one of the five terminal oxidases that have been characterized in *P. putida*. Inactivation of the Cyo terminal oxidase partially relieves the repression exerted on the alkane degradation pathway under several conditions, while inactivation of any of the other four terminal oxidases does not (Dinamarca et al., 2002; Morales et al., 2006). Cyo affects the expression of many other genes, and this enzyme has been proposed to be a component of a global regulatory network that transmits information regarding the activity of the electron transport chain to coordinate respiration and carbon metabolism (Petruschka et al., 2001; Morales et al., 2006). The expression of the *cyo* genes encoding the subunits of Cyo terminal oxidase varies depending on oxygen levels and carbon source, and there is a clear correlation between Cyo levels and the extent of alkane degradation pathway repression (Dinamarca et al., 2003).

CONCLUDING REMARKS

Research in the last few years has resulted in many new insights into the mechanism of alkane degradation by microorganisms, including the upstream regulations and the long-chain length alkane oxidation. Investigations using "omics" strategies will help us to better understand the global metabolic networks within a microbial cell and the overall process of bacterial alkane-dependent chemotaxis, alkane transport, gene expression regulation and complete mineralization.

ACKNOWLEDGMENTS

This work was financially supported by the Public Welfare Project of SOA(201005032), COMRA project (DY125-15-R-01), National Science Foundation of China (41106151,41176154), International Sci and Tech Cooperation Program of China (2010DFB23320) and the Project sponsored by the Scientific Research Foundation of Third Institute of Oceanography, SOA (2011036).

REFERENCES

Austin, R. N., and Groves, J. T. (2011). Alkane-oxidizing metalloenzymes in the carbon cycle. *Metallomics* 3, 775–787.

Beal, R., and Betts, W. B. (2000). Role of rhamnolipid biosurfactants in the uptake and mineralization of hexadecane in *Pseudomonas aeruginosa*. *J. Appl. Microbiol.* 89, 158–168.

Canosa, I., Sa'nchez-Romero, J. M., Yuste, L., and Rojo, F. (2000). A positive feedback mechanism controls expression of AlkS, the transcriptional regulator of the *Pseudomonas oleovorans* alkane degradation pathway. *Mol. Microbiol.* 35, 791–799.

Coon, M. J. (2005). Omega oxygenases: nonheme-iron enzymes and P450 cytochromes. *Biochem. Biophys. Res. Commun.* 338, 378–385.

Coulon, F., McKew, B. A., Osborn, A. M., McGenity, T. J., and Timmis, K. N. (2007). Effects of temperature and biostimulation on oil-degrading microbial communities in temperate estuarine waters. *Environ. Microbiol.* 9, 177–186.

Dinamarca, M. A., Aranda-Olmedo, I., Puyet, A., and Rojo, F. (2003). Expression of the *Pseudomonas putida* OCT plasmid alkane degradation pathway is modulated by two different global control signals: evidence from continuous cultures. *J. Bacteriol.* 185, 4772–4778.

Dinamarca, M. A., Ruiz-Manzano, A., and Rojo, F. (2002). Inactivation of cytochrome o ubiquinol oxidase relieves catabolic repression of the *Pseudomonas putida* GPo1 alkane degradation pathway. *J. Bacteriol.* 184, 3785–3793.

Duran, R. (2010). "Marinobacter," in *Handbook of Hydrocarbon and Lipid Microbiology* , eds T. McGenity, J. R. van der Meer, V. de Lorenzo, and K. N. Timmis (Berlin: Springer-Verlag), 1725–1735.

Feng, L., Wang, W., Cheng, J., Ren, Y., Zhao, G., Gao, C., et al. (2007). Genome and proteome of long-chain alkane degrading *Geobacillus thermodenitrificans* NG80-2 isolated from a deep-subsurface oil reservoir. *Proc. Natl. Acad. Sci. U.S.A.* 104, 5602–5607.

Golyshin, P. N., Chernikova, T. N., Abraham, W. R., Lunsdorf, H., Timmis, K. N., and Yakimov, M. M. (2002). Oleiphilaceae fam. nov., to include *Oleiphilus messinensis* gen. nov., sp. nov., a novel marine bacterium that obligately utilizes hydrocarbons. *Int. J. Syst. Evol. Microbiol.* 52, 901–911.

Hara, A., Syutsubo, K., and Harayama, S. (2003). *Alcanivorax* which prevails in oil-contaminated seawater exhibits broad substrate specificity for alkane degradation. *Environ. Microbiol.* 5, 746–753.

Harayama, S., Kasai, Y., and Hara, A. (2004). Microbial communities in oil-contaminated seawater. *Curr. Opin. Biotechnol.* 15, 205–214.

Hazen, T. C., Dubinsky, E. A., DeSantis, T. Z., Andersen, G. L., Piceno, Y. M., and Singh, N. et al. (2010). Deep-sea oil plume enriches indigenous oil-degrading bacteria. *Science* 330, 204–208.

Head, I. M., Jones, D. M., and Roling, W. F. (2006). Marine microorganisms make a meal of oil. *Nat. Rev. Microbiol.* 4, 173–182.

Hearn, E., M., Patel, D., R., and van den Berg, B. (2008). Outer-membrane transport of aromatic hydrocarbons as a first step in biodegradation. *Proc. Natl. Acad. Sci. U.S.A.* 105, 8601–8606.

Hearn, E., M., Patel, D., R., Lepore, B., W., Indic, M., and van den Berg, B. (2009). Transmembrane passage of hydrophobic compounds through a protein channel wall. *Nature* 458, 367–370.

Hernández-Arranz, S., Moreno, R., and Rojo, F. (2013). The translational repressor Crc controls the *Pseudomonas putida* benzoate and alkane catabolic pathways using a multi-tier regulation strategy. *Environ. Microbiol.* 15, 227–241.

Johnson, E. L., and Hyman, M. R. (2006). Propane and n-butane oxidation by *Pseudomonas putida* GPo1. *Appl. Environ. Microbiol.* 72, 950–952.

Kasai, Y., Kishira, H., Sasaki, T., Syutsubo, K., Watanabe, K., and Harayama, S. (2002). Predominant growth of *Alcanivorax* strains in oil-contaminated and nutrient-supplemented sea water. *Environ. Microbiol.* 4, 141–147.

Kok, M., Oldenhuis, R., van der Linden, M. P., Raatjes, P., Kingma, J., van Lelyveld, P. H., et al. (1989). The *Pseudomonas oleovorans* alkane hydroxylase gene. Sequence and expression. *J. Biol. Chem.* 264, 5435–5441.

Kurth, E. G., Doughty, D. M., Bottomley, P. J., Arp, D. J., and Sayavedra-Soto, L. A. (2008). Involvement of BmoR and BmoG in n-alkane metabolism in "*Pseudomonas butanovora*." *Microbiology* 154, 139–147.

Lanfranconi, M. P., Alvarez, H. M., and Studdert, C. A. (2003). A strain isolated from gas oil-contaminated soil displays chemotaxis towards gas oil

and hexadecane. *Environ. Microbiol.* 5, 1002–1008.

Lai, Q., Li, W., and Shao, Z. (2012). Complete genome sequence of *Alcanivorax dieselolei* type strain B5. *J. Bacteriol.* 194, 6674.

Li, L., Liu, X., Yang, W., Xu, F., Wang, W., Feng, L., et al. (2008). Crystal structure of long-chain alkane monooxygenase (LadA) in complex with coenzyme FMN: unveiling the long-chain alkane hydroxylase. *J. Mol. Biol.* 376, 453–465.

Liu, C., and Shao, Z. (2005). *Alcanivorax dieselolei* sp. nov., a novel alkane-degrading bacterium isolated from sea water and deep-sea sediment. *Int. J. Syst. Evol. Microbiol.* 55, 1181–1186.

Liu, C., Wang, W., Wu, Y., Zhou, Z., Lai, Q., and Shao, Z. (2011). Multiple alkane hydroxylase systems in a marine alkane degrader, *Alcanivorax dieselolei* B-5. *Environ. Microbiol.* 13, 1168–1178.

Marchant, R., Sharkey, F. H., Banat, I. M., Rahman, T. J., and Perfumo, A. (2006). The degradation of n-hexadecane in soil by thermophilic geobacilli. *FEMS. Microbiol. Ecol.* 56, 44–54.

Marín, M. M., Yuste, L., and Rojo, F. (2003). Differential expression of the components of the two alkane hydroxylases from *Pseudomonas aeruginosa*. *J. Bacteriol.* 185, 3232–3237.

McKew, B. A., Coulon, F., Osborn, A. M., Timmis, K. N., and McGenity, T. J. (2007a). Determining the identity and roles of oil-metabolizing marine bacteria from the Thames estuary, UK. *Environ. Microbiol.* 9, 165–176.

McKew, B. A., Coulon, F., Yakimov, M. M., Denaro, R., Genovese, M., Smith, C. J., et al. (2007b). Efficacy of intervention strategies for bioremediation of crude oil in marine systems and effects on indigenous hydrocarbonoclastic bacteria. *Environ. Microbiol.* 9, 1562–1571.

Meintanis, C., Chalkou, K. I., Kormas, K. A., and Karagouni, A. D. (2006). Biodegradation of crude oil by thermophilic bacteria isolated from a volcano island. *Biodegradation* 17, 105–111.

Mooney, A., O'Leary, N. D., and Dobson, A. D. (2006). Cloning and functional characterization of the styE gene, involved in styrene transport in *Pseudomonas putida* CA-3. *Appl. Environ. Microbiol.* 72, 1302–1309.

Morales, G., Ugidos, A., and Rojo, F. (2006). Inactivation of the *Pseudomonas putida* cytochrome o ubiquinol oxidase leads to a significant change in the transcriptome and to increased expression of the CIO and cbb3-1 terminal oxidases. *Environ. Microbiol.* 8, 1764–1774.

Moreno, R., Ruiz-Manzano, A., Yuste, L., and Rojo, F. (2007). The *Pseudomonas putida* Crc global regulator is an RNA binding protein that inhibits translation of the AlkS transcriptional regulator. *Mol. Microbiol.* 64, 665–675.

Noordman, W. H., and Janssen, D. B. (2002). Rhamnolipid stimulates uptake of hydrophobic compounds by *Pseudomonas aeruginosa*. *Appl. Environ. Microbiol.* 68, 4502–4508.

Panke, S., Meyer, A., Huber, C. M., Witholt, B., and Wubbolts, M. G. (1999). Analkane-responsive expression system for the production of fine chemicals. *Appl. Environ. Microbiol.* 65, 2324–2332.

Parales, R. E., and Ditty, J. L. (2010). "Chemotaxis," in *Handbook of Hydrocarbon and Lipid Microbiology*, eds T. McGenity, J. R. van der Meer, V. de Lorenzo, and K. N. Timmis (Berlin: Springer-Verlag), 1532–1540.

Parales, R. E., and Harwood, C. S. (2002). Bacterial chemotaxis to pollutants and plant-derived aromatic molecules. *Curr. Opin. Microbiol.* 5, 266–273.

Parales, R. E., Ju, K.-S., Rollefson, J., and Ditty, J. L. (2008). "Bioavailability, transport and chemotaxis of organic pollutants," in *Microbial Bioremediation*. ed. E. Diaz (Norfolk: Caister Academic Press), 145–187.

Peng, F., Liu, Z., Wang, L., and Shao, Z. (2007). An oil-degrading bacterium: *Rhodococcus erythropolis* strain 3C-9 and its biosurfactants. *J. Appl. Microbiol.* 102, 1603–1611.

Peng, F., Wang, Y., Sun, F., Liu, Z., Lai, Q., and Shao, Z. (2008). A novel lipopeptide produced by a Pacific Ocean deep-sea bacterium, *Rhodococcus* sp. TW53. *J. Appl. Microbiol.* 105, 698–705.

Petruschka, L., Burchhardt, G., Müller, C., Weihe, C., and Herrmann, H. (2001). The cyo operon of *Pseudomonas putida* is involved in catabolic repression of phenol degradation. *Mol. Genet. Genomics* 266, 199–206.

Pirnik, M. P., Atlas, R. M., and Bartha, R. (1974). Hydrocarbon metabolism by Brevibacterium erythrogenes: normal and branched alkanes. *J. Bacteriol.* 119, 868–878.

Qiao, N., and Shao, Z. (2010). Isolation and characterization of a novel biosurfactant produced by hydrocarbon-degrading bacterium *Alcanivorax dieselolei* B-5. *J. Appl. Microbiol.* 108, 1207–1216.

Ratajczak, A., Geissdorfer, W., and Hillen, W. (1998). Expression of alkane hydroxylase from *Acinetobacter* sp. strain ADP1 is induced by a broad range of n-alkanes and requires the transcriptional activator AlkR. *J. Bacteriol.* 180, 5822–5827.

Rojo, F. (2009). Degradation of alkanes by bacteria. *Environ. Microbiol.* 11, 2477–2490.

Sabirova, J. S., Becker, A., Lünsdorf, H., Nicaud, J., Timmis, K. N., and Golyshin, P. N. (2011). Transcriptional profiling of the marine oil-degrading bacterium *Alcanivorax borkumensis* during growth on n-alkanes. 319, 160–168.

Sabirova, J. S., Ferrer, M., Regenhardt, D., Timmis, K. N., and Golyshin, P. N. (2006). Proteomic insights into metabolic adaptations in *Alcanivorax borkumensis* induced by alkane utilization. *J. Bacteriol.* 188, 3763–3773.

Schneiker, S., Martins dos Santos, V. A., Bartels, D., Bekel, T., Brecht, M., Buhrmester, J., et al. (2006). Genome sequence of the ubiquitous hydrocarbon-degrading marine bacterium *Alcanivorax borkumensis*. *Nat. Biotechnol.* 24, 997–1004.

Shao, Z. (2010). "Trehalolipids," in *Biosurfactant: from Genes to Application*, ed. G. Soberon-Chavez (Berlin: Springer), 121-144.

Sluis, M. K., Sayavedra-Soto, L. A., and Arp, D. J. (2002). Molecular analysis of the soluble butane monooxygenase from "*Pseudomonas butanovora*." *Microbiology* 148, 3617–3629.

Smits, T. H., Witholt, B., and van Beilen, J. B. (2003). Functional characterization of genes involved in alkane oxidation by *Pseudomonas aeruginosa*. *Antonie Van Leeuwenhoek* 84, 193–200.

Sticher, P., Jaspers, M. C., Stemmler, K., Harms, H., Zehnder, A. J., and van der Meer, J. R. (1997). Development and characterization of a whole-cell bioluminescent sensor for bioavailable middle-chain alkanes in contaminated groundwater samples. *Appl. Environ. Microbiol.* 63, 4053–4060.

Tani, A., Ishige, T., Sakai, Y., and Kato, N. (2001). Gene structures and regulation of the alkane hydroxylase complex in Acinetobacter sp. strain M-1. *J. Bacteriol.* 183, 1819–1823.

Throne-Holst, M., Wentzel, A., Ellingsen, T., Kotlar, H., and Zotchev, S. (2007). Identification of novel genes involved in long-chain nalkane degradation by *Acinetobacter* sp. strain DSM 17874. *Appl. Environ. Microbiol.* 73, 3327–3332.

van Beilen, J. B., and Funhoff, E. G. (2007). Alkane hydroxylases involved in microbial alkane degradation. *Appl. Microbiol. Biotechnol.* 74. 13–21.

van Beilen, J. B., Holtackers, R., Luscher, D., Bauer, U., Witholt, B., and Duetz, W. A. (2005). Biocatalytic production of perillyl alcohol from limonene by using a novel *Mycobacterium* sp. cytochrome P450 alkane hydroxylase expressed in *Pseudomonas putida*. *Appl. Environ. Microbiol.* 71, 1737–1744.

van Beilen, J. B., Li, Z., Duetz, W. A., Smits, T. H. M., and Witholt, B. (2003). Diversity of alkane hydroxylase systems in the environment. *Oil Gas Sci. Technol.* 58, 427–440.

van Beilen, J. B., Marin, M. M., Smits, T. H., Rothlisberger, M., Franchini, A. G., Witholt, B., et al. (2004). Characterization of two alkane hydroxylase genes from the marine hydrocarbonoclastic bacterium *Alcanivorax borkumensis*. *Environ. Microbiol.* 6, 264–273.

van Beilen, J. B., Panke, S., Lucchini, S., Franchini, A. G., Röthlisberger, M., and Witholt, B. (2001). Analysis of *Pseudomonas putida* alkane degradation gene clusters and flanking insertion sequences: evolution and regulation of the alk-genes. *Microbiology* 147, 1621–1630.

van Beilen, J. B., Wubbolts, M. G., and Witholt, B. (1994). Genetics of alkane oxidation by *Pseudomonas oleovorans*. *Biodegradation* 5, 161–174.

van den Berg, B. (2005). The FadL family: unusual transporters for unusual substrates. *Curr. Opin. Struct. Biol.* 15, 401–407.

van Hamme, J. D., Singh, A., and Ward, O. P. (2003). Recent advances in petroleum microbiology. *Microbiol. Mol. Biol. Rev.* 67, 503–549.

Wang, L., Tang, Y., Wang, S., Liu, R. L., Liu, M. Z., Zhang, Y., et al. (2006). Isolation and characterization of a novel thermophilic *Bacillus* strain degrading long-chain n-alkanes. *Extremophiles* 10, 347–356.

Wang, L., Wang, W., and Shao, Z. (2010a). Gene diversity of CYP153A and AlkB alkane hydroxylases in oil-degrading bacteria isolated from the Atlantic Ocean. *Environ. Microbiol.* 12, 1230–1242.

Wang, W., Wang, L., and Shao, Z. (2010b). Diversity and abundance of oil-degrading bacteria and

alkane hydroxylase (alkB) genes in the subtropical seawater of Xiamen Island. *Microb. Ecol.* 60, 429–439.

Wang, W., and Shao, Z. (2012a). Diversity of flavin-binding monooxygenase genes (almA) in marine bacteria capable of degradation long-chain alkanes. *FEMS Microbiol. Ecol.* 80, 523–533.

Wang, W., and Shao, Z. (2012b). Genes involved in alkane degradation in the *Alcanivorax hongdengensis* strain A-11-3. *Appl. Microbiol. Biotechnol.* 94, 437–448.

Watkinson, R. J., and Morgan, P. (1990). Physiology of aliphatic hydrocarbon-degrading microorganisms. *Biodegradation* 1, 79–92.

Wentzel, A., Ellingsen, T. E., Kotlar, H. K., Zotchev, S. B., and Throne-Holst, M. (2007). Bacterial metabolism of long chain n-alkanes. *Appl. Microbiol. Biotechnol.* 76, 1209–1221.

Wu, Y., Lai, Q., Zhou, Z., Qiao, N., Liu, C., and Shao, Z. (2008). *Alcanivorax hongdengensis* sp. nov., a alkane-degrading bacterium isolated from surface seawater of the straits of Malacca and Singapore, producing a lipopeptide as its biosurfactant. *Int. J. Syst. Evol. Microbiol.* 59, 1474–1479.

Yakimov, M. M., Giuliano, L., Denaro, R., Crisafi, E., Chernikova, T. N., Abraham, W. R., et al. (2004). Thalassolituus oleivorans general nov., sp. nov., a novel marine bacterium that obligately utilizes hydrocarbons. *Int. J. Syst. Evol. Microbiol.* 54, 141–148.

Yakimov, M. M., Giuliano, L., Gentile, G., Crisafi, E., Chernikova, T. N., Abraham, W. R., et al. (2003). Oleispira antarctica gen. nov., sp. nov., a novel hydrocarbonoclastic marine bacterium isolated from Antarctic coastal sea water. *Int. J. Syst. Evol. Microbiol.* 53, 779–785.

Yakimov, M. M., Golyshin, P. N., Lang, S., Moore, E. R., Abraham, W. R., Lunsdorf, H., et al. (1998). *Alcanivorax borkumensis* gen. nov., sp. nov., a new, hydrocarbon-degrading and surfactant-producing marine bacterium. *Int. J. Syst. Bacteriol.* 48, 339–348.

Yakimov, M. M., Timmis, K. N., and Golyshin, P. N. (2007). Obligate oil-degrading marine bacteria. *Curr. Opin. Biotechnol.* 18, 257–266.

Yuste, L., and Rojo, F. (2001). Role of the crc gene in catabolic repression of the *Pseudomonas putida* GPo1 alkane degradation pathway. *J. Bacteriol.* 183, 6197–6206.

Conflict of Interest Statement: The authors declare that the research was conducted in the absence of any commercial or financial relationships that could be construed as a potential conflict of interest.

Received: 30 November 2012; accepted: 25 April 2013; published online: 28 May 2013.

*Citation: Wang W and Shao Z (2013) Enzymes and genes involved in aerobic alkane degradation. Front. Microbiol. **4**:116. doi: 10.3389/fmicb.2013.00116*

This article was submitted to Frontiers in Microbiological Chemistry, a specialty of Frontiers in Microbiology.

frontiers in
MICROBIOLOGY

REVIEW ARTICLE
published: 21 March 2013
doi: 10.3389/fmicb.2013.00058

Structural insights into diversity and *n*-alkane biodegradation mechanisms of alkane hydroxylases

Yurui Ji [1,2], ***Guannan Mao*** [1], ***Yingying Wang*** [1]* ***and Mark Bartlam*** [2,3]*

[1] *Key Laboratory of Pollution Processes and Environmental Criteria (Ministry of Education), Tianjin Key Laboratory of Environmental Remediation and Pollution Control, College of Environmental Science and Engineering, Nankai University, Tianjin, China*
[2] *State Key Laboratory of Medicinal Chemical Biology, Nankai University, Tianjin, China*
[3] *College of Life Sciences, Nankai University, Tianjin, China*

Edited by:
Rachel N. Austin, Bates College, USA

Reviewed by:
Rachel N. Austin, Bates College, USA
Michael J. Maroney, University of Massachusetts, USA
Amy C. Rosenzweig, Northwestern University, USA

***Correspondence:**
Mark Bartlam, College of Life Sciences, Nankai University, 94 Weijin Road, Tianjin 300071, China. e-mail: bartlam@nankai.edu.cn;
Yingying Wang, Key Laboratory of Pollution Processes and Environmental Criteria (Ministry of Education), Tianjin Key Laboratory of Environmental Remediation and Pollution Control, College of Environmental Science and Engineering, Nankai University, 94 Weijin Road, Tianjin 300071, China. e-mail: wangyy@nankai.edu.cn

Environmental microbes utilize four degradation pathways for the oxidation of *n*-alkanes. Although the enzymes degrading *n*-alkanes in different microbes may vary, enzymes functioning in the first step in the aerobic degradation of alkanes all belong to the alkane hydroxylases. Alkane hydroxylases are a class of enzymes that insert oxygen atoms derived from molecular oxygen into different sites of the alkane terminus (or termini) depending on the type of enzymes. In this review, we summarize the different types of alkane hydroxylases, their degrading steps, and compare typical enzymes from various classes with regard to their three-dimensional structures, in order to provide insights into how the enzymes mediate their different roles in the degradation of *n*-alkanes and what determines their different substrate ranges. Through the above analyzes, the degrading mechanisms of enzymes can be elucidated and molecular biological methods can be utilized to expand their catalytic roles in the petrochemical industry or in bioremediation of oil-contaminated environments.

Keywords: alkane hydroxylases, biodegradation mechanism, (an)aerobic, pMMO, sMMO, AlkB, cytochrome P450, LadA

Alkanes are major constituents of natural gas and petroleum. Many living organisms such as plants, green algae, bacteria, or animals can also produce alkanes. For example, methanogenic bacteria produce methane as a metabolic end product. Plants and animals can secrete alkanes as part of their surface waxes, which they use in order to prevent water loss (Cheesbrough and Kolattukudy, 1988). As the major components of petroleum and natural gas, alkanes play an important role in modern life. However, the inertness and viscosity of solid alkanes present a significant challenge for environmental scientists once they enter soil and water bodies via accidental oil spills and leakage. After considerable efforts to try to restore oil-contaminated soil and water, microbial degradation of these contaminants may present the best solution as a large number of microorganisms, which have various uptake mechanisms and enzyme systems, can grow by utilizing these contaminants as their sole carbon and energy source. In doing so, these microbes convert the inert alkanes into less inert substances that are easier to be oxidized and employed by other microorganisms. Accordingly, studying the enzyme systems employed by these alkane-degrading microorganisms has considerable importance for environmental and industrial applications. Understanding the mechanisms of alkane degradation by these enzyme systems may help in the control of oil pollution and in the modification of those energy-intensive industrial processes producing more valuable chemicals from the inert alkanes, such as converting methane to methanol.

In this review, we briefly summarize both the aerobic and anaerobic degradation pathways and degradation mechanisms of *n*-alkanes by microbes. We focus on the key enzymes involved in the initial activation step of aerobic degradation of *n*-alkanes, i.e., alkane hydroxylases, and discuss their structural features, structure–function relationship, and potential applications in industry.

n-ALKANE DEGRADATION PATHWAY

Activation of alkanes by microbes can be carried out under both aerobic and anaerobic conditions with different enzyme systems. Under aerobic conditions, oxygen serves as the electron acceptor, while under anaerobic conditions, sulfate and nitrite accept electrons in order to complete the process.

AEROBIC DEGRADATION PATHWAY

Under aerobic conditions, the alkane degradation reaction is initiated by oxygenases, which introduce oxygen atom(s) into alkane substrates. Four pathways for the initial attack on *n*-alkanes have been identified, and the reactions have been elucidated (**Figure 1**). First is the monoterminal (or terminal) oxidation pathway, which has been found in many bacteria such as *Geobacillus thermodenitrificans* NG80-2 (Li et al., 2008). In this pathway, the reaction proceeds as follows: alkanes are first attacked at their terminal methyl group to yield the corresponding primary alcohols, which are further oxidized by alcohol dehydrogenases and

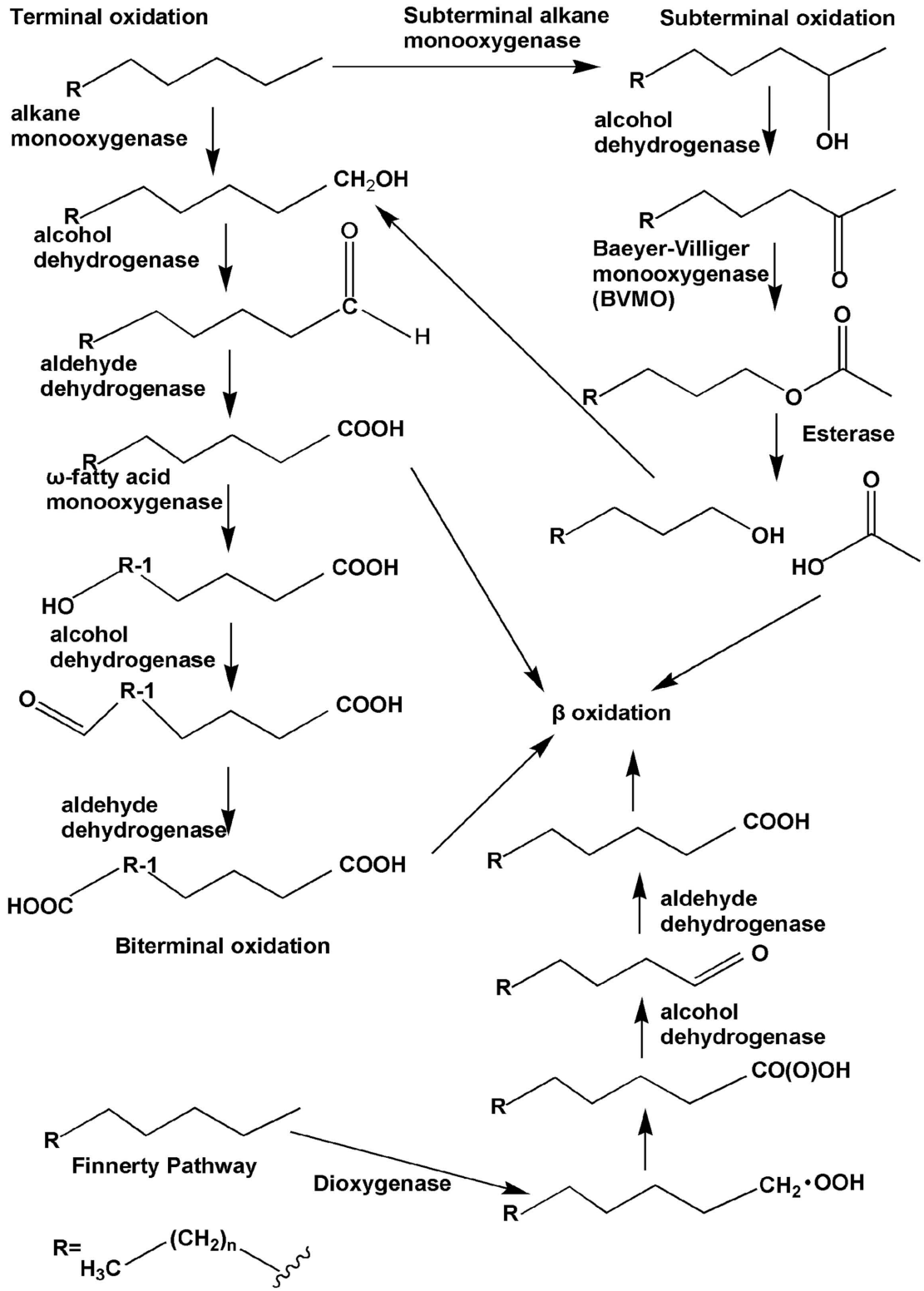

FIGURE 1 | The four types of aerobic degradation pathway (adapted from van Beilen et al., 2003). Fatty acids produced via terminal oxidation can either enter β-oxidation or be oxygenated further by the ω-fatty acid monooxygenases to form dicarboxylic acid, i.e., biterminal oxidation. Subterminal oxidation leads to the secondary alcohol or methyl acetone, which can further be oxidated by the subsequent Baeyer–Villiger monooxygenase and esterase, generating an alcohol and a fatty acid. The Finnerty pathway is initiated by dioxygenases to form *n*-alkyl hydroperoxides, which are then in turn oxidized to peroxy acids, alkyl aldehydes, and fatty acids.

aldehyde dehydrogenases to fatty acids. The fatty acids then enter β-oxidation (Watkinson and Morgan, 1990). Second is biterminal oxidation, in which the termini of the *n*-alkane undergo oxidation to the corresponding fatty acid without rupturing of the carbon chain. In this pathway, the fatty acid produced in the monoterminal oxidation pathway undergoes ω-hydroxylation at the terminal methyl group (the ω position), yielding an ω-hydroxy fatty acid that is further converted to a dicarboxylic acid, which then also enters β-oxidation (Kester and Foster, 1963; Watkinson and Morgan, 1990; Coon, 2005). Subterminal oxidation has been recognized in *Pseudomonas aeruginosa* (Forney and Markovetz, 1970) and *Gordonia* sp. strain TY-5 (Kotani et al., 2003). This process takes place when alkanes are oxidized at the subterminal position to form a primary alcohol and a secondary alcohol or methyl acetone with the same chain length as the substrate (Forney and Markovetz, 1970). A recent study has also found subterminal oxidation of *n*-alkanes in the *Gordonia* sp. strain TY-5, degrading propane into a secondary alcohol. The secondary alcohol is converted to the corresponding ketone, and then oxidized by a Baeyer–Villiger monooxygenase to form an ester. The ester is hydroxylated by an esterase, generating an alcohol and a fatty acid (Kotani et al., 2007).

The three aforementioned pathways have been known for several decades and were verified through studies with bacteria from different genera. Enzymes participating in the first step of each of the three pathways, usually called alkane hydroxylases or alkane oxygenases, form the focus of this review.

Another long-chain *n*-alkane oxidation pathway is unique to *Acinetobacter* sp. strain HO1-N, as postulated by Finnerty (1988). In this pathway, it is proposed that *n*-alkanes are oxidized to form *n*-alkyl hydroperoxides and then peroxy acids, alkyl aldehydes, and finally fatty acids. The first step involves a dioxygenase, which has been reported to be common in *n*-alkane-using *Acinetobacter* spp. (Maeng et al., 1996). However, further studies are needed in order to elucidate this process in greater detail.

ANAEROBIC DEGRADATION PATHWAY

Under anaerobic conditions, nitrate or sulfate is used as a terminal electron acceptor. To date, there are two known mechanisms of *n*-alkane anaerobic degradation (**Figure 2**). One is the fumarate addition pathway and the other is the carboxylation pathway. The anaerobic *n*-alkane degradation microorganisms that have been studied thoroughly are the sulfate-reducing bacterial strain AK-01 (So and Young, 1999), strain CV2803^T (Cravo-Laureau et al.,

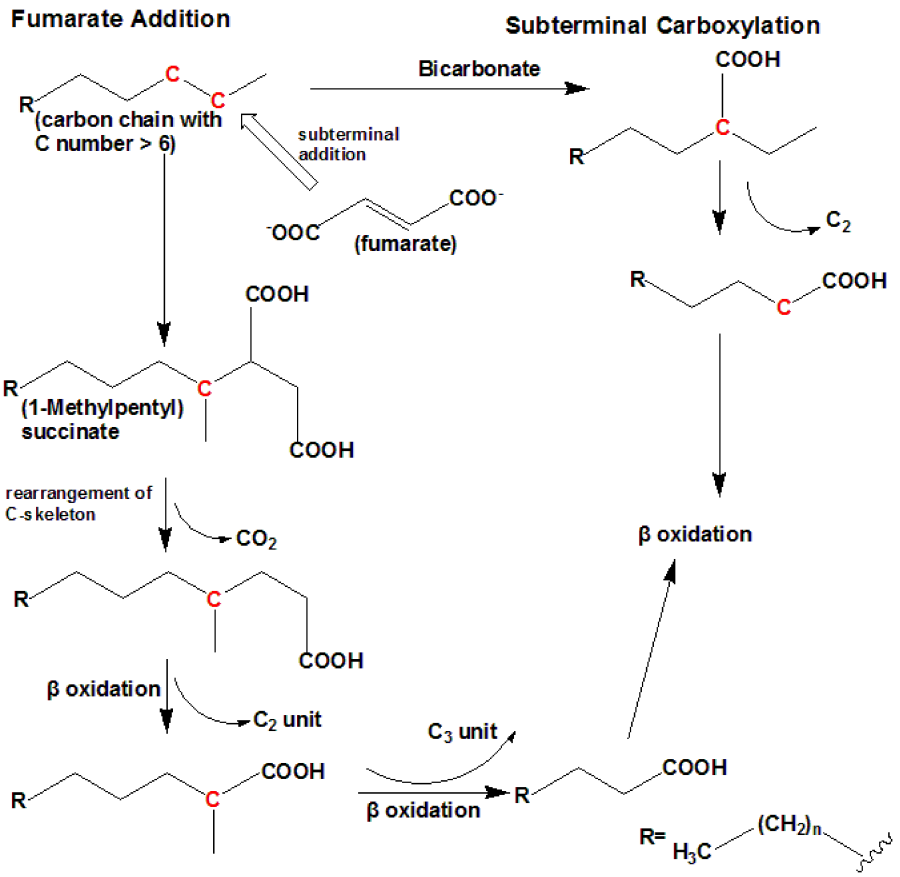

FIGURE 2 | The anaerobic degradation pathway (adapted from So et al., 2003; Cravo-Laureau et al., 2005). It shows the two types of anaerobic degradation pathway that have currently been identified. To date, subterminal carboxylation has only been found in the sulfate-reducing bacterium strain Hxd3. For short-chain *n*-alkanes, such as propane, please refer to Kniemeyer et al. (2007).

2005), strain Hxd3 (So et al., 2003), strain Pnd3 (Aeckersberg et al., 1998), and denitrifying bacterial strain HxN1 (Rabus et al., 2001). Anaerobic biodegradation of *n*-alkanes with bacterial enrichment culture has also been studied (Kropp et al., 2000; Callaghan et al., 2006, 2009). Strain Hxd3 is the first anaerobe shown to grow definitely on saturated hydrocarbons (Aeckersberg et al., 1991). Before the monooxygenase reaction was generally accepted as the initial step of alkane metabolism in aerobic microorganisms, it had been suggested that an oxygen-independent formation of a terminal double bond occurred as an alternative mechanism during aerobic growth on alkanes (Watkinson and Morgan, 1990). This mechanism also provided an explanation for the assumed anaerobic growth of certain bacteria on alkanes. It has previously been demonstrated that some microorganisms degrade *n*-alkanes via dehydrogenation and then addition of water to produce alcohols under anaerobic conditions (Parekh et al., 1977; Aeckersberg et al., 1991). Strain Hxd3 was later shown not to degrade alkanes anaerobically via a desaturation to the corresponding 1-alkenes (Aeckersberg et al., 1998). Instead, it transforms an alkane to a fatty acid via subterminal carboxylation at the C_3 position of the alkane and elimination of the two adjacent terminal carbon atoms (So et al., 2003). Researchers observed that the initial attack of alkanes includes both carboxylation with inorganic bicarbonate and the removal of two carbon atoms from the alkane chain terminus, resulting in a fatty acid that is shorter by one carbon than the original alkane. In other words, following the degradation mechanism that strain Hxd3 employed, it can transform C-odd alkanes substrates to C-even fatty acids and vice versa (So et al., 2003). To date, it is the only isolated and identified strain that anaerobically degrades via the subterminal carboxylation pathway.

Fumarate addition proceeds via subterminal addition (at the C_2 position) of the alkane to the double bond of fumarate, resulting in the formation of an alkylsuccinate. The alkylsuccinate is further degraded via carbon skeleton rearrangement and β-oxidation. The fumarate addition pathway has been found in both sulfate-reducing bacteria and denitrifying bacteria and a nitrate-reducing consortium (Kropp et al., 2000; Rabus et al., 2001; Cravo-Laureau et al., 2005; Davidova et al., 2005; Callaghan et al., 2006, 2009; Kniemeyer et al., 2007). For instance, the sulfate-reducing bacterium *Desulfatibacillum aliphaticivorans* strain CV2803^T oxidizes *n*-alkanes into fatty acids anaerobically via the addition of fumarate at C_2 position, and unlike strain Hxd3, total cellular fatty acids of this strain had predominantly odd numbers of carbon atoms when the strain was grown on a C-odd alkane (pentadecane) and even numbers of carbon atoms when it was grown on a C-even alkane (hexadecane). The same is true for other strains employing the fumarate addition pathway (Cravo-Laureau et al., 2005). A more recent study on the *Desulfosarcina/Desulfococcus* cluster strain BuS5 degrading propane indicates a subterminal as well as a novel terminal alkane addition with fumarate, i.e., the fumarate adds to the primary carbon atom of propane (Kniemeyer et al., 2007).

It has been reported that different alkane degradation pathways could occur simultaneously within mixed sulfate-reducing consortia (Callaghan et al., 2006). To sum up, these findings underline that fumarate addition and carboxylation are important alkane anaerobic degradation mechanisms that may be widespread among phylogenetically and/or physiologically distinct microorganisms.

Anaerobic methane oxidation (AMO) has also recently been identified. Purified nickel-containing methyl-coenzyme M reductase (MCR) from *Methanothermobacter marburgensis* can convert methane into methyl-coenzyme M under equilibrium conditions; the apparent V_{max} (maximum rate) and K_m (Michaelis constant) are both consistent with the observed *in vivo* kinetics for the anaerobic oxidation of methane with sulfate (Scheller et al., 2010). In another recent study, AMO is also observed to be coupled with the reduction of nitrite to dinitrogen in an enrichment culture (Ettwig et al., 2010). This is a very interesting phenomenon as the anaerobic bacterium, *Methylomirabilis oxyfera*, essentially features a methane aerobic oxidation pathway with the oxygen derived from the conversion of two nitric oxide molecules. It remains to be seen how widespread this mechanism is among anaerobic bacteria, although such a process is predicted to offer certain ecological advantages for recalcitrant substrates including aromatic compounds, alkanes and alkenes under dynamic oxic/anoxic conditions. Microbial mats collected at cold methane seeps in the Black Sea have also been shown to oxidize methane anaerobically using sulfate as an electron acceptor (Mayr et al., 2008). These microbial mats predominantly consist of sulfate-reducing bacteria and archaea of the ANME-1 and ANME-2 type. Nevertheless, further studies are required to understand the mechanisms and the enzymes involved.

DIVERSITY OF ALKANE HYDROXYLASES

Only four types of *n*-alkane aerobic degradation pathways have been identified to date, and the number of alkane hydroxylases that have been isolated, characterized, and analyzed by structural biology techniques remains limited. Studies have shown that they belong to different enzyme families. In the following section, we will classify the alkane hydroxylases into several groups according to their substrate range, degradation characteristics, and so on.

METHANE MONOOXYGENASES AND PROPANE, BUTANE OXYGENASES

The first step in the catabolism of methane is catalyzed by methane monooxygenase (MMO) to form methanol. Methanol is then oxidized by methanol dehydrogenase to form formaldehyde, which is then converted to formate and carbon dioxide by formaldehyde and formate dehydrogenases to provide energy for the cell. It is reported that methanotrophs could also assimilate formaldehyde via the ribulose monophosphate pathway or serine pathway (Lieberman and Rosenzweig, 2004). Besides MMO-containing methanotrophic bacteria, only one other enzyme, ammonia monooxygenase, can activate the C–H bond in methane (Hyman et al., 1988). Due to the inert nature of methane (104 kcal mol^{-1} C–H bond), it has proven difficult for industries to convert it to methanol under ambient temperature and pressure (Lieberman and Rosenzweig, 2005).

There are two types of MMO: a membrane-bound, particulate MMO (pMMO) and a cytoplasmic, soluble MMO (sMMO). For most methanotrophs such as *Methylococcus capsulatus* (Bath), which contain both pMMO and sMMO, it is the concentration of copper ions in the medium that determines which MMO is

expressed. Under low copper concentration conditions, the cells express only sMMO, while only pMMO is expressed when there is a high copper to biomass ratio (Stanley et al., 1983; Prior and Dalton, 1985; Murrell et al., 2000; Choi et al., 2003).

pMMO

Unlike sMMO, pMMO has a relatively narrow substrate specificity. It can only oxidize short chain *n*-alkanes (fewer than five carbon atoms). The oxidation of propane, *n*-butane and *n*-pentane preferentially occurs at the C_2 position (Chan et al., 2004). Furthermore, it is reported that pMMO could also epoxidate alkenes at the double bond. Unlike the limited existence of sMMOs, pMMO is ubiquitous in methanotrophic bacteria. As a membrane-bound protein, difficulties in solubilizing and purifying active pMMO present challenges for understanding its structure, including concentration of metal ions and location of the active site. Furthermore, difficulties in obtaining enzymatically active, pure pMMO have led to conflicting results of *in vitro* biochemical characterization (Kitmitto et al., 2005). Two groups reported structures of pMMO from the methanotroph *Methylococcus capsulatus* (Bath) in 2005 by X-ray crystallography (Lieberman and Rosenzweig, 2005) or by electron microscopy and single-particle analysis (Kitmitto et al., 2005). The research findings from the two studies are consistent and provide structural information for an enzyme that play an important role in the transformation of methane to methanol, and which may have potential applications in tackling global warming given that methane is a type of greenhouse gas. The enzyme consists of a hydroxylase formed by three polypeptides with molecular masses of approximately 47 (α, pmoB), 26 (β, pmoA), and 23 kDa (γ, pmoC). The enzyme has also been reported to form a complex with an additional component called pMMO-R formed by two polypeptides with molecular masses of 63 and 8 kDa (Basu et al., 2003; Myronova et al., 2006), although this remains controversial. A further study showed that pMMO-R is methanol dehydrogenase, the subsequent enzyme in the methane oxidation pathway by methanotrophs (Myronova et al., 2006).

Both pMMO structural studies confirmed that the hydroxylase adopts a cylindrical trimer with an $\alpha_3\beta_3\gamma_3$ polypeptide topology, with approximate dimensions of 105 Å in length and 90 Å in diameter (Lieberman and Rosenzweig, 2005; **Figure 3A**). A soluble region is composed of six β-barrel structures, two from each protomer, and extends approximately 45 Å from the membrane. pMMO is anchored into the membrane by 42 transmembrane (TM) helices, 14 from each protomer. An 11 Å hole in the center of the trimer in the soluble region is lined with glutamic acid, aspartic acid, and arginine residues, which serve to stabilize the trimer. This hole extends through the structure into the membrane where it is lined with hydrophobic residues and widens to approximately 22 Å at the opposing end to the soluble region.

Three metal centers were identified per protomer from the crystal structure: the first and second sites are located in pmoB, and the third site is located within the lipid bilayer. The first site contains a single metal ion assigned as copper, while the second metal site is a conserved dinuclear site that contains two copper ions, which was also found in subsequent pMMO structures from *Methylosinus trichosporium* OB3b (Hakemian et al., 2008) and *Methylocystis* species Strain M (Smith et al., 2011), respectively. The third metal center, modeled as a single zinc ion, is located within the lipid bilayer; it was proposed to be derived from the crystallization buffer but could be occupied by other metal ions *in vivo*. Structural analysis therefore identified a total of four metal ions per protomer, which differs significantly from other previous studies (Chan et al., 2004; Lieberman and Rosenzweig, 2005).

Activity experiments and mutagenesis have subsequently confirmed that the copper active site is located in the soluble domain of the pmoB subunit and is a dicopper center (Balasubramanian et al., 2010). The reactivity of a recombinant soluble fragment of the pmoB subunit (denoted as spmoB) and inactive spmoB, in which the dicopper center is disrupted, with oxidants were compared and an absorbance feature at 345 nm in spmoB was not produced in the inactive spmoB. Reaction of the 345 nm species with methane resulted in the disappearance of the spectroscopic feature, suggesting that this O_2 intermediate should be mechanistically relevant. These observations support the idea that the dicopper center is the activation site and molecular oxygen binds at the dicopper center (Culpepper et al., 2012).

sMMO

Soluble MMO is a soluble, cytoplasmic monooxygenase that can oxidize a broad range of substrates including saturated alkanes, alkenes, aromatics, and chlorinated aromatics (McDonald et al., 2006). As sMMO is soluble and can oxidize many chemicals, it has drawn the attention and efforts of researchers and it is better understood than pMMO. sMMO systems isolated from *Methylococcus capsulatus* (Bath) and *Methylosinus trichosporium* OB3b have been studied extensively, and the first three-dimensional structure of one component of sMMO from *Methylococcus capsulatus* (Bath) was obtained in 1993 (Rosenzweig et al., 1993). sMMO is a complex enzyme system comprised of three protein components: MMOH, MMOR, and MMOB. MMOH is a 251-kDa heterodimeric hydroxylase with an $\alpha_2\beta_2\gamma_2$ topology, containing a carboxylate- and hydroxo-bridged dinuclear iron center. MMOR is a 38.5-kDa iron-sulfur flavoprotein that utilizes flavin adenine dinucleotide (FAD) and [2Fe-2S] cofactors to transfer electrons from NADH to the hydroxylase active site. MMOB is reported to regulate MMO reactivity (Merkx et al., 2001). The dioxygen activation reaction and substrate oxidation occurs at the di-iron centers in the α subunits of MMOH.

The structure of MMOH reveals a heart-shaped dimer, with the interface between the monomers forms a canyon that is approximately 80 Å × 40 Å × 20 Å in size (**Figure 3B**; Rosenzweig et al., 1993). The di-iron centers reside in the core of the α subunit and are coordinated by four glutamate and two histidine residues. Available $MMOH_{ox}$ structures suggest that dioxygen-binding most likely occurs via replacement of the weakly coordinating bridging water molecule distal to the histidines. A hydrophobic substrate-binding pocket distal to the histidines houses the MMO active site and preferentially binds hydrophobic molecules, such as methane and dioxygen. Several possibilities have been raised for substrate ingress into and product egress from the active site. One possibility is that the substrate enters into the cavity via a gap between two helices that form part of the α subunit and constitute the di-iron centers. Another possibility

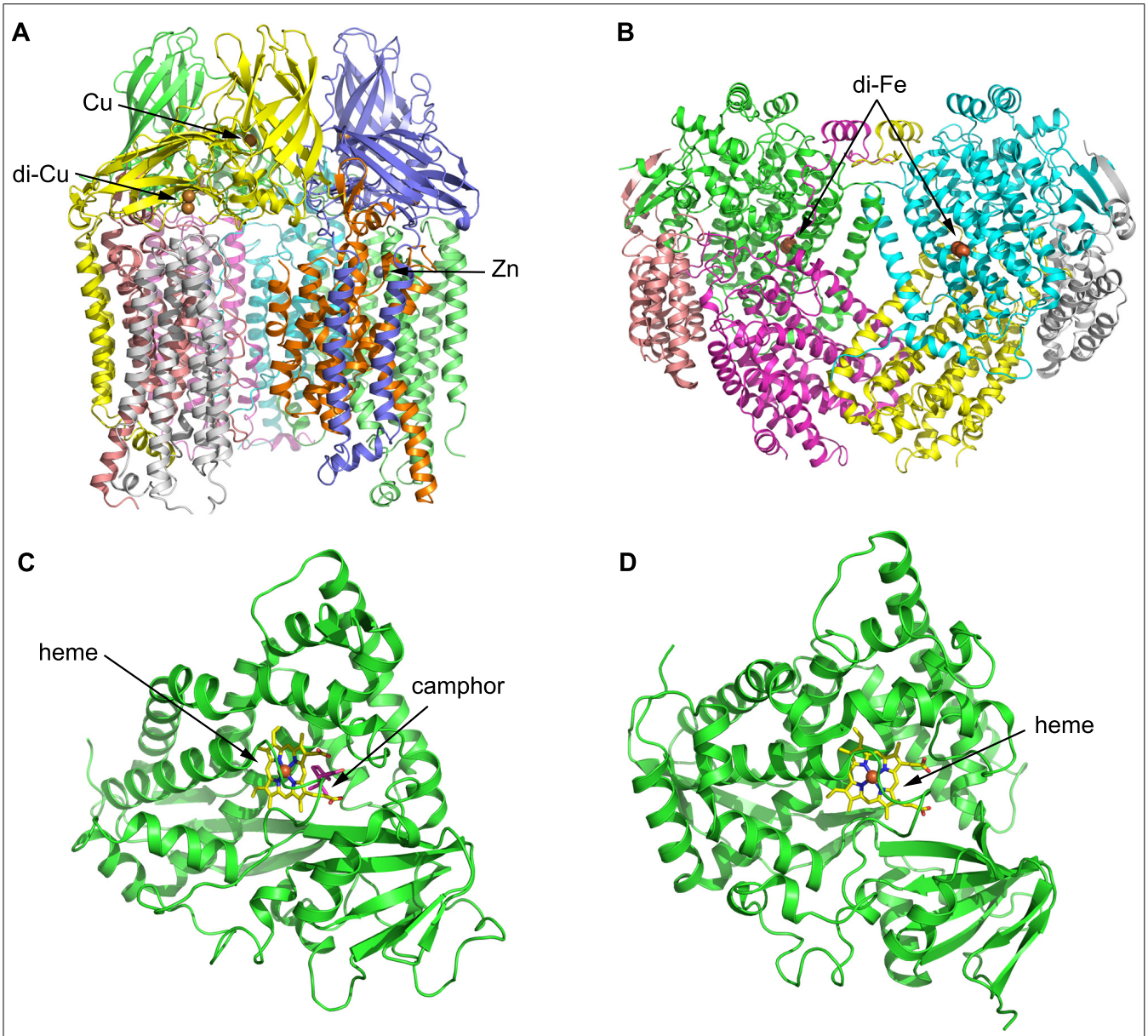

FIGURE 3 | Three-dimensional structures of alkane hydroxylase enzymes. **(A)** The crystal structure of particulate methane monooxygenase (pMMO) from *Methylococcus capsulatus* (Lieberman and Rosenzweig, 2005). The structure is shown in cartoon representation and colored by chain; the Zn and Cu ions are shown as spheres. **(B)** The crystal structure of soluble methane monooxygenase (sMMO) from *Methylococcus capsulatus* (Rosenzweig and Lippard, 1994). The structure is shown in cartoon representation and colored by chain; the di-iron centers are shown as spheres. **(C)** The crystal structure of P450cam from *Pseudomonas putida* (Poulos et al., 1987). The structure is shown in cartoon representation, with the heme shown in stick representation and the iron shown as a sphere. Camphor is also shown in stick representation and colored magenta. **(D)** The crystal structure of P450 BM-3 from *Bacillus megaterium* (Ravichandran et al., 1993). The structure is shown in cartoon representation, with the heme shown in stick representation and the iron shown as a sphere.

is that the substrate enters the active site through one or more of the five hydrophobic cavities identified in the α subunit (Merkx et al., 2001).

Many spectroscopic techniques suggest that MMOB exerts its influences on MMOH by binding in the vicinity of the di-iron site and slightly altering its structure. The regulatory protein MMOB controls the substrate selectivity of MMO. MMOB binds to MMOH, which contains the active site, and appears to create a pore consistent with the size of methane in the active site. Mutagenesis of MMOB may therefore broaden the substrate range (Zhang et al., 2006).

MMOR contains one [2Fe-2S] cluster and one FAD cofactor, which both promote electron transfer from NADH to MMOH. The [2Fe-2S] cluster is located in the N-terminal portion of MMOR. The FAD cofactor is located in the C-terminal domain of MMOR, as is the NADH-binding region.

Soluble MMO utilizes a complex electron shuttle system with the function of NADH-oxidation and hydroxylation of methane played respectively by two proteins. Activation of dioxygen and the actual hydroxylation reaction both occur within the MMOH protein.

Other oxygenases for short-chain n-alkanes

Other gaseous alkanes are metabolized by strains expressing propane or butane monooxygenases (BMOs) that are related to pMMO or sMMO. A new isolate, *Gordonia* sp. strain TY-5, is capable of growth on propane and *n*-alkanes from C_{13} to C_{22} as the sole carbon source. A gene cluster designated prmABCD, which encodes the components of a putative dinuclear-iron-containing multicomponent monooxygenase, was cloned and sequenced. It was found that prmABCD disrupted mutants cannot grow on propane, suggesting that prmABCD gene products play an essential role in propane oxidation by the bacterium. Further studies show that it oxidizes propane via subterminal oxidation to 2-propanol via a monooxygenase (Kotani et al., 2003) and then further to acetone (Kotani et al., 2007). A gene cluster designated acmAB was cloned in which the acmA and acmB genes encode a Baeyer–Villiger monooxygenase and esterase, respectively. Further studies show that acmAB gene products play an important role in the metabolism of acetone derived from propane oxidation. The propane metabolism pathway in *Gordonia* sp. strain TY-5 started with the oxidization of propane to 2-propanol, which is further converted to acetone, followed by methyl acetate, which is finally oxidized to acetic acid and methanol (Kotani et al., 2007).

Butane monooxygenase from the Gram-negative β-proteobacterium *Thauera butanivorans*, previously called "*Pseudomonas butanovora*" (Dubbels et al., 2009), can oxidize alkanes C_2–C_9 (Halsey et al., 2006) and has received considerable attention from researchers. It is a three-component di-iron monooxygenase system that consists of an iron-containing hydroxylase (BMOH), a flavo-iron sulfur-containing NADH-oxidoreductase (BMOR), and a small regulatory component protein (BMOB). BMO has a strong regiospecificity of hydroxylation at the terminal carbon atom (Dubbels et al., 2007). Although BMO shares high homology with sMMO, researchers had not identified any oxidation of methane by BMO prior to the study by Halsey et al. (2006). Due to geometric constraints in the active site, product release is believed to be rate limiting, and accumulation of 23 μM methanol led to complete inhibition of methane oxidation in the *T. butanivorans* wild-type strain. Site-directed amino acid mutations were made in the α subunit of BMOH and a mutant form of BMOH found to partly abolish this restriction, resulting in a less methanol-sensitive enzyme that can tolerate a methanol concentration as high as 83 μM (Halsey et al., 2006). Propionate is a potent repressor of BMO expression: 10 μM propionate is able to reduce transcriptional activity of the BMO promoter. Propionate catabolism was inactive during growth of *Pseudomonas butanovora* on even-chain-length alkanes. However, propionate consumption was induced following growth on the odd-chain-length alkanes propane and pentane, resulting in a striking difference in the response to even- versus odd-chain-length alkanes (Doughty et al., 2006).

Recently, researchers have identified a novel membrane-associated monooxygenase (pBMO) from the Gram-positive bacterium *Nocardioides* sp. strain CF8 growing on butane. The arrangement of the genes encoding pBMO and the genes encoding pMMO from the methane-oxidizing bacteria are similar. Phylogenetic analysis suggests that pBMO represents a deeply branching third lineage of the bacterial family (Sayavedra-Soto et al., 2011), although further studies are needed to provide a comprehensive understanding of pBMO.

THE AlkB FAMILY OF ALKANE HYDROXYLASES

The most widely characterized alkane degradation system is the Alk system of *Pseudomonas putida* GPo1 (commonly known as *Pseudomonas oleovorans* GPo1 = TF4-1L = ATCC 29347), which oxidizes C_5–C_{12} *n*-alkanes to 1-alkanols (van Beilen et al., 1994). The 1-alkanol products are then sequentially converted to the corresponding aldehydes, carboxylic acids, and acyl-coenzymes A (CoAs), which then enter the β-oxidation pathway (Throne-Holst et al., 2007). The Alk system can also catalyze versatile reactions including the hydroxylation of linear and branched aliphatic, alicyclic, and alkylaromatic compounds, demethylation of branched methyl ethers, and epoxidation of terminal olefins (van Beilen et al., 2005). This enzyme system has also been reported to oxidize gaseous alkanes such as propane and *n*-butane (Johnson and Hyman, 2006).

The *Pseudomonas putida* GPo1 alkane hydroxylase system is composed of three components: alkane hydroxylase (AlkB), rubredoxin (AlkG), and rubredoxin reductase (AlkT; Smits et al., 2002). AlkB is a non-heme iron integral membrane protein that carries out the hydroxylation reaction (Kok et al., 1989; van Beilen et al., 1992). The NADH-dependent flavoprotein rubredoxin reductase transfers electrons from reduced nicotinamide to rubredoxin (Lode and Coon, 1971). Rubredoxin, a small red-colored iron-sulfur protein, transfers reducing equivalents to AlkB (McKenna and Coon, 1970; Smits et al., 2002).

The OCT plasmid of GPo1 encodes two rubredoxins, AlkF and AlkG. AlkG is unusual in that it is more than three times the size of other bacterial rubredoxins. It is composed of two rubredoxin domains connected by a 70-amino acid linker (Kok et al., 1989). Each domain binds a single iron atom, although the iron in the N-terminal domain is very loosely bound and is usually lost in the isolated protein (van Beilen et al., 1994). Rubredoxins cloned from microbes that grow on *n*-alkanes can be grouped into AlkG1- and AlkG2-type rubredoxins based on their amino acid sequences. All of the alkane-degrading strains contain AlkG2-type rubredoxins, whereas AlkG1-type rubredoxins are only present in a limited number of alkane-degrading strains. Two iron-binding CXXCG motifs are common to most alkane-degrading rubredoxins. Insertion of arginine downstream of the second CXXCG motif results in the failure of AlkG1 to transfer electrons to the alkane hydroxylase, thus providing a means of distinguishing AlkG1-type rubredoxins from the AlkG2-type rubredoxins.

Researchers have employed protein engineering to study the substrate specificity of AlkB and found that W55 (in the case of *Pseudomonas putida* AlkB) or W58 (in the case of *Alcanivorax borkumensis* AlkB1) plays a key role in determining the substrate range. Interestingly, mutation of this amino acid to a much less

bulky amino acid enables AlkB in *Pseudomonas putida* to oxidize longer *n*-alkanes than the wild-type (van Beilen et al., 2005).

To date, there is no detailed structural information for AlkB, nor is there much biochemical data for AlkB with an extended substrate range. Nevertheless, a topology model of AlkB has provided some insight into its structure–function relationship. AlkB is predicted to contain six alpha-helical TM segments (van Beilen et al., 1992), which are thought to form a hydrophobic pocket. The N-terminus, two hydrophilic loops, and a large C-terminal domain are all located in the cytoplasm. Only three very short loops close to the amino acid positions 62, 112, and 251 are exposed to the periplasm (van Beilen et al., 1992). Mutagenesis experiments have verified that the eight histidines on the TM segment are very important for activity of AlkB, such as coordinating the Fe ions in the di-iron active site (Shanklin and Whittle, 2003). AlkB is proposed to belong to a larger family containing the non-heme integral membrane desaturases, epoxidases, acetylenases, conjugases, ketolases, decarbonylase, and methyl oxidases; all of the enzymes feature eight conserved histidine residues in a similar relative position with respect to the TM domains.

Researchers have also cloned novel genes encoding AlkB-rubredoxin fusion proteins from Gram-positive bacteria, such as *Dietzia* strain DQ12-45-1b, *Dietzia* sp. E1, *Prauserella rugosa* NRRL B-2295, and *Nocardioides* sp. strain CF8 (Hamamura et al., 2001; Smits et al., 2002; Bihari et al., 2011; Nie et al., 2011). The fusion protein encoded by *alkW1* from *Dietzia* strain DQ12-45-1b, consisting of an integral membrane alkane monooxygenase (AlkB) conserved domain and a rubredoxin conserved domain, can degrade C_8–C_{32} *n*-alkanes and is experimentally verified to be favorable for the oxidation of long-chain alkanes. Two possibilities for the mechanism of the favorable oxidation have been proposed. The first involves steric effects on the binding between the substrate and enzyme, or between the enzyme and rubredoxin. The second is easier electron transport caused by a shorter distance between the two fused proteins. Phylogenetic analysis of the fused rubredoxins identified from different species clearly showed that all AlkB-fused rubredoxins constitute a novel third cluster of rubredoxins that are significantly distinct from either AlkG1-type or AlkG2-type rubredoxins. In addition, all AlkB-fused rubredoxins contain the conserved C(P/S)DCGVR motif in addition to the first CXXCG motifs (Nie et al., 2011).

CYTOCHROME P450 ALKANE HYDROXYLASES

Cytochrome P450 enzymes are terminal monooxygenases that have been detected in nearly all domains of life, from prokaryotes such as *Pseudomonas putida* to eukaryotes, where yeasts can serve as an example. Their ubiquitous existence in nature determines their diverse substrate range, including fatty acids, steroids, prostaglandins, as well as many exogenous materials such as drugs, anesthetics, organic solvents, ethanol, alkylaryl hydrocarbon products, pesticides, and carcinogens (Bernhardt, 2006). Based on differences in the components of the P450 monooxygenase systems, they can be grouped into two classes. Class I P450s are represented by P450s isolated from mitochondria and bacteria. Electron transfer to these enzymes from NAD(P)H is mediated by an FAD-containing reductase (which accepts electrons from NAD(P)H) and an iron-sulfur protein (which shuttles electrons from the reductase to the substrate-bound P450; Huang and Kimura, 1973). The class II P450s consist of microsomal drug-metabolizing forms that receive electrons from NAD(P)H via an FAD- and flavin mononucleotide (FMN)-containing cytochrome P450 reductase (van Beilen and Funhoff, 2005). P450s from bacteria are mostly soluble while P450s from yeast and mammals are usually membranous, which makes their further study more challenging. At the time of writing, more than 4,000 P450 enzymes are known (van Beilen and Funhoff, 2005). However, with regard to P450s degrading *n*-alkanes, the number is rather small.

To date, the P450s that have received the most attention and been extensively studied are the P450cam system from *Pseudomonas putida* ATCCl7453, which require putidaredoxin and putidaredoxin reductase to transfer electrons from NADH to P450cam for the oxidation of camphor to 5-exo-hydroxycamphor (**Figure 3C**; Trudgill et al., 1966; Poulos et al., 1987), and P450 BM-3 from *Bacillus megaterium* 14581 that hydroxylates medium-chain (from C_{12} to C_{18}) saturated fatty acids (**Figure 3D**; Narhi and Fulco, 1986; Ravichandran et al., 1993). P450 BM-3 is the most active of all P450 enzymes, and this has been suggested to be due to the fusion of a hydroxylase domain and a reductase domain into a single polypeptide chain, which is different to other P450 enzymes (Narhi and Fulco, 1986). Although these two enzymes have been studied intensively, none of their substrates are *n*-alkanes, which are the most inert molecules. Researchers have thus employed molecular biology and other related methods in combination with structural information to modify the substrate-binding pockets and active sites of the enzymes, in order to make them more suitable for binding to and degrading smaller *n*-alkane molecules. For instance, P450cam was engineered into an alkane hydroxylase with amino acid residues in the active site replaced by residues with bulkier and more hydrophobic side chains. The resulting mutant (F87W/Y96F/T101L/V247L) had a comparable catalytic turnover rate for *n*-butane oxidization to that of the wild-type and exhibited the highest propane oxidation rate of the P450cam enzymes studied (Bell et al., 2003). Rational evolution of P450 BM-3 produced a triple mutant (Phe87Val, Leu188Gln, Ala74Gly) that is capable of oxidation of *n*-octane at a similar rate as *n*-dodecanoic acid (Appel et al., 2001). Directed evolution of P450 BM-3 produced mutant 139-3 that can degrade *n*-alkanes (from C_3 to C_8) at the subterminal position, which resembles the native enzyme's regioselectivity on fatty acids (Glieder et al., 2002). CYP102A3 from *B. subtilis* hydroxylates medium-chain fatty acids in subterminal positions, as does P450 BM-3 (CYP102A1) from *B. megaterium* (Whitehouse et al., 2010). Two CYP102A3 mutants can oxidize octane with ratios of 43% (S189Q) and 49% (F88V/S189Q), respectively, which shows that F88 and S189 are important in determining the substrate spectrum of CYP102A3 (Lentz et al., 2004).

CYP153 enzymes are class I P450 proteins requiring the presence of an electron-delivering protein system (ferredoxin and ferredoxin reductase protein). Cytochrome P450 enzymes from the CYP153 family are the first soluble P450 enzymes that specifically display hydroxylating activity toward the terminal position of alkanes (Scheps et al., 2011). CYP153A6 from *Mycobacterium* sp. HXN-1500 is the first soluble P450 that hydroxylates unreactive aliphatic alkanes, mainly medium-chain-length alkanes (from

C_6 to C_{11}), with high regioselectivity on terminal positions to 1-alkanols. Longer alkanes bind more strongly than shorter alkanes, while the introduction of sterically hindering groups reduces the affinity. This suggests that the substrate-binding pocket is shaped such that linear alkanes are preferred (Funhoff et al., 2006). CYP153 is a cytochrome P450 from *Acinetobacter* sp. EB104, which constitutes a new P450 family; it catalyzes the hydroxylation of unsubstituted *n*-alkanes (Maier et al., 2001). CYP153C1 from the oligotrophic bacterium *Novosphingobium aromaticivorans* DSM 12444 can bind linear alkanes such as heptane, octane, and nonane (Zhou et al., 2011).

Several species of yeast belonging to the genus *Candida* excrete α,ω-diacids as a by-product when grown on *n*-alkanes or fatty acids as the carbon source. One such yeast species, *Candida tropicalis* ATCC 20336, has been studied in detail in regard to the CYP52 family, which is important for the conversion of *n*-alkanes and fatty acids to α,ω-dicarboxylic acids. For alkanes, the first reaction occurs in the ω-oxidation pathway with the formation of the corresponding alcohol. A cytochrome P450 hydroxylase complex, which composes of a cytochrome P450 monooxygenase and the accompanying NADPH cytochrome P450 reductase, is responsible for the first and rate-limiting step of ω-oxidation of *n*-alkanes and fatty acids (van Beilen and Funhoff, 2005).

LONG-CHAIN ALKANE MONOOXYGENASE (LadA)

Several bacterial strains can assimilate *n*-alkanes with carbon chain length longer than C_{20}. However, enzymes involved in these degradation processes usually do not belong to the three groups mentioned above. To date, few long-chain alkane hydroxylases have been cloned and characterized. Three-dimensional structures of long-chain alkane hydroxylases remained unclear until the 2.7 Å apoenzyme and 1.9 Å holoenzyme structures of LadA, a long-chain alkane monooxygenase, were reported in 2008 (**Figure 4A**; Li et al., 2008). LadA, isolated from the thermophilic bacillus *Geobacillus thermodenitrificans* NG80-2, utilizes a terminal oxidation pathway for the conversion of long-chain *n*-alkanes (from C_{15} to at least C_{36}) to corresponding primary alcohols. The terminal oxidation pathway from *Geobacillus thermodenitrificans* NG80-2 has been well characterized and consists of three components: LadA, which is the key initiating enzyme; two alcohol dehydrogenases (ADH1 and ADH2) for the conversion of alkyl alcohols to alkyl aldehydes (Ji et al., 2013); and an aldehyde dehydrogenase (ALDH) for the conversion of alkyl aldehydes to fatty acids (Feng et al., 2007).

LadA was revealed to belong to the SsuD subfamily of the bacterial luciferase family via a surprising structural relationship (Li et al., 2008). The structure of LadA contains a triosephosphate isomerase (TIM) barrel fold that differs from the prototypical TIM barrel structure due to five extended insertion regions (IS1-5) and an extension at the C-terminus of the polypeptide chain (Li et al., 2008). A pocket at the C-terminal entrance of the TIM barrel is sufficiently large enough to accommodate a FMN, O_2, and part of the terminal of a long-chain *n*-alkane. LadA was thus confirmed to be a flavoprotein monooxygenase that utilizes dioxygen to insert an oxygen atom into the substrate. The flavin ring of FMN lies in the barrel with its plane almost parallel to the staves of the barrel and its *Si*-face exposed to solvent (**Figure 4B**). The ribityl side chain and phosphate moieties insert between strands β4 and β5 of LadA in an elongated manner. A cavity above the *Si*-face of FMN is lined by the residues F10, M12, H17, A57, V59, Y63, Q79, H138, H311, W348, and F349, with polar residues concentrated on the left sphere and hydrophobic residues on the right sphere (**Figure 4B**).

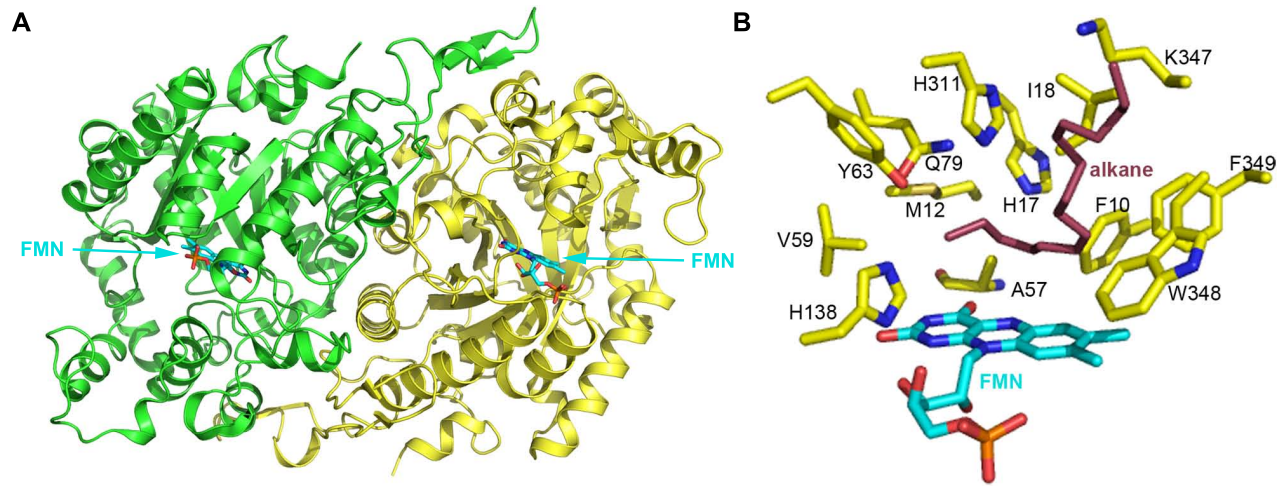

FIGURE 4 | (A) The crystal structure of long-chain alkane monooxygenase (LadA) from *Geobacillus thermodenitrificans* NG80-2 (Li et al., 2008). The structure is shown in cartoon representation and colored by chain, with the FMN cofactor shown in stick representation and colored cyan. **(B)** The putative active pocket lined by several residues above the FMN *Si*-face. H138 possibly acts as a proton donor in the reaction between reduced flavin and oxygen that leads to the formation of the C4a-hydroperoxyflavin intermediate. A hydrophobic cavity formed by M12, A57, V59 and the 4′ OH group of the FMN ribityl chain and the terminal carbon of the alkane chain act to protect the C4a-hydroperoxyflavin from solvent. H17, Y63, Q79, and H311 are believed to be involved in substrate activation and electron transfer during hydroxylation. F10, I18, K347, W348, and F349 should be involved in binding the alkane substrate. LadA amino acids are shown as yellow sticks and labeled; the FMN coenzyme is shown in cyan stick representation. A docked alkane substrate is shown in red stick representation and labeled.

In the absence of a LadA:FMN:alkane ternary complex, *in silico* docking of C_{15}–C_{22} alkanes was used to provide insights into substrate binding and the terminal hydroxylation of long-chain aliphatic alkanes. All substrates were identically coordinated with the terminal carbon located above the FMN *Si*-face, located close to the C4a atom, and interposing the cavity mentioned above. The carbon chain adopts a sinuous conformation along the surface of the insert region IS4, with its terminal lying parallel to the plane of flavin *Si*-face. The substrates bind to the protein via hydrophobic interactions between the majority of the alkane chain and a cluster of hydrophobic residues in LadA, including F10, I18, K347, W348, and F349 (**Figure 4B**). Li et al. (2008) speculated that the substrate-binding mode requires substrate specificity and thus determines the range of the alkane carbon chain length for catalysis. It was predicted that alkane chains of C_{14} and lower would be of insufficient length for the terminal carbon to reach the active site while the opposing terminal part was anchored to the protein.

As the carbon–hydrogen bond is inert in aliphatic alkanes, the activation of the substrate is rationally required before it reacts with the C4a-hydroperoxyflavin intermediate. Four polar residues, H17, Y63, Q79, and H311, are located above the terminal carbon of the alkane (**Figure 4B**). Enzyme inactivation activity assays performed on single point mutants indicate that mutation of each of these four residues completely abolishes the catalytic activity of LadA. Thus, they are likely to play crucial roles in the catalytic reaction, and it was suggested that their polar side chains may be involved in substrate activation and electron transfer. Mutation of a fifth residue, C_{14}, was also shown to abolish LadA catalytic activity, but this was achieved by disrupting the homodimer interface, indicating that dimerization is also important for catalytic activity. Although the process of activation and the precise catalytic mechanism could not be elucidated from the reported LadA structure, the structural analysis of LadA has provided a rational basis for further biochemical studies.

A recent study by Dong et al. (2012) reported the use of random- and site-directed mutagenesis to enhance the activity of LadA. Three mutants, A102D, L320V, and F146C/N376I from random-mutagenesis, together with six more mutants, A102E, L320A, F146Q/N376I, F146E/N376I, F146R/N376I, and F146N/N376I from site-directed mutagenesis, were obtained and the hydroxylation activity of purified mutants on hexadecane was found to be between 2- and 3.4-fold higher than that of the wild-type LadA, with the activity of F146N/N376I being the highest. In the same study, *Pseudomonas fluorescens* KOB2Δ1 strains expressing the LadA mutants were found to grow more rapidly with hexadecane than the strain expressing wild-type LadA, confirming the enhanced activity of LadA mutants *in vivo* (Dong et al., 2012). Both the wild-type LadA and mutants were active at temperatures ranging from 40 to 90°C and at pH values from 6.0 to 8.8. This study thus confirms the suitability of LadA for industrial utilization.

Another noteworthy phenomenon is that although LadA belongs to the flavoproteins, the activity of the enzyme appears to be independent of flavin reductase, as indicated by *in vitro* activity assays performed with and without the presence of a reductase. Flavoprotein monooxygenases catalyze an overall reaction involving three general chemical processes: (a) reduction of the cofactor flavin by NAD(P)H; (b) reaction of the reduced flavin with O_2 to provide a C4a-flavin(hydro)peroxide, which is the oxygenating reagent; and (c) binding, orienting, and activating the substrate for oxygenation by C4a-(hydro)peroxyflavin. A new group of flavoprotein monooxygenases has recently been identified that consist of two components: a NAD(P)H-dependent flavin reductase for reduction of flavin, and a monooxygenase that uses reduced flavin as a substrate for the oxidation reaction. The luciferase systems, to which LadA is related, are the first and the most extensively studied two-component flavin-dependent oxygenases. It was previously proposed that electrons may be directly transferred from NAD(P)H to the flavin during hydroxylation in some flavoproteins, including the well-studied PHBH (p-hydroxybenzoate hydroxylase; Moonen et al., 2002), and LadA. However, this hypothesis needs to be further confirmed (Dong et al., 2012).

OTHER LONG-CHAIN *n*-ALKANE HYDROXYLASES

Other studies focused on long-chain alkane degradation have remained mainly at the level of genetic studies, with little or no further research on the enzymes involved. A novel dioxygenase isolated from *Acinetobacter* sp. strain M-1 utilizes *n*-alkanes ranging in length from C_{10} to C_{30} as its sole carbon and energy source with the presence of FAD and Cu^{2+} for its activity via the Finnerty pathway (Maeng et al., 1996). *Acinetobacter haemolyticus* strain AR-46, which is evolutionally distant from the known hydrocarbon-degrading *Acinetobacter* spp., is reported to be able to utilize long-chain *n*-alkanes ranging from C_{16} to C_{35} through the monoterminal oxidation pathway (Bihari et al., 2007). Based on these results, it is evident that an alkM encoded non-heme iron integral membrane alkane hydroxylase is the first key enzyme in the monoterminal oxidation pathway.

Acinetobacter sp. strain DSM 17874 can utilize C_{10}–C_{40} *n*-alkanes as its sole carbon source (Throne-Holst et al., 2007). *almA* was identified as the gene encoding a putative flavin-binding monooxygenase which enables the strain to utilize long-chain alkanes ($>C_{32}$). An interesting phenomenon whereby an *almA*-deficient mutant was still able to grow with C_{24} and shorter alkanes as its sole carbon source, indicated that the same strain uses another enzyme system for degradation of shorter alkanes (Throne-Holst et al., 2007). By using highly degenerate primers, Liu et al. (2011) amplified the *almA* gene, with a *n*-alkane substrate range from C_{22} to C_{36}, from the marine alkane degrader *Alcanivorax dieselolei* B-5. This substrate range complements those of *alkB* and *p450* genes that also exist in the strain. Studies using the same methods indicate that *almA* is more likely to be found in marine hydrocarbon-degrading bacteria, which implies that the *almA* gene is very important for the degradation of long-chain alkanes in the ocean (Wang and Shao, 2012).

OUTLOOK

Alkane hydroxylases are widespread in petroleum-degrading bacteria and a number of them are quite efficient in oxidizing substrates. Therefore, there is considerable interest in employing alkane hydroxylases for industrial applications. Thermophilic long-chain *n*-alkane-degrading bacterial strains are of particular interest for their biotechnological applications. There are several

advantages of using thermophilic microorganisms for bioremediation of hydrocarbons over mesophilic organisms. Generally speaking, elevated temperature can increase the solubility of hydrophobic pollutants, decrease their viscosity, enhance their diffusion, and transfer long-chain *n*-alkanes from the solid phase to liquid phase (Feitkenhauer et al., 2003). Most alkane hydroxylases are relatively complex and difficult to use *in vitro* as they are composed of multiple components, such as the P450 system and the AlkB system, leading to low electron transfer rates. They also usually require the presence of cofactors, which are sensitive to inactivation by activated oxygen species and sensitive to product inhibition. Furthermore, the substrates and the products of these enzymes tend to be quite hydrophobic and toxic to the host cell. Enzymes such as the long-chain monooxygenase LadA could be a favorable candidate in industrial oxygenation reactions as it meets most of the demands of an ideal enzyme used in industry (van Beilen and Funhoff, 2007): it is cofactor-independent, less sensitive to high temperature, and abundant quantities of the enzyme can be produced through heterologous expression in *E. coli*. Although there are problems that hinder their application in industry, protein engineering, site-directed mutagenesis and random mutagenesis, together with structural information for such enzymes, can help to overcome any problems and aid the development of alkane hydroxylase enzymes into efficient, highly selective catalysts.

ACKNOWLEDGMENTS

The authors are grateful to the financial support from the Ministry of Science & Technology 973 Project (2010CB912602), the National Science Foundation of China (31270545), and the Tianjin Municipal Science and Technology Commission (12JCZDJC29700).

REFERENCES

Aeckersberg, F., Bak, F., and Widdel, F. (1991). Anaerobic oxidation of saturated hydrocarbons to CO2 by a new type of sulfate-reducing bacterium. *Arch. Microbiol.* 156, 5–14.

Aeckersberg, F., Rainey, F. A., and Widdel, F. (1998). Growth, natural relationships, cellular fatty acids and metabolic adaptation of sulfate-reducing bacteria that utilize long-chain alkanes under anoxic conditions. *Arch. Microbiol.* 170, 361–369.

Appel, D., Lutz-Wahl, S., Fischer, P., Schwaneberg, U., and Schmid, R. D. (2001). A P450 BM-3 mutant hydroxylates alkanes, cycloalkanes, arenes and heteroarenes. *J. Biotechnol.* 88, 167–171.

Balasubramanian, R., Smith, S. M., Rawat, S., Yatsunyk, L. A., Stemmler, T. L., and Rosenzweig, A. C. (2010). Oxidation of methane by a biological dicopper centre. *Nature* 465, 115–119.

Basu, P., Katterle, B., Andersson, K. K., and Dalton, H. (2003). The membrane-associated form of methane mono-oxygenase from *Methylococcus capsulatus* (Bath) is a copper/iron protein. *Biochem. J.* 369, 417–427.

Bell, S. G., Orton, E., Boyd, H., Stevenson, J.-A., Riddle, A., Campbell, S., et al. (2003). Engineering cytochrome P450cam into an alkane hydroxylase. *Dalton Trans.* 2133–2140.

Bernhardt, R. (2006). Cytochromes P450 as versatile biocatalysts. *J. Biotechnol.* 124, 128–145.

Bihari, Z., Pettko-Szandtner, A., Csanadi, G., Balazs, M., Bartos, P., Kesseru, P., et al. (2007). Isolation and characterization of a novel *n*-alkane-degrading strain, *Acinetobacter haemolyticus* AR-46. *Z. Naturforsch. C.* 62, 285–295.

Bihari, Z., Szvetnik, A., Szabo, Z., Blastyak, A., Zombori, Z., Balazs, M., et al. (2011). Functional analysis of long-chain *n*-alkane degradation by *Dietzia* spp. *FEMS Microbiol. Lett.* 316, 100–107.

Callaghan, A. V., Gieg, L. M., Kropp, K. G., Suflita, J. M., and Young, L. Y. (2006). Comparison of mechanisms of alkane metabolism under sulfate-reducing conditions among two bacterial isolates and a bacterial consortium. *Appl. Environ. Microbiol.* 72, 4274–4282.

Callaghan, A. V., Tierney, M., Phelps, C. D., and Young, L. Y. (2009). Anaerobic biodegradation of *n*-hexadecane by a nitrate-reducing consortium. *Appl. Environ. Microbiol.* 75, 1339–1344.

Chan, S. I., Chen, K. H.-C., Yu, S. S.-F., Chen, C.-L., and Kuo, S. S.-J. (2004). Toward delineating the structure and function of the particulate methane monooxygenase from methanotrophic bacteria. *Biochemistry* 43, 4421–4430.

Cheesbrough, T. M., and Kolattukudy, P. E. (1988). Microsomal preparation from an animal tissue catalyzes release of carbon monoxide from a fatty aldehyde to generate an alkane. *J. Biol. Chem.* 263, 2738–2743.

Choi, D. W., Kunz, R. C., Boyd, E. S., Semrau, J. D., Antholine, W. E., Han, J. I., et al. (2003). The membrane-associated methane monooxygenase (pMMO) and pMMO-NADH: quinone oxidoreductase complex from *Methylococcus capsulatus* Bath. *J. Bacteriol.* 185, 5755–5764.

Coon, M. J. (2005). Omega oxygenases: nonheme-iron enzymes and P450 cytochromes. *Biochem. Biophys. Res. Commun.* 338, 378–385.

Cravo-Laureau, C., Grossi, V., Raphel, D., Matheron, R., and Hirschler-Rea, A. (2005). Anaerobic *n*-alkane metabolism by a sulfate-reducing bacterium, *Desulfatibacillum aliphaticivorans* strain CV2803T. *Appl. Environ. Microbiol.* 71, 3458–3467.

Culpepper, M. A., Cutsail, G. E. III., Hoffman, B. M., and Rosenzweig, A. C. (2012). Evidence for oxygen binding at the active site of particulate methane monooxygenase. *J. Am. Chem. Soc.* 134, 7640–7643.

Davidova, I. A., Gieg, L. M., Nanny, M., Kropp, K. G., and Suflita, J. M. (2005). Stable isotopic studies of *n*-alkane metabolism by a sulfate-reducing bacterial enrichment culture. *Appl. Environ. Microbiol.* 71, 8174–8182.

Dong, Y., Yan, J., Du, H., Chen, M., Ma, T., and Feng, L. (2012). Engineering of LadA for enhanced hexadecane oxidation using random- and site-directed mutagenesis. *Appl. Environ. Microbiol.* 94, 1019–1029.

Doughty, D. M., Sayavedra-Soto, L. A., Arp, D. J., and Bottomley, P. J. (2006). Product repression of alkane monooxygenase expression in *Pseudomonas butanovora*. *J. Bacteriol.* 188, 2586–2592.

Dubbels, B. L., Sayavedra-Soto, L. A., and Arp, D. J. (2007). Butane monooxygenase of '*Pseudomonas butanovora*': purification and biochemical characterization of a terminal-alkane hydroxylating diiron monooxygenase. *Microbiology* 153, 1808–1816.

Dubbels, B. L., Sayavedra-Soto, L. A., Bottomley, P. J., and Arp, D. J. (2009). *Thauera butanivorans* sp. nov., a C2–C9 alkane-oxidizing bacterium previously referred to as '*Pseudomonas butanovora*'. *Int. J. Syst. Evol. Microbiol.* 59, 1576–1578.

Ettwig, K. F., Butler, M. K., Le Paslier, D., Pelletier, E., Mangenot, S., Kuypers, M. M., et al. (2010). Nitrite-driven anaerobic methane oxidation by oxygenic bacteria. *Nature* 464, 543–548.

Feitkenhauer, H., Müller, R., and Märkl, H. (2003). Degradation of polycyclic aromatic hydrocarbons and long chain alkanes at 6070°C by *Thermus* and *Bacillus* spp. *Biodegradation* 14, 367–372.

Feng, L., Wang, W., Cheng, J., Ren, Y., Zhao, G., Gao, C., et al. (2007). Genome and proteome of long-chain alkane degrading *Geobacillus thermodenitrificans* NG80-2 isolated from a deep-subsurface oil reservoir. *Proc. Natl. Acad. Sci. U.S.A.* 104, 5602–5607.

Finnerty, W. (1988). "Lipids of *Acinetobacter*," in *Proceedings of the World Conference on Biotechnology for the Fats and Oil Industry*, ed. T. H. Applewhite (Urbana: Amer Oil Chemists Society), 184–188.

Forney, F. W., and Markovetz, A. J. (1970). Subterminal oxidation of aliphatic hydrocarbons. *J. Bacteriol.* 102, 281–282.

Funhoff, E. G., Bauer, U., Garcia-Rubio, I., Witholt, B., and Van Beilen, J. B. (2006). CYP153A6, a soluble P450 oxygenase catalyzing terminal-alkane hydroxylation. *J. Bacteriol.* 188, 5220–5227.

Glieder, A., Farinas, E. T., and Arnold, F. H. (2002). Laboratory evolution of a soluble, self-sufficient, highly active alkane hydroxylase. *Nat. Biotechnol.* 20, 1135–1139.

Hakemian, A. S., Kondapalli, K. C., Telser, J., Hoffman, B. M., Stemmler, T. L., and Rosenzweig, A. C. (2008). The metal centers of particulate methane monooxygenase from *Methylosinus trichosporium* OB3b. *Biochemistry* 47, 6793–6801.

Halsey, K. H., Sayavedra-Soto, L. A., Bottomley, P. J., and Arp, D. J. (2006). Site-directed amino acid substitutions in the hydroxylase alpha subunit of butane monooxygenase from *Pseudomonas butanovora*: implications for substrates knocking at the gate. *J. Bacteriol.* 188, 4962–4969.

Hamamura, N., Yeager, C. M., and Arp, D. J. (2001). Two distinct monooxygenases for alkane oxidation in *Nocardioides* sp. strain CF8. *Appl. Environ. Microbiol.* 67, 4992–4998.

Huang, J. J., and Kimura, T. (1973). Studies on adrenal steroid hydroxylases. Oxidation-reduction properties of adrenal iron-sulphur protein (adrenodoxin). *Biochemistry* 12, 406–409.

Hyman, M. R., Murton, I. B., and Arp, D. J. (1988). Interaction of ammonia monooxygenase from Nitrosomonas europaea with alkanes, alkenes, and alkynes. *Appl. Environ. Microbiol.* 54, 3187–3190.

Ji, Y., Mao, G., Wang, Y., and Bartlam, M. (2013). Crystallization and preliminary X-ray characterization of an NAD(P)-dependent butanol dehydrogenase A from *Geobacillus thermodenitrificans* NG80-2. *Acta Crystallogr. Sect. F Struct. Biol. Cryst. Commun.* F69, 184–187.

Johnson, E. L., and Hyman, M. R. (2006). Propane and *n*-butane oxidation by *Pseudomonas putida* GPo1. *Appl. Environ. Microbiol.* 72, 950–952.

Kester, A. S., and Foster, J. W. (1963). Diterminal oxidation of long-chain alkanes by bacteria. *J. Bacteriol.* 85, 859–869.

Kitmitto, A., Myronova, N., Basu, P., and Dalton, H. (2005). Characterization and structural analysis of an active particulate methane monooxygenase trimer from *Methylococcus capsulatus* (Bath). *Biochemistry* 44, 10954–10965.

Kniemeyer, O., Musat, F., Sievert, S. M., Knittel, K., Wilkes, H., Blumenberg, M., et al. (2007). Anaerobic oxidation of short-chain hydrocarbons by marine sulphate-reducing bacteria. *Nature* 449, 898–901.

Kok, M., Oldenhuis, R., Van Der Linden, M. P. G., Raatjes, P., Kingma, J., Van Lelyveld, P. H., et al. (1989). The *Pseudomonas oleovorans* alkane hydroxylase gene. Sequence and expression. *J. Biol. Chem.* 264, 5435–5441.

Kotani, T., Yamamoto, T., Yurimoto, H., Sakai, Y., and Kato, N. (2003). Propane monooxygenase and NAD^+-dependent secondary alcohol dehydrogenase in propane metabolism by *Gordonia* sp. strain TY-5. *J. Bacteriol.* 185, 7120–7128.

Kotani, T., Yurimoto, H., Kato, N., and Sakai, Y. (2007). Novel acetone metabolism in a propane-utilizing bacterium, *Gordonia* sp. strain TY-5. *J. Bacteriol.* 189, 886–893.

Kropp, K. G., Davidova, I. A., and Suflita, J. M. (2000). Anaerobic oxidation of *n*-dodecane by an addition reaction in a sulfate-reducing bacterial enrichment culture. *Appl. Environ. Microbiol.* 66, 5393–5398.

Lentz, O., Urlacher, V., and Schmid, R. D. (2004). Substrate specificity of native and mutated cytochrome P450 (CYP102A3) from *Bacillus subtilis*. *J. Biotechnol.* 108, 41–49.

Li, L., Liu, X., Yang, W., Xu, F., Wang, W., Feng, L., et al. (2008). Crystal structure of long-chain alkane monooxygenase (LadA) in complex with coenzyme FMN: unveiling the long-chain alkane hydroxylase. *J. Mol. Biol.* 376, 453–465.

Lieberman, R. L., and Rosenzweig, A. C. (2004). Biological methane oxidation: regulation, biochemistry, and active site structure of particulate methane monooxygenase. *Crit. Rev. Biochem. Mol. Biol.* 39, 147–164.

Lieberman, R. L., and Rosenzweig, A. C. (2005). Crystal structure of a membrane-bound metalloenzyme that catalyses the biological oxidation of methane. *Nature* 434, 177–182.

Liu, C., Wang, W., Wu, Y., Zhou, Z., Lai, Q., and Shao, Z. (2011). Multiple alkane hydroxylase systems in a marine alkane degrader, *Alcanivorax dieselolei* B-5. *Environ. Microbiol.* 13, 1168–1178.

Lode, E. T., and Coon, M. J. (1971). Enzymatic ω-Oxidation V. Forms of *Pseudomonas Oleovorans* rubredoxin containing one or two iron atoms: structure and function in ω-hydroxylation. *J. Biol. Chem.* 246, 791–802.

Maeng, J. H., Sakai, Y., Tani, Y., and Kato, N. (1996). Isolation and characterization of a novel oxygenase that catalyzes the first step of *n*-alkane oxidation in *Acinetobacter* sp. strain M-1. *J. Bacteriol.* 178, 3695–3700.

Maier, T., Forster, H. H., Asperger, O., and Hahn, U. (2001). Molecular characterization of the 56-kDa CYP153 from *Acinetobacter* sp. EB104. *Biochem. Biophys. Res. Commun.* 286, 652–658.

Mayr, S., Latkoczy, C., KrüGer, M., GüNther, D., Shima, S., Thauer, R. K., et al. (2008). Structure of an F430 variant from archaea associated with anaerobic oxidation of methane. *J. Am. Chem. Soc.* 130, 10758–10767.

McDonald, I. R., Miguez, C. B., Rogge, G., Bourque, D., Wendlandt, K. D., Groleau, D., et al. (2006). Diversity of soluble methane monooxygenase-containing methanotrophs isolated from polluted environments. *FEMS Microbiol. Lett.* 255, 225–232.

McKenna, E. J., and Coon, M. J. (1970). Enzymatic ω-oxidation IV. Purification and properties of the ω-hydroxylase of *Pseudomonas Oleovorans*. *J. Biol. Chem.* 245, 3882–3889.

Merkx, M., Kopp, D. A., Sazinsky, M. H., Blazyk, J. L., Müller, J., and Lippard, S. J. (2001). Dioxygen activation and methane hydroxylation by soluble methane monooxygenase a tale of two irons and three proteins. *Angew. Chem. Int. Ed. Engl.* 40, 2782–2807.

Moonen, M. J. H., Fraaije, M. W., Rietjens, I. M. C. M., Laane, C., and Van Berkel, W. J. H. (2002). Flavoenzyme-catalyzed oxygenations and oxidations of phenolic compounds. *Adv. Synth. Catal.* 344, 1023–1035.

Murrell, J. C., Mcdonald, I. R., and Gilbert, B. (2000). Regulation of expression of methane monooxygenases by copper ions. *Trends Microbiol.* 8, 221–225.

Myronova, N., Kitmitto, A., Collins, R. F., Miyaji, A., and Dalton, H. (2006). Three-dimensional structure determination of a protein super-complex that oxidizes methane to formaldehyde in *Methylococcus capsulatus* (Bath). *Biochemistry* 45, 11905–11914.

Narhi, L. O., and Fulco, A. J. (1986). Characterization of a catalytically self-sufficient 119,000-Dalton cytochrome P-450 monooxygenase induced by barbiturates in *Bacillus megaterium*. *J. Biol. Chem.* 261, 7160–7169.

Nie, Y., Liang, J., Fang, H., Tang, Y. Q., and Wu, X. L. (2011). Two novel alkane hydroxylase-rubredoxin fusion genes isolated from a *Dietzia* bacterium and the functions of fused rubredoxin domains in long-chain *n*-alkane degradation. *Appl. Environ. Microbiol.* 77, 7279–7288.

Parekh, V. R., Traxler, R. W., and Sobek, J. M. (1977). *n*-Alkane oxidation enzymes of a pseudomonad. *Appl. Environ. Microbiol.* 33, 881–884.

Poulos, T. L., Finzel, B. C., and Howard, A. J. (1987). High-resolution crystal structure of cytochrome P450cam. *J. Mol. Biol.* 195, 687–700.

Prior, S. D., and Dalton, H. (1985). The effect of copper ions on membrane content and methane monooxygenase activity in methanol-grown cells of *Methylococcus capsulatus* (Bath). *J. Gen. Microbiol.* 131, 155–163.

Rabus, R., Wilkes, H., Behrends, A., Armstroff, A., Fischer, T., Pierik, A. J., et al. (2001). Anaerobic initial reaction of *n*-alkanes in a denitrifying bacterium: evidence for (1-methylpentyl)succinate as initial product and for involvement of an organic radical in *n*-hexane metabolism. *J. Bacteriol.* 183, 1707–1715.

Ravichandran, K. G., Boddupalli, S. S., Hasermann, C. A., Peterson, J. A., and Deisenhofer, J. (1993). Crystal structure of hemoprotein domain of P450BM-3, a prototype for microsomal P450′s. *Science* 261, 731–736.

Rosenzweig, A. C., Frederick, C. A., Lippard, S. J., and Nordlund, P. (1993). Crystal structure of a bacterial nonhaem iron hydroxylase that catalyses the biological oxidation of methane. *Nature* 366, 537–543.

Rosenzweig, A. C., and Lippard, S. J. (1994). Determining the structure of a hydroxylase enzyme that catalyzes the conversion of methane to methanol in methanotrophic bacteria. *Acc. Chem. Res.* 27, 229–236.

Sayavedra-Soto, L. A., Hamamura, N., Liu, C.-W., Kimbrel, J. A., Chang, J. H., and Arp, D. J. (2011). The membrane-associated monooxygenase in the butane-oxidizing Gram-positive bacterium *Nocardioides* sp. strain CF8 is a novel member of the AMO/PMO family. *Environ. Microbiol. Rep.* 3, 390–396.

Scheller, S., Goenrich, M., Boecher, R., Thauer, R. K., and Jaun, B. (2010). The key nickel enzyme of methanogenesis catalyses the anaerobic oxidation of methane. *Nature* 465, 606–608.

Scheps, D., Malca, S. H., Hoffmann, H., Nestl, B. M., and Hauer, B. (2011). Regioselective omega-hydroxylation of medium-chain *n*-alkanes and primary alcohols by CYP153 enzymes from *Mycobacterium marinum* and *Polaromonas* sp. strain JS666. *Org. Biomol. Chem.* 9, 6727–6733.

Shanklin, J., and Whittle, E. (2003). Evidence linking the *Pseudomonas oleovorans* alkane ω-hydroxylase, an integral membrane diiron enzyme, and the fatty acid desaturase family. *FEBS Lett.* 545, 188–192.

Smith, S. M., Rawat, S., Telser, J., Hoffman, B. M., Stemmler, T. L., and Rosenzweig, A. C. (2011). Crystal structure and characterization of particulate methane monooxygenase from *Methylocystis* species

strain M. *Biochemistry* 50, 10231–10240.

Smits, T. H. M., Balada, S. B., Witholt, B., and Van Beilen, J. B. (2002). Functional analysis of alkane hydroxylases from Gram-negative and Gram-positive bacteria. *J. Bacteriol.* 184, 1733–1742.

So, C. M., Phelps, C. D., and Young, L. Y. (2003). Anaerobic transformation of alkanes to fatty acids by a sulfate-reducing bacterium, strain Hxd3. *Appl. Environ. Microbiol.* 69, 3892–3900.

So, C. M., and Young, L. Y. (1999). Initial reactions in anaerobic alkane degradation by a sulfate reducer, strain AK-01. *Appl. Environ. Microbiol.* 65, 5532–5540.

Stanley, S. H., Prior, S. D., Leak, D. J., and Dalton, H. (1983). Copper stress underlies the fundamental change in intracellular location of methane monooxygenase in methane-oxidizing organisms: studies in batch and continuous cultures. *Biotechnol. Lett* 5, 487–492.

Throne-Holst, M., Wentzel, A., Ellingsen, T. E., Kotlar, H. K., and Zotchev, S. B. (2007). Identification of novel genes involved in long-chain *n*-alkane degradation by *Acinetobacter* sp. strain DSM 17874. *Appl. Microbiol. Biotechnol.* 73, 3327–3332.

Trudgill, P. W., Dubus, R., and Gunsalus, I. C. (1966). Mixed Function Oxidation. V. Flavin interaction with a reduced diphosphopyridine nucleotide dehydrogenase, one of the enzymes participating in camphor lactonization. *J. Biol. Chem.* 241, 1194–1205.

van Beilen, J. B., and Funhoff, E. G. (2005). Expanding the alkane oxygenase toolbox: new enzymes and applications. *Curr. Opin. Biotechnol.* 16, 308–314.

van Beilen, J. B., and Funhoff, E. G. (2007). Alkane hydroxylases involved in microbial alkane degradation. *Appl. Microbiol. Biotechnol.* 74, 13–21.

van Beilen, J. B., Li, Z., Duetz, W. A., Smits, T. H. M., and Witholt, B. (2003). Diversity of alkane hydroxylase systems in the environment. *Oil Gas Sci. Technol.* 58, 427–440.

van Beilen, J. B., Penninga, D., and Witholt, B. (1992). Topology of the membrane-bound alkane hydroxylase of *Pseudomonas oleovorans*. *J. Biol. Chem.* 267, 9194–9201.

van Beilen, J. B., Smits, T. H., Roos, F. F., Brunner, T., Balada, S. B., Rothlisberger, M., et al. (2005). Identification of an amino acid position that determines the substrate range of integral membrane alkane hydroxylases. *J. Bacteriol.* 187, 85–91.

van Beilen, J. B., Wubbolts, M. G., and Witholt, B. (1994). Genetics of alkane oxidation by *Pseudomonas oleovorans*. *Biodegradation* 5, 161–174.

Wang, W., and Shao, Z. (2012). Diversity of flavin-binding monooxygenase genes (almA) in marine bacteria capable of degradation long-chain alkanes. *FEMS Microbiol. Ecol.* 80, 523–533.

Watkinson, R. J., and Morgan, P. (1990). Physiology of aliphatic hydrocarbon-degrading microorganisms. *Biodegradation* 1, 79–92.

Whitehouse, C. J. C., Yang, W., Yorke, J. A., Rowlatt, B. C., Strong, A. J. F., Blanford, C. F., et al. (2010). Structural basis for the properties of two single-site proline mutants of CYP102A1 (P450BM3). *Chembiochem* 11, 2549–2556.

Zhang, J., Zheng, H., Groce, S. L., and Lipscomb, J. D. (2006). Basis for specificity in methane monooxygenase and related non-heme iron-containing biological oxidation catalysts. *J. Mol. Catal. A Chem.* 251, 54–65.

Zhou, R., Huang, C., Zhang, A., Bell, S. G., Zhou, W., and Wong, L. L. (2011). Crystallization and preliminary X-ray analysis of CYP153C1 from *Novosphingobium aromaticivorans* DSM12444. *Acta Crystallogr. Sect. F Struct. Biol. Cryst. Commun.* 67, 964–967.

Conflict of Interest Statement: The authors declare that the research was conducted in the absence of any commercial or financial relationships that could be construed as a potential conflict of interest.

Received: 06 December 2012; accepted: 28 February 2013; published online: 21 March 2013.

Citation: Ji Y, Mao G, Wang Y and Bartlam M (2013) Structural insights into diversity and n-alkane biodegradation mechanisms of alkane hydroxylases. Front. Microbiol. ***4****:58. doi: 10.3389/fmicb.2013.00058*

This article was submitted to Frontiers in Microbiological Chemistry, a specialty of Frontiers in Microbiology.

frontiers in
MICROBIOLOGY

ORIGINAL RESEARCH ARTICLE
published: 03 April 2013
doi: 10.3389/fmicb.2013.00040

Global molecular analyses of methane metabolism in methanotrophic alphaproteobacterium, *Methylosinus trichosporium* OB3b. Part I: transcriptomic study

Janet B. Matsen[1], Song Yang[1], Lisa Y. Stein[2], David Beck[1,3] and Marina G. Kalyuzhnaya[4]*

[1] *Department of Chemical Engineering, University of Washington, Seattle, WA, USA*
[2] *Department of Biological Sciences, University of Alberta, Edmonton, AB, Canada*
[3] *eScience Institute, University of Washington, Seattle, WA, USA*
[4] *Department of Microbiology, University of Washington, Seattle, WA, USA*

Edited by:
Amy V. Callaghan, University of Oklahoma, USA

Reviewed by:
Svetlana N. Dedysh, Russian Academy of Sciences, Russia
Jeremy Semrau, The University of Michigan, USA

***Correspondence:**
Marina G. Kalyuzhnaya, Department of Microbiology, University of Washington, Benjamin Hall IRB RM 455, 616 NE Northlake Place, Seattle, WA 98105, USA.
e-mail: mkalyuzh@uw.edu

Methane utilizing bacteria (methanotrophs) are important in both environmental and biotechnological applications, due to their ability to convert methane to multicarbon compounds. However, systems-level studies of methane metabolism have not been carried out in methanotrophs. In this work we have integrated genomic and transcriptomic information to provide an overview of central metabolic pathways for methane utilization in *Methylosinus trichosporium* OB3b, a model alphaproteobacterial methanotroph. Particulate methane monooxygenase, PQQ-dependent methanol dehydrogenase, the H_4MPT-pathway, and NAD-dependent formate dehydrogenase are involved in methane oxidation to CO_2. All genes essential for operation of the serine cycle, the ethylmalonyl-CoA (EMC) pathway, and the citric acid (TCA) cycle were expressed. PEP-pyruvate-oxaloacetate interconversions may have a function in regulation and balancing carbon between the serine cycle and the EMC pathway. A set of transaminases may contribute to carbon partitioning between the pathways. Metabolic pathways for acquisition and/or assimilation of nitrogen and iron are discussed.

Keywords: methanotrophic proteobacteria, serine cycle, ethylmalonyl-CoA pathway in methanotrophs, TCA, gene expression

INTRODUCTION

Aerobic methanotrophic bacteria (methanotrophs) are a highly specialized group of microbes utilizing methane as a sole source of carbon and energy (Hanson and Hanson, 1996; Murrell and Jetten, 2009). As the recognition of methane's impact on global climate change increases, a multitude of research activities have been directed toward understanding the natural mechanisms for reducing methane emissions, including consumption by methanotrophs. The number of described microbial species capable of methane oxidation has recently expanded dramatically. A number of novel methanotrophic phyla have been isolated and described in the past few years, including new members of the Alpha- and Gammaproteobacteria, and Verrucomicrobia (Trotsenko and Murrell, 2008; Chistoserdova et al., 2009; Murrell and Jetten, 2009). Several genomes of methanotrophic bacteria have been sequenced opening new dimensions in characterization of methane metabolism (Ward et al., 2004; Dunfield et al., 2007; Hou et al., 2008; Chen et al., 2010; Stein et al., 2010, 2011; Dam et al., 2012b). Initial genome-based reconstructions of methane metabolism in methanotrophic proteobacteria and Verrucomicrobia have been performed (Ward et al., 2004; Kelly et al., 2005; Hou et al., 2008; Khadem et al., 2011).

Methylosinus trichosporium OB3b, an obligate alphaproteobacterial methanotroph, has served as a model system for years (first described in Whittenbury et al., 1970). Research on both fundamental and biotechnological aspects of methanotrophy in *M. trichosporium* OB3b has been carried out with applications involving cometabolism of contaminants (Oldenhuis et al., 1991; EPA, 1993; Fitch et al., 1996), epoxidation of propene (Hou et al., 1979), and synthesis of polyhydroxybutyrate (PHB) (Williams, 1988; Doronina et al., 2008). *M. trichosporium* OB3b possesses two systems for methane oxidation, a particulate methane monooxygenase (pMMO), expressed under high biomass/copper ratios, and a soluble methane monooxygenase (sMMO) which is expressed at low copper conditions (Hakemian and Rosenzweig, 2007; Semrau et al., 2010). It has been shown that the strain is capable of fixing nitrogen (Oakley and Murrell, 1988; Auman et al., 2001). Although significant progress has been made in the understanding of primary methane and methanol oxidation pathways in this model bacterium, little work has been carried out on carbon assimilation by *M. trichosporium* OB3b. The reconstruction of the core metabolic pathways for alphaproteobacterial methanotrophs has been primarily based on a restricted set of enzymatic studies and extrapolations relying on similarity to non-methane utilizing methylotrophs (Lawrence and Quayle, 1970; Strom et al., 1974). A draft genome of *M. trichosporium* OB3b has recently been generated (Stein et al., 2010). This genetic blueprint provides an essential background for revisiting the established model of methanotrophy in Alphaproteobacteria using modern system-level approaches. For this research, we

integrated heterogeneous multi-scale genomic, transcriptomic, and metabolomic data to redefine the metabolic framework of C_1-utilization in *M. trichosporium* OB3b grown in batch culture under copper, oxygen, and iron sufficiency on methane and nitrate as the sources of carbon and nitrogen, respectively. In this part of our work we present transcriptomic-based analysis of the methanotrophic metabolic network. Metabolomic and ^{13}C-labeling studies are presented in a follow-up paper (Yang et al., 2013).

RESULTS AND DISCUSSION

GENE EXPRESSION STUDIES

Gene expression studies were carried out with *M. trichosporium* OB3b cultures grown on methane at N (10 mM), Cu (9 μM), and Fe (9 μM) sufficiency conditions. The maximum specific growth rate of *M. trichosporium* OB3b in shake flasks during the exponential growth phase was $\mu = 0.038 \pm 0.004\,h^{-1}$. The methane consumption rate during the period of maximum growth rate was 8.95 mmol of $CH_4 h^{-1}$ L culture^{-1} ($OD_{600} = 1$).

All experiments were performed with at least two biological replicates. RNA samples were prepared as described in the Section "Materials and Methods." Illumina sequencing for two biological replicates (BR1 and BR2) returned 28 and 29 million 36-bp reads. The Burrows–Wheeler Aligner (BWA, Li and Durbin, 2009) aligned 98% of the reads to the *M. trichosporium* OB3b genome annotated by MaGE[1] using the default parameters for small genomes. Reads per kilobase of coding sequence per million (reads) mapped (RPKM) (Mortazavi et al., 2008) was calculated to compare gene expression within and across replicates, and no further normalization (other than RPKM) was applied. The samples were in good agreement with each other, with per gene coding sequence RPKM correlations of 0.959 and 0.989 for the Pearson and Spearman correlations, respectively. In total, 4,762 of 4,812 ORFs (CDS, tRNA, and rRNA predicted from the draft genome) were detected. Based on relative expression, genes (omitting rRNAs) could be grouped into six major expression categories (**Table 1**): *very high* (RPKM ≥ 15,000), *high* (RPKM ≥ 1,500), *moderate* (1,500 > RPKM ≥ 500), *modest* (500 > RPKM ≥ 250), *low* (250 > RPKM ≥ 150) *very low* (150 > RPKM ≥ 15), and *not expressed* (RPKM < 15). The majority of genes fell into *low/very low expression* categories (74%). About 14% of genes displayed *moderate/modest* expression and only a small fraction of the genome showed very *high/high expression* (2.7%).

In order to determine whether the draft genome of the strain is missing some functional genes, we performed *de novo* assembly of the transcriptome. Using this approach, a total of 173 genes that are not present in the genome sequence, but have homologs in the non-redundant database were detected. Among those are key subunits of succinate dehydrogenase (*sdhABCD*), 2-oxoglutarate dehydrogenase (E2), and nitric oxide reductase (*norB*) (Table S1 in Supplementary Material). The *de novo* transcriptome assembly provides additional information for highly expressed genes and it was used for verification of some metabolic functions that were predicted by enzymatic studies but were not detected in the draft genome assembly (see below).

[1]https://www.genoscope.cns.fr/agc/microscope/mage

Table 1 | Classification of gene expression level based on replicate averaged RPKMs.

Description of expression level	RPKM range	% of ORFs	Number of ORFs
Very high	>15,000	0.23	11
High	1,500–15,000	2.49	120
Moderate	500–1,500	5.30	255
Modest	250–500	8.61	414
Low	50–250	40.41	1,944
Very low	15–50	23.70	1,140
Not expressed	<15	19.27	927

In addition, the reads obtained from RNA-seq were aligned to the reference genome in order to identify transcription boundaries and transcription start sites for the most highly expressed genes, including the *pmoCAB* operons, *mxaFJGI* operon, *fae1*, *pqqA*, and key genes of the serine cycle (Table S2 in Supplementary Material, see description below). Gene expression data were used to reconstruct central metabolic pathways in *M. trichosporium* OB3b (**Table 2**; **Figure 1**; Table S2 in Supplementary Material). Core functions are described below.

C_1-OXIDATION: METHANE-TO-METHANOL

It has been previously demonstrated that *M. trichosporium* OB3b possesses two types of methane oxidation enzymes: pMMO and sMMO. The expression of the enzymes is determined by copper availability; sMMO is dominant in copper-limited environments while pMMO dominates under copper sufficiency (Hakemian and Rosenzweig, 2007; Semrau et al., 2010). Structures of both enzymes are available (Elango et al., 1997; Hakemian et al., 2008). In this study, *M. trichosporium* OB3b was grown at a copper concentration that has been shown to be sufficient to suppress the expression of sMMO (Park et al., 1991; Phelps et al., 1992; Nielsen et al., 1997; Lloyd et al., 1999; Murrell et al., 2000). Indeed, virtually no expression of the sMMO gene cluster (*mmoXYBZC*) was observed. In contrast, the *pmoCAB* genes were the most highly expressed in the transcriptome, representing about 14% of all reads mapped to the coding regions (**Table 2**). It has previously been shown that PMMO in *M. trichosporium* OB3b is encoded by two copies of the *pmoCAB* operon that appear to be identical (Gilbert et al., 2000). The current genome assembly failed to resolve these closely related duplicated regions. The *pmoCAB* genes were found within one relatively short contig, which includes 320 bp upstream from *pmoC*, and about 66 bp downstream from *pmoB*. It is possible that in the genome assembly, the *pmo* contig represents only those parts of the duplicated regions that are highly similar. Thus, it was not possible to determine relative expression of the two operons with the transcriptomic data.

Previous attempts to identify transcriptional starts of the *pmoCAB* operons in *M. trichosporium* OB3b using a conventional primer extension approach were not successful (Gilbert et al., 2000). The RNA-seq data were used for identification of transcriptional starts for the *pmoCAB* operons. Because the published METTOv1 genome did not contain a complete *pmoCAB* cluster, a separate alignment run was performed using a previously

Table 2 | Gene expression profile in methane-grown cells of *M. trichosporium* OB3b.

Gene ID	Predicted function	Gene	Replicate 1	Replicate 2
METHANE AND METHANOL OXIDATION				
METTOv1_1270003	Particulate methane monooxygenase subunit C	*pmoC*	123026	127241
METTOv1_1270002	Particulate methane monooxygenase subunit A	*pmoA*	37102	31813
METTOv1_1270001	Particulate methane monooxygenase subunit B	*pmoB*	27371	22917
METTOv1_310040	Particulate methane monooxygenase subunit C2	*pmoC2*	532	492
METTOv1_50081	Soluble methane monooxygenase alpha subunit	*mmoX*	9	8
METTOv1_50082	Soluble methane monooxygenase beta subunit	*mmoY*	13	9
METTOv1_50084	Soluble methane monooxygenase gamma subunit	*mmoZ*	20	19
METTOv1_240014	PQQ-dependent methanol dehydrogenase	*mxaF*	15313	13760
METTOv1_240011	PQQ-dependent methanol dehydrogenase	*mxaI*	24552	28474
METTOv1_240012	Cytochrome *c* class I	*mxaG*	5712	6117
METTOv1_240013	Extracellular solute-binding protein family 3	*mxaJ*	1942	1838
METTOv1_240001	Putative methanol utilization control sensor protein	*mxaY*	36	41
METTOv1_240002	Putative two-component response regulator	*mxaB*	303	317
METTOv1_240003	MxaH protein, involved in methanol oxidation	*mxaH*	399	391
METTOv1_240004	MxaD protein, involved in methanol oxidation	*mxaD*	1137	1077
METTOv1_240005	von Willebrand factor type A, involved in methanol oxidation	*mxaL*	191	201
METTOv1_240006	Protein of unknown function, involved in methanol oxidation	*mxaK*	124	132
METTOv1_240007	von Willebrand factor type A, involved in methanol oxidation	*mxaC*	144	141
METTOv1_240008	MxaA protein, involved in methanol oxidation	*mxaA*	137	127
METTOv1_240009	MxaS protein, involved in methanol oxidation	*mxaS*	202	167
METTOv1_240010	ATPase, involved in methanol oxidation	*mxaR*	563	538
METTOv1_110056	Coenzyme PQQ biosynthesis protein A	*pqqA*	11857	13927
METTOv1_160001	Coenzyme PQQ biosynthesis protein E	*pqqE*	166	161
METTOv1_160002	Coenzyme PQQ biosynthesis protein PqqC/D	*pqqC/D*	372	344
METTOv1_160003	Coenzyme PQQ biosynthesis protein B	*pqqB*	306	313
METTOv1_20046	Coenzyme PQQ biosynthesis protein F	*pqqF*	183	185
METTOv1_20047	Coenzyme PQQ biosynthesis protein G	*pqqG*	157	142
METTOv1_610028	Aldehyde dehydrogenase	*aldh*	37	37
METTOv1_290006	Aldehyde oxidase	*aor*	45	38
METTOv1_100046	Aldehyde dehydrogenase	*aldh-F7*	7	9
FORMALDEHYDE OXIDATION				
METTOv1_40010	Methenyltetrahydromethanopterin cyclohydrolase	*mch*	393	312
METTOv1_40011	Tetrahydromethanopterin-linked C1 transfer pathway protein. Orf5	*orf5*	128	111
METTOv1_40012	Tetrahydromethanopterin-linked C1 transfer pathway protein, Orf7	*orf7*	73	72
METTOv1_40013	Formaldehyde activating enzyme	*fae1*	24353	24787
METTOv1_40014	Formaldehyde activating enzyme	*fae1-2*	4024	3676
METTOv1_840013	Formaldehyde activating enzyme homolog	*fae2*	535	581
METTOv1_40015	Tetrahydromethanopterin-linked C1 transfer pathway protein	*orf17*	38	45
METTOv1_110058	Tetrahydromethanopterin formyltransferase, subunit C	*fhcC*	535	453
METTOv1_110059	Tetrahydromethanopterin formyltransferase, subunit D	*fhcD*	496	470
METTOv1_110060	Tetrahydromethanopterin formyltransferase, subunit A	*fhcA*	591	546
METTOv1_110061	Tetrahydromethanopterin formyltransferase, subunit B	*fhcB*	620	570
METTOv1_560001	Tetrahydromethanopterin -linked C1 transfer pathway protein	*orf9*	172	167
METTOv1_560002	Methylenetetrahydrofolate dehydrogenase (NAD)	*mtdB*	688	607
METTOv1_440045	Ribofuranosylaminobenzene 5′-phosphate synthase	*mptG*	94	80
FORMATE OXIDATION				
METTOv1_630016	Transcriptional regulator, LysR family	*fdsR*	52	39
METTOv1_630017	NAD-linked formate dehydrogenase, subunit G	*fdsG*	672	608
METTOv1_630018	NAD-linked formate dehydrogenase, subunit B	*fdsB*	585	531
METTOv1_630019	NAD-linked formate dehydrogenase, subunit A	*fdsA*	593	554
METTOv1_370001	Formate dehydrogenase family accessory protein	*fdsC*	210	199

(Continued)

Table 2 | Continued

Gene ID	Predicted function	Gene	Replicate 1	Replicate 2
METTOv1_370002	NAD-linked formate dehydrogenase, subunit D	*fdsD*	368	312
METTOv1_220028	NAD-linked formate dehydrogenase, subunit A	*fdhA2*	9	7
C1-ASSIMILATION:SERINE CYCLE				
METTOv1_130002	Phosphoenolpyruvate carboxylase	*ppc2*	104	89
METTOv1_400011	Glycerate kinase	*gckA*	229	211
METTOv1_400012	Conserved protein of unknown function	*orf1*	626	708
METTOv1_400013	Malyl-CoA lyase/beta-methylmalyl-CoA lyase	*mclA*	1713	1615
METTOv1_400014	Phosphoenolpyruvate carboxylase	*ppc1*	141	139
METTOv1_400015	Malate thiokinase, small subunit	*mtkB*	516	485
METTOv1_400016	Malate thiokinase, large subunit	*mtkA*	534	455
METTOv1_400017	Methenyltetrahydrofolate cyclohydrolase	*fch*	355	281
METTOv1_400018	NADP-dependent methylenetetrahydrofolate dehydrogenase	*mtdA*	281	243
METTOv1_400019	2-Hydroxyacid dehydrogenase NAD-binding	*hprA*	375	348
METTOv1_400020	Serine-glyoxylate transaminase	*sga*	1840	1969
METTOv1_400021	Formate-tetrahydrofolate ligase	*ftfL*	448	412
METTOv1_670019	Serine hydroxymethyltransferase	*glyA*	1342	1197
METTOv1_20135	Enolase	*eno*	432	408
C1-ASSIMILATION:EMP PATHWAY AND PHB CYCLE				
METTOv1_100079	Acetyl-CoA acetyltransferase	*phaA*	597	561
METTOv1_100080	Acetoacetyl-CoA reductase	*phaB*	1160	1060
METTOv1_50006	Crotonase	*croR*	235	275
METTOv1_110068	Crotonyl-CoA reductase	*ccr*	577	523
METTOv1_60013	Ethylmalonyl-CoA mutase	*ecm*	187	162
METTOv1_510010	Methylsuccinyl-CoA dehydrogenase	*ibd*	309	295
METTOv1_110043	Mesaconyl-CoA hydratase	*meaC*	341	317
METTOv1_30129	Methylmalonyl-CoA epimerase	*epm*	428	394
METTOv1_220010	Malyl-CoA lyase/beta-Methylmalyl-CoA lyase	*mclA2*	137	135
METTOv1_200020	Acetyl/propionyl-CoA carboxylase	*ppcA*	353	310
METTOv1_220035	Propionyl-CoA carboxylase	*ppcB*	472	455
METTOv1_50067	Methylmalonyl-CoA mutase, large subunit	*mcmA*	201	188
METTOv1_10062	Methylmalonyl-CoA mutase small subunit B	*mcmB*	144	144
METTOv1_270063	3-Hydroxybutyrate dehydrogenase	*bdhA*	235	232
METTOv1_130047	Poly-beta-hydroxybutyrate polymerase	*phaC*	30	30
METTOv1_200042	Acetoacetate decarboxylase	*aad*	123	114
METTOv1_200022	Acetoacetyl-coenzyme A synthetase	*aas*	116	114
METTOv1_630008	Polyhydroxyalkanoate depolymerase	*phaZ*	237	263
C1-ASSIMILATION:TCA CYCLE				
METTOv1_360040	Malate dehydrogenase	*mdh*	539	473
METTOv1_360041	Succinyl-CoA synthetase, beta subunit	*sucC*	660	631
METTOv1_510003	Succinyl-CoA synthetase, alpha subunit	*sucD*	1198	1135
METTOv1_510002	2-Oxoglutarate dehydrogenase E1	*sucA*	236	237
METTOv1_370050	2-Oxoglutarate dehydrogenase E2	*sucB*	191	181
METTOv1_80046	Succinate:ubiquinone oxidoreductase	*sdhB*	327	348
METTOv1_80046	Succinate:ubiquinone oxidoreductase	*sdhA*	311	299
METTOv1_80051	Succinate:ubiquinone oxidoreductase, cytochrome b556 subunit	*sdhC*	318	329
METTOv1_40061	Fumarate hydratase	*fum*	196	185
METTOv1_1080004	2-Oxoacid ferredoxin oxidoreductase	*ofr*	79	77
INTERMEDIARY METABOLISM AND ANAPLEROTIC CO_2-FIXATION				
METTOv1_70038	Phosphoenolpyruvate synthase	*pps*	28	26
METTOv1_120036	Pyruvate carboxylase	*pcx*	145	140
METTOv1_830002	Acetyl-coenzyme A carboxylase subunit beta	*accD*	246	228
METTOv1_380021	Acetyl-CoA carboxylase subunit alpha	*accA*	211	204

(Continued)

Table 2 | Continued

Gene ID	Predicted function	Gene	Replicate 1	Replicate 2
METTOv1_130018	Acetyl-CoA carboxylase, biotin carboxyl carrier protein	*accB*	307	276
METTOv1_150014	Pyruvate kinase	*pyk1*	245	224
METTOv1_340039	Pyruvate dehydrogenase (acetyl-transferring) E1	*pdhA*	181	175
METTOv1_340041	Pyruvate dehydrogenase subunit beta	*pdhB*	160	158
METTOv1_340042	Pyruvate dehydrogenase	*pdhC*	101	106
METTOv1_350050	Pyruvate phosphate dikinase	*pdk*	50	52
METTOv1_80025	Malic enzyme	*mae*	107	106
METTOv1_680013	Phosphoglycerate mutase	*gpmA*	136	135
METTOv1_100061	Phosphoglycerate mutase (modular protein)	*pgm*	101	99
METTOv1_10180	Phosphoglycerate mutase (modular protein)	*pgm*	72	65
METTOv1_280049	Phosphoglycerate kinase	*pgk*	199	208
METTOv1_280047	Glyceraldehyde-3-phosphate dehydrogenase	*gpd*	391	407
METTOv1_620016	Ribokinase	*rik*	140	144
METTOv1_620017	Phosphoribulokinase	*prk*	173	164
METTOv1_620018	Transketolase	*tkl*	147	123
METTOv1_620019	Fructose-bisphosphate aldolase, class II	*fba*	427	461
METTOv1_220030	6-Phosphofructokinase	*pfk*	243	239
METTOv1_200031	Fructose 1,6-bisphosphatase II	*glp*	68	56
METTOv1_550029	Glucose-6-phosphate isomerase	*pgi*	88	84
METTOv1_620022	Ribulose-phosphate 3-epimerase	*rpe*	51	53
NITROGEN, Cu, Fe METABOLISM				
METTOv1_310019	Nitrate transporter component	*nrtA*	151	154
METTOv1_310020	Nitrite reductase (NAD(P)H), large subunit	*nasB*	1762	1562
METTOv1_310021	Nitrite reductase (NAD(P)H), small subunit	*nasD*	726	610
METTOv1_310022	Nitrate reductase, large subunit	*nasA*	646	597
METTOv1_130049	Ammonium transporter	*amtB*	2029	1766
METTOv1_300058	Glutamate synthase large subunit (NADPH/GOGAT)	*gltB*	199	183
METTOv1_300033	Glutamate synthase small subunit (NADPH/GOGAT)	*gltD*	431	401
METTOv1_190023	Glutamate dehydrogenase	*gdh*	2	2
METTOv1_200046	Glutamate-ammonia ligase	*glnS*	1413	1375
METTOv1_200047	Nitrogen regulatory protein P-II	*glnK*	2400	2277
METTOv1_200048	Glutamine synthetase, type I	*glnA*	2452	2321
METTOv1_280018	Alanine dehydrogenase	*aldA*	29	36
METTOv1_80043	Phosphoserine aminotransferase	*serC*	415	364
METTOv1_560023	Cytochrome *c′*-alpha	*cycA*	336	370
METTOv1_230076	Putative oxygenase		6	8
METTOv1_230077	Hydroxylamine reductase	*hcp*	21	16
METTOv1_230078	Putative transcriptional regulator	*nsrR*	38	35
METTOv1_730005	Putative FecR iron sensor protein	*fecR*	48	58
METTOv1_730006	Putative TonB-dependent receptor protein	*tonB*	382	383
METTOv1_CDS4222756D	Methanobactin precursor	*Mb*	1439	2177
METTOv1_730007	Putative lyase		306	384
METTOv1_730008	Conserved protein of unknown function	*hp*	170	175
METTOv1_730009	Conserved protein of unknown function	*hp*	116	143
METTOv1_660011	l-Ornithine 5-monooxygenase	*pvdA1*	1410	1450
METTOv1_760004	Putative hydroxy-l-ornithine formylase	*pvdF*	2255	2676
METTOv1_760006	l-Ornithine 5-monooxygenase	*pvdA2*	979	1116
METTOv1_760007	Diaminobutyrate-2-oxoglutarate aminotransferase	*pvdH*	720	770
METTOv1_760008	Sigma-24 (FecI-like)	*pvdS*	1260	1522
METTOv1_760009	Putative pyoverdine ABC export system, permease	*pvdE*	532	500
METTOv1_760010	TonB-dependent siderophore receptor	*fpvA*	2197	2174
METTOv1_760011	FecR-like protein	*fecR*	330	321

(Continued)

Table 2 | Continued

Gene ID	Predicted function	Gene	Replicate 1	Replicate 2
METTOv1_760012	FecI-family sigma factor	*fecI*	922	951
METTOv1_870003	Ferribactin synthase	*pvdL*	433	441
METTOv1_870004	Pyoverdine biosynthesis regulatory protein-TauD/TfdA family protein		932	1039
METTOv1_870005	Pyoverdine synthetase, thioesterase component	*pvdG*	1542	1473
METTOv1_870006	Integral components of bacterial non-ribosomal peptide synthetases	*MbtH*	4176	5481
METTOv1_1220001	Putative pyoverdine sidechain peptide synthetase IV, d-Asp-l-Ser component	*pvdI/J*	480	564
METTOv1_1220002	Putative non-ribosomal peptide synthase	*pvdJ/D*	379	396

Values represent reads per kilobase of coding sequence per million (reads) mapped (RPKM).

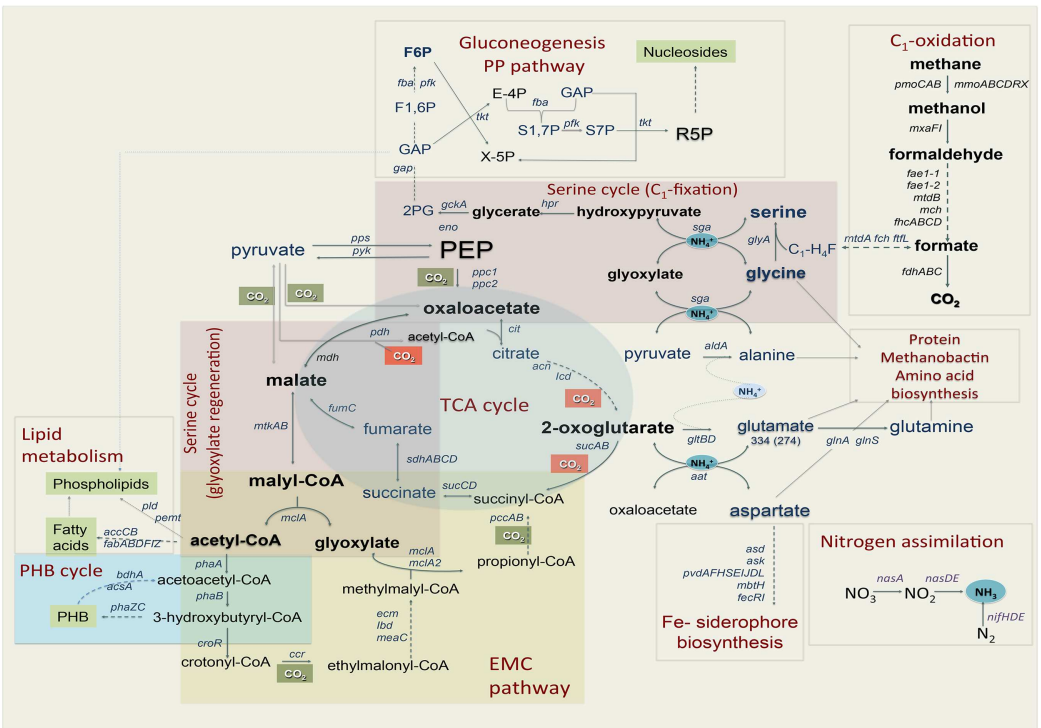

FIGURE 1 | Central metabolism of *Methylosinus trichosporium* OB3b grown on methane as sole source of energy and carbon as deduced from the genome sequences and transcriptomic studies. Font size of the gene name indicates the expression level.

published sequence as the scaffold (Holmes et al., 1995). For this sequence, two possible transcriptional start sites were identified. It is not known whether these reflect the same start sites of both operons, different start sites for each, or expression of only one operon with two start sites. The position −274nt (A) from the translational start of the *pmoC* gene was predicted as the most prominent start of transcription of the operon (Figure S1 in Supplementary Material). Putative σ^{70}-like -10 and -35 regions could be identified upstream of the predicted start (Table S3 in Supplementary Material). The structure of the putative promoter region from *M. trichosporium* OB3b shows significant similarity to a *pmoCAB* promoter region previously identified in *Methylocystis* sp. M (Gilbert et al., 2000). Another potential transcriptional start is at position −324 from the translational start of the *pmoC* gene. It should be noted that the region between the two predicted start sites was also covered with relatively high count (region between −324 and −274nt with respect to the translational start of *pmoC*). No putative promoter sequences were found upstream of position 324.

The genome predicts an additional copy of the *pmoC* gene by itself (*pmoC2, METTOv1_310040*), which can be distinguished from the other *pmoC* genes in the transcriptomics data due to sequence divergence. It has previously been demonstrated that additional copies of *pmoC* are essential for methanotrophic growth in other strains (Stolyar et al., 1999; Dam et al., 2012a). It has also been shown that the homologous *amoC* (additional lone copy of amoC in ammonia-oxidizing bacterium *Nitrosomonas europaea*) plays role in cell recovery from ammonium starvation (Berube and Stahl, 2012). However the functional role of PmoC is

not known. The relative expression of *pmoC2* was approximately 450-fold less than the expression of the two *pmoC* genes from the *pmo*-operons (**Table 2**). Low relative expression of the *pmoC* homolog may suggest a role in regulation or sensing rather than catalytic activity.

C_1-OXIDATION: METHANOL-TO-FORMALDEHYDE

The product of methane oxidation (i.e., methanol) is converted to formaldehyde by a PQQ-dependent methanol dehydrogenase (MDH) (Anthony, 1982, 2002; Yamada et al., 1991; Anthony et al., 1994). The enzyme has been previously purified from *M. trichosporium* OB3b and well characterized (Yamada et al., 1991). MDH is a hetero-tetrameric enzyme encoded by *mxaF* and *mxaI*. The activity of the enzyme *in vivo* requires cytochrome c_L (*mxaG*) and a number of chaperones, regulators, and enzymes, including genes required for Ca^{2+} insertion (Anthony et al., 1994; Anthony, 2002). Most of the genes essential for this methanol conversion step in *M. trichosporium* OB3b are organized in one large operon in an order similar to that found in other methylotrophs (Figure S2A in Supplementary Material). The first four genes of the operon (*mxaFJGI*), encoding the two subunits of the MDH, the associated cytochrome, and a gene of unknown function (*mxaJ*) were detected at relatively high RPKM counts. The relative expression of genes downstream from *mxaI,* including those for chaperones, regulators, and Ca^{2+} insertion functions drops by 10- to 50-fold (**Table 2**). The overall mapping pattern of the *mxa*-cluster is as follows: *mxaFJGI* (highly expressed), *mxaD* (moderate expression), *mxaRSACKL, mxaB* (low expression), and *mxaY* (very low expression*)*. It remains to be elucidated if the *mxaRSACKL* transcripts arise from the same start as *mxaF* and are attenuated by some transcriptional or post-transcriptional mechanism, or whether separate, lower expression promoter(s) is/are present. Orientations and/or the expression patterns of *mxaD*, *mxaB*, and *mxaY*, suggest that they are not part of the major *mxaF*-operon (Figure S2A in Supplementary Material) and most likely have independent regulatory/promoter regions. According to RNA-seq mapping data, a putative transcriptional start of the *mxaFJGI* operon is predicted at position −164 from the predicted translational start (Figure S3 in Supplementary Material). Just upstream from the predicted transcriptional start, putative σ^{70}-like −10 and −35 sequences were identified (Table S3 in Supplementary Material).

The genome of *M. trichosporium* OB3b contains the following three homologs of the large subunit of the MDH: *xoxF1, xoxF2*, and *xoxF3*. Relative expression of all *xoxF*-homologs is very low. The most highly expressed *xox*-homolog (*xoxF1*) showed only about 2% of the *mxaF* expression. The function of the *xox*-gene products has not been studied in *M. trichosporium* OB3b. In the non-methanotrophic methylotroph *Methylobacterium extorquens* AM1, it has been shown that *xoxF* may display methanol-oxidizing activity (Schmidt et al., 2010), and can contribute to the complex regulation of *mxa*-genes (Skovran et al., 2011). Furthermore, there are suggestions that *xoxF* may play a role in formaldehyde oxidation (Wilson et al., 2008). The low expression of all *xoxF*-homologs in *M. trichosporium* OB3b compared to *mxaFI* or H_4MTP-linked pathway genes suggests that *xox*-genes may have no or a minor contribution to methanol oxidation in *M. trichosporium* OB3b under the tested growth conditions. However, our data do not rule out the possibility that one or more of the *xoxF* gene products are involved in regulation, either of methanol or formaldehyde oxidation.

Pyrroloquinoline quinone (PQQ) biosynthesis is another function essential for operation of the primary methanol oxidation system (Toyama et al., 1997; Anthony, 2002). A total of six *pqq* genes appear to be present in the *M. trichosporium* OB3b genome in two clusters: *pqqBCDE* and *pqqFG*. Moderate expression of both clusters was observed (**Table 2**). No gene for the small PQQ precursor (PqqA) is predicted in the current version of the genome. Our manual review of the sequences revealed a fragment within the METTOv1_110055 – METTOv1_110057 gene locus (positions 1424678 – 1424755 of current version of the genome) with high sequence identity [83% nucleic acid (NA) identity and 96% amino acid (AA) similarity] to the *pqqA* sequence from *Methylobacterium* spp (**Figures 2A,B**). Transcript mapping data indicated that only the *pqqA*-like region of the locus is highly expressed (**Figure 2C**). The relative expression of the putative PQQ precursor gene is comparable to the high expression of the *mxaFI* genes. The rest of the genes involved in PQQ biosynthesis showed modest to low expression (Figure S2B in Supplementary Material).

C_1-OXIDATION: FORMALDEHYDE-TO-FORMATE

Previous enzymatic studies predict three possible pathways for formaldehyde oxidation: (1) direct oxidation through dye-linked heme-containing formaldehyde dehydrogenase (Patel et al., 1980), (2) H_4folate-, and (3) H_4MTP-mediated C_1 transfers (Vorholt et al., 1999; Doronina et al., 2008). Contrary to enzymatic studies, BLAST searches of the draft genome of *M. trichosporium* OB3b did not reveal any obvious system that could be attributed to heme-containing formaldehyde oxidation. Three broad-specificity aldehyde-detoxification systems, including two NAD-dependent aldehyde dehydrogenases (Aldh-F7 METTOv1_100046 and Aldh, METTOv1_610028) and one aldehyde oxidase (*Aor*, METTOv1_290006) were predicted in the genome. Two of them, *aldh* and *aor* show low expression (**Table 2**), while *aldh-F7* was barely detected in the transcriptome. None of the putative genes identified by *de novo* transcriptome assembly could be readily attributed to any dye-linked aldehyde dehydrogenases (Schwartz et al., 2004). Thus, even if the enzyme is present in the genome, its expression during growth of the strain on methane must be low.

For years it has been assumed that methylene H_4F is formed as a result of the spontaneous (non-enzymatic) condensation of formaldehyde with H_4F (Large and Quayle, 1963). It has recently been demonstrated that formate, rather than formaldehyde serves as an entry substrate for assimilation in serine cycle methylotrophs (Crowther et al., 2008). With this metabolic arrangement, the H_4Folate C_1 transfer could be considered as a part of the assimilatory network that converts formate into methylene H_4F. In *M. trichosporium* OB3b genes encoding all three steps of the H_4Folate pathway converting methylene-H_4F to formate (formyl-H_4F ligase, *ftfL,* methenyl-H_4F cyclohydrolase, *fch,* and methylene-H_4F dehydrogenase *mtdA*) were co-localized and co-transcribed with genes encoding the serine cycle enzymes

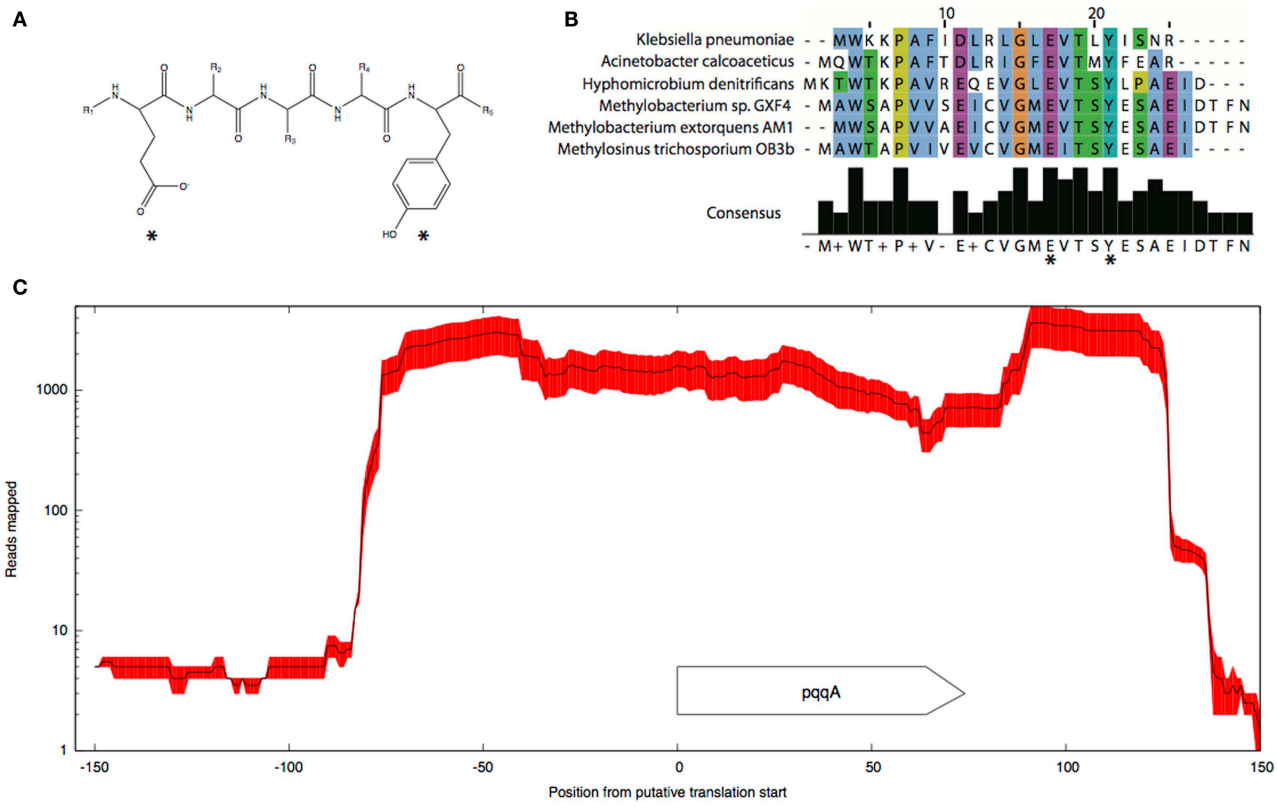

FIGURE 2 | Predicted structure (A) and alignment of the putative *pqqA* peptide (B) from *M. trichosporium* OB3b and *pqqA* peptides from *Methylobacterium* sp. GXF4, *M. extorquens* AM1, *Hyphomicrobium denitrificans* ATCC51888, *K. pneumoniae*, and *A. calcoaceticus*. (C) Mapping.

(Figure S4 in Supplementary Material). While the assimilatory function of the pathway is more apparent, it is still possible that key enzymes of the pathway contribute to formaldehyde oxidation in *M. trichosporium* OB3b.

The tetrahydromethanopterin (H_4MTP) pathway was proposed to be the key pathway for formaldehyde oxidation/detoxification in alphaproteobacterial methylotrophs (Chistoserdova et al., 1998). It was speculated that this pathway contributes to formaldehyde oxidation in methane utilizing proteobacteria (Vorholt et al., 1999). Nineteen genes encoding enzymes and genes for tetrahydromethanopterin biosynthesis were identified in the *M. trichosporium* OB3b genome. These genes were not clustered together in the genome, but formed five different gene islands: (1) *mch-orf5-orf7-fae1/1-fae1/2-orf17* (Figure S2C in Supplementary Material); (2) *orf19-orf20-afpA-orf21-orf22*; (3) *fhcCDAB*; (4) *orf9-mtdB*; and (5) *pcbD-mptG*. No homologs of o*rfY, dmrA*, and *pabB* genes, which are commonly associated with tetrahydromethanopterin biosynthesis in methylotrophs (Caccamo et al., 2004; Rasche et al., 2004; Chistoserdova et al., 2005; Kalyuzhnaya et al., 2005), were found in the genome or detected in transcriptome.

Formaldehyde activating enzyme (FAE) is the first enzyme of the H_4MTP-pathway, which has been shown to catalyze the condensation of formaldehyde and H_4MPT to form methylene-H_4MPT (Vorholt et al., 2000). The draft genome of *M. trichosporium* OB3b predicts three homologs of Fae; two of them (*fae1/1* and *fae1/2*) share a high degree of identity (NA 82.2%) and are co-localized in the genome (Figure S2C in Supplementary Material). Though both *fae* genes are clustered with four other genes involved in the H_4MTP-pathway, they are expressed in dramatically different patterns. The abundance of *fae1-1* transcripts was almost 40-fold higher than the abundance of any other gene in the cluster, except *fae1-2* (**Table 2**; Figure S2C in Supplementary Material). The relative abundance of the second homolog (*fae1-2*) was one fifth of that observed for *fae1-1*, and *fae1-2* was the second highest expressed gene in the pathway. Mapping data indicate that *fae1-1* and *fae1-2* are most likely co-transcribed (Figure S5 in Supplementary Material). RNA-Seq mapping data suggest two putative transcriptional starts at the positions −215 (with σ^{70}-like −10 and −35 sequences upstream) and −105 (with a conserved "AATGGTTG" sequence in the −35 region) upstream from the *fae1-1* translational start (Figure S5 in Supplementary Material; Table S3 in Supplementary Material).

The third homolog of Fae (*fae2*) demonstrates moderate expression. The rest of the genes encoding key enzymes of the pathway (*mtdB*, methylene-H_4MPT dehydrogenase; *mch*, methenyl-H_4MPT cyclohydrolase; *fhcABCD*, formyltransferase/hydrolase) have a similarly moderate expression. The relative abundance of genes encoding key enzymes of the pathway were 5- to

10-fold higher than those involved in cofactor biosynthesis. Overall, transcriptomic data indicate that the H_4MTP-pathway serves as the key pathway for formaldehyde oxidation in *M. trichosporium* OB3b.

FORMATE OXIDATION

Formate is oxidized to CO_2 by a NAD-dependent formate dehydrogenase in most, if not all, methanotrophs (Anthony, 1982). It has been suggested that most of the reducing power required for methane metabolism is produced by formaldehyde oxidation to formate and then to CO_2 (Hanson and Hanson, 1996). It has been speculated that in microbes with a functional serine pathway, formate serves as a key branch point between assimilation and catabolism (Chistoserdova, 2011). NAD-dependent formate dehydrogenase from *M. trichosporium* OB3b has been purified and characterized (Jollie and Lipscomb, 1991). The enzyme is composed of four subunit types and contained flavin, iron, and molybdenum (Jollie and Lipscomb, 1991). The genome of *M. trichosporium* OB3b predicts one NAD-dependent molybdenum-containing formate dehydrogenase encoded by *fdsABGCD* and an additional single copy of the alpha subunit (*fdhA)*. The two genes *fdsA* and *fdhA* share 81% identity. Only one of them, *fdsA* as well as the rest of the *fds* cluster genes were expressed in the transcriptome (**Table 2**).

C_1-ASSIMILATION: SERINE CYCLE

It has been previously suggested that the serine cycle is the major pathway for C_1-assimilation in *M. trichosporium* OB3b (Strom et al., 1974). All genetic elements essential for operation of the cycle were predicted in the genome and cluster together (Stein et al., 2010). However, genes of the pathway show deferent levels of expression (**Table 2**). While *sga*, *glyA*, and *mclA* have high expression levels, the rest of the genes involved in the pathway show modest expression (**Table 2**; Figure S4 in Supplementary Material). In addition to the serine-glyoxylate aminotransferase (*sga*), a key aminotransferase in the central metabolism of serine cycle microbes, moderate levels of expression were observed for two other aminotransferases, phosphoserine aminotransferase, and aspartate aminotransferase (**Table 2**).

The genome of *M. trichosporium* OB3b encodes two copies of phosphoenolpyruvate (PEP) carboxylase (*ppc1* and *ppc2*). The two enzymes are only distantly related to each other and share 33% identity at the amino acid level. One of them, Ppc1, clusters with PEP carboxylases usually found in bacteria possessing the serine

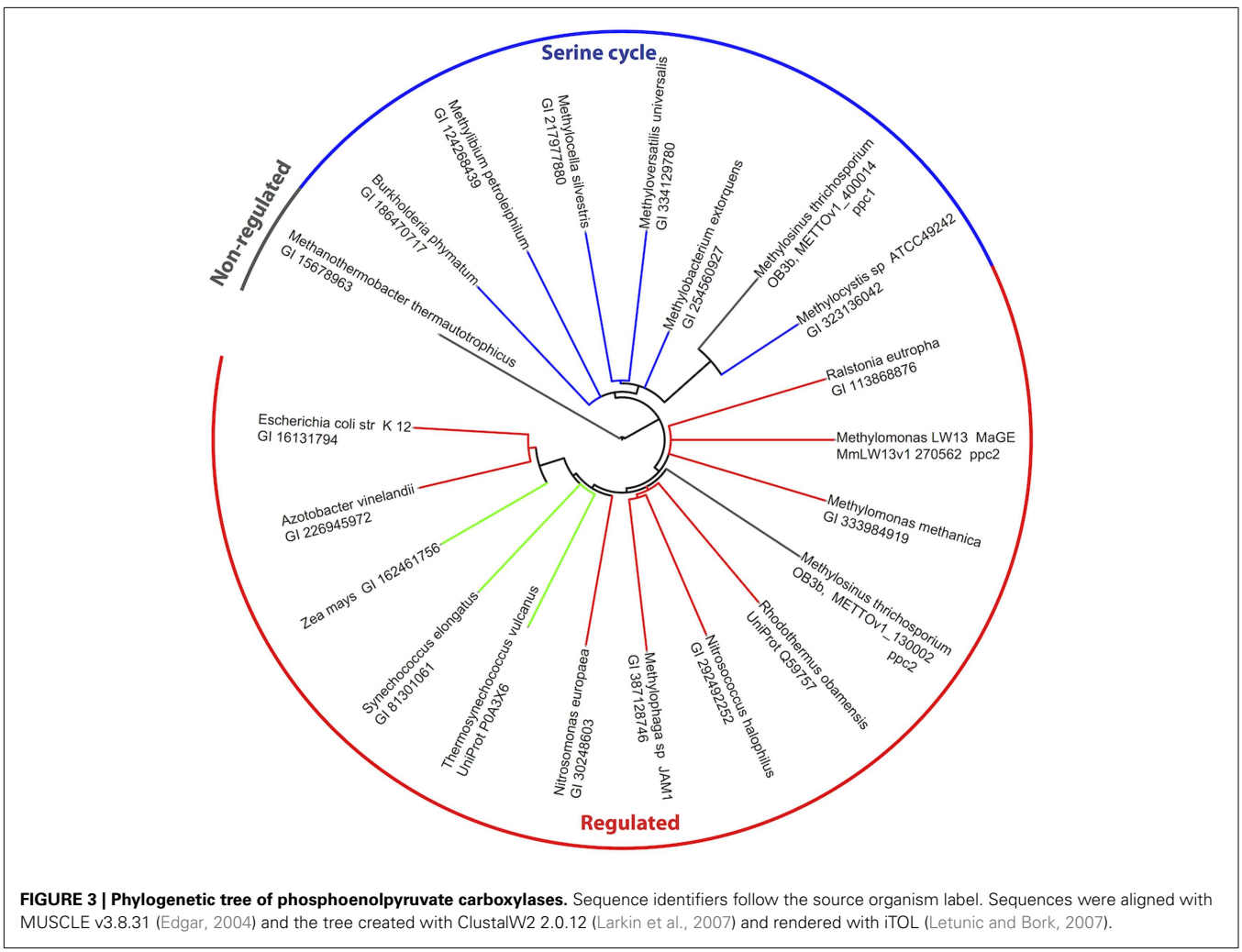

FIGURE 3 | Phylogenetic tree of phosphoenolpyruvate carboxylases. Sequence identifiers follow the source organism label. Sequences were aligned with MUSCLE v3.8.31 (Edgar, 2004) and the tree created with ClustalW2 2.0.12 (Larkin et al., 2007) and rendered with iTOL (Letunic and Bork, 2007).

cycle for C_1-assimilation (**Figure 3**). Serine cycle Ppcs belong to a "*non-regulated*" group of PEP carboxylases (Anthony, 1982). The activity of these enzymes is not controlled by intermediates of the TCA cycle or glycolysis/gluconeogenesis (Newaz and Hersh, 1975). The second homolog of Ppc (*ppc2*) clusters with anaplerotic "*regulated*" PEP carboxylases, which are controlled by a variety of metabolic effectors (Takahashi et al., 1993; Kai et al., 2003). Both *ppc1* and *ppc2* transcripts demonstrate comparable levels of abundance in this study (**Table 2**). The sequences of the two genes were further investigated in an attempt to better understand the rationale for the enzymatic redundancy at the PEP to oxaloacetate conversion step. We used multiple sequence alignments of Ppc1, Ppc*2*, and other characterized PEP carboxylases and homology models (not shown) built from tensed and relaxed state crystal structures (Matsumura et al., 2002) to investigate the predicted allosteric regulation sites of these two enzymes. The alignment shows that only the catalytic elements, such as PEP-binding-site residues, are conserved in both proteins (Ppc1 and Ppc2, Figure S6 in Supplementary Material). However, sequence features required for the allosteric regulation of the enzyme activity show several structural differences. The majority of the characterized bacterial PEP carboxylases are activated by acetyl-CoA, FBP, long-chain fatty acids, and pGp. Inhibition occurs in the presence of aspartate and L-malate. In the case of Ppc1 from *M. trichosporium* OB3b, two of the four highly conserved polar amino acids that bind allosteric inhibitors (e.g., aspartate, malate) were hydrophobic: L805 and A912 (K and N in *E. coli* respectively) suggesting alternate inhibitors or a lack of sensitivity to L-malate and aspartate. The activator-binding residues were conserved except for a R159 instead of K. By contrast, Ppc2 was well conserved relative to the well characterized PEP carboxylases and for those with structures, only minor rearrangements of the monomeric interfaces were predicted. It is tempting to speculate that the presence of two functionally identical but differently regulated enzymatic systems in *M. trichosporium* OB3b evolved as a way to control flux through PEP-oxaloacetate in response to levels of the serine cycle and EMC pathway intermediates. The flux is never completely blocked, due to the insensitivity of Ppc1 to the metabolic state of the cell. Increases in the intracellular levels of acetyl-CoA, aspartate, or malate (as a result of saturation of the downstream EMC pathway and the TCA cycle) can reduce the flux through the PEP-oxaloacetate presumably twofold via allosteric inhibition and lack of activation of Ppc2 activity. In this case, C_1-carbon assimilated via the serine cycle is re-directed to gluconeogenesis or converted into pyruvate.

Regeneration of glyoxylate is an essential part of the serine cycle (Anthony, 1982, 2011; Peyraud et al., 2009). Like other obligate methanotrophic bacteria, *M. trichosporium* OB3b lacks isocitrate lyase, a key enzyme of the glyoxylate shunt (Trotsenko and Murrell, 2008). Homologs of enzymes involved in the ethylmalonyl-CoA (EMC) pathway, an alternative route for glyoxylate regeneration (Peyraud et al., 2009), were identified in the draft genomes of *M. trichosporium* OB3b and another obligate methanotroph *Methylocystis* sp. (Stein et al., 2010, 2011). However, a functional EMC pathway has not yet been demonstrated in methanotrophs. Furthermore, the recent investigation of PHB-metabolism in *Methylocysctis parvus* OBBP, an alphaproteobacterial methanotroph, suggested that this metabolic module can not supply C_2 (glyoxylate) units for biosynthesis (Pieja et al., 2011). As the initial steps of the EMC pathway are shared with PHB biosynthesis [acetyl-CoA acetyltransferase (*phaA*) and acetoacetyl-CoA reductase (*phaB*), see **Figure 1**] in context with the data presented by Pieja et al. (2011) call into question the operation of the EMC pathway in methanotrophs.

We found that genes encoding the initial steps of the PHB-synthesis (*phaA/phaB)* show moderate levels of expression. As could be expected for cells in early-mid exponential growth, the expression of the gene encoding PHB synthase (*phaC*) was low. The data are consistent with previous observations of high activity of PhaA and PhaB and low activity of PHB synthase (PhaC) in exponentially grown cells of *M. trichosporium* OB3b (Williams, 1988; Doronina et al., 2008). The PHB-degradation pathway genes, including 3-hydroxybutyrate dehydrogenase, acetoacetate decarboxylase, and acetoacetyl-coenzymeA synthetase, show modest expression levels (**Table 2**).

All homologs of the EMC pathway enzymes were expressed in *M. trichosporium* OB3b during growth on methane (**Table 2**). Several putative acetyl/propionyl-CoA carboxylases are predicted in the genome, however only METTOv1_200020 (putative *ppcA*) and METTOv1_220035 (putative *ppcB*) were expressed. Furthermore, the PpcAB and crotonyl-CoA reductase (*ccr*) genes display the highest level of expression among all CO_2-fixing enzymes in the *M. trichosporium* OB3b transcriptome. Thus, the transcriptional profile of *M. trichosporium* OB3b indicates the methanotroph may possess an active EMC pathway.

C_1-ASSIMILATION: TCA CYCLE AND ANAPLEROTIC CO_2-FIXATION

All previous enzymatic studies predict that the tricarboxylic acid cycle (TCA cycle) in alphaproteobacterial methanotrophs is complete (Trotsenko and Murrell, 2008). However, the functional role of this metabolic pathway in methanotrophs is not fully understood. It has been suggested that the main role of the TCA cycle in the methanotrophs is carbon assimilation rather than energy production, due to low enzyme activity and lack of pyruvate dehydrogenase (Trotsenko, 1976; Anthony, 1982; Shishkina and Trotsenko, 1982; Trotsenko and Murrell, 2008). However, labeling studies on acetate and pyruvate utilization have predicted the presence of a catabolic TCA cycle in type II methanotrophs (Wadzink and Ribbons, 1975; reviewed in Higgins et al., 1981). *In silico* genome analysis indicates that *M. trichosporium* OB3b contains predicted genes for all key enzymes of the TCA cycle and pyruvate dehydrogenase (*pdh*). All of these genes were expressed (**Table 2**). These steps of the TCA cycle are shared between the EMC pathway and the serine cycle (**Figure 1**). *De novo* transcriptome assembly indicated that *M. trichosporium* OB3b possesses an additional homolog of succinate:ubiquinone oxidoreductase (*sucABCD,* Table S1 in Supplementary Material). Genes encoding the succinate:ubiquinone oxidoreductase and succinyl-CoA synthase (*sucCD*) are among the most highly expressed TCA cycle functions. The reductive branch of the pathway (including genes for citrate synthase, aconitase, isocitrate dehydrogenase, and 2-ketoglutarate dehydrogenase) displays moderate-to-low expression. Low expression of *pdh* genes is consistent with the

previous enzymatic studies that show low/no activity of pyruvate dehydrogenase (Trotsenko, 1976).

It has been shown that the CO_2-fixation potential is maximal during early stages of logarithmic growth (Park et al., 1991, 1992). However, data on carboxylation system(s) in *M. trichosporium* OB3b are controversial. Most previous enzymatic studies predict that the PEP carboxylase (Ppc), a key enzyme of the serine cycle, is the major entry point for CO_2 in alphaproteobacterial methanotrophs (Shishkina and Trotsenko, 1982). On the other hand Naguib (1979) has shown that *M. trichosporium* OB3b possesses different carboxylation systems, including membrane bound and cytoplasmic enzymes. It could be predicted that the EMC pathway also contributes to CO_2 assimilation. *In silico* analysis of the genome sequence also revealed that in addition to the CO_2-fixing functions described above, genes for NAD(P)-dependent malic enzyme (*mae*), acetyl-CoA carboxylase (*accABD*), phosphoribosyl aminoimidazole carboxylase, pyruvate carboxylase (*pcx*), and a putative 2-oxoacid ferredoxin oxidoreductase are all present. All of these genes were expressed (**Table 2**).

GLYCOLYSIS/GLUCONEOGENESIS AND PENTOSE-PHOSPHATE PATHWAYS

The absence of enzymatic activity for the initial steps of the gluconeogenic pathway including pyruvate-PEP or oxaloacetate-PEP conversions was one of the most common explanations for the inability of alphaproteobacterial methanotrophic bacteria to grow on poly-carbon compounds such as pyruvate or acetate (Patel et al., 1979; Shishkina and Trotsenko, 1982). No homolog of PEP-carboxykinase was found in the *M. trichosporium* OB3b genome. However, contrary to expectations based on enzymatic inferences, a set of pyruvate-acetyl-CoA, pyruvate-PEP, and pyruvate-malate interconversions could be predicted from the genome annotation. Homologs of PEP synthase (*pps*), pyruvate kinase (*pyk*1 and *pyk*2), and pyruvate phosphate dikinase were detected. The relative abundances of *pyk1*, *pps*, and *pdk* transcripts were low, but a second pyruvate kinase (*pyk*2) displayed modest expression (**Table 2**).

During growth on C_1 compounds (methane or methanol), gluconeogenesis starts with conversion of 2-phosphoglycerate into 3-phosphoglycerate by phosphoglycerate mutase (*pgm*). This metabolic step represents the main branch point of the serine cycle. Four homologs of *pgm* were identified in the *M. trichosporium* OB3b genome. Three of them (METTOv1_10180, METTOv1_100061, and METTOv1_680013) were expressed at tested conditions. Homologs of the genes for the rest of the enzymes in the pathway were detected in the genome, mostly in single copies. All gene transcripts were observed in the RNA-Seq data (**Table 2**).

The genome analysis suggests that the pentose-phosphate pathway (PPP) is incomplete in *M. trichosporium* OB3b. Glucose-6-phosphate dehydrogenase, gluconolactonase and phosphogluconate dehydrogenase (oxidative PPP), and transaldolase or sedoheptulose bisphosphatase (non-oxidative PPP), are missing in the genome. In addition, no homologs of the genes were detected among *de novo* assembled transcripts. The lack of the oxidative branch of the PPP is consistent with previous enzymatic data and the inability of alphaproteobacterial methanotrophs to utilize sugars. However if the non-oxidative PPP operates as a route for generation of ribose-5-phosphate for the synthesis of nucleotides, an unknown enzyme must be involved in the sedoheptulose-phosphate interconversion. One possible system is a pyrophosphate-dependent phosphofructokinase (Pfk). It has been shown that Pfks from methanotrophic bacteria have surprisingly high affinity for sedoheptulose phosphate, and can catalyze the conversion of sedoheptulose-1,7-bisphosphate to sedoheptulose-7-phosphate (Reshetnikov et al., 2008; Rozova et al., 2012). It is possible that Pfk contributes to sedoheptulose-1,7-bisphosphate conversion in *M. trichosporium* OB3b.

LIPID METABOLISM

Methane oxidation via particulate methane monooxygenase is linked to formation of extensive intracellular membranes. It has been shown that lipid/biomass content of *M. trichosporium* OB3b cells grown on methane is 9.2% and that phospholipids represent a significant fraction of membrane lipids (83.4%) (Weaver et al., 1975; Guckert et al., 1991). Concurrent with previous observation, genes essential for biosynthesis of major fatty acids (stearic, oleic, and palmitoleic acids) and phospholipids (including phosphotidylcholine, phosphatidylglycerol, phosphatidylserine, and phosphatidylethanolamine) show moderate level of expression (Table S2 in Supplementary Material).

NITROGEN, COPPER, AND IRON METABOLISM

The pathways of nitrogen assimilation have been studied in a number of obligate methanotrophic species including *M. trichosporium* OB3b. Methanotrophs are able to grow with ammonia, nitrate, and molecular nitrogen as N-sources (Whittenbury et al., 1970; Shishkina and Trotsenko, 1979; Murrell and Dalton, 1983a,b; Chu and Alvarez-Cohen, 1998; Kim and Graham, 2001). No activities of alanine or glutamate dehydrogenases were detected in cell extracts of *M. trichosporium* OB3b grown on any source of nitrogen (Shishkina and Trotsenko, 1979; Murrell and Dalton, 1983a,b). It has been concluded that ammonia was assimilated exclusively via the glutamine synthetase/glutamate synthase pathway (Murrell and Dalton, 1983b).

In this study, cells of *M. trichosporium* OB3b were grown using nitrate as the N-source. Despite the presence of an exogenous source of nitrogen, some (very low) expression of the nitrogenase gene cluster was observed. Relative expression of nitrogenase structural genes (*nifHDK*) was about four to five times higher than expression of the chaperone and cofactor biosynthesis genes (Table S2 in Supplementary Material). High expression of genes involved in assimilatory nitrate reduction, including the nitrate transporter (*nrtA*), nitrate reductase (*nasA*), and nitrite reductase (*nasDE*) was detected. Interestingly, moderate expression of a putative ammonium transporter (METTOv1_130049) was detected, although a gene cluster with putative involvement in hydroxylamine detoxification (METTOv1_230076-78), which should only be needed under conditions of high ammonium concentration, showed low expression (**Table 2**). The gene encoding cytochrome *c′*-alpha (METTOv1_560023), a protein implicated in NOx detoxification, was moderately expressed. Homologs of alanine dehydrogenase (METTOv1_280018) and glutamate dehydrogenase (METTOv1_190023) were identified; however, neither gene was expressed (**Table 2**). High expression of glutamate synthase (both NADH and Fd-dependent), glutamate-ammonia

ligase (METTOv1_200046), and Type I glutamine synthetase (METTOv1_200048) was observed. Based on these transcriptomic studies and genome analysis, the only pathway for alanine biosynthesis is transamination of pyruvate. The most likely enzymatic system for this conversion is the serine-glyoxylate aminotransferase (Sga), which is known to catalyze serine-pyruvate transamination (Liepman and Olsen, 2001). It has been shown that alanine may serve as alternative substrate for SGA in methylotrophs (Karsten et al., 2001).

Copper is an important microelement in the physiology of methanotrophic bacteria possessing pMMO (Anthony, 1982). Methanotrophic bacteria synthetize methanobactin (Mb), a copper-chelating compound (Kim et al., 2004; Balasubramanian and Rosenzweig, 2008; Semrau et al., 2010). It has been suggested that Mb provides copper for the regulation and activity of methane oxidation machinery in methanotrophs (Balasubramanian et al., 2010; Semrau et al., 2010). It has been shown that Mb is a peptide-derived molecule. A gene encoding the Mb precursor in *M. trichosporium* OB3b has recently been identified (Krentz et al., 2010). We found that the Mb-gene is among the top 5% most abundant transcripts despite the fact that the culture in our experiments was grown with sufficient Cu (**Table 2**). It is not known how Mb is synthesized or cleaved, however it has been suggested that genes downstream of *mb* are involved (Krentz et al., 2010). These genes were also expressed, but the expression level was low.

Iron is another essential metal in C_1-metabolism. It has been previously observed that *M. trichosporium* OB3b can produce a Fe-chelating compound (Yoon et al., 2010); however the siderophore structure and pathways for its biosynthesis remain to be discovered. The production of a fluorescent compound was observed on plates at tested growth conditions (data not shown). Our transcriptomic studies revealed relatively high expression of genes homologous to those involved in pyoverdine (*pvd*) I biosynthesis, excretion, uptake, and regulation (**Table 2**), making this a possibility for a siderophore. All four essential non-ribosomal peptide synthetases (*pvdLIJD*) were identified. Unfortunately, the *pvd* genes are represented in fragments in the current genome assembly, making it impossible to predict the order of the amino acids in the peptide product.

CONCLUSION

In this work we performed genomic- and transcriptomic-based reconstruction of the central metabolic pathways in *Methylosinus trichosporium* OB3b grown on methane as a sole source of carbon and energy. The overview of the methane metabolism is summarized in **Figure 1**. While some metabolic functions correlate well with previous enzymatic and genetic studies, several novel functions were detected and characterized. The major outcomes of our work are listed below:

1. Exceptionally high expression of pMMO in comparison to other central pathway functions (such as methanol or formaldehyde oxidation) implies a relatively low turn over at the first step of methane conversion.
2. We propose that *M. trichosporium* OB3b uses the EMC variant of the serine cycle for carbon assimilation. In addition to carbon fixing reactions of the EMC-serine cycle, a number of carboxylation reactions are predicted. The role of CO_2 fixation during methanotrophic growth has further been explored by Yang et al. (2013).
3. The diversity of predicted reactions at the PEP-pyruvate-oxaloacetate node suggests that metabolic interconversions may play an important role in the distribution of carbon flux between the serine cycle, EMC pathway, and TCA cycle. In *M. trichosporium* OB3b the PEP-oxaloacetate conversion is predicted to be performed by two enzymatic systems under different metabolic control. Increases in the intracellular pools of malate, aspartate, and acetyl-CoA could activate flow of C_1-derived carbon into gluconeogenesis and/or pyruvate. Our results indicate that multiple PEP-pyruvate conversion reactions may be taking place in the strain during growth on methane as a way to regenerate energy and to provide pyruvate for biosynthesis. Due to the lack of PEP-carboxykinase, the PEP synthesis from C_4 compounds is also possible and could be achieved via decarboxylation of malate (MalE). Two reactions are predicted for PEP synthesis from pyruvate, however both of them seem to be of minor importance during growth on methane.
4. A number of transamination reactions contribute to carbon partitioning and nitrogen assimilation. It has been predicted that the growth of majority of alphaproteobacterial methylotrophic bacteria is NAD(P)H-limited due to the high NADH-requirements for formaldehyde assimilation via serine cycle (Anthony, 1978). Biosynthesis of key amino acids (such as alanine, glutamate and aspartate) via transamination seems to be a rational metabolic compensation to NAD(P)H-limitation.
5. While copper acquisition is quite well characterized in *M. trichosporium* OB3b, relatively little is known about iron uptake systems. Transcriptomic data provide initial evidence for siderophore production in this methanotroph.

MATERIALS AND METHODS

STRAIN AND CULTIVATION CONDITIONS

Methylosinus trichosporium strain OB3b was kindly provided by Dr. Lisa Stein. The culture was grown in 250 mL glass bottles on modified NMS medium (Whittenbury et al., 1970) containing (per liter of distilled water): 1 g·KNO_3, 1 g·$MgSO_4 \cdot 7H_2O$, 0.134 g·$CaCl_2 \cdot 2H_2O$, 0.25 g·KH_2-PO, 0.7 g·$Na_2HPO_4 \cdot 12H_2O$, and 2 mL of trace elements solution. The trace elements solution contained 0.5 g·Na_2-EDTA, 1.0 g·$FeSO_4 \cdot 7H_2O$, 0.75 g·Fe-EDTA, 0.8 g·$ZnSO_4 \cdot 7H_2O$, 0.005 g·$MnCl_2 \cdot 4H_2O$, 0.03 g·H_3BO_3, 0.05 g·$CoCl_2 \cdot 6H_2O$, 0.4 g·Cu-EDTA, 0.6 g·$CuCl_2 \cdot 2H_2O$, 0.002 g·$NiCl_2 \cdot 6H_2O$, and 0.05 g·$Na_2MoO_4 \cdot 2H_2O$. The bottles were sealed with rubber stoppers and aluminum caps, then 50 mL of methane was added to the 200 mL headspace. Bottles were shaken at 250 RPM at 30°C for 1–4 days.

GROWTH PARAMETERS AND METHANE CONSUMPTION RATE MEASUREMENTS

Methane consumption rates and cell density (OD_{600}) were measured in triplicate as cultures grew. Methane measurements were made on a Shimadzu Gas Chromatograph GC-14A, using the FID detection with helium as the carrier gas. Concentrations

were deduced from standard curves. OD_{600} was measured on a Beckman DU®640B spectrophotometer in plastic 1.5 mL cuvettes with a 1 cm path length.

RNA-seq

Two replicate cultures were grown to mid exponential phase (OD_{600} 0.29 ± 0.01) for approximately 24 h, then collected by pouring 45 mL of culture into 50 mL tubes containing 5 mL of *stop solution* comprised of 5% water-equilibrated phenol, pH 6.6 (Sigma; St. Louis, MO, USA), and 95% ethanol (200 Proof; Deacon Labs, Inc., King of Prussia, PA, USA). The cells were collected by centrifugation at 4,300 × *g* at 4˚C for 10 min. The resultant pellet was re-suspended in 0.75 mL of extraction buffer [2.5% CTAB (Sigma; St. Louis, MO, USA), 0.7 M NaCl, and 0.075 M pH 7.6 phosphate buffer] and transferred to a 2 mL sterilized screw-cap tube containing 0.75 mL of phenol:chloroform:isoamylic alcohol with a volume ratio of 25:24:1 (Ambion®; Austin, TX, USA), 0.5 g of 0.1 mm silica beads (Biospec products; Bartlesville, OK, USA), 0.2% SDS (Ambion®; Austin, TX, USA), and 0.2% lauryl sarkosine (Sigma; St. Louis, MO, USA). The mixtures were homogenized in a bead beater (Mini-Beadbeater; Biospec Products; Bartlesville, OK, USA) for 2 min (75% of the maximum power). The resulting slurry was centrifuged for 5 min at 4˚C and 20,800 × *g*. The aqueous layer was transferred to a fresh tube containing 0.75 mL of chloroform:isoamylic alcohol with a volumetric ratio of 24:1 (Sigma; St. Louis, MO, USA) and centrifuged again for 5 min at 4˚C and 20,800 × *g* to remove dissolved phenol. The aqueous phase was transferred to a new tube. $MgCl_2$ (final concentration 3 mM), sodium acetate (10 mM, pH 5.5), and 0.8 mL icecold isopropanol were added. Nucleic acids were transferred to −80˚C for overnight precipitation. Precipitated samples were centrifuged for 45 min at 4˚C and 14,000 RPM (20,800 × *g*), washed with 0.5 mL of 75% ethanol (made from 200 proof; Deacon Labs, Inc., King of Prussia, PA, USA), and dried for 15 min at room temperature.

An RNeasy Mini Kit (Qiagen©; Venlo, Netherlands) with two types of DNA digestions was used to isolate the mRNA. Initially, the DNA/RNA pellet was re-suspended in 80 mL of a DNase I (RNase-free) mixture (Ambion®; Austin, TX, USA) and incubated for 30 min at 37˚C. Then, the samples were purified on RNeasy Mini Kit columns as described in the *RNA cleanup* section of the manual, including the optional on-column DNAse digestion. The MICROBExpress™(Ambion®; Austin, TX, USA) kit was applied to each sample to reduce the rRNA concentration and increase the mRNA sequencing depth.

The sample quality was monitored with three techniques: (1) by electrophoresis in TAE buffer in 1% agarose gels (2) using an Agilent 2100 Bioanalyzer with Agilent RNA 6000 Nano-kit as suggested by the manufacturer, and (3) by real-time reverse-transcriptase PCR (RT-RT PCR) with 16S rRNA (27F/536R) and *pmoA*-specific (Auman et al., 2001) primers.

TRANSCRIPT SEQUENCING, ALIGNMENT, AND MAPPING

Enriched RNA samples (i.e., two biological replicates) were submitted to the University of Washington's High-Throughput Sequencing Solutions Center on dry ice for single-read Illumina®sequencing (Department of Genome Sciences, University of Washington[2]). The replicates were aligned to the reference genome using BWA under default parameters (Li and Durbin, 2009). The "METTOv1" genome sequence was downloaded from MaGE (Vallenet et al., 2006). The single large pseudo scaffold distributed by MaGE was split into 187 separate contigs at each stretch of *N* bases. In addition, chimeric contigs from the assembly and low quality gene calls were removed (Table S5 in Supplementary Material). The summary of RNA-seq (Illumina) reads can be found in Table S4 in Supplementary Material. The METTOv1 genome did not have a complete *pmoCAB* cluster suitable for alignment. In order to include *pmoCAB*, a separate alignment run was performed with the previously published sequence of this gene cluster (Holmes et al., 1995). After the alignment with BWA, SAM tools was used to generate a *pileup* file that was loaded into a MySQL database for normalization from Reads Per Kilobase of gene per Million mapped reads (RPKM) to coding sequences (Mortazavi et al., 2008).

TRANSCRIPTION SITE MAPPING AND TRANSCRIPTOME BASED GENE ASSEMBLY

The reads mapped at each base position in the genomic scaffolds generated from the *pileup* were manually examined to identify putative transcription starts and stops. Briefly, reads mapped per base data for the two replicates were plotted on a log scale. The boundary of a rapid transition from near zero reads mapped to 10, 100 RPKM or more that was upstream of a gene start was designated a transcription start. Stops were similarly identified as a rapid transition to low numbers of reads mapped downstream of a gene termination codon.

Given the fragmented nature of the *M. trichosporium* OB3b genome, we performed *de novo* assembly of the RNA-Seq reads, in an attempt to identify transcripts whose genomic sequences were incomplete. The assembly was performed with Velvet 1.2.06 (Zerbino and Birney, 2008) and Oases 0.2.08 (Schulz et al., 2012). The oases pipeline tool distributed with Oases was used to survey assemblies across the range of odd k-mers from 17 to 35 where the minimum fragment length was set to 100 bp. The final merged assembly from the pipeline tool was stripped down to the highest confidence transcript for each locus with confidence ties resolved by taking the longest sequence. The high confidence assembled transcripts were aligned to the *M. trichosporium* OB3b scaffolds using BLASTn. Transcripts without significant matches were aligned with BLASTx to the protein non-redundant database, as retrieved on January 13, 2012.

ACKNOWLEDGMENTS

This project was funded by the DOE (DE-SC0005154). Authors are very grateful to Mary E. Lidstrom, Ludmila Chistoserdova, and Valentina N. Khmelenina for many insightful suggestions on the manuscript.

SUPPLEMENTARY MATERIAL

The Supplementary Material for this article can be found online at http://www.frontiersin.org/Microbiological_Chemistry/10.3389/fmicb.2013.00040/abstract

[2]http://www.htseq.org/

Figure S1 | RNA-Seq reads mapped per base relative to start of pmo-operon. Left, the average number of reads mapped to the region −330 to −270 upstream from the start of *pmoC* for two biological replicates. The sequence at each base is shown above the bars. Right, the range (shown in red) and mean of two biological replicates (shown as black line) for the number of reads mapped per base for the coding and downstream region of the *pmo*-operon.

Figure S2 | Genetic organization and relative expression (RPKM) of the mxa gene cluster (A), the pqq gene cluster (B) and cluster of genes encoding reactions of the H_4MPT-linked C1 transfer pathway (C).

Figure S3 | RNA-Seq reads mapped per base relative to start of *mxaF* ORF. Left, the average number of reads mapped to the region −200 to −140 upstream from the start of *mxaF* for two biological replicates. The sequence at each base is shown above the bars. Right, the range (shown in red) and mean of two biological replicates (shown as black line) for the number of reads mapped per base for the coding and downstream region of the *mxaF* cluster.

Figure S4 | RNA-Seq reads mapped per base relative to start of serine cycle gene operon. The log10 average number of reads mapped at each base from biological replicates one and two is shown. In **(A)**, the upstream location spanning −250 to −190 from putative start of ftfL. **(B)** The expression over the entire operon. Note the several drop to near zero upstream indicating the operon is not co-transcribed. **(C)** The −230 to −170 region upstream from sga. Bases from the +strand are shown across the top of the figure. **(D)** The −270 to −210 region upstream of *mclA*.

Figure S5 | RNA-Seq reads mapped per base relative to start of *fae1-1*. Left, the average number of reads mapped to the region −235 to −185 upstream from the start of *fae1-1* gene for two biological replicates. The sequence at each base is shown above the bars. Right, the range (shown in red) and mean of two biological replicates (shown as black line) for the number of reads mapped per base for the coding and downstream region of the *fae1-1* and *fae1-2* genes.

Figure S6 | Primary structure alignment for phosphoenolpyruvate carboxylases (Ppc1 and Ppc2) from *M. trichosporium* OB3b and Ppc-homologs.

Table S1 | Transcripts detected by de novo assembly RNA-Seq data.

Table S2 | Gene expression profile in methane-grown cells of *M. trichosporium* OB3b. Values represent reads per kilobase of coding sequence per million (reads) mapped (RPKM).

Table S3 | Summary of putative transcription site mapping (Note that the published sequences need references added).

Table S4 | Summary of RNA-seq (Illumina) reads.

Table S5 | Genes removed from reference scaffold before alignment.

REFERENCES

Anthony, C. (1978). The prediction of growth yields in methylotrophs. *J. Gen. Microbiol.* 104, 91–104.

Anthony, C. (1982). *The Biochemistry of Methylotrophs.* New York: Academic Press Inc.

Anthony, C. (2002). Methanol dehydrogenase, a PQQ-containing quinoprotein dehydrogenase. *Subcell. Biochem.* 35, 73–117.

Anthony, C. (2011). How half a century of research was required to understand bacterial growth on C1 and C2 compounds; the story of the serine cycle and the ethylmalonyl-CoA pathway. *Sci. Prog.* 94, 109–137.

Anthony, C., Ghosh, M., and Blake, C. C. (1994). The structure and function of methanol dehydrogenase and related quinoproteins containing pyrrolo-quinoline quinone. *Biochem. J.* 304, 665–674.

Auman, A. J., Speake, C. C., and Lidstrom, M. E. (2001). nifH sequences and nitrogen fixation in type I and type II methanotrophs. *Appl. Environ. Microbiol.* 67, 4009–4016.

Balasubramanian, R., and Rosenzweig, A. C. (2008). Copper methanobactin: a molecule whose time has come. *Curr. Opin. Chem. Biol.* 12, 245–249.

Balasubramanian, R., Smith, S. M., Rawat, S., Yatsunyk, L. A., Stemmler, T. L., and Rosenzweig, A. C. (2010). Oxidation of methane by a biological dicopper centre. *Nature* 465, 115–119.

Berube, P. M., and Stahl, D. A. (2012). The divergent AmoC3 subunit of ammonia monooxygenase functions as part of a stress response system in *Nitrosomonas europaea*. *J. Bacteriol.* 189, 3448–3456.

Caccamo, M. A., Malone, C. M., and Rasche, M. E. (2004). Biochemical characterization of a dihydromethanopterin reductase involved in tetrahydromethanopterin biosynthesis in *Methylobacterium extorquens* AM1. *J. Bacteriol.* 186, 2068–2073.

Chen, Y., Crombie, A., Rahman, M. T., Dedysh, S. N., Liesack, W., Stott, M. B., et al. (2010). Complete genome sequence of the aerobic facultative methanotroph *Methylocella silvestris* BL2. *J. Bacteriol.* 192, 3840–3841.

Chistoserdova, L. (2011). Modularity of methylotrophy, revisited. *Environ. Microbiol.* 13, 2603–2622.

Chistoserdova, L., Kalyuzhnaya, M. G., and Lidstrom, M. E. (2009). The expanding world of methylotrophic metabolism. *Annu. Rev. Microbiol.* 63, 477–499.

Chistoserdova, L., Rasche, M. E., and Lidstrom, M. E. (2005). Novel dephosphotetrahydromethanopterin biosynthesis genes discovered via mutagenesis in *Methylobacterium extorquens* AM1. *J. Bacteriol.* 187, 2508–2512.

Chistoserdova, L., Vorholt, J. A., Thauer, R. K., and Lidstrom, M. E. (1998). C1 transfer enzymes and coenzymes linking methylotrophic bacteria and methanogenic archaea. *Science* 281, 99–102.

Chu, K. H., and Alvarez-Cohen, L. (1998). Effect of nitrogen source on growth and trichloroethylene degradation by methane-oxidizing bacteria. *Appl. Environ. Microbiol.* 64, 3451–3457.

Crowther, G. J., Kosály, G., and Lidstrom, M. E. (2008). Formate as the main branch point for methylotrophic metabolism in *Methylobacterium extorquens* AM1. *J. Bacteriol.* 190, 5057–5062.

Dam, B., Kube, M., Dam, S., Reinhardt, R., and Liesack, W. (2012a). Complete sequence analysis of two methanotroph-specific repABC-containing plasmids from *Methylocystis* sp. strain SC2. *Appl. Environ. Microbiol.* 78, 4373–4379.

Dam, B., Dam, S., Kube, M., Reinhardt, R., and Liesack, W. (2012b). Complete genome sequence of *Methylocystis* sp. strain SC2, an aerobic methanotroph with high-affinity methane oxidation potential. *J. Bacteriol.* 194, 6008–6009.

Doronina, N. V., Ezhov, V. A., and Trotsenko, Yu. A. (2008). Growth of *Methylosinus trichosporium* OB3b on methane and poly-beta-hydroxybutyrate biosynthesis. *Prikl. Biokhim. Mikrobiol.* 44, 182–185.

Dunfield, P. F., Yuryev, A., Senin, P., Smirnova, A. V., Stott, M. B., Hou, S., et al. (2007). Methane oxidation by an extremely acidophilic bacterium of the phylum Verrucomicrobia. *Nature* 450, 879–882.

Edgar, R. C. (2004). MUSCLE: multiple sequence alignment with high accuracy and high throughput. *Nucleic Acids Res.* 32, 1792–1797.

Elango, N., Radhakrishnan, R., Froland, W. A., Wallar, B. J., Earhart, C. A., Lipscomb, J. D., et al. (1997). Crystal structure of the hydroxylase component of methane monooxygenase from *Methylosinus trichosporium* OB3b. *Protein Sci.* 6, 556–568.

EPA. (1993). *Emerging Technology Summary Pilot-Scale Demonstration of a Two-Stage Methanotrophic Bioreactor for Biodegradation of Trichloroethylene in Groundwater.* Available at: http://nepis.epa.gov

Fitch, M. W., Speitel, G. E., and Georgiou, G. (1996). Degradation of trichloroethylene by methanol-grown cultures of *Methylosinus trichosporium* OB3b PP358. *Appl. Environ. Microbiol.* 62, 1124–1128.

Gilbert, B., McDonald, I. R., Finch, R., Stafford, G. P., Nielsen, A. K., and Murrell, J. C. (2000). Molecular analysis of the *pmo* (particulate methane monooxygenase) operons from two type II methanotrophs. *Appl. Environ. Microbiol.* 66, 966–975.

Guckert, J. B., Ringelberg, D. B., White, D. C., Hanson, R. S., and Bratina, B. J. (1991). Membrane fatty acids as phenotypic markers in the polyphasic taxonomy of methylotrophs within the Proteobacteria. *J. Gen. Microbiol.* 137, 2631–2641.

Hakemian, A. S., Kondapalli, K. C., Telser, J., Hoffman, B. M., Stemmler, T. L., and Rosenzweig, A. C. (2008). The metal centers of particulate methane monooxygenase from *Methylosinus trichosporium* OB3b. *Biochemistry* 47, 6793–6801.

Hakemian, A. S., and Rosenzweig, A. C. (2007). The biochemistry of methane oxidation. *Annu. Rev. Biochem.* 76, 223–241.

Hanson, R. S., and Hanson, T. E. (1996). Methanotrophic bacteria. *Microbiol. Rev.* 60, 439–471.

Higgins, I. J., Best, D. J., Hammond, R. C., and Scott, D. (1981). Methane-oxidizing microorganisms. *Microbiol. Rev.* 45, 556–590.

Holmes, A. J., Costello, A., Lidstrom, M. E., and Murrell, J. C. (1995). Evidence that particulate methane monooxygenase and ammonia monooxygenase may be evolutionarily related. *FEMS Microbiol. Lett.* 132, 203–208.

Hou, C. T., Patel, R., Laskin, A. I., and Barnabe, N. (1979). Microbial oxidation of gaseous hydrocarbons: epoxidation of C2 to C4 n-alkenes by methylotrophic bacteria. *Appl. Environ. Microbiol.* 38, 127–134.

Hou, S., Makarova, K. S., Saw, J. H., Senin, P., Ly, B. V., Zhou, Z., et al. (2008). Complete genome sequence of the extremely acidophilic methanotroph isolate V4, *Methylacidiphilum infernorum*, a representative of the bacterial phylum Verrucomicrobia. *Biol. Direct* 3, 26.

Jollie, D. R., and Lipscomb, J. D. (1991). Formate dehydrogenase from *Methylosinus trichosporium* OB3b. Purification and spectroscopic characterization of the cofactors. *J. Biol. Chem.* 266, 21853–21863.

Kai, Y., Matsumura, H., and Izui, K. (2003). Phosphoenolpyruvate carboxylase: three-dimensional structure and molecular mechanisms. *Arch. Biochem. Biophys.* 414, 170–179.

Kalyuzhnaya, M. G., Korotkova, N., Crowther, G., Marx, C. J., Lidstrom, M. E., and Chistoserdova, L. (2005). Analysis of gene islands involved in methanopterin-linked C1 transfer reactions reveals new functions and provides evolutionary insights. *J. Bacteriol.* 187, 4607–4614.

Karsten, W. E., Ohshiro, T., Izumi, Y., and Cook, P. F. (2001). Initial velocity, spectral, and pH studies of the serine-glyoxylate aminotransferase from *Hyphomicrobiuim methylovorum. Arch. Biochem. Biophys.* 388, 267–275.

Kelly, D. P., Anthony, C., and Murrell, J. C. (2005). Insights into the obligate methanotroph *Methylococcus capsulatus. Trends Microbiol.* 13, 195–198.

Khadem, A. F., Pol, A., Wieczorek, A., Mohammadi, S. S., Francoijs, K. J., Stunnenberg, H. G., et al. (2011). Autotrophic methanotrophy in Verrucomicrobia: *Methylacidiphilum fumariolicum* SolV uses the Calvin-Benson-Bassham cycle for carbon dioxide fixation. *J. Bacteriol.* 193, 4438–4446.

Kim, H. J., and Graham, D. W. (2001). Effect of oxygen level on simultaneous nitrogenase and sMMO expression and activity in *Methylosinus trichosporium* OB3b and its sMMoC mutant, PP319: aerotolerant N2 fixation in PP319. *FEMS Microbiol. Lett.* 201, 133–138.

Kim, H. J., Graham, D. W., DiSpirito, A. A., Alterman, M. A., Galeva, N., Larive, C. K., et al. (2004). Methanobactin, a copper-acquisition compound from methane-oxidizing bacteria. *Science* 305, 1612–1615.

Krentz, B. D., Mulheron, H. J., Semrau, J. D., Dispirito, A. A., Bandow, N. L., Haft, D. H., et al. (2010). A comparison of methanobactins from *Methylosinus trichosporium* OB3b and *Methylocystis* strain Sb2 predicts methanobactins are synthesized from diverse peptide precursors modified to create a common core for binding and reducing copper ions. *Biochemistry* 49, 10117–10130.

Large, P. J., and Quayle, J. R. (1963). Microbial growth on C(1) compounds. 5. Enzyme activities in extracts of *Pseudomonas* AM1. *Biochem. J.* 87, 386–396.

Larkin, M. A., Blackshields, G., Brown, N. P., Chenna, R., McGettigan, P. A., McWilliam, H., et al. (2007). Clustal W and Clustal X version 2.0. *Bioinformatics* 23, 2947–2948.

Lawrence, A. J., and Quayle, J. R. (1970). Alternative carbon assimilation pathways in methane-utilizing bacteria. *J. Gen. Microbiol.* 63, 371–374.

Letunic, I., and Bork, P. (2007). Interactive Tree Of Life (iTOL): an online tool for phylogenetic tree display and annotation. *Bioinformatics* 23, 127–128.

Li, H., and Durbin, R. (2009). Fast and accurate short read alignment with Burrows-Wheeler transform. *Bioinformatics* 25, 1754–1760.

Liepman, A. H., and Olsen, L. J. (2001). Peroxisomal alanine: glyoxylate aminotransferase (AGT1) is a photorespiratory enzyme with multiple substrates in *Arabidopsis thaliana. Plant J.* 25, 487–498.

Lloyd, J. S., Finch, R., Dalton, H., and Murrell, J. C. (1999). Homologous expression of soluble methane monooxygenase genes in *Methylosinus trichosporium* OB3b. *Microbiology* 145, 461–470.

Matsumura, H., Xie, Y., Shirakata, S., Inoue, T., Yoshinaga, T., Ueno, Y., et al. (2002). Crystal structures of C4 form maize and quaternary complex of *E. coli* phosphoenolpyruvate carboxylases. *Structure* 10, 1721–1730.

Mortazavi, A., Williams, B. A., McCue, K., Schaeffer, L., and Wold, B. (2008). Mapping and quantifying mammalian transcriptomes by RNA-Seq. *Nat. Methods* 5, 621–628.

Murrell, C. J., and Dalton, H. (1983a). Ammonia assimilation in *Methylococcus capsulatus* (Bath) and other obligate methanotrophs. *Microbiology* 129, 1197–1206.

Murrell, J. C., and Dalton, H. (1983b). Purification and properties of glutamine synthetase from *Methylococcus capsulatus* (Bath). *J. Gen. Microbiol.* 129, 1187–1196.

Murrell, J. C., and Jetten, M. S. M. (2009). The microbial methane cycle. *Environ. Microbiol. Rep.* 1, 279–284.

Murrell, J. C., McDonald, I. R., and Gilbert, B. (2000). Regulation of expression of methane monooxygenases by copper ions. *Trends Microbiol.* 8, 221–225.

Naguib, M. (1979). Alternative carboxylation reactions in type II methylotrophs and the localization of carboxylase activities in the intracytoplasmic membranes. *Z. Allg. Mikrobio.* 19, 333–342.

Newaz, S. S., and Hersh, L. B. (1975). Reduced nicotinamide adenine dinucleotide-activated phosphoenolpyruvate carboxylase in *Pseudomonas* MA: potential regulation between carbon assimilation and energy production. *J. Bacteriol.* 124, 825–833.

Nielsen, A. K., Gerdes, K., and Murrell, J. C. (1997). Copper-dependent reciprocal transcriptional regulation of methane monooxygenase genes in *Methylococcus capsulatus* and *Methylosinus trichosporium. Mol. Microbiol.* 25, 399–409.

Oakley, C. J., and Murrell, J. C. (1988). nifH genes in the obligate methane oxidizing bacteria. *FEMS Micriobiol. Lett.* 49, 53–57.

Oldenhuis, R., Oedzes, J. Y., van der Waarde, J. J., and Janssen, D. B. (1991). Kinetics of chlorinated hydrocarbon degradation by *Methylosinus trichosporium* OB3b and toxicity of trichloroethylene. *Appl. Environ. Microbiol.* 57, 7–14.

Park, S., Hanna, L. M., Taylor, R. T., and Droege, M. W. (1991). Batch cultivation of *Methylosinus trichosporium* OB3b. I: production of soluble methane monooxygenase. *Biotechnol. Bioeng.* 38, 423–433.

Park, S., Shah, N. N., Taylor, R. T., and Droege, M. W. (1992). Batch cultivation of *Methylosinus trichosporium* OB3b: II. production of particulate methane monooxygenase. *Biotechnol. Bioeng.* 40, 151–157.

Patel, R. N., Hoare, S. L., and Hoare, D. S. (1979). (14C) acetate assimilation by obligate methylotrophs, *Pseudomonas methanica* and *Methylosinus trichosporium. Antonie Van Leeuwenhoek* 45, 499–511.

Patel, R. N., Hou, C. T., Derelanko, P., and Felix, A. (1980). Purification and properties of a heme-containing aldehyde dehydrogenase from *Methylosinus trichosporium. Arch. Biochem. Biophys.* 203, 654–662.

Peyraud, R., Kiefer, P., Christen, P., Massou, S., Portais, J. C., and Vorholt, J. A. (2009). Demonstration of the ethylmalonyl-CoA pathway by using 13C metabolomics. *Proc. Natl. Acad. Sci. U.S.A.* 106, 4846–4851.

Phelps, P. A., Agarwal, S. K., Speitel, G. E. Jr., and Georgiou, G. (1992). *Methylosinus trichosporium* OB3b mutants having constitutive expression of soluble methane monooxygenase in the presence of high levels of copper. *Appl. Environ. Microbiol.* 58, 3701–3708.

Pieja, A. J., Sundstrom, E. R., and Criddle, C. S. (2011). Poly-3-hydroxybutyrate metabolism in the type II methanotroph *Methylocystis parvus* OBBP. *Appl. Environ. Microbiol.* 77, 6012–6019.

Rasche, M. E., Havemann, S. A., and Rosenzvaig, M. (2004). Characterization of two methanopterin biosynthesis mutants of *Methylobacterium extorquens* AM1 by use of a tetrahydromethanopterin bioassay. *J. Bacteriol.* 5, 1565–1570.

Reshetnikov, A. S., Rozova, O. N., Khmelenina, V. N., Mustakhimov, I. I., Beschastny, A. P., Murrell, J. C., et al. (2008). Characterization of the pyrophosphate-dependent 6-phosphofructokinase from Methylococcus capsulatus Bath. *FEMS Microbiol. Lett.* 288, 202–210.

Rozova, O. N., Khmelenina, V. N., and Trotsenko, Y. A. (2012). Characterization of recombinant PPi-dependent 6-phosphofructokinases

from *Methylosinus trichosporium* OB3b and *Methylobacterium nodulans* ORS 2060. *Biochemistry Mosc.* 77, 288–295.

Schmidt, S., Christen, P., Kiefer, P., and Vorholt, J. A. (2010). Functional investigation of methanol dehydrogenase-like protein XoxF in *Methylobacterium extorquens* AM1. *Microbiology* 156, 2575–2586.

Schulz, M. H., Zerbino, D. R., Vingron, M., and Birney, E. (2012). Oases: robust de novo RNA-seq assembly across the dynamic range of expression levels. *Bioinformatics* 28, 1086–1092.

Schwartz, A. C., Gockel, G., Gross, J., Moritz, B., and Meyer, H. E. (2004). Relations and functions of dye-linked formaldehyde dehydrogenase from *Hyphomicrobium zavarzinii* revealed by sequence determination and analysis. *Arch. Microbiol.* 182, 458–466.

Semrau, J. D., DiSpirito, A. A., and Yoon, S. (2010). Methanotrophs and copper. *FEMS Microbiol. Rev.* 34, 496–531.

Shishkina, V. N., and Trotsenko, Y. A. (1979). Pathways of ammonia assimilation in obligate methane utilizers. *FEMS Microbiol. Lett.* 5, 187–191.

Shishkina, V. N., and Trotsenko, Y. A. (1982). Multiple enzymatic lesions in obligate methanotrophic bacteria. *FEMS Microbiol. Lett.* 13, 237–242.

Skovran, E., Palmer, A. D., Rountree, A. M., Good, N. M., and Lidstrom, M. E. (2011). XoxF is required for expression of methanol dehydrogenase in *Methylobacterium extorquens* AM1. *J. Bacteriol.* 193, 6032–6038.

Stein, L. Y., Bringel, F., DiSpirito, A. A., Han, S., Jetten, M. S., Kalyuzhnaya, M. G., et al. (2011). Genome sequence of the methanotrophic alphaproteobacterium *Methylocystis* sp. strain Rockwell (ATCC 49242). *J. Bacteriol.* 193, 2668–2669.

Stein, L. Y., Yoon, S., Semrau, J. D., Dispirito, A. A., Crombie, A., Murrell, J. C., et al. (2010). Genome sequence of the obligate methanotroph *Methylosinus trichosporium* strain OB3b. *J. Bacteriol.* 192, 6497–6498.

Stolyar, S., Costello, A. M., Peeples, T. L., and Lidstrom, M. E. (1999). Role of multiple gene copies in particulate methane monooxygenase activity in the methane-oxidizing bacterium *Methylococcus capsulatus* Bath. *Microbiology* 145, 1235–1244.

Strom, T., Ference, T., and Quayle, J. R. (1974). The carbon assimilation pathways of *Methylococcus capsulatus*, *Pseudomonas methanica*, and *Methylosinus trichosporium* (OB3B) during growth on methane. *Biochemistry* 144, 465–476.

Takahashi, R., Ohmori, T., Watanabe, K., and Tokuyama, T. (1993). Phosphoenolpyruvate carboxylase of an ammonia-oxidizing chemoautotrophic bacterium, *Nitrosomonas europaea* ATCC 25978. *J. Ferment. Bioeng.* 76, 232–234.

Toyama, H., Chistoserdova, L., and Lidstrom, M. E. (1997). Sequence analysis of pqq genes required for biosynthesis of pyrroloquinoline quinone in *Methylobacterium extorquens* AM1 and the purification of a biosynthetic intermediate. *Microbiology* 143, 595–602.

Trotsenko, Y. A. (1976). "Isolation and characterization of obligate methanotrophic bacteria," in *Microbial Production and Utilization of Gases*, eds H. G. Schlegel, G. Gottschalk, and N. Pfennig (Gottingen: Goltze), 329–336.

Trotsenko, Y. A., and Murrell, J. C. (2008). Metabolic aspects of aerobic obligate methanotrophy. *Adv. Appl. Microbiol.* 63, 183–229.

Vallenet, D., Labarre, L., Rouy, Z., Barbe, V., Bocs, S., Cruveiller, S., et al. (2006). MaGe: a microbial genome annotation system supported by synteny results. *Nucleic Acids Res.* 10, 53–65.

Vorholt, J. A., Chistoserdova, L., Stolyar, S. M., Thauer, R. K., and Lidstrom, M. E. (1999). Distribution of tetrahydromethanopterin-dependent enzymes in methylotrophic bacteria and phylogeny of methenyl tetrahydromethanopterin cyclohydrolases. *J. Bacteriol.* 181, 5750–5757.

Vorholt, J. A., Marx, C. J., Lidstrom, M. E., and Thauer, R. K. (2000). Novel formaldehyde-activating enzyme in *Methylobacterium extorquens* AM1 required for growth on methanol. *J. Bacteriol.* 182, 6645–6650.

Wadzink, A. M., and Ribbons, D. W. (1975). Utilization of acetate by *Methanomonas methanooxidans*. *J. Bacteriol.* 123, 380–381.

Ward, N., Larsen, O., Sakwa, J., Bruseth, L., Khouri, H., Durkin, A. S., et al. (2004). Genomic insights into methanotrophy: the complete genome sequence of *Methylococcus capsulatus* (Bath). *PLoS Biol.* 2:e303. doi:10.1371/journal.pbio.0020303

Weaver, T. L., Patrick, M. A., and Dugan, P. R. (1975). Whole-cell and membrane lipids o the methanotrophic bacterium *Methylosinus trichosporium*. *J. Bacteriol.* 124, 602–605.

Whittenbury, R., Phillips, K. C., and Wilkinson, J. F. (1970). Enrichment, isolation and some properties of methane-utilizing bacteria. *J. Gen. Microbiol.* 61, 205–218.

Williams, A. M. (1988). *The Biochemistry and Physiology of Poly-beta-Hydroxybutyrate Metabolism in Methylosinus trichosporium OB3b.* Ph.D. thesis, Biotechnology Centre, Cranfield Institute of Technology, Cranfield.

Wilson, S. M., Gleisten, M. P., and Donohue, T. J. (2008). Identification of proteins involved in formaldehyde metabolism by *Rhodobacter sphaeroides*. *Microbiology* 154, 296–305.

Yamada, K., Shimoda, M., and Okura, I. (1991). Purification and characterization of methanol dehydrogenase from *Methylosinus trichosporium* (OB3b). *J. Mol. Catal.* 73, 381–386.

Yang, S., Matsen, J. B., Konopka, M., Green-Saxena, A., Clubb, J., Sadilek, M., et al. (2013). Global molecular analyses of methane metabolism in methanotrophic Alphaproteobacterium, *Methylosinus trichosporium* OB3b. Part II. Metabolomics and 13C-labeling study. *Front. Microbiol. 4:70* doi:10.3389/fmicb.2013.00070

Yoon, S., Kraemer, S. M., DiSpirito, A. A., and Semrau, J. D. (2010). An assay for screen microbial cultures for chalkophore production. *Environ. Microbiol.* 2, 295–303.

Zerbino, D. R., and Birney, E. (2008). Velvet: algorithms for de novo short read assembly using de Bruijn graphs. *Genome Res.* 18, 821–829.

Conflict of Interest Statement: The authors declare that the research was conducted in the absence of any commercial or financial relationships that could be construed as a potential conflict of interest.

Received: 01 January 2013; paper pending published: 28 January 2013; accepted: 17 February 2013; published online: 03 April 2013.

Citation: Matsen JB, Yang S, Stein LY, Beck D and Kalyuzhnaya MG (2013) Global molecular analyses of methane metabolism in methanotrophic alphaproteobacterium, Methylosinus trichosporium OB3b. Part I: transcriptomic study. Front. Microbiol. ***4****:40. doi:10.3389/fmicb.2013.00040*

This article was submitted to Frontiers in Microbiological Chemistry, a specialty of Frontiers in Microbiology.

frontiers in
MICROBIOLOGY

ORIGINAL RESEARCH ARTICLE
published: 03 April 2013
doi: 10.3389/fmicb.2013.00070

Global molecular analyses of methane metabolism in methanotrophic Alphaproteobacterium, *Methylosinus trichosporium* OB3b. Part II. metabolomics and 13C-labeling study

Song Yang[1], Janet B. Matsen[1], Michael Konopka[1], Abigail Green-Saxena[2], Justin Clubb[1], Martin Sadilek[3], Victoria J. Orphan[4], David Beck[1,5] and Marina G. Kalyuzhnaya[6]*

[1] *Department of Chemical Engineering, University of Washington, Seattle, WA, USA*
[2] *Division of Biology, California Institute of Technology, Pasadena, CA, USA*
[3] *Department of Chemistry, University of Washington, Seattle, WA, USA*
[4] *Division of Geological and Planetary Sciences; California Institute of Technology, Pasadena, CA, USA*
[5] *eScience Institute, University of Washington, Seattle, WA, USA*
[6] *Department of Microbiology, University of Washington, Seattle, WA, USA*

Edited by:
Amy V. Callaghan, University of Oklahoma, USA

Reviewed by:
Alan A. DiSpirito, Ohio State University, USA
Amy V. Callaghan, University of Oklahoma, USA

****Correspondence:***
Marina G. Kalyuzhnaya, Department of Microbiology, University of Washington, Benjamin Hall IRB RM 455, 616 NE Northlake Place, Seattle, WA 98105, USA.
e-mail: mkalyuzh@uw.edu

In this work we use metabolomics and ^{13}C-labeling data to refine central metabolic pathways for methane utilization in *Methylosinus trichosporium* OB3b, a model alphaproteobacterial methanotrophic bacterium. We demonstrate here that similar to non-methane utilizing methylotrophic alphaproteobacteria the core metabolism of the microbe is represented by several tightly connected metabolic cycles, such as the serine pathway, the ethylmalonyl-CoA (EMC) pathway, and the citric acid (TCA) cycle. Both *in silico* estimations and stable isotope labeling experiments combined with single cell (NanoSIMS) and bulk biomass analyses indicate that a significantly larger portion of the cell carbon (over 60%) is derived from CO_2 in this methanotroph. Our^{13} C-labeling studies revealed an unusual topology of the assimilatory network in which phosph(enol) pyruvate/pyruvate interconversions are key metabolic switches. A set of additional pathways for carbon fixation are identified and discussed.

Keywords: methanotrophic proteobacteria, serine cycle, ethylmalonyl-CoA pathway in methanotrophs, metabolic fluxes labeling

INTRODUCTION

Microbial oxidation of methane is one of the key elements of the global carbon cycle. The ability to oxidize methane has been demonstrated in two classes of Proteobacteria, Alpha, and Gamma. *Methylosinus trichosporium* OB3b was first described by Whittenbury et al. (1970) and has served as a model system for the investigation of methane utilization in obligate alphaproteobacterial methanotrophs for decades (Lawrence and Quayle, 1970; Strom et al., 1974; Cornish et al., 1984; Jollie and Lipscomb, 1991; Park et al., 1991, 1992; DiSpirito et al., 1998; Lontoh and Semrau, 1998; Gilbert et al., 2000; Trotsenko and Murrell, 2008). While the key metabolic pathways for carbon assimilation in *M. trichosporium* OB3b have been predicted (Strom et al., 1974), several fundamental questions have never been answered, such as how cells regenerate glyoxylate (Anthony, 1982), what is the role of the TCA cycle in methanotrophic metabolism is (Patel et al., 1979; Shishkina and Trotsenko, 1982), and why CO_2 supplementation has a significant positive effect on cell growth (Park et al., 1991, 1992). A draft genome of *M. trichosporium* OB3b has recently been generated (Stein et al., 2010), providing a genetic framework for characterization of the methanotrophy. In this work, models of carbon assimilation pathways in *M. trichosporium* OB3b predicted by biochemical characterization (Strom et al., 1974; Trotsenko and Murrell, 2008) and global gene expression analysis (Matsen et al., 2013) are further tested by metabolomic and ^{13}C-labeled studies.

RESULTS AND DISCUSSION

GROWTH PARAMETERS AND INCORPORATION FROM METHANE AND CO_2 VIA ^{13}C-LABELING EXPERIMENTS

A strong dependence of the *Methylosinus trichosporium* OB3b growth upon CO_2 supplementation has been previously demonstrated (Park et al., 1991, 1992). Similarly, a lag-period (up to 24 h) was observed in methane supplemented cultures inoculated at low cell density ($OD_{600} < 0.05$) at ambient concentrations of CO_2. The initial lag-period was shortened by the addition of CO_2 (5% of head space). Furthermore, the specific growth rate was also increased to $0.057 \pm 0.002\,h^{-1}$ (versus $\mu = 0.038 \pm 0.004\,h^{-1}$, in cultures grown without additional CO_2). CO_2 supplementation did not have any significant effect on the final cell density (data not shown).

It has been speculated that the positive effect of CO_2 is a result of the high demand of the serine pathway for CO_2 (Park et al., 1991, 1992). However, addition of extra CO_2 does not affect the growth of non-methane utilizing methylotrophs such as *Methylobacterium extorquens* AM1 with the serine pathway for carbon utilization (Yanfen Fu, Mary E. Lidstrom personal communication).

Several putative carboxylating systems were identified in the *M. trichosporium* OB3b genome: phosphoenolpyruvate carboxylase (Ppc); two propionyl-CoA carboxylases; crotonyl-CoA reductase (*ccr*); NAD(P)-dependent malic enzyme (*mae*), acetyl-CoA carboxylase (*accABD*), phosphoribosylaminoimidazole carboxylase, pyruvate carboxylase (*pcx*), and a putative 2-oxoacid ferredoxin oxidoreductase. To investigate the fate of CO_2 in OB3b, we estimated the C_1-carbon incorporation derived from methane (at the level of methylene-tetrahydrofolate, MeH4F) and/or bicarbonate into biomass using stable isotope labeling experiments and bulk biomass analyses. For these experiments, cells of *M. trichosporium* OB3b were grown on $^{13}CH_4$ (20%) with or without external CO_2 supplementation (5% atmosphere). A Cameca nanoSIMS 50 L was used to analyze the $^{13}C/^{12}C$ ratio of individual cells from either methane only or methane + carbon dioxide treatment. Individual *M. trichosporium* OB3b cells from the $^{13}CH_4$ treatment showed substantial ^{13}C enrichment ($^{13}C/^{12}C$ ratio of 0.351 ± 0.231), albeit with significant cell-to-cell variation (**Table 1**). Cells grown on $^{13}CH_4$ in the presence of added $^{12}CO_2$ showed less cell-to-cell variation. The amount of ^{13}C-enriched biomass derived from methane dropped dramatically in the presence of elevated CO_2 ($^{13}C/^{12}C$ ratio of 0.134 ± 0.046), reflecting the reincorporation of $^{13}CO_2$ derived from $^{13}CH_4$ when $^{12}CO_2$ is not elevated (Crowther et al., 2008; **Table 1**). Analysis of bulk cell pellets from *M. trichosporium* OB3b cultures incubated under the same conditions ($^{13}CH_4$ with and without elevated $^{12}CO_2$) also showed a similar trend with significantly lower ^{13}C enrichment in biomass from cultures incubated with additional CO_2 relative to treatments with only methane (data not shown). Overall, ^{13}C-labeling data suggest significant assimilation of CO_2 relative to CH_4. Assuming that in the presence of 5% $^{12}CO_2$, no reincorporation of $^{13}CH_4$-derived $^{13}CO_2$ occurred, our results suggest that at least 62% of the assimilated carbon is from CO_2, significantly greater than the 50% observed for *M. extorquens* AM1, a non-methane utilizing serine cycle methylotroph (Peyraud et al., 2011).

ASSIMILATION: *IN SILICO* AND METABOLOMICS STUDIES

The functional organization of the *M. trichosporium* OB3b metabolic network operating during growth on methane has been discussed in an accompanying manuscript by Matsen et al. (2013). A summary of the central metabolism is shown in **Figure 1**. The chemical composition of *M. trichosporium* OB3b (RNA, DNA, protein, polyhydroxybutyrate (PHB), fatty acids, intracellular metabolites) was determined experimentally or taken from available literature (Weaver et al., 1975; Williams, 1988; Guckert et al., 1991; Sun and Wood, 1996; Lloyd et al., 1999; Doronina et al., 2008). Proteins comprise a significant portion of the cell dry weight (55%). The specific amino acid composition of the cell proteins was estimated from RNA-seq data, and the data were used to estimate contribution of C2-C6 intermediates into biomass (shown in **Figure 1**, **Table A1** in Appendix).

As background information for physiological pathways, 27 targeted intermediates involved in the serine cycle, EMC pathway, TCA cycle, and gluconeogenesis were quantified (**Table 2**). Among those, the lowest concentration was observed for propionyl-CoA (108.6 μM) and the highest concentration was 24 mM for glutamate (**Table 2**). Relatively high concentrations of pyruvate (1 mM) and its corresponding amino acid, alanine (4.5 mM) were detected.

METABOLOME ANALYSIS: ^{13}C-LABELING

To address some of the hypotheses generated by gene expression and *in silico* studies and to probe metabolic pathways for methane and CO_2 assimilation in *M. trichosporium* OB3b, we monitored the dynamic ^{13}C-incorporation of intermediates through two different ^{13}C-tracing experiments: switching from $^{12}CH_4$ to $^{13}CH_4$ (*switch* experiment) and spiking $^{13}CO_2$ into cell cultures grown on $^{12}CH_4$ (*spike* experiment) (**Figures 2–4**, **Figure A1** in Appendix). The data generated were compared with predicted pathways for carbon assimilation (summarized in **Figure 1**, see also Matsen et al., 2013). All key intermediates of central pathways could be divided into three groups: (1) efficiently labeled with methane-derived carbon, such as serine, alanine, G6P/F6P, citric acid (**Figures 2A–F**); (2) more efficiently labeled with CO_2-derived carbon, such as malate, fumarate, and succinate (**Figures 2G–I**); and (3) similarly labeled by both CO_2 and CH_4 carbon, such as glutamate (**Figure 2J**).

As was expected during the switch from $^{12}CH_4$ to $^{13}CH_4$, singly labeled serine was generated quickly, demonstrating that any unlabeled glycine rapidly reacted with labeled methylene H_4F (**Figure 3**). Doubly labeled serine appeared later, followed by triply labeled serine. About 25% of the total serine pool (as determined by normalization to total pool of serine) was labeled after 20 min. The low ^{13}C-incorporation suggested a slow uptake that was consistent with the methane consumption rate (in *M. trichosporium* OB3b). The labeling distribution of glycine (herein an indicator of glyoxylate) is shown in **Figures 3B** and **4A**. Around 25% of the glycine (an indicator of glyoxylate) was labeled in 20 min in the switch experiment. Ten percent of the singly label glycine occurred after 10 min in the $^{13}CO_2$ spiking experiments (**Figure 4A**), which is also consistent with regeneration of glyoxylate via the EMC pathway (**Figure 4**).

In addition, two metabolites involved in the EMC pathway [3-OHB-CoA (entry) and propionyl-CoA (exit)] were monitored during CH_4 spike (**Figures 3C,D**). Both compounds were singly

Table 1 | ^{13}Carbon enrichment of *Methylosinus trichosporium* OB3b cells grown on ^{13}C-labeled methane with or without additional supplementation with unlabeled carbon dioxide.

Treatment	$^{13}C/^{12}C$ ratio	Mean	Lower 95%	Upper 95%	Number of cells analyzed
^{13}C-methane	0.351 ± 0.231	0.04	0.264	0.437	30
^{13}C-methane + $^{12}CO_2$ (5%)	0.134 ± 0.046	0.01	0.113	0.155	21

^{13}C of cells grown on unlabeled $^{12}CH_4$ is 55.19± 0.21.

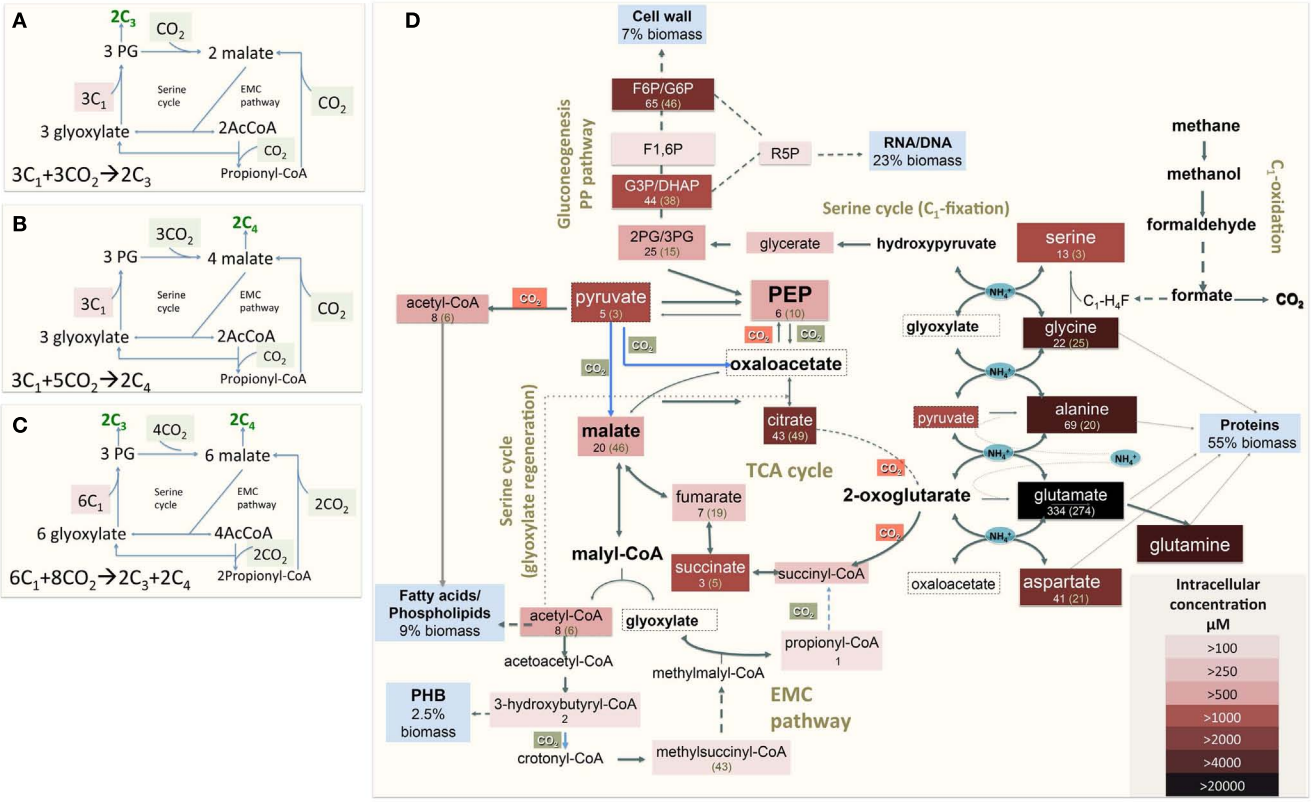

FIGURE 1 | (A) Schematic representation of the serine cycle with the EMC pathway for carbon assimilation [adapted from (Peyraud et al., 2009, 2011)]. **(B)** Schematic representation of the serine cycle with the EMC pathway for carbon assimilation (adapted from Anthony, 2011); **(C)** Schematic representation of the serine cycle with the EMC pathway for carbon assimilation in *Methylosinus trichosporium* OB3b (see description in the text). **(D)** Central metabolism of *Methylosinus trichosporium* OB3b grown on methane as deduced from the genome sequences, transcriptomic, and metabolomic studies. Metabolites boxed were measured. Box color is an indicator of the metabolite pool, with darker colors indicating a larger pool. Numbers under a metabolite names are rates of ^{13}C-carbon incorporation: the first number is the rate of CH_4-derived carbon; number in parentheses- is the rate of CO_2-derived carbon incorporation. PHB-polyhydroxybutyrate; F1, 6P, Fructose-1, 6-bisphosphate; F6P/G6P, fructose-6-phosphate/ glucose-6-phosphate; GAP/DHAP, glyceraldehyde-3-phosphate/ dihydroxyacetone phosphate; 2PG/3PG, 2-phosphoglycerate/ 3-phosphoglycerate.

labeled quickly. These could be generated from one singly labeled acetyl-CoA and one unlabeled acetyl-CoA (**Figure 3E**). The low incorporation for the second carbon can be explained by the additional synthesis of unlabeled acetyl-CoA via the EMC pathway itself. $^{13}CO_2$-carbon was also quickly incorporated into propionyl-CoA (**Figure 4G**). These data also provide metabolic proof of EMC operation in the strain.

About 40% of the total malate pool was labeled throughout the course of the $^{13}CH_4$-experiments (**Figure 3F**). Both methane and CO_2 (generated from $^{13}CH_4$-oxidation) can contribute to the label. However, the rate of CO_2 incorporation into malate and fumarate was high too (**Figures 2G,H**). The possible routes for the CO_2 incorporation into malate labeling are through the serine cycle, EMC pathway and carboxylation of pyruvate (**Figure 1**). As shown in **Figure 4D**, singly labeled malate increased to around 20% after 0.5 min and remained at a similarly high percentage throughout the experiment, adding support to the hypothesis that the carboxylation via the EMC pathway and pyruvate contributes significantly to the pool of malate in addition to PEP-carboxylation. The labeling pattern of fumarate favors the hypothesis of the EMC pathway is a major source of malate. However, it should be noted that the $^{13}CO_2$-fumarate labeling may be explained by the reversible reaction catalyzed by *fumC*. On the other hand, the rate of CO_2 incorporation into aspartate (herein an indicator of oxaloacetate) was slow compared to malate (**Figures 4D,E**). The rates of C_1-incorporation ($^{13}CH_4$-derived carbon) into malate and aspartate are almost identical in the switch over experiment (**Figures 3F,H**). Thus, the much slower rate of CO_2 incorporation into aspartate at the early time points could not be attributed only to the large pool of the compound. The labeling patterns of malate and aspartate during $^{13}CO_2$-spikes indicate that at least one of the compounds (most likely malate) comes from alternative sources. Doubly labeled malate was observed throughout the experiment (**Figure 4D**). The reversible conversions of malyl-CoA to malate and malate to fumarate may result in fumarate scrambling and contribute to doubly labeled malate. However, $^{13}CO_2$ is incorporated into fumarate and succinate more efficiently than C_1-labeled carbon (**Figures 2H,I**).

Table 2 | Intracellular pool of key metabolites in *M. trichosporium* OB3b.

Metabolite	Concentration μM	SD
SERINE CYCLE AND ETHYLMALONYL-CoA PATHWAY		
Serine	1504.9	142.0
Glycine	4631.9	484.1
Glycerate	365.4	41.8
Phosphoglycerate	811.9	118.3
3-Hydroxybutyryl-CoA	185.2	54.3
Methylsuccinic acid	119.7	37.6
Phosphoenolpyruvate	661.5	103.4
Propionyl-CoA	108.6	26.5
TCA CYCLE AND RELATED AMINO ACIDS		
Acetyl-CoA	519.3	162.9
Citrate	3149.2	528.1
Fumarate	400.5	85.7
Malate	950.2	154.7
Succinate	1304.4	323.9
Succinyl-CoA	320.0	80.7
Aspartate	1998.0	481.7
Glutamate	24034.1	4060.4
Glutamine	9864.0	2457.3
GLUCONEOGENESIS/PYRUVATE-PEP AND RELATED AMINO ACIDS		
Fructose-1,6-bisphosphate	136.4	37.6
Fructose-6-phosphate/Glucose-6-phosphate	2836.0	654.3
Glyceraldehyde-3-phosphate/ Dihydroxyacetonephosphate	1968.6	509.6
Phosphoenolpyruvate	661.5	103.4
Pyruvate	1134.7	299.3
Ribulose-5-phosphate/Ribose-5-phosphate	140.6	57.1
Alanine	4495.5	766.2

Together the presented data indicate that the ECM pathway may serve as a significant source of intracellular malate.

According to current pathway prediction, both acetyl-CoA and glyoxylate are generated from malyl-CoA. The labeling rate of these two compounds was similar during the switch over experiments (**Figures 3B,E**). The incorporation of CO_2-labeling into intracellular acetyl-CoA was slow compared to the ^{13}C-carbon label that originated from methane. The labeling pattern of acetyl-CoA is similar to other intermediates of the serine cycle generated upstream from phosphoenolpyruvate, including all intermediates of gluconeogenesis/PPP, and pyruvate/alanine (**Figures 3C,I**; **Figures A1D** and **A2A-D** in Appendix). As a rule, these intermediates were labeled with methane-derived carbon faster than with CO_2 (**Figure 2**). This suggests that significant flux of carbon assimilated as MeH_4F is incorporated into biomass via gluconeogenesis/PPP and that pyruvate contributes to at least 1/3 of the intracellular pool of acetyl-CoA. Such conversion seems to be essential in the strain, which is known to have high demand for acetyl-CoA as a key metabolite for membrane and PHB biosynthesis.

Singly and doubly $^{13}C_1$-labeled citric acid and glutamate were generated quickly, followed by triply and quadruple labeled variants (**Figures 3** and **4**). About 32% of the total pool of citric acid was labeled throughout the experiments demonstrating significant flux through the forward TCA cycle. During $^{13}CO_2$ experiments, singly labeled citric acid appeared quickly at the early time points most likely as a result of CO_2 incorporation into oxaloacetate (**Figure 4F**). The concentration of doubly labeled citric acid eventually increased to 15%, yet triply labeled citric acid (the limit of detection of citric acid was less than 0.2 pmol on column) was not clearly detected within 20 min. For glutamate, singly and doubly labeled patterns rose slowly due to its high concentration (**Figure 4H**). However, 4.7% of the glutamate pool (567 ± 268 μM) was triply labeled after 20 min. ^{13}C-labeling data indicate that cells could produce α-ketoglutarate from succinyl-CoA. The genome analysis suggests one system that may perform this function, namely related to 2-oxoacid ferredoxin oxidoreductase (METTOv1_1080004). This gene is expressed (Matsen et al., 2013). The presence of a partially reversible TCA has never been predicted for methanotrophic bacteria and represents an interesting subject for follow-up studies.

CONCLUSION

In this work we used ^{13}C-labeling to test and refine the previous genome/transriptome based reconstruction of the central metabolic pathways in *Methylosinus trichosporium* OB3b grown on methane (Matsen et al., 2013). While some metabolic functions correlate well with previous enzymatic and genetic studies, several novel functions are newly predicted. The major outcomes of our work are listed below:

1. *M. trichosporium* OB3b uses the EMC variant of the serine cycle for carbon assimilation. Both *in silico* and *in vivo* labeling data indicate that a significant fraction of biomass comes from C_4-metabolites (after carboxylation step). Thus the overall balance of the pathway is shifted to a higher CO_2-assimilation mode, whereby eight molecules of CO_2 are consumed per six molecules of MeH4F (**Figure 1C**). The data also suggest that a significant fraction of methane oxidized to CO_2 is incorporated back via the EMC pathway. Thus this methanotroph differs from facultative methanol utilizers with respect to overall CO_2 assimilation. Type II methanotrophs may represent a better system for C_1-based commercial production of chemicals than serine cycle methylotrophs, as the methanotrophs will reincorporate more CO_2 per unit of substrate oxidized.
2. Both genomic and trancriptomic data predict a variety of reactions at the PEP-pyruvate-oxaloacetate node. Metabolomic data indicate that the metabolic interconversions play an important role in the distribution of carbon flux between the major metabolic pathways. A significant fraction of PEP is converted to pyruvate, which serves as a precursor for alanine and is also used as an acceptor in two anaplerotic CO_2-fixation reactions: pyruvate carboxytransferase and malic enzyme. ^{13}C-labeling data strongly suggest that a part of the intracellular pool of the acetyl-CoA comes from pyruvate most likely via pyruvate dehydrogenase. The contribution of pyruvate to acetyl-CoA has never been discussed before, as it was assumed that the serine cycle refills the cellular needs for this intermediate.

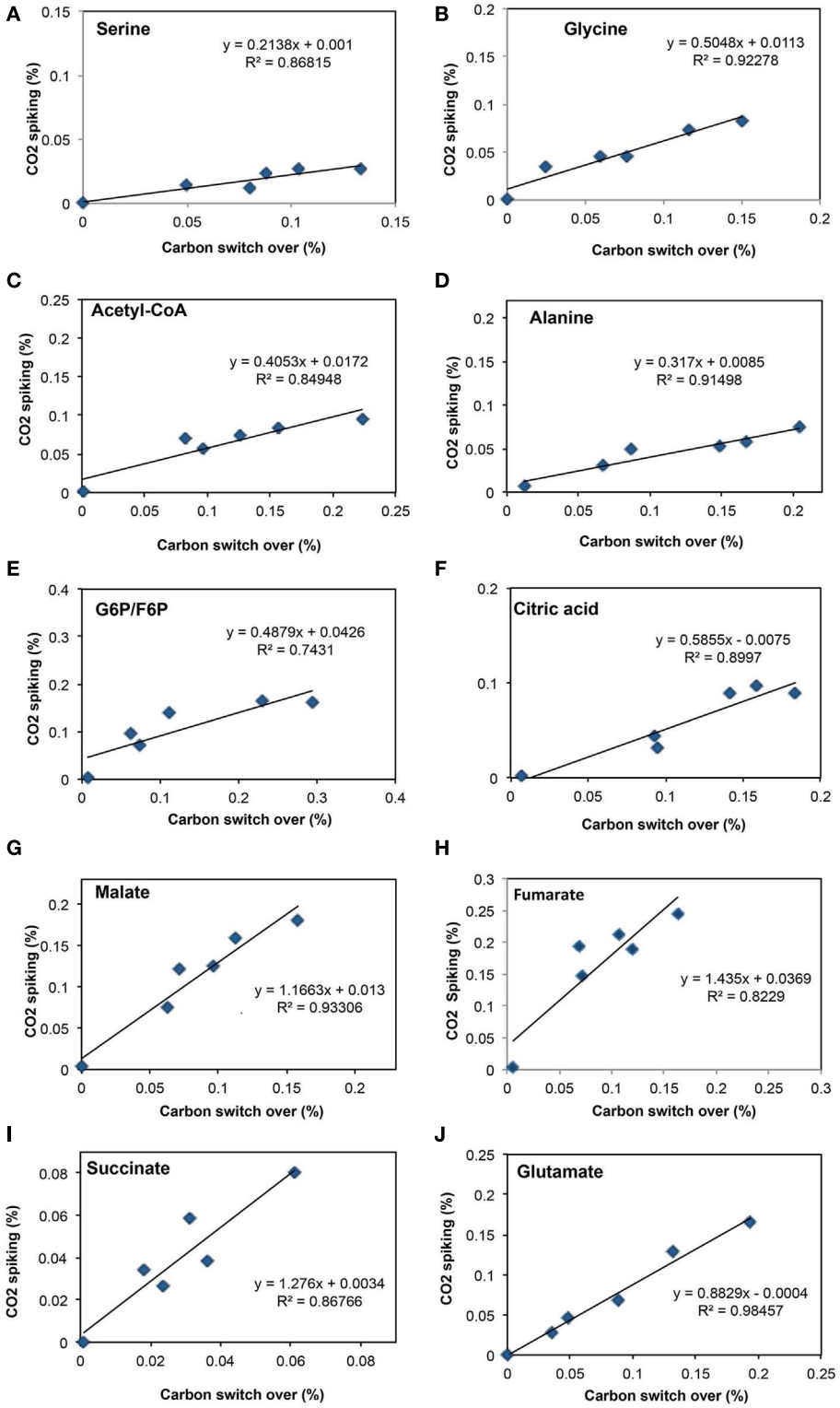

FIGURE 2 | Comparison of total ^{13}C-incorporation (%) between switch from $^{12}CH_4$ to $^{13}CH_4$ versus that of $^{13}CO_2$ spiking in a time course (0, 1, 2, 5, 10, 20 min). In each panel, the total 13C-incorporation under carbon switchover and CO_2 spiking conditions are plotted against each other for each time point. The six points corresponding to 0, 1, 2, 4, 10, and 20 min were best fit and the slope of the resulting line used to estimate the relative rate of incorporation into serine **(A)**, glycine **(B)**, acetyl-CoA **(C)**, alanine **(D)**, glucose-6-phosphate/fructose-6-phosphate **(E)**, citric acid **(F)**, malate **(G)**, fumarate **(H)**, succinate **(I)**, and glutamate **(J)**.

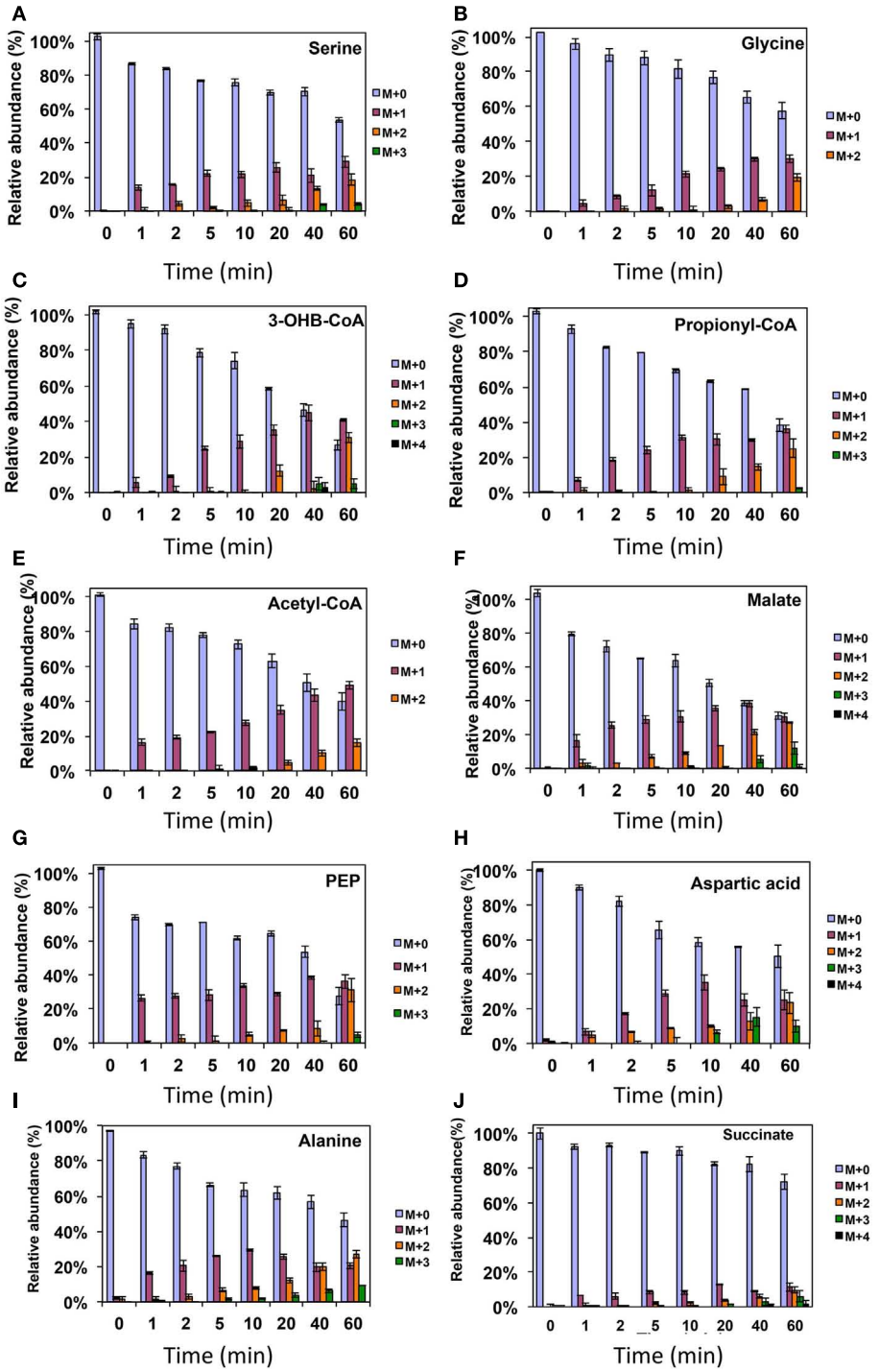

FIGURE 3 | ^{13}C-incorporation during the switch from $^{12}CH_4$ to $^{13}CH_4$ in *Methylosinus trichosporium* OB3b. **(A)** ^{12}C/^{13}C-isotopomer distributions of serine **(A)**, glycine **(B)**, 3-hydroxybutyric acid **(C)**, propionyl-CoA **(D)**, acetyl-CoA **(E)**, malate **(F)**, phosphoenolpyruvate **(G)**, aspartic acid **(H)**, alanine **(I)**, and succinate **(J)**. Additional data are shown in **Figure A1** in Appendix. M + 0 represented non-labeled compound, M + 1 represented compound with one ^{13}C-label, M + 2 represented compound with two ^{13}C-labels and so on.

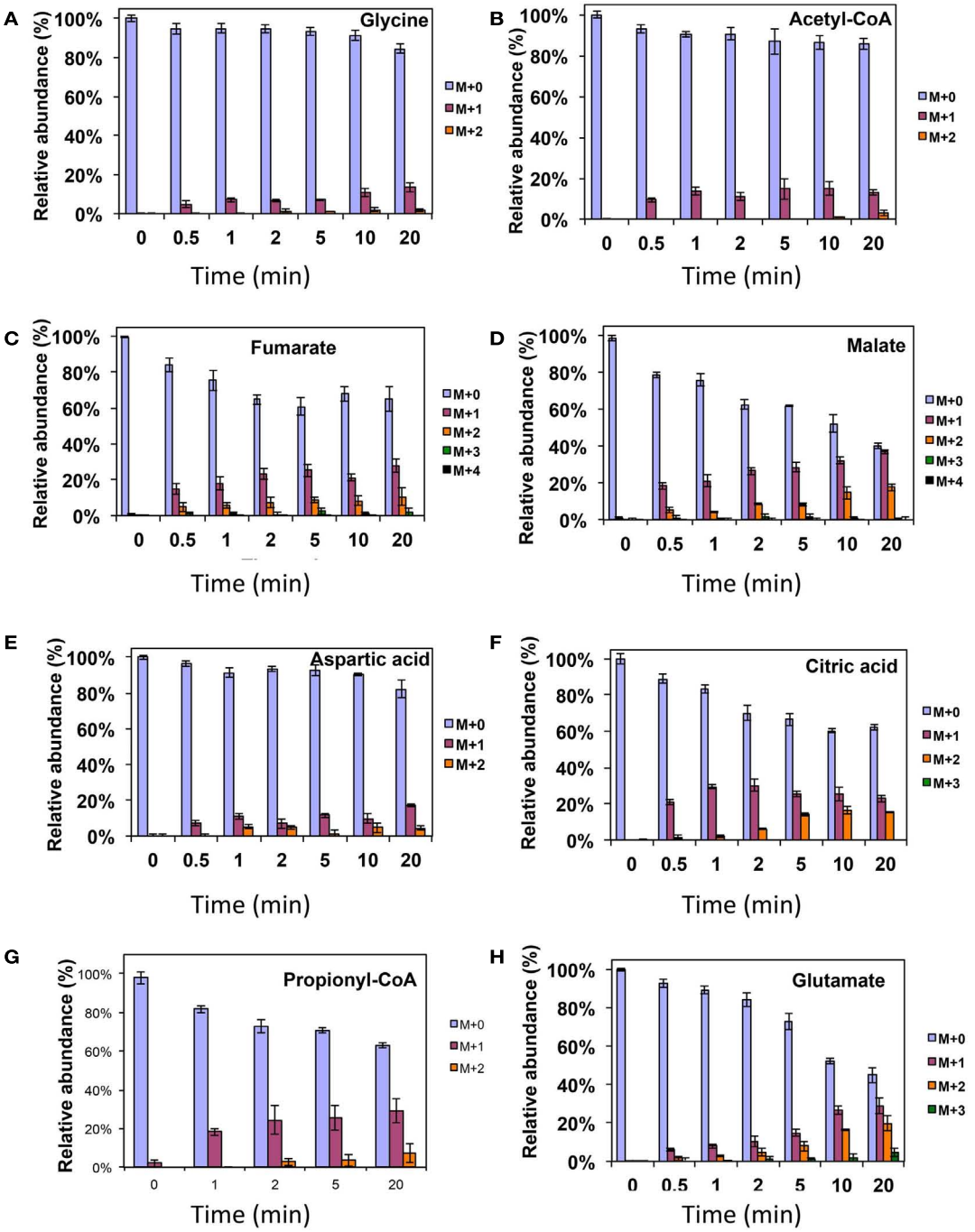

FIGURE 4 | ^{13}C-incorporation during $^{12}CO_2$ spiking in *Methylosinus trichosporium* OB3b grown on $^{12}CH_4$. ^{12}C/^{13}C-isotopomer distributions of glycine **(A)**, acetyl-CoA **(B)**, fumarate **(C)**, malate **(D)**, aspartic acid **(E)**, citric acid **(F)**, propionyl-CoA **(G)**, glutamate **(H)**. Additional data are shown in **Figure A2** in Appendix. $M+0$ represented non-labeled compound, $M+1$ represented compound with one ^{13}C-label, $M+2$ represented compound with two ^{13}C-labels and so on.

3. A significant fraction of intracellular malate comes from the EMC pathway. The data suggest that the serine cycle is split into two functional branches that have different metabolic control. The first, labeled as "C1-fixation" part (**Figure 1**), includes all steps from glycine to PEP. This branch of the assimilatory pathway contributes to 53% of biomass. Most of the C1-carbon incorporated at first step of the branch is directed to gluconeogenesis (RNA/DNA, cell wall biosynthesis) and amino acid (serine, cysteine, tryptophan tyrosine, and phenylalanine) biosynthesis. The second part of the serine cycle (named

"glyoxylate regeneration" in **Figure 1**) overlaps with the EMC pathway. Our data suggest the EMC pathway contributes significantly to replenish the intermediates (mostly malate, acetyl-CoA, and glyoxylate) of this part of the assimilation.

EXPERIMENTAL PROCEDURES

STRAIN AND CULTIVATION CONDITIONS

Methylosinus trichosporium strain OB3b was kindly provided by Dr. Lisa Stein. The culture was grown in 250 mL glass bottles on modified NMS that contained the following contents (Whittenbury et al., 1970): 1 g KNO_3, 1 g $MgSO_4{\cdot}7H_2O$, 0.134 g $CaCl_2{\cdot}2H_2O$, 0.25 g KH_2PO_4, 0.7 g $Na_2HPO_4{\cdot}12H_2O$, and 2 mL of trace elements solution. The trace elements solution contained 0.5 g Na_2-EDTA, 1.0 g $FeSO_4{\cdot}7H_2O$, 0.75 g Fe-EDTA, 0.8 g $ZnSO_4{\cdot}7H_2O$, 0.005 g $MnCl_2{\cdot}4H_2O$, 0.03 g H_3BO_3, 0.05 g $CoCl_2{\cdot}6H_2O$, 0.4 g Cu-EDTA, 0.6 g $CuCl_2{\cdot}2H_2O$, 0.002 g $NiCl_2{\cdot}6H_2O$, and 0.05 g $Na_2MoO_4{\cdot}2H_2O$ in 1 L of water. The bottles were sealed with rubber stoppers and aluminum caps. 50 mL of methane were added to the 200 mL headspace. If necessary, 10 mL of CO_2 were added to the headspace. Bottles were shaken at 250 RPM at 30˚C for 1–4 days.

GROWTH PARAMETERS AND METHANE CONSUMPTION RATE MEASUREMENTS

Methane consumption rates and cell density (OD_{600}) were measured in triplicate as cultures grew. Methane measurements were collected on a Shimadzu Gas Chromatograph GC-14A, using FID detection with helium as the carrier gas. Concentrations were deduced from standard curves. OD_{600} was measured on a Beckman DU®640B spectrophotometer in plastic 1.5 mL cuvettes with a 1 cm path length.

$^{13}CO_2$ AND $^{13}CH_4$ LABELING EXPERIMENTS FOR SINGLE CELLS AND BULK BIOMASS: EA-IRMS AND NanoSIMS ANALYSES

Experiments to determine the relative contributions of methylene H_4F (produced from methane) and CO_2 to labeled biomass were performed by modifying a previous method (Crowther et al., 2008). Cells were grown in NMS medium supplemented with either 20% $^{13}CH_4$, 20% $^{12}CH_4$, 20% $^{13}CH_4$ and 5% $^{12}CO_2$, or 20% $^{12}CH_4$ and 5% $^{13}CO_2$. After initial incubations at the described gas mixtures, cell cultures ($OD_{600} = 0.4$) were diluted (1:50) with fresh medium and transferred into new vials containing the same gases. For bulk and single cell NanoSIMS measurements, cells were harvested at $OD_{600} = 0.4$.

BULK $\delta^{13}C$ ISOTOPIC ANALYSIS VIA ELEMENTAL ANALYSIS COUPLED TO ISOTOPIC RATIO MASS SPECTROMETRY

For bulk elemental analysis coupled to isotopic ratio mass spectrometry (EA-IRMS) measurements, harvested cell pellets were initially frozen at −80˚C, then lyophilized prior to $\delta^{13}C$ analysis. As these were isotopically enriched samples, cell material was initially diluted in unlabeled glucose in order to lower the $\delta^{13}C$ values to an acceptable range for the instrument. Specifically, 2 mg of dry cell mass was re-suspended in a glucose solution (1.455 M final concentration, Mallinckrodt Chemicals) and diluted to create a 3 point standard curve. Samples were then aliquoted into tin capsules, dried under desiccant, and sealed. The $\delta^{13}C$ values of these samples were measured using an ECS 4010 Elemental Analyzer (Costech, Valencia, CA, USA) connected to a Finnigan ThermoQuest Delta^{plus}XL IRMS and using CO_2 as reference gas. $\delta^{13}C$ values were calculated using the ISODAT 2.0 software (ThermoFisher Scientific, Bremen, Germany) and are reported in permil (‰) relative to the VPDB standard. Blank tin capsules along with urea and acetanilide standards of known $\delta^{13}C$ value were analyzed after every 15 samples as well as at the beginning and end of each run in order to track instrument accuracy and precision.

As the cell cultures were diluted in unlabeled glucose, the raw $\delta^{13}C$ values represented that of cellular carbon + glucose, and a back calculation was necessary in order to determine the $\delta^{13}C$ of the cellular carbon. Three-point pure glucose standard curves were run in order to generate a linear regression of μmoles carbon versus peak area. The resulting equation was then used to determine the total μmoles carbon (glucose + cells) added to each sample run, in order to calculate μmoles of cellular carbon added. This value was then used to determine the $\delta^{13}C$ of the cellular carbon.

$\delta^{13}C$ ISOTOPIC ANALYSIS VIA NANOSCALE SECONDARY ION MASS SPECTROMETRY

For bulk and single cell Nanoscale Secondary Ion Mass Spectrometry (NanoSIMS) measurements, cells were harvested at $OD_{600} = 0.4$ and fixed in 3% formaldehyde. Fixed cells were then washed in sterile buffer and deposited onto indium tin oxide (ITO) coated glass slides. Samples were analyzed using a CAMECA NanoSIMS 50 L housed at Caltech, using a mass resolving power approximately 5,000. A primary Cs^+ ion beam (2.5 pA) was used to raster over target cells, and ion images ranging from 5 to 20 μm were collected at 256 × 256 pixel resolution with a dwell time of 14,000 ct/pixel. Several masses were collected in parallel including: $^{12}C^-$, $^{13}C^-$, $^{14}N^{12}C^-$, and $^{14}N^{13}C^-$ using electron multiplier detectors. Resulting ion images were processed using L'Image software (http://www.dtm.ciw.edu/users/nittler/limage_manual.pdf). In order to compare bulk (average $\delta^{13}C$ over entire rastor) and single cell $\delta^{13}C$ values, NanoSIMS targets included both aggregated cells as well as less densely populated areas of the slide containing single cells. $\delta^{13}C$ values for single cells were calculated by creating "regions of interest" around individual cells in L'Image, using a 0.636 micron diameter circle which matched the $^{12}C^{14}N$ count space for an individual cell.

CO_2 incorporation was determined by assuming that the ^{13}C in the cells incubated with 5% $^{12}CO_2$ was solely from direct $^{13}CH_4$ incorporation, while in the sample without external $^{12}CO_2$, incorporation of $^{12}CO_2$ was minimal. Instead, CO_2 incorporation in the latter samples was assumed to be from $^{13}CO_2$ generated from $^{13}CH_4$. These assumptions have been shown to be valid for the serine cycle methanol-utilizer, *M. extorquens* AM1 (Crowther et al., 2008). It was not possible to carry out experiments with *M. trichosporium* OB3b in the absence of any external CO_2 to confirm these assumptions directly, since this strain grows poorly under these conditions. Therefore the calculation represents a minimum, and may be higher.

IN SILICO AMINO ACID USAGE ESTIMATION

The amino acid usage data were generated from the codon usage as follows: nucleotide sequences for each predicted ORF were split

into consecutive codons. The start and stop codons were ignored. The frequency of each codon was tabulated for each ORF. The amino acid usage table for each predicted protein product was multiplied by the mean number of reads mapped from replicates one and two. For each amino acid, the aggregate sum across predicted protein products was then normalized by the aggregate sum of all amino acids. Those fractions were also weighted by the neutral amino acid mass to predict the percent of the total pool by weight. The contribution of each amino acid into biomass was re-calculated using the estimation that proteins comprise 55% of biomass. The data are shown in **Table A1** in Appendix.

METABOLOMICS: CHEMICALS, SAMPLING, AND METABOLITE EXTRACTION

Acyl-CoAs, amino acids, organic acids, and sugar phosphates used as standards were of analytical grade and obtained from Sigma (St. Louis, MO, USA). Absolute ethanol (EMD Chemicals; Gibbstown, NJ, USA) was used in the metabolite extraction. All solvents used for liquid chromatography were LC-MS grade (Fisher Scientific; Fair Lawn, NJ, USA). Millipore purified water was used in the preparation of standard and sample solutions. For GC-MS sample derivatization, pyridine was purchased from EMD Chemicals (Gibbstown, NJ, USA), the trimethylsilylation (TMS) reagent [*N,O*–Bis (trimethylsilyl) trifluoroacetamide (BSTFA) + trimethylchlorosilane (TMCS), 99:1] and methoxyamine hydrochloride were both obtained from Sigma (St. Louis, MO, USA).

Samples (3 mL) of mid-exponential cultures ($OD_{600} = 0.35 \pm 0.02$) were rapidly harvested by vacuum filtration using S-Pak™membrane filters (0.22 μm, 47 mm) (Millipore; Billerica, MA, USA) and washed with 3 mL of fresh medium. The filter was immediately transferred to a petri dish located on the surface of a Cool Beans Chill Bucket™(ISC Bioexpress; Kaysville, UT, USA) at −5°C. To collect cells, the following three sequential rinse solutions were applied: (i) 0.5 mL of 25 mM ice cold HEPES buffer (pH 5.2), (ii) 0.5 mL of −20°C ethanol solution (75/25, v/v, ethanol/aqueous 25 mM HEPES buffer, pH 5.2), and (iii) 1.5 mL of −20°C ethanol. The resulting solution was transferred to a pre-cooled tube and stored in a −80°C freezer until it was ready for subsequent extractions.

Extraction of metabolites from *M. trichosporium* OB3b samples were carried out as previously published for *M. extorquens* AM1 (Yang et al., 2009). Briefly, the samples were incubated in a 100°C water bath for 3 min. The extracted cell suspension was cooled on ice for 5 min, then cell debris was removed by centrifugation at 5,000 RPM (4,300 × *g*) for 5 min. The cell-free metabolite extract was centrifuged at 14,000 RPM (20,800 × *g*) for 8 min. The supernatant was dried in a vacuum centrifuge (CentriVap®Concentrator System; Labconco, MO, USA) and stored at −80°C. For LC-MS/MS analysis, each dried sample was dissolved in 50 μL of purified water. For GC-MS analysis, each sample was further derivatized in two steps. First, keto group were methoximated by adding 50 μL of methoxyamine solution (25 mg/ml methoxyamine hydrochloride in pyridine) and incubated at 60°C for 30 min. Second, trimethylsilylation was performed by adding 50 μl of a TMS reagent (BSTFA/TMCS, 99:1) and incubated at 30°C for 90 min.

METABOLITE MEASUREMENT AND ABSOLUTE QUANTIFICATION

LC-MS/MS experiments were carried out on a Waters© (Milford, MA, USA) LC-MS system consisting of a 1,525 μ binary HPLC pump with a 2,777°C autosampler coupled to a Quattro *Micro*™ API triple-quadrupole mass spectrometer (Micromass®; Manchester, UK). The HILIC method employing gradient elution was carried out using the previously described column (Luna NH_2, 250 mm × 2 mm, 5 μm; Phenomenex®; Torrance, CA, USA) and nearly identical conditions as described below. Gradient elution was carried out with 20 mM ammonium acetate +0.35% NH_4OH (28%) in water (v/v)/acetonitrile (95:5, v/v) with pH 9.7 (mobile phase A), and acetonitrile (mobile phase B). The linear gradients used were 85–0% B for 15 min, 0% B for 11 min, 0–85% B for 1 min, and 85% B for 15 min. The total run time was 42 min at 0.15 mL/min. The injection volume was 10 μL. The eluent from each LC column was directed into the ion source of a mass spectrometer. The multiple reaction monitoring (MRM) experiments were carried out as previously described (Yang et al., 2010). The dwell time for each MRM transition was 0.08 s. All peaks were integrated using MassLynx™ Applications Manager (version 4.1) software.

GC-MS experiments were performed using an Agilent 7890/5975C GC-MS (Agilent Corp; Santa Clara, CA, USA). The column was HP-5MS (30 m × 0.25 mm × 0.25 μm film; Restek; Bellefonte, PA, USA). Ultra high purity helium was used as a carrier gas at a constant flow rate of 1 mL/min, 1 μL of a given sample was injected in split-less mode through an Agilent 7890 auto sampler. The inlet temperature was set to 250°C. The temperature began at 60°C, was held for 0.25 min, and then increased at 8°C/min to 280°C where it held for 10 min. The ion source temperature was set to 250°C. Mass spectra were collected from m/z 50–500 at 3 spectra/s with a 7.4 min solvent delay. The peaks were evaluated using Agilent data analysis software.

The absolute intracellular metabolite quantification was determined using an isotope ratio-based approach as previously published (Yang et al., 2010). Briefly, ^{13}C-labeled cell extracts produced from the continuous cultivation of *M. extorquens* AM1 served as ^{13}C-labeled internal standards (^{13}C-labeled IS). After fast filtration of *M. trichosporium* OB3b, a fixed amount of ^{13}C-labeled IS was added to the petri dish prior to the cell storage. After the metabolites were extracted, they were analyzed by LC-MS/MS and GC-MS as previously described. The calibration curve was developed by adding a fixed amount of ^{13}C-labeled IS to different dilutions of primary stock solutions of ^{12}C-standard mixtures. Calibration plots were obtained by plotting the ratio of ^{12}C-standard to ^{13}C-labeled IS versus the ^{12}C-standard concentration.

DYNAMIC ^{13}C-INCORPORATION

For the $^{13}CH_4$ labeling experiment, *M. trichosporium* OB3b grown on ^{12}C-methane to mid-exponential phase (corresponding to 25% of the added methane consumed) were rapidly transferred to a fresh flask and supplemented with the same percentage of $^{13}CH_4$. At the defined time points (0, 1, 2, 5, 10, 20, 40, and 60 min), the cell culture was harvested, and metabolites were analyzed as previously described. The mass isotopomer distributions were corrected for the natural isotope contribution by using a matrix-based method (Yang et al., 2012) and calculated as the

relative abundances of the different possible mass isotopomers of a metabolite.

For the $^{13}CO_2$ tracing experiment, mid-exponential cultures were spiked with $^{13}CO_2$, resulting in 5% $^{13}CO_2$ in the headspace. These were also harvested at 0, 0.5, 1, 2, 5, 10, and 20 min, and metabolites were analyzed as previously described.

CALCULATION OF ^{13}C-INCORPORATION RATE

Total ^{13}C-incorporation of each metabolite was obtained by normalizing to its total carbon number. Relative isotopic abundance (M_i) for a metabolite in which i ^{13}C atoms were incorporated was calculated by the Eq. 1:

$$M_i\,(\%) = \frac{m_i}{\sum_{j=0}^{n} m_j} \quad (1)$$

Where m_i represented the isotopic abundance for a metabolite in which i ^{13}C atoms were incorporated and n represented the maximum number of ^{13}C atoms incorporated.

Total ^{13}C-incorporation of a metabolite with N carbon atoms was obtained by normalizing to its total carbon number according to the following Eq. 2:

$$\text{Total } ^{13}\text{C-incorporation } (\%) = \frac{\sum_{i=1}^{N} (i \times M_i)}{N} \quad (2)$$

^{13}C-incorporation rate was calculated from the initial slope of all ^{13}C-isotopologues versus time. Comparison of ^{13}C-incorporation was obtained by plotting ^{13}C-incorporation (%) during a switchover from $^{12}CH_4$ to $^{13}CH_4$ versus $^{13}CO_2$ spiking in a time course. The correlation coefficients (R^2) between $^{13}CO_2$ vs. $^{13}CH_4$ were calculated using linear regression.

CELL VOLUME DETERMINATION

An average OB3b cell volume was determined based on confocal images of OB3b cells stained with the lipid dye FM 1–43 (Invitrogen™). After growing colonies on agar plates, OB3b cells were re-suspended in NMS1 media as described and stained for 1 h at 20°C with FM 1–43 (5 μg/mL). The cells were then washed with NMS1 media, seeded on a poly lysine coated slide, and imaged on a Zeiss Axiovert 200 M microscope with an LSM 510 META confocal attachment with a 100× oil immersion objective (NA = 1.30). Image spacing in the Z-axis was 0.5 μm. Complete images of non-mobile cells were analyzed using ImageJ with the Volumest plug-in to determine the average volume (3.79 fL/cell; $n = 60$). The concentration of cells per mL was estimated using a CyFlow®(Partec) flow cytometer with true volumetric absolute counting (TVAC). An average *M. trichosporium* OB3b cell number per 1 mL per OD = 1 is $8.6 \times 10^7 \pm 2.6 \times 10^6$.

ACKNOWLEDGMENTS

We are very grateful to Dr. Mary E. Lidstrom, Dr. Ivan Berg and Dr. Ludmila Chistoserdova for insightful suggestions on the manuscript. This work was supported by the DOE (DE-SC0005154).

REFERENCES

Anthony, C. (1982). *The Biochemistry of Methylotrophs.* New York: Academic Press Inc.

Anthony, C. (2011). How half a century of research was required to understand bacterial growth on C1 and C2 compounds; the story of the serine cycle and the ethylmalonyl-CoA pathway. *Sci. Prog.* 94, 109–137.

Cornish, A., Nicholls, K. M., Scott, D., Hunter, B. K., Aston, W. J., Higgins, I. J., et al. (1984). *In vivo* super ^{13}C NMR investigations of methanol oxidation by the obligate methanotroph *Methylosinus trichosporium* OB3b. *J. Gen. Microbiol.* 130, 2565–2575.

Crowther, G. J., Kosály, G., and Lidstrom, M. E. (2008). Formate as the main branch point for methylotrophic metabolism in *Methylobacterium extorquens* AM1. *J. Bacteriol.* 190, 5057–5062.

DiSpirito, A. A., Zahn, J. A., Graham, D. W., Kim, H. J., Larive, C. K., Derrick, T. S., et al. (1998). Copper-binding compounds from *Methylosinus trichosporium* OB3b. *J. Bacteriol.* 180, 3606–3613.

Doronina, N. V., Ezhov, V. A., and Trotsenko, Y. uA. (2008). Growth of *Methylosinus trichosporium* OB3b on methane and poly-beta-hydroxybutyrate biosynthesis. *Appl. Biochem. Microbiol.* 44, 182–185.

Gilbert, B., McDonald, I., Finch, R., Stafford, G., Nielsen, A., and Murrell, J. (2000). Molecular analysis of the pmo (particulate methane monooxygenase) operon from two type II methano- trophs. *Appl. Environ. Microbiol.* 66, 966–975.

Guckert, J. B., Ringelberg, D. B., White, D. C., Hanson, R. S., and Bratina, B. J. (1991). Membrane fatty acids as phenotypic markers in the polyphasic taxonomy of methylotrophs within the proteobacteria. *J. Gen. Microbiol.* 137, 2631–2641.

Jollie, D. R., and Lipscomb, J. D. (1991). Formate dehydrogenase from *Methylosinus trichosporium* OB3b. Purification and spectroscopic characterization of the cofactors. *J. Biol. Chem.* 266, 21853–21863.

Lawrence, A. J., and Quayle, J. R. (1970). Alternative carbon assimilation pathways in methane-utilizing bacteria. *J. Gen. Microbiol.* 63, 371–374.

Lloyd, J. S., Finch, R., Dalton, H., and Murrell, J. C. (1999). Homologous expression of soluble methane monooxygenase genes in *Methylosinus trichosporium* OB3b. *Microbiology* 145, 461–470.

Lontoh, S., and Semrau, J. D. (1998). Methane and trichloroethylene degradation by *Methylosinus trichosporium* OB3b expressing particulate methane monooxygenase. *Appl. Environ. Microbiol.* 64, 1106–1114.

Matsen, J. B., Yang, S., Stein, L. Y., Beck, D., and Kalyuzhnaya, M. G. (2013). Global molecular analyses of methane methabolism in methanotrophic Alphaproteobacterium, *Methylosinus trichosporium* OB3b. Part I. Transcripomic study. *Front. Microbiol.* 4:40. doi:10.3389/fmicb.2013.00040.

Neidhardt, F. C., Curtiss, R. III, Ingraham, J. L., Lin, E. C. C., Low, K. B., Magasanik, B., et al. (1996). *Escherichia Coli and Salmonella Typhimurium: Cellular and Molecular Biology*, 2nd Edn. Washington: ASM Press.

Park, S., Hanna, L. M., Taylor, R. T., and Droege, M. W. (1991). Batch cultivation of *Methylosinus trichosporium OB3b.* I: production of soluble methane monooxygenase. *Biotechnol. Bioeng.* 38, 423–433.

Park, S., Shah, N. N., Taylor, R. T., and Droege, M. W. (1992). Batch cultivation of *Methylosinus trichosporium OB3b:* II. production of particulate methane monooxygenase. *Biotechnol. Bioeng.* 40, 151–157.

Patel, R. N., Hoare, S. L., and Hoare, D. S. (1979). (14C) acetate assimilation by obligate methylotrophs, *Pseudomonas methanica* and *Methylosinus trichosporium. Antonie Van Leeuwenhoek* 45, 499–511.

Peyraud, R., Kiefer, P., Christen, P., Massou, S., Portais, J. C., and Vorholt, J. A. (2009). Demonstration of the ethylmalonyl-CoA pathway by using 13C metabolomics. *Proc. Natl. Acad. Sci. U.S.A.* 106, 4846–4851.

Peyraud, R., Schneider, K., Kiefer, P., Massou, S., Vorholt, J., and Portais, J. P. (2011). Genome-scale reconstruction and system level investigation of the metabolic network of *Methylobacterium extorquens* AM1. *BMC Syst. Biol.* 5:189. doi:10.1186/1752-0509-5-189

Shishkina, V. N., and Trotsenko, Y. A. (1982). Multiple enzymatic lesions in obligate methanotrophic bacteria. *FEMS Microbiol. Lett.* 13, 237–242.

Stein, L. Y., Yoon, S., Semrau, J. D., Dispirito, A. A., Crombie, A., Murrell, J. C., et al. (2010). Genome sequence of the obligate methanotroph *Methylosinus trichosporium* strain OB3b. *J. Bacteriol.* 192, 6497–6498.

Strom, T., Ference, T., and Quayle, J. R. (1974). The carbon assimilation

pathways of *Methylococcus capsulatus, Pseudomonas methanica*, and *Methylosinus trichosporium* (OB3B) during growth on methane. *Biochem. J.* 144, 465–476.

Sun, A. K., and Wood, T. K. (1996). Trichloroethylene degradation and mineralization by pseudomonads and *Methylosinus trichosporium* OB3b. *Appl. Microbiol. Biotechnol.* 45, 248–256.

Trotsenko, Y. A., and Murrell, J. C. (2008). Metabolic aspects of aerobic obligate methanotrophy. *Adv. Appl. Microbiol.* 63, 183–229.

Weaver, T. L., Patrick, M. A., and Dugan, P. R. (1975). Whole-cell and membrane lipids o the methanotrophic bacterium *Methylosinus trichosporium*. *J. Bacteriol.* 124, 602–605.

Whittenbury, R., Phillips, K. C., and Wilkinson, J. F. (1970). Enrichment, isolation and some properties of methane-utilizing bacteria. *J. Gen. Microbiol.* 61, 205–218.

Williams, A. M. (1988). *The Biochemistry and Physiology of Poly-Beta-Hydroxybutyrate Metabolism in Methylosinus trichosporium OB3b.* Ph.D. thesis, Cranfield Institute of Technology, Biotechnology Centre, Cranfield.

Yang, S., Nadeau, J. S., Humston-Fulmer, E. M., Hoggard, J. C., Lidstrom, M. E., and Synovec, R. E. (2012). Gas chromatography-mass spectrometry with chemometric analysis for determining ^{12}C and ^{13}C labeled contributions in metabolomics and ^{13}C flux analysis. *J. Chromatogr. A* 1240, 156–164.

Yang, S., Sadilek, M., and Lidstrom, M. E. (2010). Streamlined pentafluorophenyl propyl column liquid chromatography-tandem quadrupole mass spectrometry and global (13)C-labeled internal standards improve performance for quantitative metabolomics in bacteria. *J. Chromatogr. A* 1217, 7401–7410.

Yang, S., Sadilek, M., Synovec, R. E., and Lidstrom, M. E. (2009). Liquid chromatography-tandem quadrupole mass spectrometry and comprehensive two-dimensional gas chromatography-time-of-flight mass spectrometry measurement of targeted metabolites of *Methylobacterium extorquens* AM1 grown on two different carbon sources. *J. Chromatogr. A* 1216, 3280–3289.

Conflict of Interest Statement: The authors declare that the research was conducted in the absence of any commercial or financial relationships that could be construed as a potential conflict of interest.

Received: 01 January 2013; paper pending published: 28 January 2013; accepted: 12 March 2013; published online: 03 April 2013.

Citation: Yang S, Matsen JB, Konopka M, Green-Saxena A, Clubb J, Sadilek M, Orphan VJ, Beck D and Kalyuzhnaya MG (2013) Global molecular analyses of methane metabolism in methanotrophic Alphaproteobacterium, Methylosinus trichosporium OB3b. Part II. metabolomics and 13C-labeling study. Front. Microbiol. ***4****:70. doi: 10.3389/fmicb.2013.00070*

This article was submitted to Frontiers in Microbiological Chemistry, a specialty of Frontiers in Microbiology.

APPENDIX

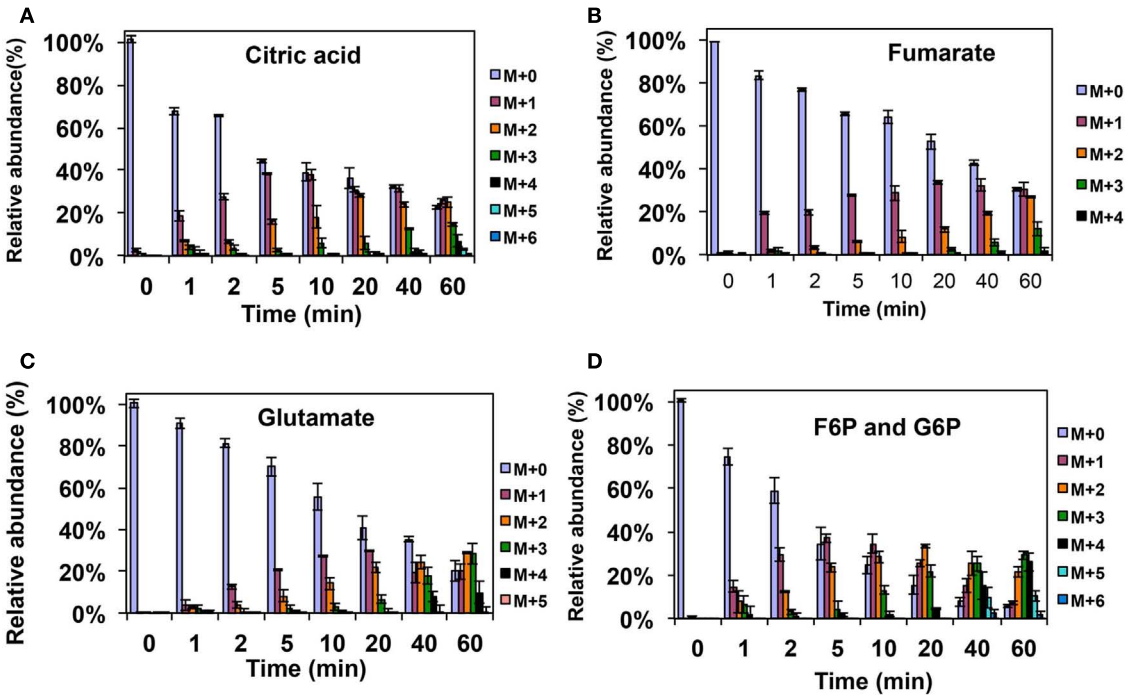

FIGURE A1 | ^{13}C-incorporation during the switch from $^{12}CH_4$ to $^{13}CH_4$ in *Methylosinus trichosporium* OB3b. **(A)** ^{12}C/^{13}C-isotopomer distributions of citric acid **(A)**, fumarate **(B)**, glutamate **(C)**, and fructose-6-phosphate/glucose-6-phosphate **(D)**.

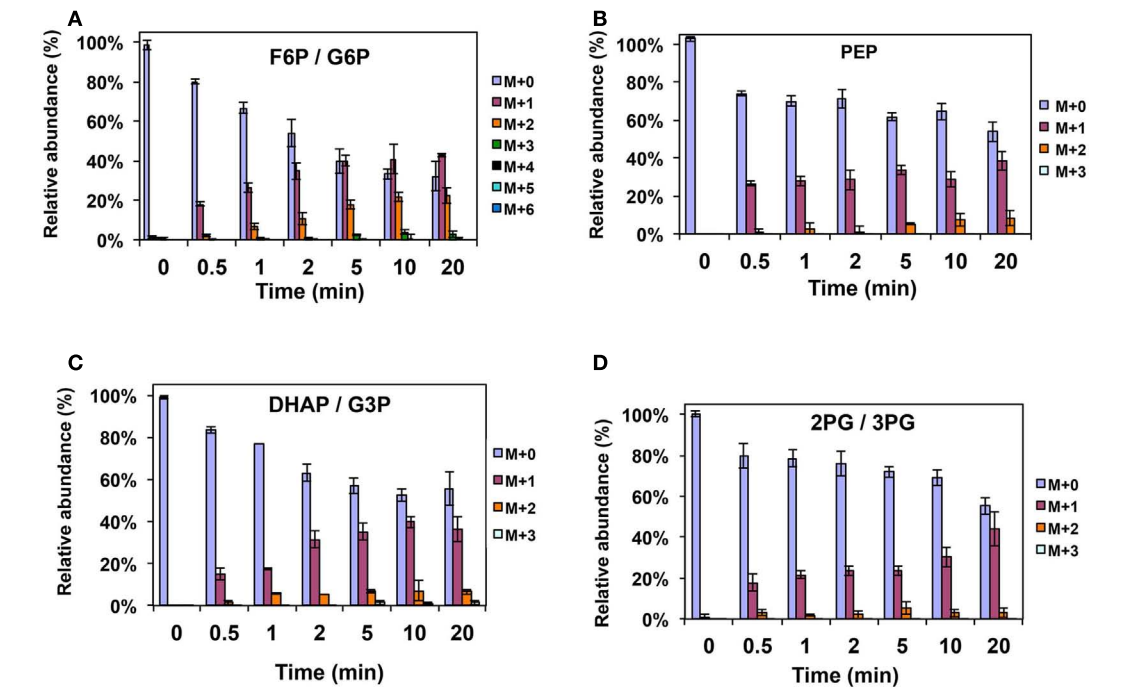

FIGURE A2 | ^{13}C-incorporation during $^{12}CO_2$ spiking in *Methylosinus trichosporium* OB3b grown on $^{12}CH_4$. ^{12}C/^{13}C-isotopomer distributions of fructose-6-phosphate/glucose-6-phosphate **(A)**, phosphoenolpyruvate **(B)**, dihydroxyacetone phosphate/glyceraldehyde 3-phosphate **(C)**, 2-phosphoglycerate/3-phosphoglycerate **(D)**.

Table A1 | Macromolecule and amino acid composition of cells grown on methane.

	Compound	% Cell dry weight	Source of data
C2	PHB	2.5 ± 2	Weaver et al. (1975), Doronina et al. (2008)
	Lipids (FA/PL)	9.2	Weaver et al. (1975)
	Glycine	2.9	This study
C3	DNA/RNA	23	This study
	Serine	2.6	This study
	Cysteine	0.4	This study
	Tryptophan	1.2	This study
	Tyrosine	2	This study
	Phenylalanine	2.9	This study
	Alanine	4.7	This study
	Leucine	5.4	This study
	Valine	3.9	This study
	Cell wall (LPS/PG)	7	Neidhardt et al. (1996)*
C4	Aspartate	3.2	This study
	Asparagine	1.6	This study
	Lysine	2.5	This study
	Methionine	1.3	This study
	Threonine	2.9	This study
	Isoleucine	2.9	This study
C5	Proline	2.5	This study
	Glutamate	3.7	This study
	Glutamine	1.9	This study
	Arginine	5.2	This study
	Histidine	1.4	This study
	Small metabolites, cofactors, ions	3.5	Neidhardt et al. (1996)*
	Total	97.6	

FA, fatty acids; PL, phospholipids; LPS, lipopolysaccharide; PG, peptidoglycan; PHB, polyhydroxybutyrate.

**Data for E. coli, from Neidhardt et al. (1996).*

frontiers in
MICROBIOLOGY

MINI REVIEW ARTICLE
published: 14 May 2013
doi: 10.3389/fmicb.2013.00089

Enzymes involved in the anaerobic oxidation of *n*-alkanes: from methane to long-chain paraffins

Amy V. Callaghan*

Department of Microbiology and Plant Biology, University of Oklahoma, Norman, OK, USA

Edited by:
Rachel N. Austin, Bates College, USA

Reviewed by:
Julia Foght, University of Alberta, Canada
Amy M. Grunden, North Carolina State University, USA
Ian M. Head, Newcastle University, UK

***Correspondence:**
Amy V. Callaghan, Department of Microbiology and Plant Biology, University of Oklahoma, 770 Van Vleet Oval, Norman, OK 73019, USA.
e-mail: acallaghan@ou.edu

Anaerobic microorganisms play key roles in the biogeochemical cycling of methane and non-methane alkanes. To date, there appear to be at least three proposed mechanisms of anaerobic methane oxidation (AOM). The first pathway is mediated by consortia of archaeal anaerobic methane oxidizers and sulfate-reducing bacteria (SRB) via "reverse methanogenesis" and is catalyzed by a homolog of methyl-coenzyme M reductase. The second pathway is also mediated by anaerobic methane oxidizers and SRB, wherein the archaeal members catalyze both methane oxidation and sulfate reduction and zero-valent sulfur is a key intermediate. The third AOM mechanism is a nitrite-dependent, "intra-aerobic" pathway described for the denitrifying bacterium, '*Candidatus Methylomirabilis oxyfera*'. It is hypothesized that AOM proceeds via reduction of nitrite to nitric oxide, followed by the conversion of two nitric oxide molecules to dinitrogen and molecular oxygen. The latter can be used to functionalize the methane via a particulate methane monooxygenase. With respect to non-methane alkanes, there also appear to be novel mechanisms of activation. The most well-described pathway is the addition of non-methane alkanes across the double bond of fumarate to form alkyl-substituted succinates via the putative glycyl radical enzyme, alkylsuccinate synthase (also known as methylalkylsuccinate synthase). Other proposed mechanisms include anaerobic hydroxylation via ethylbenzene dehydrogenase-like enzymes and an "intra-aerobic" denitrification pathway similar to that described for '*Methylomirabilis oxyfera*'.

Keywords: anaerobic, oxidation, alkanes, methane, paraffins

INTRODUCTION

Alkanes are saturated hydrocarbons that are derived from both natural and anthropogenic sources. Due to their apolar C-H σ bonds, alkanes are considered to be among the least chemically reactive organic compounds. The activation or functionalization of alkanes is initiated via cleavage of a C-H bond. Aerobic microorganisms achieve this step via monooxygenase or dioxygenase enzymes, in which oxygen serves as both the physiological terminal electron acceptor and as a reactant (for review of mechanisms and enzymes see Austin and Groves, 2011). The role of oxygen in the functionalization of alkanes led to the belief for many years that anaerobic microorganisms would be unable to activate and utilize these compounds as growth substrates. However, research during the last 25 years has demonstrated that anaerobic microorganisms have their own novel mechanisms of activating alkanes.

ANAEROBIC OXIDATION OF METHANE

The shortest alkane, methane, is the most environmentally relevant hydrocarbon due to its biological production by methanogenic archaea in freshwater systems, swamps, landfills, marine sediments and seeps, rice fields, and other anaerobic environments, as well as its role as a greenhouse gas (Conrad, 2009). Anaerobic methane oxidation (AOM) is thought to account for the removal of over 300 Tg of methane per year in oceanic systems (Hinrichs and Boetius, 2002; Reeburgh, 2007). Therefore, from the perspective of climate change, AOM serves as a significant greenhouse "sink." AOM can be coupled to the reduction of sulfate, nitrate and nitrite (for reviews see Knittel and Boetius, 2011; Shen et al., 2012), manganese (Beal et al., 2009), and iron (Beal et al., 2009; Crowe et al., 2011; Sivan et al., 2011; Amos et al., 2012; Zhu et al., 2012). Although the mechanisms of aerobic methane oxidation are well-described (Austin and Groves, 2011), the mechanisms of AOM have been hotly debated.

REVERSE METHANOGENESIS

To date, several studies have revealed that AOM coupled to sulfate reduction is mediated by consortia of archaeal anaerobic methane oxidizers (ANME-1, ANME-2, and ANME-3) and sulfate-reducing bacteria (SRB) (Knittel and Boetius, 2011). AOM with sulfate as the terminal electron acceptor appears to proceed via "reverse methanogenesis" (Zehnder and Brock, 1979; Hoehler et al., 1994; Hallam et al., 2004) and is catalyzed by a homolog of methyl-coenzyme M reductase (MCR), the Ni-containing enzyme responsible for the last step of methanogenesis (Krüger et al., 2003; Scheller et al., 2010a; **Figure 1A**). MCR homologues have been found in high concentrations in methanotrophic archaea associated with SRB (Hallam et al., 2003; Krüger et al., 2003; Heller et al., 2008; Mayr et al., 2008; Nunoura et al., 2008). In a recent study, an ANME-1 MCR complex was isolated from a Black Sea microbial mat, and the X-ray structure was reported (Shima et al., 2012). Compared to the methanogenic MCR, the ANME-1 MCR

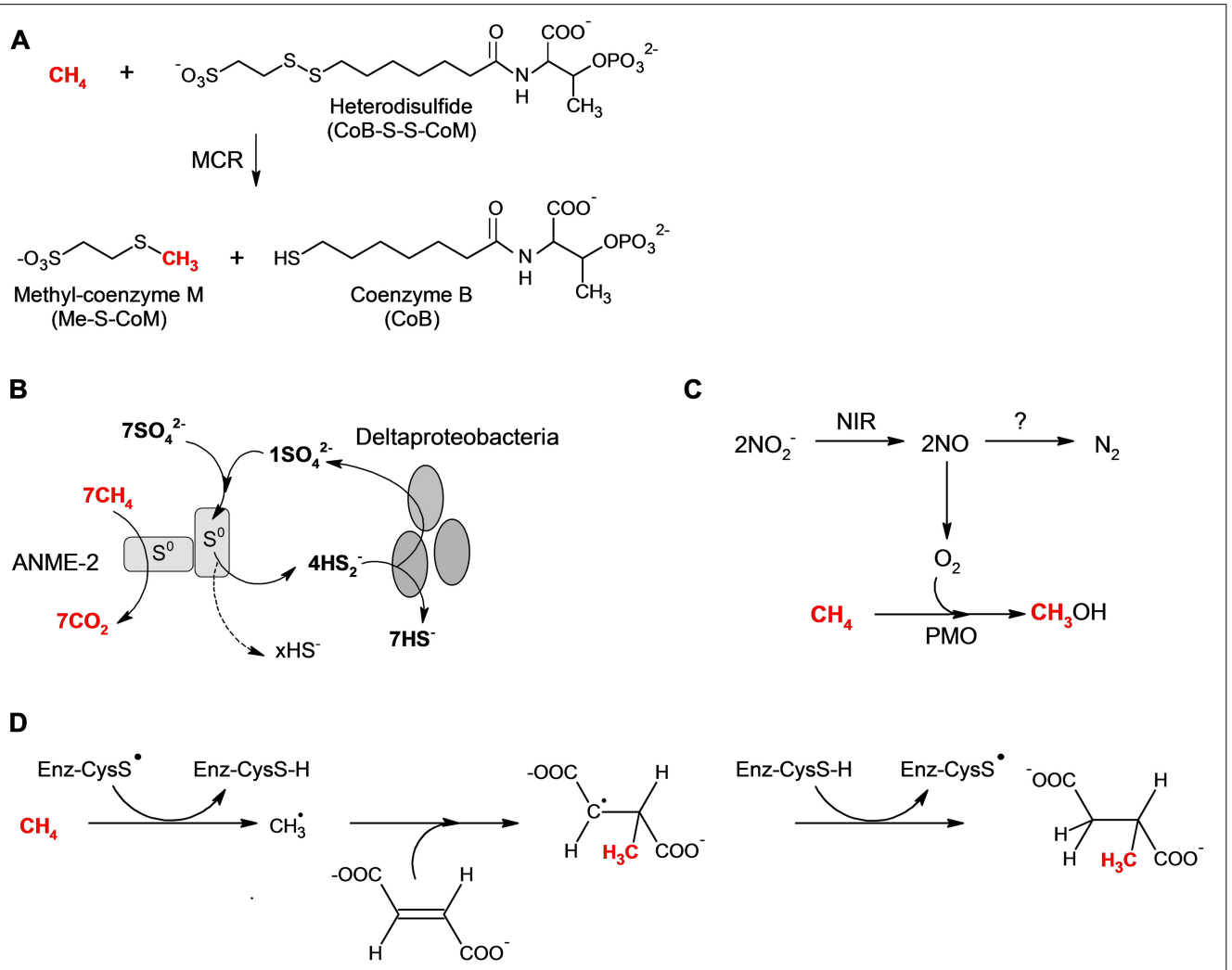

FIGURE 1 | Proposed pathways for the anaerobic oxidation of methane (AOM) via: (A) Reverse methanogenesis (adapted from Scheller et al., 2010a,b); (B) Zero-valent sulfur as a key intermediate in AOM (adapted from Milucka et al., 2012); (C) Nitrite-dependent anaerobic methane oxidation ("intra-aerobic denitrification"; adapted from (Ettwig et al., 2010); and (D) Methane addition to fumarate (adapted from Beasley and Nanny, 2012). Enzyme nomenclature: methyl-coenzyme M reductase (MCR); nitrite reductase (NIR); particulate methane monooxygenase (PMO); and the putative thiyl radical of the alkylsuccinate/methylalkylsuccinate synthase-like enzyme (Enz-CysS).

complex is similar in overall structure and contains coenzyme M and coenzyme B. However, it differs from the methanogenic MCR in that it contains an F_{430} variant, as well as a cysteine-rich region and an altered post-translational amino acid modification pattern (Shima et al., 2012). Although not clearly elucidated, the role of the cysteine-rich region between the F_{430} and the protein surface may be to operate as a redox-relay system for electron or H^+/e^- transport for the reduction of ANME-1 MCR from the inactive Ni^{2+} to the active Ni^{1+} oxidation state (Mayr et al., 2008; Shima et al., 2012), whereas, the altered post-translational amino acid modifications may reflect phylogenetic adaptation to environmental conditions (Shima et al., 2012) based on the distribution of different ANME groups within microbial mats (Krüger et al., 2008).

The "reversibility" of MCR is supported by thermodynamic and kinetic considerations (Thauer, 2011), as well as activity assays with purified MCR from *Methanothermobacter marburgensis* (Scheller et al., 2010a). However, there are still several hypotheses regarding the reaction intermediates of both methane formation and methane oxidation by MCR. The two main competing theories argue either for an organometallic methyl-$Ni^{III}F_{430}$ intermediate (Ermler et al., 1997; Dey et al., 2010) or the formation of a methyl radical and a CoM-S-$Ni^{II}F_{430}$ intermediate (Pelmenschikov et al., 2002; Pelmenschikov and Siegbahn, 2003). The latter was challenged in an experimental study which predicted the formation of (σ-alkane)-NiF_{430} and (H)(alkyl)NiF_{430} complexes as intermediates (Scheller et al., 2010b). However, recent active site models of the MCR X-ray crystal structure (PDB code 1HBN) from *Methanothermobacter thermautotrophicus* support the theory that methane oxidation proceeds via a methyl radical and a CoM-S-$Ni^{II}F_{430}$ intermediate (Chen et al., 2012).

ALTERNATIVE AOM MECHANISMS UNDER SULFATE-REDUCING CONDITIONS

There has been tremendous debate regarding the interspecies intermediates of sulfate-dependent AOM, and several mechanisms have been proposed for consortia of ANME and SRB. One hypothesis proposes the formation of acetic acid and H_2 from methane and water by methane-oxidizing archaea, with subsequent utilization of the acetic acid and H_2 by SRB (Valentine and Reeburgh, 2000). Another variation of this process was previously proposed as "reverse acetoclastic methanogenesis" in which methane-oxidizing archaea produce acetate from CO_2 and CH_4, and the acetate is utilized by SRB (Zehnder and Brock, 1980; Hoehler et al., 1994). More recently, a "methylogenesis" mechanism was proposed, in which methanethiol (MeSH) serves as an interspecies compound that transfers methane-derived carbon from the methanotroph to the SRB (Moran et al., 2008). With respect to the latter, there is some evidence that methanethiol inhibits AOM (Moran et al., 2008; Meulepas et al., 2010) and sulfate reduction (Meulepas et al., 2010). Therefore, the role of methylsulfides is still unclear. Additionally, several studies have provided experimental evidence and theoretical predictions that compounds such as acetate, hydrogen, formate, methanol, and carbon monoxide are unlikely to serve as interspecies compounds based on their effects on sulfate reduction and AOM, their diffusion distances, and thermodynamic considerations (see Meulepas et al., 2010 and references therein). Finally, extracellular electron transfer between archaea and deltaproteobacteria via nanowires (Reguera et al., 2005; Gorby et al., 2006) or direct electron transfer via multi-heme *c*-type cytochromes (Meyerdierks et al., 2010) has also been proposed. These processes, however, would require the archaea and deltaproteobacteria to be in direct physical contact with each other.

NEW MODEL FOR AOM MECHANISM UNDER SULFATE-REDUCING CONDITIONS: ZERO-VALENT SULFUR AS A KEY INTERMEDIATE

The studies focusing on the identification of AOM intermediates under sulfate-reducing conditions (see above) have mainly been predicated on the hypothesis that the ANME/SRB consortia catalyze AOM via an *obligate* syntrophic mechanism (for review see Knittel and Boetius, 2009). However, a new study of an enrichment culture obtained from sediments of the Mediterranean mud volcano Isis challenges that paradigm and also provides new insight to potential intermediates that may be transferred from the archaeal members to the SRB (Milucka et al., 2012). The culture consists of ANME-2 and bacteria belonging to the *Desulfosarcina*/*Desulfococcus* (DSS) cluster (Schreiber et al., 2010), and evidence suggests that the ANME-2 assimilate dissolved inorganic carbon (DIC) and catalyze both the anaerobic oxidation of methane and the reduction of sulfate to zero-valent sulfur (S^0) and possibly to sulfide. Although experimental evidence is not yet available, the reduction of sulfate by ANME-2 is proposed to proceed via a non-canonical enzymatic pathway in which the electron donor may be the formylmethanofuran (MFR)/CO_2 + MFR redox couple. The zero-valent sulfur can react with sulfide to form polysulfides, such as disulfide. The DSS then couple disproportionation of disulfide to sulfide and sulfate (**Figure 1B**) with autotrophic carbon assimilation. Presumably, the disproportionation reaction in DSS could be catalyzed by enzymes such as sulfate adenylyltransferase (SAT) and adenylylsulfate reductase (APR), which have been shown to be involved in the disproportionation of compounds such as elemental sulfur, thiosulfate, and sulfite (Krämer and Cypionka, 1989). The sulfate generated by the DSS can be partly reused by the ANME-2. Stoichiometrically, no net sulfate production occurs. Given these findings, it appears as though the ANME-2 are not necessarily dependent upon the sulfate-reducing partner and may be able to associate with any bacteria capable of scavenging disulfide and coupling it to energy generation and growth. This has important implications with respect to the biogeochemistry of methane oxidation and sulfur cycling as well as studies investigating interspecies compounds that are indicative of an obligate syntrophic AOM mechanism (see above).

NITRITE-DEPENDENT ANAEROBIC METHANE OXIDATION ("INTRA-AEROBIC DENITRIFICATION")

Anaerobic methane oxidation coupled to denitrification through "reverse methanogenesis" was first proposed for a consortium ("Twente") enriched from Twentekanaal sediment (Netherlands) (Raghoebarsing et al., 2006). The culture consisted of a bacterium belonging to the candidate division, "NC10," and archaea distantly related to *Methanosaeta* and ANME–II (Raghoebarsing et al., 2006; Ettwig et al., 2009). Subsequent investigations of the "Twente" culture showed AOM in the *absence* of the archaea (Ettwig et al., 2008, 2009), and further characterization of "Twente" and another culture ("Ooij")(Ettwig et al., 2009) revealed microbial populations dominated by the denitrifying bacterium, '*Candidatus Methylomirabilis oxyfera*' (Ettwig et al., 2010). Genome assembly obtained from metagenomic analyses shows that '*Methylomirabilis oxyfera*' contains genes encoding enzymes for the complete pathway for aerobic methane oxidation, including a particulate monooxygenase (pMMO). The genome also contains several genes for denitrification, but lacks the genes encoding the enzymes for the reduction of nitrous oxide to dinitrogen (*nosZDFY*), an interesting finding given the observed production of N_2 in the "Twente" and "Ooij" cultures during AOM (Raghoebarsing et al., 2006; Ettwig et al., 2008, 2009). '*Methylomirabilis oxyfera*' also lacks genes encoding homologs of MCR or alkane-activating glycyl radical enzymes (Ettwig et al., 2010). Isotopic labeling experiments suggest that AOM by '*Methylomirabilis oxyfera*' proceeds via reduction of nitrite to nitric oxide, followed by the conversion of two nitric oxide molecules to dinitrogen and molecular oxygen. The latter can be used to functionalize the methane via the pMMO (**Figure 1C**). Based on stoichiometry ($3CH_4 + 8NO_2^- + 8H^+ \rightarrow 3CO_2 + 4N_2 + 10H_2O$), four molecules of O_2 could be generated from eight molecules of nitrite, of which only three are required for methane activation by pMMO (Wu et al., 2011). Based on oxygen uptake and inhibition experiments with cell extracts and UV–visible absorption spectral characteristics and electron spin resonance (EPR) spectroscopy of solubilized membranes, the remaining oxygen might be consumed by a membrane-bound *bo*-type terminal oxidase (Wu et al., 2011).

METHANE ADDITION TO FUMARATE

The addition of non-methane alkanes to fumarate (i.e., fumarate addition) is a prevalent anaerobic alkane activation mechanism observed under nitrate- and sulfate-reducing conditions (see below). Although the majority of studies have focused on longer-chain alkanes, a few investigations have revealed that short alkanes, such as propane, are also added to fumarate terminally or subterminally under sulfate-reducing conditions (Kniemeyer et al., 2007; Savage et al., 2010). These findings are supported by field metabolomic studies of petroleum reservoirs and coalbeds in which low molecular weight gases such as methane are prevalent and low molecular weight alkylsuccinates, including methylsuccinate, have been detected (Duncan et al., 2009; Gieg et al., 2010; Wawrik et al., 2012). Due to the complex mixture of hydrocarbons in oil reservoirs and coalbeds, it is possible that the low molecular weight alkylsuccinates are derived from cometabolic hydrocarbon metabolism, as has been observed for toluene in anaerobic alkane-degrading bacteria (Rabus et al., 2011). However, the detection of methylsuccinate is intriguing nonetheless because it suggests that AOM via fumarate addition may be possible (**Figure 1D**). Thermodynamically, however, there are several considerations with respect to the formation of the methyl radical and the terminal electron accepting conditions. The formation of a methyl radical (439 kJ mol^{-1}) (Lide, 2003) would be at the expense of the glycyl radical formation (350 kJ mol^{-1}) (Armstrong et al., 1996). The difference in dissociation energies (90 kJ) is considerably larger than that for other alkane substrates (∼60 kJ) (Thauer and Shima, 2008), and at first glance, it would not appear that the transition state of the enzyme could overcome such a barrier. A study using quantum chemical calculations to investigate the energetics of methane addition to fumarate (Beasley and Nanny, 2012) also predicts that the initial reaction (i.e., homolytic cleavage of the C-H bond in methane by the methylethyl radical) is unfavorable, but that all other steps in the proposed reaction are favorable, with an overall energy change that is exothermic. Given that glycyl radical enzymes are functional dimers, it is possible that the initial energy barrier might be overcome via coupling the endergonic steps of the catalytic cycle in one active site with exergonic steps in the catalytic cycle of the second active site (Thauer and Shima, 2008).

Whether AOM via fumarate addition proceeds with sulfate versus nitrate or nitrite as the terminal electron acceptor has also been debated. It is hypothesized that the majority or all of the free energy generated from this process with sulfate as the terminal electron acceptor ($\Delta G^{\circ\prime} = -21$ kJ/mol) would be dissipated as heat in the initial activation step, which would not allow enough energy for subsequent reactions, whereas the free energy change using nitrate or nitrite as a terminal electron acceptor is more energetically favorable (Thauer and Shima, 2008).

ANAEROBIC OXIDATION OF NON-METHANE ALKANES

ALKANE ADDITION TO FUMARATE

One of the most well characterized mechanisms of anaerobic alkane activation and degradation is the addition of non-methane alkanes across the double bond of fumarate to form alkyl-substituted succinates. This was first demonstrated in a sulfate-reducing, dodecane-utilizing enrichment culture (Kropp et al., 2000) and was subsequently found to be applicable to a range of *n*-alkane and cycloalkane substrates (C_3–C_{16}) in several sulfate-reducing and nitrate-reducing isolates and cultures (Rabus et al., 2001; Wilkes et al., 2002, 2003; Rios-Hernandez et al., 2003; Cravo-Laureau et al., 2005; Davidova et al., 2005; Callaghan et al., 2006; Kniemeyer et al., 2007; Musat et al., 2010). Although subterminal addition of *n*-alkanes to fumarate appears to be a prevalent feature of the fumarate addition mechanism (**Figure 2A**), other modes include C3 addition (Rabus et al., 2001) and C1 addition (Kniemeyer et al., 2007), both of which have been proposed as side-reactions. The alkyl-substituted succinates are further degraded via carbon-skeleton rearrangement followed by decarboxylation and β-oxidation (Wilkes et al., 2002).

Analogous to the glycyl radical mechanism of benzylsuccinate synthase (BSS) and its homologs, which catalyze the addition of aromatic hydrocarbons to fumarate (for reviews see Boll and Heider, 2010; Meckenstock and Mouttaki, 2011), alkane activation is presumably catalyzed by the glycyl radical enzyme, alkylsuccinate synthase (ASS) (Callaghan et al., 2008b) or methylalkylsuccinate synthase (MAS) (Grundmann et al., 2008), for which the sulfate-reducing strain *Desulfatibacillum alkenivorans* AK-01 and the denitrifying strain '*Aromatoleum*' HxN1 currently serve as model strains, respectively. Comparison of *ass/mas* genes to *bss* genes has revealed several similarities. Both AK-01 and HxN1 contain genes encoding putative glycyl radical activating enzymes, belonging to the radical *S*-adenosylmethionine (SAM) superfamily. Similar to BSS activase, which generates a glycyl radical on the catalytic subunit of BSS (Leuthner et al., 1998; Krieger et al., 2001; Verfürth et al., 2004), it is thought that the ASS activase is responsible for the generation of the glycyl radical on the catalytic subunit of the alkane-activating enzyme. Subsequent generation of a thiyl radical on a conserved cysteine residue (Selmer et al., 2005) would result in the abstraction of an H atom from the hydrocarbon substrate (Heider et al., 1998). In the case of BSS, the reaction results in the stereospecific formation of *R*(+)-benzylsuccinate (Beller and Spormann, 1998; Leutwein and Heider, 1999), wherein the initially abstracted H atom is transferred to the same face of fumarate (Qiao and Marsh, 2005). Unlike benzylsuccinate, however, methylalkylsuccinic acids contain two chiral carbons. Metabolomic investigations of numerous sulfate- and nitrate-reducing cultures utilizing *n*-alkanes show the formation of two diastereomers of the methylalkylsuccinic acid metabolites (Kropp et al., 2000; Rabus et al., 2001; Wilkes et al., 2002; Cravo-Laureau et al., 2005; Callaghan et al., 2006), and gas chromatography-mass spectrometry (GC-MS) analysis of a sulfate-reducing enrichment culture utilizing ethylcyclopentane resolved up to five peaks corresponding to the requisite ethylcyclopentylsuccinic acids (Rios-Hernandez et al., 2003). Recent stereochemical investigations of '*Aromatoleum*' HxN1growing on *n*-hexane showed only the formation of (2R, 1′R) and (2S, 1′R) isomers of 1-methylpentylsuccinate and that the initial step in activation is via abstraction of the pro-*S* hydrogen from C_2 of hexane, with subsequent addition of the alkyl species intermediate to fumarate on the opposite face from which the hydrogen atom was abstracted (**Figure 2A**; Jarling et al., 2012). It is also proposed that the initial 1-methylpentylsuccinate isomer is epimerized to

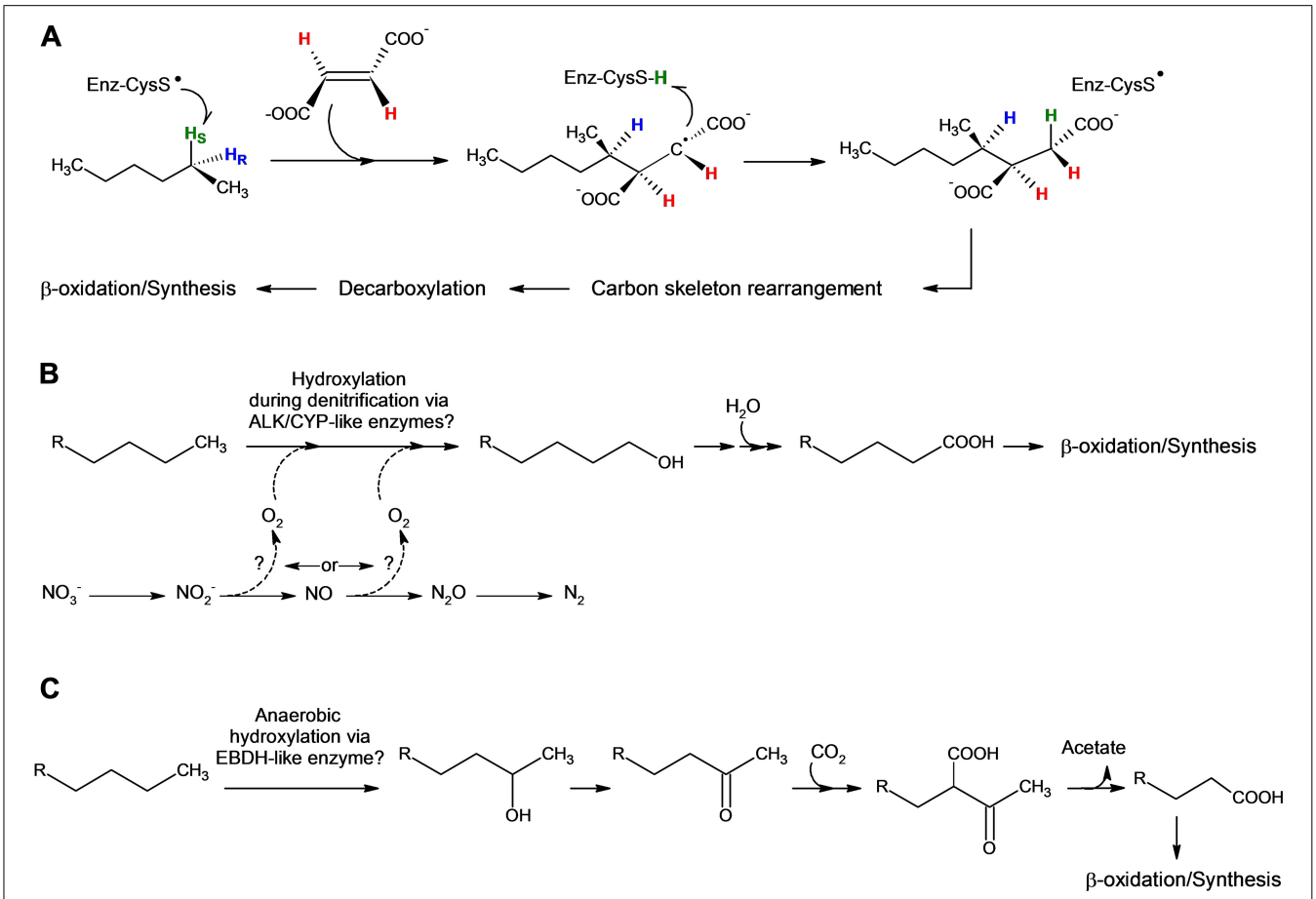

FIGURE 2 | (A) Proposed pathway and stereochemistry for the anaerobic activation and degradation of hexane via subterminal addition to fumarate (adapted from Jarling et al., 2012); **(B)** Proposed pathway of activation and degradation of non-methane alkanes via "intra-aerobic denitrification" (adapted from Zedelius et al., 2011); and **(C)** Proposed pathway of activation and degradation of non-methane alkanes via anaerobic hydroxylation by *Desulfococcus oleovorans* Hxd3 (Sünwoldt et al., 2012). Enzyme nomenclature: putative thiyl radical of the alkylsuccinate/methylalkylsuccinate synthase-like enzyme (Enz-CysS); alkane monooxygenase (ALK); cytochromes P450 (CYP); and ethylbenzene dehydrogenase (EBDH).

generate a diastereomer that then undergoes the reported carbon-skeleton rearrangement and subsequent decarboxylation (Jarling et al., 2012).

The discoveries of ASS and MAS have enabled the interrogation of hydrocarbon-impacted environments as well as isolates and enrichment cultures (Callaghan et al., 2010; Kolukirik et al., 2011; Andrade et al., 2012; Li et al., 2012; Mbadinga et al., 2012; Wang et al., 2012; Wawrik et al., 2012; Zhou et al., 2012; Cheng et al., 2013). In addition to alkanes of medium chain lengths, ASS/MAS enzymes appear to play a role in the degradation of very short alkanes (eg., propane) (Kniemeyer et al., 2007; Callaghan et al., 2010; Savage et al., 2010), and recent investigations of anaerobic biodegradation of solid paraffins under methanogenic conditions suggest that microorganisms may also activate paraffin waxes via fumarate addition (Callaghan et al., 2010). With respect to the latter, the detection and expression of several *assA* genotypes was demonstrated in a methanogenic consortium utilizing octacosane (C_{28}) (Davidova et al., 2011). However, the requisite metabolites have not been identified in this study or in other studies examining alkane activation under methanogenic conditions for which *assA* genotypes have been detected (Mbadinga et al., 2012; Wang et al., 2012; Zhou et al., 2012; Aitken et al., 2013; Cheng et al., 2013). It has been hypothesized that either the metabolites that result from fumarate addition do not accumulate to detectable levels under the slow-growing conditions and/or that other mechanisms, such as hydroxylation, may be important (Aitken et al., 2013).

INTRA-HYDROXYLATION

An "intra-aerobic" pathway of alkane oxidation similar to that of '*Methylomirabilis oxyfera*' has also been proposed to be involved in the functionalization of *n*-hexadecane by the Gammaproteobacterium HdN1 (**Figure 2B**; Zedelius et al., 2011). Unlike '*Methylomirabilis oxyfera*,' HdN1 contains genes for the complete denitrification pathway. The genome of strain HdN1 does not contain genes that encode an alkane-activating glycyl radical enzyme, but does contain genes that may encode a di-iron monooxygenase, a P_{450}-type monooxygenase and a putative third type of monooxygenase (Zedelius et al., 2011). Consistent with the absence of an alkane-activating glycyl radical enzyme,

alkyl-substituted succinates were not detected via metabolite profiling, but 1-hexadecanol was detected when the anaerobic culture was exposed to air. Based on these findings and growth experiments, the authors proposed a mechanism in which NO_2^-, NO or an unknown product of NO_2^- reduction may be required for alkane activation. Specifically, the dismutation of NO_2^- [$\Delta G^{\circ\prime} = -55.2$ kJ (mole O_2)$^{-1}$] or NO [$\Delta G^{\circ\prime} = -173.1$ kJ (mole O_2)$^{-1}$)] would provide O_2, which could then be used to hydroxylate the alkane via one of the putative monooxygenases. Alternatively, N-O species could behave as strongly oxidizing electron acceptors to generate a reactive state of a factor or enzyme site that is involved in the activation of the alkane, or an N-O species may be directly involved in the activation of the alkane (Zedelius et al., 2011).

ANAEROBIC HYDROXYLATION FOLLOWED BY CARBOXYLATION

Finally, there appears to be at least one additional pathway of anaerobic alkane oxidation. Early studies of the sulfate-reducing bacterium *Desulfococcus oleovorans* Hxd3 demonstrated that incubation with an alkane with an odd number of C atoms yielded predominantly fatty acids with an even number of C atoms, and vice versa (Aeckersberg et al., 1998; So et al., 2003). This is in contrast with what is observed in microorganisms that activate alkanes via fumarate addition (So and Young, 1999). Stable isotope studies of strain Hxd3 incubated with $NaH^{13}CO_3$ and [1,2-$^{13}C_2$]hexadecane were indicative of incorporation of carbon derived from bicarbonate at C3 and elimination of the C1 and C2 carbon atoms (So et al., 2003). Subsequently, evidence of this pathway was also observed in nitrate- and sulfate-reducing enrichment cultures utilizing *n*-hexadecane (Callaghan et al., 2006, 2009). However, although it was hypothesized that carboxylation at C3 may be the first step in degradation, the corresponding carboxylated intermediate, 2-ethylpentadecanoic acid, was not detected in any of the above studies. Under standard conditions, the direct carboxylation of alkanes is an endergonic process ($\Delta G^{\circ\prime} = +28$ kJ/mol) (Thauer and Shima, 2008). Thus, carboxylation as the first step in alkane degradation in Hxd3 has been debated for almost 10 years.

With the continual evolution of sequencing technologies, however, genome-enabled analyses are yielding new hypotheses. Consistent with the above experimental observations, the genome of Hxd3 does not contain genes encoding an alkane-activating glycyl radical enzyme. Interestingly, the genome contains genes that encode an ethylbenzene dehydrogenase-like complex (Callaghan et al., 2008a), similar to that found in denitrifying strains *Aromatoleum aromaticum* EbN1 (Kniemeyer and Heider, 2001) and *Azoarcus* sp. strain EB1 (Johnson and Spormann, 1999; Johnson et al., 2001). Ethylbenzene dehydrogenase is a molybdenum-cofactor-containing enzyme of the dimethylsulfoxide reductase family that catalyzes the anaerobic hydroxylation of ethylbenzene (Ball et al., 1996; Rabus and Heider, 1998). Based on these findings, it is possible that the activation of alkanes by Hxd3 may also occur via anaerobic hydroxylation. Analogous to the steps involved in the anaerobic hydroxylation of ethylbenzene, hydroxylation of the alkane at C2 would produce a secondary alcohol that could be further oxidized to a ketone, similar to the formation of acetophenone during ethylbenzene degradation (**Figure 2C**; Ball et al., 1996; Rabus and Heider, 1998) Subsequent transformation of the ketone may involve carboxylation at C3, with elimination of the C1 and C2 carbons, to produce a fatty acid that is one carbon shorter than the parent alkane. The latter would be consistent with previous studies (So and Young, 1999; Callaghan et al., 2006, 2009). Proteomic investigations of alkane-degrading cells of Hxd3 implicate the putative ethylbenzene dehydrogenase (Sünwoldt et al., 2012). However, further study is needed to elucidate the transformation reactions that would ultimately result in the formation of the observed fatty acids.

CONCLUSION

The anaerobic oxidation of alkanes plays an important role in the biogeochemical cycling of methane and the bioremediation of hydrocarbon-impacted environments. As we look to the future, advances in next-generation sequencing and annotation will facilitate genome-enabled transcriptomic and proteomic investigations of anaerobic alkane oxidation. The complete genome sequences of several model alkane utilizers are now publicly available and include: *Desulfatibacillum alkenivorans* AK-01, *Desulfococcus oleovorans* Hxd3, '*Candidatus Methylomirabilis. oxyfera*,' and the Gammaproteobacterium, strain HdN1. Future work will rely on these model organisms for the purification and characterization of relevant enzymes.

ACKNOWLEDGMENTS

The author would like to thank Rachel N. Austin, Johann Heider, Jana Milucka, and Mark A. Nanny for editorial comments and suggestions. The preparation of this review was funded by a National Science Foundation grant (MCB-0921265).

REFERENCES

Aeckersberg, F., Rainey, F. A., and Widdel, F. (1998). Growth, natural relationships, cellular fatty acids and metabolic adaptation of sulfate-reducing bacteria that utilize long-chain alkanes under anoxic conditions. *Arch. Microbiol.* 170, 361–369.

Aitken, C. M., Jones, D. M., Maguire, M. J., Gray, N. D., Sherry, A., Bowler, B. F. J., et al. (2013). Evidence that crude oil alkane activation proceeds by different mechanisms under sulfate-reducing and methanogenic conditions. *Geochim. Cosmochim. Acta* 109, 162–174.

Amos, R. T., Bekins, B. A., Cozzarelli, I. M., Voytek, M. A., Kirshtein, J. D., Jones, E. J., et al. (2012). Evidence for iron-mediated anaerobic methane oxidation in a crude oil-contaminated aquifer. *Geobiology* 10, 506–517.

Andrade, L. L., Leite, D., Ferreira, E., Ferreira, L., Paula, G. R., Maguire, M., et al. (2012). Microbial diversity and anaerobic hydrocarbon degradation potential in an oil-contaminated mangrove sediment. *BMC Microbiol.* 12:186. doi: 10.1186/1471-2180-12-186

Armstrong, D. A., Yu, D., and Rauk, A. (1996). Oxidative damage to the glycyl alpha-carbon site in proteins: an ab initio study of the C-H bond dissociation energy and the reduction potential of the C-centered radical. *Can. J. Chem.* 74, 1192–1199.

Austin, R. N., and Groves, J. T. (2011). Alkane-oxidizing metalloenzymes in the carbon cycle. *Metallomics* 3, 775–787.

Ball, H. A., Johnson, H. A., Reinhard, M., and Spormann, A. M. (1996). Initial reactions in anaerobic ethylbenzene oxidation by a denitrifying bacterium, strain EB1. *J. Bacteriol.* 178, 5755–5761.

Beal, E. J., House, C. H., and Orphan, V. J. (2009). Manganese- and iron-dependent marine methane oxidation. *Science* 325, 184–187.

Beasley, K. K., and Nanny, M. A. (2012). Potential energy surface for anaerobic

oxidation of methane via fumarate addition. *Environ. Sci. Technol.* 46, 8244–8252.

Beller, H. R., and Spormann, A. M. (1998). Analysis of the novel benzylsuccinate synthase reaction for anaerobic toluene activation based on structural studies of the product. *J. Bacteriol.* 180, 5454–5457.

Boll, M., and Heider, J. (2010). "Anaerobic degradation of hydrocarbons: mechanisms of C–H-bond activation in the absence of oxygen," in *Handbook of Hydrocarbon and Lipid Microbiology*, eds K. N. Timmis, T. Mcgenity, J. R. Van Der Meer, and V. De Lorenzo (Berlin Heidelberg: Springer-Verlag), 1011–1024.

Callaghan, A. V., Austin, R. N., Groves, J. T., Kukor, J. J., Rabus, R., Widdel, F., et al. (2008a). "The complete genome sequence of *Desulfococcus oleovorans* Hxd3, a sulfate-reducing, alkane-degrading bacterium," in *American Society for Microbiology 108th General Meeting.* (Boston: Amer Society for Microbiology).

Callaghan, A. V., Wawrik, B., Ní Chadhain, S. M., Young, L. Y., and Zylstra, G. J. (2008b). Anaerobic alkane-degrading strain AK-01 contains two alkylsuccinate synthase genes. *Biochem. Biophys. Res. Commun.* 366, 142–148.

Callaghan, A. V., Davidova, I. A., Savage-Ashlock, K., Parisi, V. A., Gieg, L. M., Suflita, J. M., et al. (2010). Diversity of benzyl- and alkylsuccinate synthase genes in hydrocarbon-impacted environments and enrichment cultures. *Environ. Sci. Technol.* 44, 7287–7294.

Callaghan, A. V., Gieg, L. M., Kropp, K. G., Suflita, J. M., and Young, L. Y. (2006). Comparison of mechanisms of alkane metabolism under sulfate-reducing conditions among two bacterial isolates and a bacterial consortium. *Appl. Environ. Microbiol.* 72, 4274–4282.

Callaghan, A. V., Tierney, M., Phelps, C. D., and Young, L. Y. (2009). Anaerobic biodegradation of *n*-hexadecane by a nitrate-reducing consortium. *Appl. Environ. Microbiol.* 75, 1339–1344.

Chen, S. L., Blomberg, M. R., and Siegbahn, P. E. (2012). How is methane formed and oxidized reversibly when catalyzed by Ni-containing methyl-coenzyme M reductase? *Chemistry* 18, 6309–6315.

Cheng, L., Rui, J., Li, Q., Zhang, H., and Lu, Y. (2013). Enrichment and dynamics of novel syntrophs in a methanogenic hexadecane-degrading culture from a Chinese oilfield. *FEMS Microbiol. Ecol.* 83, 757–766.

Conrad, R. (2009). The global methane cycle: recent advances in understanding the microbial processes involved. *Environ. Microbiol. Rep.* 1, 285–292.

Cravo-Laureau, C., Grossi, V., Raphel, D., Matheron, R., and Hirschler-Réa, A. (2005). Anaerobic *n*-alkane metabolism by a sulfate-reducing bacterium, *Desulfatibacillum aliphaticivorans* strain CV2803^T. *Appl. Environ. Microbiol.* 71, 3458–3467.

Crowe, S. A., Katsev, S., Leslie, K., Sturm, A., Magen, C., Nomosatryo, S., et al. (2011). The methane cycle in ferruginous Lake Matano. *Geobiol.* 9, 61–78.

Davidova, I. A., Callaghan, A. V., Duncan, K. E., Sunner, J., Biri, B., Wawrik, B., et al. (2011). "Long-chain paraffin metabolism by a methanogenic bacterial consortium enriched from marine sediments," in *8th International Symposium of Subsurface Microbiology*, (Garmisch-Partenkirchen: International Symposium of Subsurface Microbiology).

Davidova, I. A., Gieg, L. M., Nanny, M., Kropp, K. G., and Suflita, J. M. (2005). Stable isotopic studies of *n*-alkane metabolism by a sulfate-reducing bacterial enrichment culture. *Appl. Environ. Microbiol.* 71, 8174–8182.

Dey, M., Li, X. H., Kunz, R. C., and Ragsdale, S. W. (2010). Detection of organometallic and radical intermediates in the catalytic mechanism of methyl-coenzyme M reductase using the natural substrate methyl-coenzyme M and a coenzyme B substrate analogue. *Biochemistry* 49, 10902–10911.

Duncan, K. E., Gieg, L. M., Parisi, V. A., Tanner, R. S., Tringe, S. G., Bristow, J., et al. (2009). Biocorrosive thermophilic microbial communities in Alaskan North Slope oil facilities. *Environ. Sci. Technol.* 43, 7977–7984.

Ermler, U., Grabarse, W., Shima, S., Goubeaud, M., and Thauer, R. K. (1997). Crystal structure of methyl coenzyme M reductase: the key enzyme of biological methane formation. *Science* 278, 1457–1462.

Ettwig, K. F., Butler, M. K., Le Paslier, D., Pelletier, E., Mangenot, S., Kuypers, M. M. M., et al. (2010). Nitrite-driven anaerobic methane oxidation by oxygenic bacteria. *Nature* 464, 543–550.

Ettwig, K. F., Shima, S., Van De Pas-Schoonen, K. T., Kahnt, J., Medema, M. H., Op Den Camp, H. J. M., et al. (2008). Denitrifying bacteria anaerobically oxidize methane in the absence of Archaea. *Environ. Microbiol.* 10, 3164–3173.

Ettwig, K. F., Van Alen, T., Van De Pas-Schoonen, K. T., Jetten, M. S. M., and Strous, M. (2009). Enrichment and molecular detection of denitrifying methanotrophic bacteria of the NC10 phylum. *Appl. Environ. Microbiol.* 75, 3656–3662.

Gieg, L. M., Davidova, I. A., Duncan, K. E., and Suflita, J. M. (2010). Methanogenesis, sulfate reduction and crude oil biodegradation in hot Alaskan oilfields. *Environ. Microbiol.* 12, 3074–3086.

Gorby, Y. A., Yanina, S., Mclean, J. S., Rosso, K. M., Moyles, D., Dohnalkova, A., et al. (2006). Electrically conductive bacterial nanowires produced by *Shewanella oneidensis* strain MR-1 and other microorganisms. *Proc. Natl. Acad. Sci. U.S.A.* 103, 11358–11363.

Grundmann, O., Behrends, A., Rabus, R., Amann, J., Halder, T., Heider, J., et al. (2008). Genes encoding the candidate enzyme for anaerobic activation of *n*-alkanes in the denitrifying bacterium, strain HxN1. *Environ. Microbiol.* 10, 376–385.

Hallam, S. J., Girguis, P. R., Preston, C. M., Richardson, P. M., and Delong, E. F. (2003). Identification of methyl coenzyme M reductase A *(mcrA)* genes associated with methane-oxidizing archaea. *Appl. Environ. Microbiol.* 69, 5483–5491.

Hallam, S. J., Putnam, N., Preston, C. M., Detter, J. C., Rokhsar, D., Richardson, P. M., et al. (2004). Reverse methanogenesis: testing the hypothesis with environmental genomics. *Science* 305, 1457–1462.

Heider, J., Spormann, A. M., Beller, H. R., and Widdel, F. (1998). Anaerobic bacterial metabolism of hydrocarbons. *FEMS Microbiol. Rev.* 22, 459–473.

Heller, C., Hoppert, M., and Reitner, J. (2008). Immunological localization of coenzyme M reductase in anaerobic methane-oxidizing archaea of ANME 1 and ANME 2 type. *Geomicrobiol. J.* 25, 149–156.

Hinrichs, K. U., and Boetius, A. (2002). "The anaerobic oxidation of methane: new insights in microbial ecology and biogeochemistry," in *Ocean Margin Systems*, eds G. Wefer, D. Billett, D. Hebbeln, B. Jørgensen, M. Schlüter, and T. Van Weering. (Berlin Heidelberg: Springer-Verlag), 457–477.

Hoehler, T. M., Alperin, M. J., Albert, D. B., and Martens, C. S. (1994). Field and laboratory studies of methane oxidation in an anoxic marine sediment – evidence for a methanogen-sulfate reducer consortium. *Glob. Biogeochem. Cycle* 8, 451–463.

Jarling, R., Sadeghi, M., Drozdowska, M., Lahme, S., Buckel, W., Rabus, R., et al. (2012). Stereochemical investigations reveal the mechanism of the bacterial activation of *n*-alkanes without oxygen. *Angew. Chem. Int. Ed. Engl.* 51, 1334–1338.

Johnson, H. A., Pelletier, D. A., and Spormann, A. M. (2001). Isolation and characterization of anaerobic ethylbenzene dehydrogenase, a novel Mo-Fe-S enzyme. *J. Bacteriol.* 183, 4536–4542.

Johnson, H. A., and Spormann, A. M. (1999). In vitro studies on the initial reactions of anaerobic ethylbenzene mineralization. *J. Bacteriol.* 181, 5662–5668.

Kniemeyer, O., and Heider, J. (2001). Ethylbenzene dehydrogenase, a novel hydrocarbon-oxidizing molybdenum/iron-sulfur/heme enzyme. *J. Biol. Chem.* 276, 21381–21386.

Kniemeyer, O., Musat, F., Sievert, S. M., Knittel, K., Wilkes, H., Blumenberg, M., et al. (2007). Anaerobic oxidation of short-chain hydrocarbons by marine sulphate-reducing bacteria. *Nature* 449, 898–901.

Knittel, K., and Boetius, A. (2009). Anaerobic oxidation of methane: progress with an unknown process. *Annu. Rev. Microbiol.* 63, 311–334.

Knittel, K., and Boetius, A. (2011). "Anaerobic oxidation of methane with sulfate," in *Encyclopedia of Geobiology*, eds V. Thiel and J. Reitner (Berlin: Springer).

Kolukirik, M., Ince, O., and Ince, B. K. (2011). Increment in anaerobic hydrocarbon degradation activity of halic bay sediments via nutrient amendment. *Microb. Ecol.* 61, 871–884.

Krämer, M., and Cypionka, H. (1989). Sulfate formation via Atp sulfurylase in thiosulfate-disproportionating and sulfite-disproportionating bacteria. *Arch. Microbiol.* 151, 232–237.

Krieger, C. J., Roseboom, W., Albracht, S. P. J., and Spormann, A. M. (2001). A stable organic free radical in anaerobic benzylsuccinate synthase of *Azoarcus* sp strain T. *J. Biol. Chem.* 276, 12924–12927.

Kropp, K. G., Davidova, I. A., and Suflita, J. M. (2000). Anaerobic oxidation of *n*-dodecane by an addition reaction in a sulfate-reducing bacterial enrichment culture. *Appl.*

Environ. Microbiol. 66, 5393–5398.

Krüger, M., Blumenberg, M., Kasten, S., Wieland, A., Kanel, L., Klock, J. H., et al. (2008). A novel, multi-layered methanotrophic microbial mat system growing on the sediment of the Black Sea. *Environ. Microbiol.* 10, 1934–1947.

Krüger, M., Meyerdierks, A., Glöckner, F. O., Amann, R., Widdel, F., Kube, M., et al. (2003). A conspicuous nickel protein in microbial mats that oxidize methane anaerobically. *Nature* 426, 878–881.

Leuthner, B., Leutwein, C., Schulz, H., Hörth, P., Haehnel, W., Schiltz, E., et al. (1998). Biochemical and genetic characterization of benzylsuccinate synthase from *Thauera aromatica*: a new glycyl radical enzyme catalysing the first step in anaerobic toluene metabolism. *Mol. Microbiol.* 28, 615–628.

Leutwein, C., and Heider, J. (1999). Anaerobic toluene-catabolic pathway in denitrifying *Thauera aromatica*: activation and beta-oxidation of the first intermediate, *(R)*-(+)-benzylsuccinate. *Microbiology* 145, 3265–3271.

Li, W., Wang, L. Y., Duan, R. Y., Liu, J. F., Gu, J. D., and Mu, B. Z. (2012). Microbial community characteristics of petroleum reservoir production water amended with *n*-alkanes and incubated under nitrate-, sulfate-reducing and methanogenic conditions. *Int. Biodeterior. Biodegration* 69, 87–96.

Lide, D. R. (ed.). (2003). *Handbook of Chemistry and Physics.* Boca Raton: CRC Press.

Mayr, S., Latkoczy, C., Krüger, M., Günther, D., Shima, S., Thauer, R. K., et al. (2008). Structure of an F430 variant from archaea associated with anaerobic oxidation of methane. *J. Am. Chem. Soc.* 130, 10758–10767.

Mbadinga, S. M., Li, K. P., Zhou, L., Wang, L. Y., Yang, S. Z., Liu, J. F., et al. (2012). Analysis of alkane-dependent methanogenic community derived from production water of a high-temperature petroleum reservoir. *Appl. Microbiol. Biotechnol.* 96, 531–542.

Meckenstock, R. U., and Mouttaki, H. (2011). Anaerobic degradation of non-substituted aromatic hydrocarbons. *Curr. Opin. Biotechnol.* 22, 406–414.

Meulepas, R. J., Jagersma, C. G., Khadem, A. F., Stams, A. J., and Lens, P. N. (2010). Effect of methanogenic substrates on anaerobic oxidation of methane and sulfate reduction by an anaerobic methanotrophic enrichment. *Appl. Microbiol. Biotechnol.* 87, 1499–1506.

Meyerdierks, A., Kube, M., Kostadinov, I., Teeling, H., Glockner, F. O., Reinhardt, R., et al. (2010). Metagenome and mRNA expression analyses of anaerobic methanotrophic archaea of the ANME-1 group. *Environ. Microbiol.* 12, 422–439.

Milucka, J., Ferdelman, T. G., Polerecky, L., Franzke, D., Wegener, G., Schmid, M., et al. (2012). Zero-valent sulphur is a key intermediate in marine methane oxidation. *Nature* 491, 541–546.

Moran, J. J., Beal, E. J., Vrentas, J. M., Orphan, V. J., Freeman, K. H., and House, C. H. (2008). Methyl sulfides as intermediates in the anaerobic oxidation of methane. *Environ. Microbiol.* 10, 162–173.

Musat, F., Wilkes, H., Behrends, A., Woebken, D., and Widdel, F. (2010). Microbial nitrate-dependent cyclohexane degradation coupled with anaerobic ammonium oxidation. *ISME J.* 4, 1290–1301.

Nunoura, T., Oida, H., Miyazaki, J., Miyashita, A., Imachi, H., and Takai, K. (2008). Quantification of *mcrA* by fluorescent PCR in methanogenic and methanotrophic microbial communities. *FEMS Microbiol. Ecol.* 64, 240–247.

Pelmenschikov, V., Blomberg, M. R. A., Siegbahn, P. E. M., and Crabtree, R. H. (2002). A mechanism from quantum chemical studies for methane formation in methanogenesis. *J. Am. Chem. Soc.* 124, 4039–4049.

Pelmenschikov, V., and Siegbahn, P. E. M. (2003). Catalysis by methyl-coenzyme M reductase: a theoretical study for heterodisulfide product formation. *J. Biol. Inorg. Chem.* 8, 653–662.

Qiao, C. H., and Marsh, E. N. G. (2005). Mechanism of benzylsuccinate synthase: stereochemistry of toluene addition to fumarate and maleate. *J. Am. Chem. Soc.* 127, 8608–8609.

Rabus, R., and Heider, J. (1998). Initial reactions of anaerobic metabolism of alkylbenzenes in denitrifying and sulfate reducing bacteria. *Arch. Microbiol.* 170, 377–384.

Rabus, R., Jarling, R., Lahme, S., Kuhner, S., Heider, J., Widdel, F., et al. (2011). Co-metabolic conversion of toluene in anaerobic n-alkane-degrading bacteria. *Environ. Microbiol.* 13, 2576–2586.

Rabus, R., Wilkes, H., Behrends, A., Armstroff, A., Fischer, T., Pierik, A. J., et al. (2001). Anaerobic initial reaction of *n*-alkanes in a denitrifying bacterium: evidence for (1-methylpentyl)succinate as initial product and for involvement of an organic radical in *n*-hexane metabolism. *J. Bacteriol.* 183, 1707–1715.

Raghoebarsing, A. A., Pol, A., Van De Pas-Schoonen, K. T., Smolders, A. J. P., Ettwig, K. F., Rijpstra, W. I. C., et al. (2006). A microbial consortium couples anaerobic methane oxidation to denitrification. *Nature* 440, 918–921.

Reeburgh, W. S. (2007). Oceanic methane biogeochemistry. *Chem. Rev.* 107, 486–513.

Reguera, G., Mccarthy, K. D., Mehta, T., Nicoll, J. S., Tuominen, M. T., and Lovley, D. R. (2005). Extracellular electron transfer via microbial nanowires. *Nature* 435, 1098–1101.

Rios-Hernandez, L. A., Gieg, L. M., and Suflita, J. M. (2003). Biodegradation of an alicyclic hydrocarbon by a sulfate-reducing enrichment from a gas condensate-contaminated aquifer. *Appl. Environ. Microbiol.* 69, 434–443.

Savage, K. N., Krumholz, L. R., Gieg, L. M., Parisi, V. A., Suflita, J. M., Allen, J., et al. (2010). Biodegradation of low-molecular-weight alkanes under mesophilic, sulfate-reducing conditions: metabolic intermediates and community patterns. *FEMS Microbiol. Ecol.* 72, 485–495.

Scheller, S., Goenrich, M., Boecher, R., Thauer, R. K., and Jaun, B. (2010a). The key nickel enzyme of methanogenesis catalyses the anaerobic oxidation of methane. *Nature* 465, U606–U697.

Scheller, S., Goenrich, M., Mayr, S., Thauer, R. K., and Jaun, B. (2010b). Intermediates in the catalytic cycle of methyl coenzyme M reductase: isotope exchange is consistent with formation of a σ-alkane-nickel complex. *Angew. Chem. Int. Ed.* 49, 8112–8115.

Schreiber, L., Holler, T., Knittel, K., Meyerdierks, A., and Amann, R. (2010). Identification of the dominant sulfate-reducing bacterial partner of anaerobic methanotrophs of the ANME-2 clade. *Environ. Microbiol.* 12, 2327–2340.

Selmer, T., Pierik, A. J., and Heider, J. (2005). New glycyl radical enzymes catalysing key metabolic steps in anaerobic bacteria. *Biol. Chem.* 386, 981–988.

Shen, L. D., He, Z. F., Zhu, Q., Chen, D. Q., Lou, L. P., Xu, X. Y., et al. (2012). Microbiology, ecology, and application of the nitrite-dependent anaerobic methane oxidation process. *Front. Microbiol.* 3:269. doi: 10.3389/fmicb.2012.00269

Shima, S., Krueger, M., Weinert, T., Demmer, U., Kahnt, J., Thauer, R. K., et al. (2012). Structure of a methyl-coenzyme M reductase from Black Sea mats that oxidize methane anaerobically. *Nature* 481, 98–101.

Sivan, O., Adler, M., Pearson, A., Gelman, F., Bar-Or, I., John, S. G., et al. (2011). Geochemical evidence for iron-mediated anaerobic oxidation of methane. *Limnol. Oceanogr.* 56, 1536–1544.

So, C. M., Phelps, C. D., and Young, L. Y. (2003). Anaerobic transformation of alkanes to fatty acids by a sulfate-reducing bacterium, strain Hxd3. *Appl. Environ. Microbiol.* 69, 3892–3900.

So, C. M., and Young, L. Y. (1999). Initial reactions in anaerobic alkane degradation by a sulfate reducer, strain AK-01. *Appl. Environ. Microbiol.* 65, 5532–5540.

Sünwoldt, K., Knack, D., and Heider, J. (2012). "New reactions in anaerobic alkane and alkene metabolism," in *DFG-Priority Programme 1319 Third Meeting: Biological Transformations of Hydrocarbons without Oxygen – from the Molecular to the Global Scale.* (Freiburg: Deutsche Forschungsgemeinschaft).

Thauer, R. K. (2011). Anaerobic oxidation of methane with sulfate: on the reversibility of the reactions that are catalyzed by enzymes also involved in methanogenesis from CO_2. *Curr. Opin. Microbiol.* 14, 292–299.

Thauer, R. K., and Shima, S. (2008). Methane as fuel for anaerobic microorganisms. *Ann. N. Y. Acad. Sci.* 1125, 158–170.

Valentine, D. L., and Reeburgh, W. S. (2000). New perspectives on anaerobic methane oxidation. *Environ. Microbiol.* 2, 477–484.

Verfürth, K., Pierik, A. J., Leutwein, C., Zorn, S., and Heider, J. (2004). Substrate specificities and electron paramagnetic resonance properties of benzylsuccinate synthases in anaerobic toluene and *m*-xylene metabolism. *Arch. Microbiol.* 181, 155–162.

Wang, L. Y., Li, W., Mbadinga, S. M., Liu, J. F., Gu, J. D., and Mu, B. Z. (2012). Methanogenic microbial community composition of oily sludge and its enrichment amended with alkanes incubated for over 500 days. *Geomicrobiol. J.* 29, 716–726.

Wawrik, B., Mendivelso, M., Parisi, V. A., Suflita, J. M., Davidova, I. A., Marks, C. R., et al. (2012). Field and laboratory studies on the bioconversion of coal to methane in the San

Juan Basin. *FEMS Microbiol. Ecol.* 81, 26–42.

Wilkes, H., Kühner, S., Bolm, C., Fischer, T., Classen, A., Widdel, F., et al. (2003). Formation of *n*-alkane- and cycloalkane-derived organic acids during anaerobic growth of a denitrifying bacterium with crude oil. *Org. Geochem.* 34, 1313–1323.

Wilkes, H., Rabus, R., Fischer, T., Armstroff, A., Behrends, A., and Widdel, F. (2002). Anaerobic degradation of *n*-hexane in a denitrifying bacterium: further degradation of the initial intermediate (1-methylpentyl)succinate via C-skeleton rearrangement. *Arch. Microbiol.* 177, 235–243.

Wu, M. L., De Vries, S., Van Alen, T. A., Butler, M. K., Den Camp, H. J. M. O., Keltjens, J. T., et al. (2011). Physiological role of the respiratory quinol oxidase in the anaerobic nitrite-reducing methanotroph '*Candidatus Methylomirabilis oxyfera*'. *Microbiology* 157, 890–898.

Zedelius, J., Rabus, R., Grundmann, O., Werner, I., Brodkorb, D., Schreiber, F., et al. (2011). Alkane degradation under anoxic conditions by a nitrate-reducing bacterium with possible involvement of the electron acceptor in substrate activation. *Environ. Microbiol. Rep.* 3, 125–135.

Zehnder, A. J. B., and Brock, T. D. (1979). Methane formation and methane oxidation by methanogenic bacteria. *J. Bacteriol.* 137, 420–432.

Zehnder, A. J. B., and Brock, T. D. (1980). Anaerobic methane oxidation – cccurrence and ecology. *Appl. Environ. Microbiol.* 39, 194–204.

Zhou, L., Li, K. P., Mbadinga, S. M., Yang, S. Z., Gu, J. D., and Mu, B. Z. (2012). Analyses of *n*-alkanes degrading community dynamics of a high-temperature methanogenic consortium enriched from production water of a petroleum reservoir by a combination of molecular techniques. *Ecotoxicology* 21, 1680–1691.

Zhu, B., Van Dijk, G., Fritz, C., Smolders, A. J., Pol, A., Jetten, M. S., et al. (2012). Anaerobic oxidization of methane in a minerotrophic peatland: enrichment of nitrite-dependent methane-oxidizing bacteria. *Appl. Environ. Microbiol.* 78, 8657–8665.

Conflict of Interest Statement: The author declares that the research was conducted in the absence of any commercial or financial relationships that could be construed as a potential conflict of interest.

Received: 14 December 2012; paper pending published: 13 January 2013; accepted: 31 March 2013; published online: 14 May 2013.

Citation: Callaghan AV (2013) Enzymes involved in the anaerobic oxidation of n-alkanes: from methane to long-chain paraffins. Front. Microbiol. ***4****:89. doi: 10.3389/fmicb.2013.00089*

This article was submitted to Frontiers in Microbiological Chemistry, a specialty of Frontiers in Microbiology.

frontiers in
MICROBIOLOGY

REVIEW ARTICLE
published: 04 June 2013
doi: 10.3389/fmicb.2013.00140

In situ detection of anaerobic alkane metabolites in subsurface environments

Akhil Agrawal and Lisa M. Gieg*

Petroleum Microbiology Research Group, Department of Biological Sciences, University of Calgary, Calgary, AB, Canada

Edited by:
Amy V. Callaghan, University of Oklahoma, USA

Reviewed by:
Rachel N. Austin, Bates College, USA
Craig Phelps, The State University of New Jersey, USA

****Correspondence:***
Lisa M. Gieg, Petroleum Microbiology Research Group, Department of Biological Sciences, University of Calgary, 2500 University Drive NW, Calgary, AB T2N 1N4, Canada
e-mail: lmgieg@ucalgary.ca

Alkanes comprise a substantial fraction of crude oil and refined fuels. As such, they are prevalent within deep subsurface fossil fuel deposits and in shallow subsurface environments such as aquifers that are contaminated with hydrocarbons. These environments are typically anaerobic, and host diverse microbial communities that can potentially use alkanes as substrates. Anaerobic alkane biodegradation has been reported to occur under nitrate-reducing, sulfate-reducing, and methanogenic conditions. Elucidating the pathways of anaerobic alkane metabolism has been of interest in order to understand how microbes can be used to remediate contaminated sites. Alkane activation primarily occurs by addition to fumarate, yielding alkylsuccinates, unique anaerobic metabolites that can be used to indicate *in situ* anaerobic alkane metabolism. These metabolites have been detected in hydrocarbon-contaminated shallow aquifers, offering strong evidence for intrinsic anaerobic bioremediation. Recently, studies have also revealed that alkylsuccinates are present in oil and coal seam production waters, indicating that anaerobic microbial communities can utilize alkanes in these deeper subsurface environments. In many crude oil reservoirs, the *in situ* anaerobic metabolism of hydrocarbons such as alkanes may be contributing to modern-day detrimental effects such as oilfield souring, or may lead to more beneficial technologies such as enhanced energy recovery from mature oilfields. In this review, we briefly describe the key metabolic pathways for anaerobic alkane (including *n*-alkanes, isoalkanes, and cyclic alkanes) metabolism and highlight several field reports wherein alkylsuccinates have provided evidence for anaerobic *in situ* alkane metabolism in shallow and deep subsurface environments.

Keywords: anaerobic, metabolites, alkylsuccinates, alkanes, subsurface

INTRODUCTION

Alkanes are carbon and hydrogen containing molecules that are abundant across the globe, found primarily in fossil energy deposits. They are most abundant in crude oil reservoirs, but can also be found associated with shale and coal seams (Formolo et al., 2008; Strąpoć et al., 2011). Straight chain alkanes (*n*-alkanes), branched alkanes (also known as isoalkanes), and cyclic alkanes form the saturate fraction of crude oils, which can comprise ∼20% (by wt.) in a heavy oil and up to ∼50% (by wt.) in a typical light oil (Hunt, 1996). The smallest alkane is methane, a C_1 compound, while the largest alkane extends beyond C_{100} in paraffinic (waxy) oils (Hsieh et al., 2000). Under ambient conditions, alkanes ranging from C_1–C_4 are gases, those ranging from C_5–C_{16} are liquids, and alkanes $>C_{17}$ are solids (Hunt, 1996). In addition to their prevalence in petroleum mixtures, alkanes can also be found in some plants and animals, where they play a protective role or function as signaling molecules among species (Thom et al., 2007; Kunst and Samuels, 2009).

Alkanes are characterized by non-polar sigma bonds, a property that renders them relatively unreactive to most chemical transformations unless high temperatures, UV light, or specialized catalysts are applied (Carey, 2007). In contrast, these compounds are readily susceptible to microbiological transformation under ambient conditions. Understanding the biodegradation of all classes of hydrocarbons including alkanes is especially important, as the transport, storage, and usage of fossil fuel as our primary global energy source has resulted in widespread contamination of hydrocarbons into natural surface or near surface ecosystems such as groundwater aquifers. Thus, the microbial degradation of hydrocarbons represents an important fate process to mitigate such contamination. In deeper subsurface environments such as oil reservoirs, it has also been suggested that anaerobic microbial activity contributed to oil biodegradation over geological time, giving rise to heavy oil reservoirs (Huang and Larter, 2005; Head et al., 2010). Thus, understanding the processes underlying hydrocarbon biodegradation in reservoirs is important because these processes can potentially lead to detrimental effects such as heavy oil generation or reservoir souring (Voordouw et al., 2009). However, such activity can also lead to the development of beneficial biotechnologies such as microbially-enhanced energy recovery by purposefully stimulating hydrocarbon biodegradation to yield methane as an alternate energy source in mature oil reservoirs or other fossil energy environments like coal or shale deposits (Formolo et al., 2008; Gieg et al., 2008; Gray et al., 2010; Strąpoć et al., 2011). Therefore, understanding the biodegradation of hydrocarbons

such as alkanes under a variety of electron-accepting conditions is important for both bioremediation and microbial-based energy recovery applications.

PATHWAYS OF ALKANE BIODEGRADATION

Alkanes have long been known to be biodegradable under aerobic conditions by microorganisms. In addition to utilizing oxygen as an electron acceptor, aerobes use oxygen as a co-reactant to activate the stable carbon-carbon bonds of alkanes using monooxygenases (Rojo, 2009). The monooxygenases incorporate oxygen into the alkane molecule typically at the terminal carbon, forming an alcohol. This metabolite is then transformed to an aldehyde, which is subsequently converted to a carboxylic acid. The latter product is then readily metabolized via β-oxidation reactions to products that can enter central metabolic pathways (Rojo, 2009). The reader is referred to other papers in this volume for more details on the aerobic microbial oxidation of alkanes.

The anaerobic oxidation of alkanes has also been documented in a few early reports (ZoBell, 1946; Muller, 1957; Jack et al., 1985) but was largely discounted due to the overwhelming evidence for and widespread prevalence of aerobic alkane biodegradation processes that can readily occur in surface soils or in aerated environments. However, mounting evidence over the last two decades has shown that petroleum mixtures spilled into natural environments such as groundwater aquifers results in a rapid depletion of oxygen, creating anaerobic conditions. Thus, much attention has now also been focused on examining the potential for anaerobic hydrocarbon metabolism primarily in the interest of applying bioremediation for site cleanup.

Research conducted in the 1990's examining the anaerobic biodegradation of alkylbenzenes such as toluene and xylene using samples collected from hydrocarbon-contaminated sites revealed that anaerobes activate hydrocarbons by a novel carbon-carbon addition mechanism known as "fumarate addition." In this mechanism, the methyl group of an alkylbenzene such as toluene is added to fumarate (a C_4-dicarboxylic acid present in central microbial metabolic pathways) forming benzylsuccinic acid (Biegert et al., 1996; Beller and Spormann, 1997). The enzyme carrying out this reaction, benzylsuccinate synthase, is known to be part of the radical SAM superfamily of enzymes (Frey, 2001; Widdel and Grundmann, 2010). Following this discovery, many more details regarding the mechanism, enzymes, and genes involved in this activation step (and further downstream metabolic reactions) have been elucidated for many aromatic hydrocarbons, including methylated mono- and polycyclic aromatic hydrocarbons [e.g., reviewed by Foght (2008)]. Subsequently, investigators examining anaerobic *n*-alkane metabolism found that this class of hydrocarbons could also be activated by carbon-carbon bond addition to fumarate, forming alkylsuccinates (Kropp et al., 2000; Rabus et al., 2001). Fumarate addition occurs primarily at the C2 subterminal carbon position of a given *n*-alkane (**Figure 1A**). Alkylsuccinates are then further transformed by a postulated carbon skeleton rearrangement followed by decarboxylation yielding branched fatty acids that can readily enter β-oxidation and other central metabolic pathways (Wilkes et al., 2002; Cravo-Laureau et al., 2005; Davidova et al., 2005; Callaghan et al., 2006; Widdel and Grundmann, 2010) (**Figure 1A**). Recently, the genes responsible for the initial "alkylsuccinate synthase" reaction were identified, known as the *masD* or *assA* genes (Callaghan et al., 2008; Grundmann et al., 2008). Laboratory-based studies examining the anaerobic degradation of pure *n*-alkanes have demonstrated that alkanes ranging from C_3 to C_{16} are susceptible to fumarate addition, as the corresponding alkylsuccinates have been identified in culture fluids (**Table 1**). A recent laboratory study has also shown that *n*-alkanes up to C_{26} in whole crude oil can be degraded via fumarate addition under sulfate-reducing conditions (Aitken et al., 2013). Further, the *assA* gene has been detected in anaerobic cultures incubated with pure *n*-alkanes as short as C_3 and as long as C_{28} (Callaghan et al., 2010). It has been suggested that fumarate addition may even be possible for anaerobic methane oxidation (Thauer and Shima, 2008; Beasley and Nanny, 2012). An alternate mechanism to fumarate addition has also been suggested involving carboxylation at the C3 position of an *n*-alkane, followed by ethyl group removal by an unknown mechanism (So et al., 2003). Studies with a nitrate-reducing enrichment culture degrading *n*-hexadecane suggested a similar mechanism (Callaghan et al., 2009). Even though recent research has shown that alkanes are biodegraded under methanogenic conditions in laboratory incubations (e.g., Zengler et al., 1999; Siddique et al., 2006; Gieg et al., 2008; Jones et al., 2008; Siddique et al., 2011; Zhou et al., 2012; Aitken et al., 2013; Cheng et al., 2013), alkylsuccinates have not been detected as metabolites during the metabolism of *n*-alkanes, prompting the hypothesis that a different pathway may be occurring under these highly reduced conditions (Mbadinga et al., 2011; Aitken et al., 2013).

A few studies have now shown that cyclic alkanes may be also be activated by fumarate addition (**Figure 1B**). In studies examining the biotransformation of hydrocarbons in whole crude oil by a nitrate-reducer (strain HxN1) capable of utilizing C_6–C_8 *n*-alkanes, Wilkes et al. (2003) detected metabolites showing that cyclopentane and methylcyclopentane were biotransformed to the corresponding fumarate addition products in co-metabolic reactions with hexane as the primary carbon source. Using sediments from a gas condensate-contaminated site, Rios-Hernandez et al. (2003) demonstrated sulfate-dependent ethylcyclopentane metabolism, and identified a putative fumarate addition metabolite from this cyclic alkane. In anoxic laboratory incubations prepared from the same contaminated sediments amended with sulfate and methylcyclohexane-d_{14}, the corresponding *d*-labeled fumarate addition metabolite was also tentatively identified from this cyclic alkane (Gieg et al., 2009). Unfortunately, the exact location on the alkylated cyclic alkanes to which fumarate was added (e.g., alkyl group or ring carbon) could not be determined in the studies. Musat et al. (2010) showed that the model unsubstituted cyclic alkane cyclohexane was also activated by a carbon-carbon addition to fumarate under nitrate-reducing conditions, a process that was also coupled to anaerobic ammonium oxidation. A proposed pathway for the anaerobic biodegradation of a model cyclic alkane (cyclohexane) via fumarate addition and subsequent reactions (Rios-Hernandez et al., 2003; Musat et al., 2010) is shown in **Figure 1B**.

Comparatively little has been reported on the anaerobic biotransformation of isoalkanes. Branched alkanes such as pristane

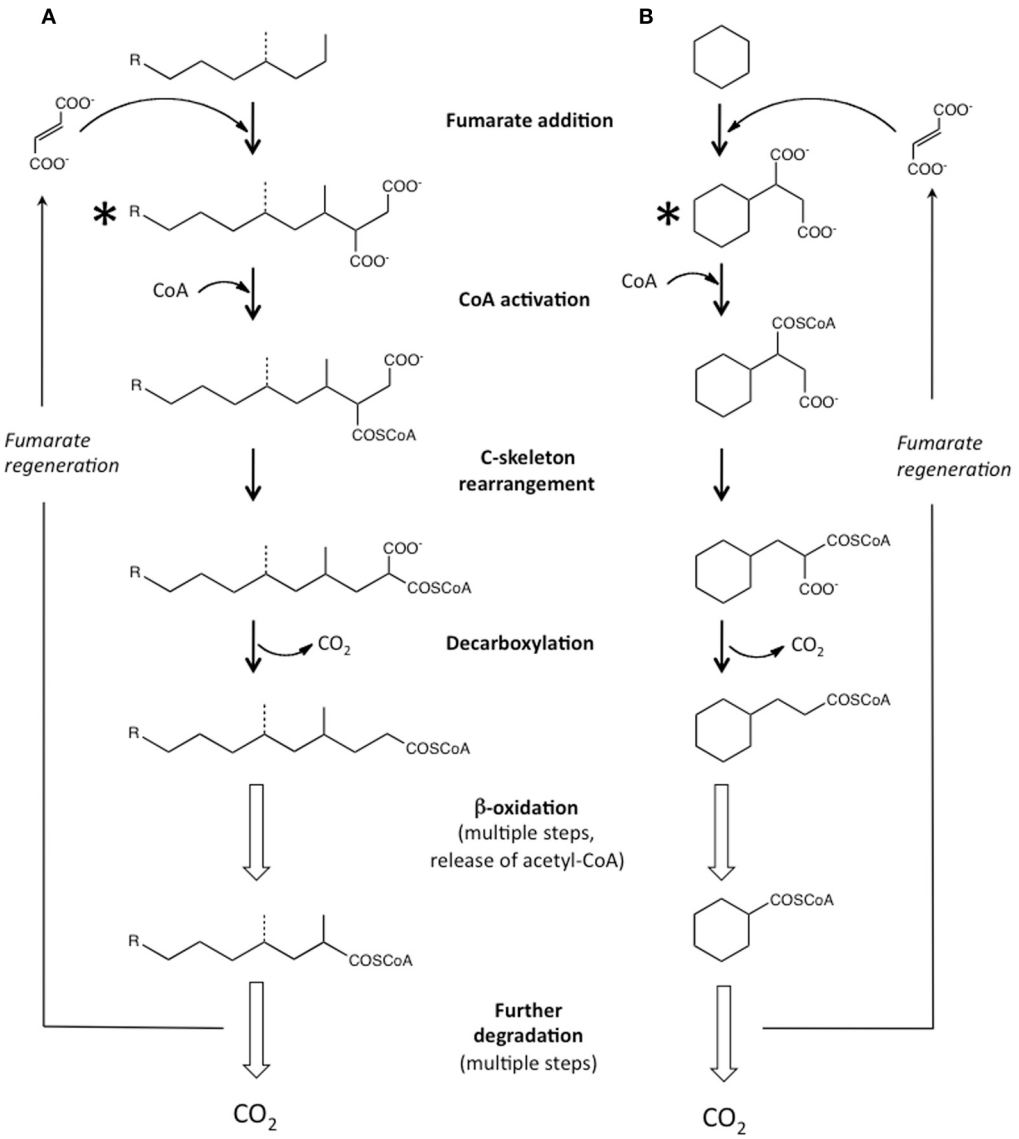

FIGURE 1 | The anaerobic biodegradation of alkanes via fumarate addition and subsequent reactions. (A) Pathway for the biodegradation of *n*-alkanes and potentially for isoalkanes (dotted lines) based on literature reports [e.g., as overviewed by Widdel and Grundmann (2010)]. **(B)** Proposed pathway for the biodegradation of cyclic alkanes using (after Rios-Hernandez et al., 2003; Musat et al., 2010). Compounds marked with asterisks indicate fumarate addition metabolites that are most diagnostic of *in situ* anaerobic biodegradation of alkanes.

and phytane have frequently been used as biomarkers with which to compare the extent of biodegradation of alkanes in crude oils, as these kinds of compounds are typically more recalcitrant than *n*-alkanes (Huang and Larter, 2005). However, there is some evidence that branched alkanes can be utilized under anaerobic conditions. Two studies carried out under anaerobic conditions showed that the branched alkane pristane was susceptible to biodegradation under nitrate-reducing or methanogenic conditions but no metabolites were reported (Bregnard et al., 1997; Grossi et al., 2000). Using oil sands tailings ponds samples as an inoculum, Abu Laban et al. (2012) recently showed that C_7 and C_8 isoalkanes could also be metabolized under sulfate-reducing or methanogenic conditions. In the study, metabolites consistent with the mass spectral (MS) profiles of the corresponding alkylsuccinates were detected, showing for the first time that isoalkanes are also susceptible to fumarate addition (**Figure 1A**).

SIGNATURE ANAEROBIC METABOLITES AS INDICATORS OF *in situ* HYDROCARBON BIODEGRADATION

Given the overwhelming evidence that microbes are able to biodegrade hydrocarbons, relying on such activity for the remediation of contaminated sites is an attractive and relatively inexpensive clean-up option. However, documenting that such anaerobic hydrocarbon biodegradation is occurring in fuel-contaminated sites or in fossil energy reservoirs remains a challenge. For example, multiple lines of evidence, both chemical and

Table 1 | Overview of literature studies wherein fumarate addition metabolites (alkylsuccinates) were detected in anaerobic laboratory incubations with *n*-alkanes added as pure substrates.

n-alkane	Electron-accepting condition and culture	Literature references
C_3	Sulfate-reducing—strain BuS5	Kniemeyer et al., 2007
	Sulfate-reducing—enrichment culture	Savage et al., 2010
C_4	Sulfate-reducing—strain BuS5	Kniemeyer et al., 2007
C_6	Nitrate-reducing—strains HxN1, OcN1	Rabus et al., 2001
	Sulfate-reducing—strain ALDC (*Desulfoglaeba alkanexedens*)	Davidova et al., 2005
C_8	Nitrate-reducing—strain HxN1	Rabus et al., 2001
	Nitrate-reducing—strains HxN1, OcN1, HdN1	Zedelius et al., 2011
	Sulfate-reducing—strain ALDC (*Desulfoglaeba alkanexedens*)	Davidova et al., 2005
C_{10}	Sulfate-reducing—strain ALDC (*Desulfoglaeba alkanexedens*)	Davidova et al., 2005
	Sulfate-reducing—strain TD3	Rabus et al., 2011
C_{12}	Sulfate-reducing—strain ALDC (*Desulfoglaeba alkanexedens*)	Kropp et al., 2000 Davidova et al., 2005
C_{15}	Sulfate-reducing—*Desulfatibacillum aliphaticovorans CV2803*	Cravo-Laureau et al., 2005
C_{16}	Sulfate-reducing—*Desulfatibacillum aliphaticovorans CV2803*	Cravo-Laureau et al., 2005
	Sulfate-reducing—*Desulfatibacillum alkenivorans AK-01*	Callaghan et al., 2006

microbiological, are required to offer support that *in situ* hydrocarbon bioremediation is occurring in contaminated aquifers (NRC, 1993; Gieg and Suflita, 2005; Beller et al., 2008; Weiss and Cozzarelli, 2008; Bombach et al., 2010; Morasch et al., 2011; Jeon and Madsen, 2012). In conjunction with the elucidation of anaerobic hydrocarbon metabolic pathways, the idea of using anaerobic metabolites to indicate that *in situ* anaerobic hydrocarbon biodegradation is occurring emerged as a powerful tool for proving *in situ* bioremediation. Beller et al. (1995) first proposed that these metabolites can be effective indicators of *in situ* anaerobic hydrocarbon biodegradation since they are uniquely anaerobic and are specific to their hydrocarbon substrate; indeed they detected these metabolites in anoxic hydrocarbon-impacted groundwater but not in uncontaminated areas. Beller (2000) proposed a list of criteria that define a signature metabolite for use as an *in situ* bioremediation indicator including that the metabolite should be (1) actively produced during biodegradation, (2) relatively chemically and biologically stable so that it can be detected, (3) a true intermediate rather than a cometabolic by-product, (4) absent in the contaminant mixture, (5) absent in uncontaminated environments, and (6) be of no commercial use.

In addition to the initial reports by Beller and colleagues, many other studies have now shown that fumarate addition metabolites of alkylbenzenes (e.g., toluene, ethylbenzene, xylenes, and trimethylbenzenes) can be detected in hydrocarbon-contaminated groundwater [see reviews by Beller (2000); Gieg and Suflita (2005), and Callaghan (2012)]. With the discovery that methylnaphthalenes and other multi-ringed aromatics (including heterocycles) can also be metabolized by fumarate addition, the corresponding succinates have also been detected in field studies (Griebler et al., 2004; Bombach et al., 2010; Jobelius et al., 2011; Morasch et al., 2011), attesting to the usefulness of this method for demonstrating the *in situ* anaerobic biodegradation of many hydrocarbon classes. Furthermore, primer sets based on the catabolic gene(s) encoding benzylsuccinate synthase have been developed by several investigators and have been used successfully to indicate the metabolic potential for microbial communities in contaminated field samples to anaerobically biodegrade alkylbenzenes (e.g., Beller et al., 2002, 2008; Winderl et al., 2007; Callaghan et al., 2010; Oka et al., 2011; von Netzer et al., 2013). It should be noted that downstream metabolites of anaerobic hydrocarbon biodegradation can also be indicators of *in situ* biodegradation, especially if they are detected in contaminated but not in unrelated, uncontaminated groundwater samples (Cozzarelli et al., 1995; Gieg and Suflita, 2002). However, these compounds are typically not specific to a parent substrate (for example, benzoate, often detected in contaminated groundwaters, is a central intermediate in the anaerobic metabolism of many aromatic compounds) or may be produced via aerobic or anaerobic processes (such as toluates from xylenes) (Beller, 2000; Gieg and Suflita, 2005). In anaerobic alkane metabolism, downstream metabolites include fatty acids, which may be produced via a variety of other cellular pathways. Thus, the fumarate addition metabolites are most diagnostic of the *in situ* anaerobic metabolism of specific hydrocarbons including alkanes. It should be noted, however, that there are some disadvantages to using signature metabolites as *sole* indicators of *in situ* bioremediation (Morasch et al., 2011). For example, these products may be below analytical detection limits, knowledge of biodegradation pathways for various hydrocarbons is required (e.g., in order to determine which metabolites to look for), and commercially-available authentic standards for many of the fumarate addition products are not available for analytical comparisons with metabolites found in field samples. Thus, using signature fumarate addition metabolites to determine whether *in situ* hydrocarbon metabolism is occurring at a given site should ideally be done in conjunction with other methods of site assessment (Bombach et al., 2010; Morasch et al., 2011).

ANAEROBIC ALKANE METABOLITES IN HYDROCARBON-CONTAMINATED AQUIFERS

In field bioremediation studies, the biodegradation of BTEX compounds has been a focus because these compounds are highly water-soluble (150–1780 mg/L; Heath et al., 1993) thus can rapidly migrate away from the spill source. Furthermore, benzene is among the most highly regulated hydrocarbons due to its carcinogenicity (Maltoni et al., 1989). However, in many fuel mixtures that spill into aquifers (such as gasoline, diesel, gas condensate, jet fuel), the saturate fraction (alkanes, isoalkanes, and cyclic alkanes) is the most abundant (e.g., up to 80% by wt., Heath

et al., 1993). Since many alkanes have appreciable water solubilites (in the tens of mg/L), some alkanes can also migrate in groundwater away from the spill source. Many alkanes have known toxicity (Ritchie et al., 2001), thus their presence in contaminated aquifers is also of concern and their levels are often regulated (Nascarella et al., 2002).

To date, though, relatively few studies have reported on the detection of signature anaerobic alkane metabolites indicative of *in situ* anaerobic alkane in hydrocarbon-contaminated near surface environments. Gieg and Suflita (2002) documented that alkylsuccinates can be detected in hydrocarbon contaminated aquifers alongside benzylsuccinates, providing evidence that alkanes are susceptible to *in situ* anaerobic biodegradation and that alkylsuccinates can also be used as indicator metabolites. In 5 of the 6 sites examined for these signature compounds, alkylsuccinates were detected in contaminated groundwater samples, ranging from C_3 to C_{11} alkylsuccinates depending on the site interrogated (Gieg and Suflita, 2002; **Table 2**). Several of the detected metabolites had MS fragments with two mass units less than those predicted to arise from straight chain (or branched) alkane metabolism, suggesting the formation of fumarate addition products from cyclic alkanes. Using sediments from a gas condensate-contaminated site, Rios-Hernandez et al. (2003) demonstrated that ethylcyclopentane could be biodegraded under sulfate-reducing conditions in laboratory incubations, and identified a putative fumarate addition metabolite that formed during

Table 2 | Summary of studies reporting the detection of alkylsuccinates [and/or alkylsuccinate synthase (*assA*) gene] in hydrocarbon-contaminated aquifer samples*.

Field location	Hydrocarbon contaminant	Electron accepting condition(s) of field Site	Alkylsuccinates (and/or *assA* gene detected)	References
Weld County, CO, USA	Gas condensate	Sulfate-reducing, methanogenic	Saturated: C_6–C_9 Unsaturated: C_6–C_9 *assA* gene detected	Gieg and Suflita, 2002; Rios-Hernandez et al., 2003; Callaghan et al., 2010
Wise County, TX, USA	Natural gas liquids	Sulfate-reducing	Saturated: C_3–C_6 Unsaturated: C_6	Gieg and Suflita, 2002
Sedgewick County, KS, USA	Gasoline range organics	Nitrate-reducing, sulfate-reducing, methanogenic	Saturated: C_5 Unsaturated: C_6	Gieg and Suflita, 2002
West central AB, Canada	Flare pit site, variable hydrocarbons	Sulfate-reducing, methanogenic	Saturated: C_5–C_{11} Unsaturated: C_7	Gieg and Suflita, 2002
East central AB, Canada	Gas condensate	Nitrate-reducing, Fe- and Mn-reducing, sulfate-reducing	Saturated: C_4, C_6, C_8 Unsaturated: C_6, C_7	Gieg and Suflita, 2002
Casper, WY, USA	Former refinery site, variable hydrocarbons	Sulfate-reducing, methanogenic	Saturated: C_5, C_6 Unsaturated: C_5–C_9	Parisi et al., 2009
Hickam AFB, HI, USA	Jet fuel	Sulfate-reducing, methanogenic	Saturated: C_5–C_9 Unsaturated: C_7	Gieg et al., 2009
Passaic River, NJ, USA	Hydrocarbon-contaminated sediments	Not reported	*assA* gene detected	Callaghan et al., 2010
Newtown Creek, NY, USA	Hydrocarbon-contaminated sediments	Not reported	*assA* gene detected	Callaghan et al., 2010
Arthur Kill Waterway, NY/NJ, USA	Hydrocarbon-contaminated sediments	Not reported	*assA* gene detected	Callaghan et al., 2010
Gowanus Canal, NY, USA	Hydrocarbon-contaminated sediments	Not reported	*assA* gene detected	Callaghan et al., 2010
Rhine River Valley (Flingern aquifer), Germany	Former gas works site, tar oil-contaminated	Primarily sulfate-reducing	*assA* gene detected	von Netzer et al., 2013
*Gulf of Mexico, USA	Crude oil	Not reported, but marine sediments	*assA* gene detected	Kimes et al., 2013

**Deep-sea marine sediments rather than groundwater aquifer sediments.*

the biodegradation of this compound. The gas chromatographic (GC) retention time and MS profile of this incubation-derived metabolite matched with that of a GC peak detected in several of the samples from the contaminated site, supporting the notion that cyclic alkanes can be anaerobically biotransformed *in situ*. Parisi et al. (2009) also detected alkylsuccinates from C_5 to C_9 *n*- or cyclic alkanes in groundwater samples collected from an aquifer contaminated with a variety of fuel mixtures while Gieg et al. (2009) detected C_5–C_9 alkylsuccinates in several anoxic groundwater samples prior to conducting push-pull tests in a jet fuel contaminated aquifer, further attesting to the *in situ* anaerobic biodegradation of alkanes (**Table 2**). In a gas condensate-contaminated site wherein alkylsuccinates were detected in groundwater samples (Gieg and Suflita, 2002; Rios-Hernandez et al., 2003), Callaghan et al. (2010) detected the presence of the alkylsuccinate synthase gene (*assA* gene), augmenting the metabolite findings. Primer sets for this gene were also used to probe samples collected from a handful of other hydrocarbon-contaminated aquifers in the US and in Germany, and indeed this gene was detected (**Table 2**; Callaghan et al., 2010; von Netzer et al., 2013). Recently, *assA* gene sequences were also detected in deep sea core samples collected from areas near the Deepwater Horizon oil spill, indicating that the extant organisms in deep-sea sediments have the potential to biodegrade alkanes and can potential contribute to bioremediation of such oil spills (Kimes et al., 2013). Although the alkylsuccinates themselves were not detected in these latter field sites, the detection of the gene catalyzing their formation in contaminated sites reveals a widespread potential for *in situ* anaerobic alkane biodegradation and usefulness of probing for the requisite metabolic genes. However, there are currently some limitations in the use of the *assA* gene. For example, this gene appears to be highly diverse, as a single primer set has not yet been designed that can be used to detect/amplify this gene (Callaghan et al., 2010; Aitken et al., 2013; von Netzer et al., 2013). Further, the *assA* genes show high similarity with the *bssA* genes, thus primer pairs designed to detect *assA* may also amplify the *bssA* genotypes (Callaghan et al., 2010). However, as stated above, such limitations can be overcome by coupling gene analysis with metabolite analysis and other indicators of biodegradation at field sites to provide strong evidence for intrinsic bioremediation of hydrocarbons like alkanes at contaminated sites. **Table 2** summarizes the reports to date wherein alkylsuccinates (and/or alkylsuccinate synthase genes) have been detected in hydrocarbon-contaminated sites, providing evidence in support of *in situ* anaerobic alkane biodegradation.

ANAEROBIC ALKANE METABOLITES IN FOSSIL ENERGY RESERVOIRS

Geochemical data suggesting the biodegradation of crude oil in reservoirs over geological time generating heavy oil has prompted an examination of these oils and fluids of oil reservoirs in general for evidence of anaerobic hydrocarbon metabolites. Upon examining 77 crude oils from across the globe, Aitken et al. (2004) detected known anaerobic metabolites of naphthalenes in 52 samples (including 2-naphthoic acid; 5,6,7,8-tetrahydro-2-naphthoic acid; decahydro-2-naphthoic acid), offering the first metabolic evidence that anaerobic *in situ* biodegradation of crude oil can occur in reservoirs. Although alkylsuccinates were also sought, none were detected in the assays. In a later study, Duncan et al. (2009) examined the metabolite profiles of several produced water samples (e.g., water removed along with oil from production wells during oil recovery) collected from high temperature Alaska North Slope (ANS) oilfields. The authors were able to detect some low molecular weight alkylsuccinates derived from C_1–C_4 alkanes in the produced water samples (**Table 3**). Downstream, branched alkanoic acids related to these alkylsuccinates were also detected (Duncan et al., 2009). Operationally, these oilfields were pressurized with natural gas to aid in oil recovery, providing the oilfield microbial community with a continuous source of low molecular weight alkanes that were likely ultimately biotransformed to the corresponding alkylsuccinates (Duncan et al., 2009). In a subsequent study, Gieg et al. (2010) examined samples collected from two different high temperature ANS oilfields, and also detected several fumarate addition metabolites including C_1–C_3 alkylsuccinates (**Table 3**). This latter study further showed that the methanogenic microbial communities present in crude oil reservoirs are able to subsist on hydrocarbons supporting the notion that oil biodegradation within fossil energy reservoirs can occur under anaerobic conditions.

A low temperature (∼30°C) heavy oil field in Alberta, Canada (Medicine Hat Glauconitic C field) has been under study for over 5 years to test the effects of nitrate treatment on souring caused by sulfate-reducing bacteria (Lambo et al., 2008; Voordouw et al., 2009; Callbeck et al., 2011; Agrawal et al., 2012). Oil analysis conducted on various samples from this field showed that toluene served as a major electron donor driving the microbial activities within the subsurface reservoir environment (Lambo et al., 2008). This result was subsequently confirmed in laboratory studies conducted under nitrate-reducing and sulfate-reducing conditions using produced water and heavy crude oil from the field. However, the laboratory incubation tests also showed that other alkylbenzenes and alkanes present in the oil served as substrates for the oilfield microbial community (Agrawal et al., 2012). Notably, several alkanes were depleted in sulfate-reducing enrichments, and numerous metabolites indicative of fumarate addition to both aromatics and alkanes were detected, including methyl- and dimethylbenzylsuccinates and alkylsuccinates derived from C_6–C_9 alkanes, confirming the anaerobic biodegradation of hydrocarbons in the oil. These laboratory-based studies prompted an investigation of produced water samples from the heavy oil field for the presence of alkylsuccinates, and indeed several of these signature anaerobic alkane metabolites were detected, ranging from C_5 to C_8 alkylsuccinates (**Table 3**). These data suggested that the anaerobic microbial communities present within this low temperature reservoir can utilize alkanes as a carbon and energy source, potentially leading to souring when sulfate is present. Although alkylsuccinates were not specifically identified in other oilfields (Li et al., 2012; Zhou et al., 2012; Cheng et al., 2013), recently identified alkylsuccinate synthase genes in incubations prepared from oilfield fluids, showing that microbes residing in the sampled oilfield harbor the potential for *in situ* anaerobic alkane

Table 3 | Summary of studies reporting the detection of alkylsuccinates [and/or alkylsuccinate synthase (*assA*) gene] in fossil energy reservoir samples.

Field location	Field details	Electron accepting condition(s)	Alkylsuccinates (and/or *assA* gene detected)	References
Alaska North Slope, USA	High temperature oilfield (50–60°C)	Sulfate-reducing, methanogenic	Saturated: C_1–C_4	Duncan et al., 2009
Alaska North Slope, USA	High temperature oilfield (50–60°C)	Primarily sulfate-reducing	Saturated: C_1–C_3	Gieg et al., 2010
Alaska North Slope, USA	High temperature oilfield (50–60°C)	Primarily methanogenic	Saturated: C_1–C_3	Gieg et al., 2010
SE Alberta, Canada	Low temperature oilfield (~30°C); oil produced via PWRI[1], nitrate treatment for souring	Nitrate-reducing, sulfate-reducing, methanogenic	Saturated: C_6–C_8 Unsaturated: C_6–C_8	Agrawal et al., 2012
Huabei Oilfield, China	Low temperature oilfield (37°C)	Not reported but incubations prepared with nitrate, sulfate, and under methanogenic conditions	*assA* gene detected in methanogenic incubations from production waters	Li et al., 2012
Shengli Oilfield, China	High temperature oilfield (70°C)	Not reported but incubations prepared under methanogenic conditions	*assA* gene detected in methanogenic incubations (55°C) from production waters	Zhou et al., 2012
Shengli Oilfield, China	High temperature oilfield (70°C)	Not reported but incubations prepared under methanogenic conditions	*assA* gene detected in methanogenic hexadecane-degrading enrichment	Cheng et al., 2013
San Juan Basin (Fruitland Coal Formation, CO and NM), USA	Coal bed methane site	Methanogenic	Saturated: C_1–C_3, C_8 Unsaturated: C_7–C_8 *ass*A gene detected	Wawrik et al., 2012

[1] *PWRI, Produced water re-injection.*

metabolism, again attesting to the usefulness of catabolic gene probes for determining *in situ* alkane biodegradation potential (**Table 2**).

Wawrik et al. (2012) recently conducted a study examining the biological conversion of coal to methane in a major coal-bed methane producing region in the USA (San Juan Basin) using a series of enrichments, functional gene assays, hydrocarbon metabolite analyses, and microbial community profiling of produced water samples. Coal is a complex, organic carbon-rich mixture derived from ancient wetland plants that were buried and transformed by heat and pressure over geological time (Strąpoć et al., 2011). While methane produced from coal beds is typically thermogenic, increasing evidence (such as the isotopic signature of methane) is showing that biologically produced methane is also occurring in many coal-bed regions (Strąpoć et al., 2011). Although not as clearly defined as crude oil, coal can contain many substrates such as alkanes (Orem et al., 2007; Strąpoć et al., 2011) that may be used by microbial communities living in coal beds to produce methane in real time, presumably via pathways similar to those shown in **Figure 1**. Using a functional gene array (GeoChip 3.1), Wawrik et al. (2012) detected the *assA* gene in several produced water samples collected from the San Juan Basin, showing that the indigenous microbial community has the metabolic potential for *in situ* anaerobic alkane biodegradation. In addition, they also detected C_1–C_3, C_7, and C_8 alkylsuccinates in several of the produced waters (**Table 3**). These data collectively showed for the first time that alkanes (and other substrates) associated with the coal can be metabolized by the associated microbial community, presumably leading to biological methane production in such fossil energy resources (Wawrik et al., 2012).

METHODS FOR ANAEROBIC ALKANE METABOLITE ANALYSIS

Tools of analytical chemistry including gas chromatography-mass spectrometry (GC-MS) and high performance liquid chromatography coupled with tandem MS (LC-MS-MS) have generally been used to detect hydrocarbon metabolites in samples collected from contaminated groundwater wells or produced water wellheads of oil or coal reservoirs. Detailed descriptions of these approaches have been described in several previous publications (e.g., Beller, 2002; Gieg and Suflita, 2002, 2005; Alumbaugh et al., 2004; Jobelius et al., 2011). Briefly, for metabolite analysis by GC-MS, at least a liter of water should be collected into clean vessels (preferably glass) and acidified immediately to pH ~2 to preserve samples and protonate metabolites. Samples can then be processed in the laboratory using liquid-liquid extraction with an organic solvent such as dichloromethane, diethyl ether, or ethylacetate. Concentrated organic solvent extracts are concentrated, then derivatized by

methylation or silylation prior to analysis by GC-MS (Gieg and Suflita, 2002). Depending on the method of derivatization, alkylsuccinates have diagnostic MS fragment ions that can be used to readily determine their presence in a given water sample. For example, trimethylsilyl esters of alkylsuccinates have diagnostic fragment ions of m/z 262, 217, 172, 147, and 73 (Gieg and Suflita, 2002, 2005). Metabolite concentrations can be estimated by comparison to calibration curves prepared from commercially available or readily synthesized alkylsuccinates (e.g., methylsuccinate or *n*-octylsuccinate). Detection limits for alkylsuccinates by GC-MS analysis are in the nanomolar range (Gieg and Suflita, 2002). Hydrocarbon metabolite analysis by LC-MS-MS analysis has the advantage of requiring little to no sample preparation prior to analysis thus is far less labor-intensive (Beller, 2002). Further, the technique requires only small amounts of sample (∼1 mL). Parent and/or daughter ions of various metabolites are typically monitored (Beller, 2002; Alumbaugh et al., 2004). Beller (2002) found the detection limits for benzylsuccinates to be ∼0.3 μg/L using LC tandem MS, while Alumbaugh et al. (2004) found that sample pre-treatment using solid-phase extraction lowered the LC-MS-MS detection level of benzylsuccinates by at least an order of magnitude (0.006–0.029 μg/L). Although high sensitivity LC-MS techniques (e.g., LC/MS-ESI-Q-TOF) have been used to successfully detect benzylsuccinates in environmental samples (Jobelius et al., 2011; Kimes et al., 2013), the detection of alkylsuccinates remains elusive, possibly because these metabolites are present at levels below detection limits (Kimes et al., 2013). Other analytical techniques such as 2-dimensional GC analysis (GC × GC) coupled with MS, currently used for separating and quantifying complex mixtures of crude oil components and related compounds (such as naphthenic acids) (e.g., Rowland et al., 2011; Reddy et al., 2012), may find future application for hydrocarbon metabolite analysis.

CONCLUSIONS AND FUTURE DIRECTIONS

Research on the topic of anaerobic alkane metabolism has increased in the last dozen years, revealing that alkanes can be activated by fumarate addition reactions as well as by other proposed mechanisms (yet to be understood). Of the saturate fraction of fuels, the anaerobic metabolism of *n*-alkanes has been the most frequently studied while less is known about how isoalkanes and cyclic alkanes are metabolized anaerobically, representing a knowledge gap that can be addressed by future research. As knowledge is gained regarding the key metabolic pathways for anaerobic alkane biodegradation, the identified metabolites can readily be sought in the natural environment to indicate biodegradation. Further, as newer fuel mixtures such as biofuels become more commonly used, metabolic insights gained from the study of alkanes and other hydrocarbons may help predict the kinds of metabolites that can serve as diagnostic indicators for the biotreatment of such alternative fuels. To date, a metabolite profiling approach using robust tools of analytical chemistry (GC-MS, LC-MS-MS) has been widely been used to garner evidence for the *in situ* anaerobic metabolism of aromatic hydrocarbons in contaminated aquifers, but has been used to a lesser extent for determining for *in situ* alkane biodegradation. Since alkanes (including *n*-alkanes, isoalkanes, and cyclic alkanes) comprise substantial components of many fuel mixtures that are spilled into aquifers, looking for their metabolic by-products should be included in more future site assessments to determine the prospects for *in situ* alkane bioremediation; details on how to look for such metabolites in environmental samples have been described (e.g., Gieg and Suflita, 2002; Duncan et al., 2009). Parallel assessments of the catabolic gene (e.g., *assA* gene) in subsurface microbial populations along with metabolite profiling offers very strong evidence for the *in situ* anaerobic biodegradation of alkanes (Callaghan et al., 2010; Wawrik et al., 2012), an approach that should also be part of future site assessments. Although many hydrocarbon biodegradation studies have been carried out in the context of petroleum contaminated site bioremediation, understanding anaerobic hydrocarbon biodegradation in fossil energy reservoirs has enormous economic implications related to detrimental effects (e.g., heavy oil generation and souring) and beneficial technologies (e.g., microbially enhanced energy recovery). Thus, more extensive research into hydrocarbon-related microbial metabolic processes including anaerobic alkane biodegradation in fossil energy resources such as crude oil reservoirs, and coal and shale deposits is warranted.

ACKNOWLEDGMENTS

The preparation of this review was supported by funding from the Natural Sciences and Engineering Research Council of Canada (NSERC) via a Discovery Grant awarded to Lisa M. Gieg. Akhil Agrawal was supported through NSERC Industrial Research Chair funding awarded to Dr. Gerrit Voordouw (University of Calgary) that was in turn supported by the partner companies Aramco Services, Baker Hughes Incorporated, British Petroleum, Intertek/CML, the Computer Modelling Group Limited, ConocoPhillips Company, YPF SA, Shell Canada Limited, Suncor Energy Developments Inc., and Yara International ASA, as well as by Alberta Innovates-Energy and Environment Solutions.

REFERENCES

Abu Laban, N., Semple, K., Young, R., Dao, A., and Foght, J. M. (2012). "Biodegradation of C7 and C8 iso-alkanes under methanogenic and sulfate-reducing conditions," in *Abstracts of the 14th International Symposium on Microbial Ecology* (Copenhagen, DK).

Agrawal, A., Park, H. S., Nathoo, S., Gieg, L. M., Jack, T. R., Miner, K., et al. (2012). Toluene depletion in produced oil contributes to souring control in a fied subjected to nitrate injection. *Environ. Sci. Technol.* 46, 1285–1292. doi: 10.1021/es203748b

Aitken, C. M., Jones, D. M., and Larter, S. R. (2004). Anaerobic hydrocarbon biodegradation in deep subsurface oil reservoirs. *Nature* 341, 291–294. doi: 10.1038/nature02922

Aitken, C. M., Jones, D. M., Maguire, M. J., Gray, N. D., Sherry, A., Bowler, B. F. J., et al. (2013). Evidence that crude oil alkane activation proceeds by different mechanisms under sulfate-reducing and methanogenic conditions. *Geochim. Cosmochim. Acta* 109, 162–174. doi: 10.1016/j.gca.2013.01.031

Alumbaugh, R. E., Gieg, L. M., and Field, J. A. (2004). Determination of alkylbenzene metabolites in groundwater by solid-phase extraction and liquid chromatography-tandem mass spectrometry. *J. Chromatog. A* 1042, 89–97. doi: 10.1016/j.chroma.2004.05.031

Beasley, K. K., and Nanny, M. A. (2012). Potential energy surface for anaerobic oxidation of methane via fumarate addition. *Environ.*

Sci. Technol. 46, 8244–8252. doi: 10.1021/es3009503

Beller, H. R. (2000). Metabolic indicators for detecting *in situ* anaerobic alkylbenzene degradation. *Biodegradation* 11, 125–139. doi: 10.1023/A:1011109800916

Beller, H. R. (2002). Analysis of benzylsuccinates in groundwater by liquid chromatography/ tandem mass spectrometry and its use for monitoring *in situ* BTEX biodegradation. *Environ. Sci. Technol.* 36, 2724–2728. doi: 10.1021/es025527l

Beller, H. R., Ding, W.-H., and Reinhard, M. (1995). Byproducts of anaerobic alkylbenzene metabolism useful as indicators of *in situ* bioremediation. *Environ. Sci. Technol.* 29, 2864–2870. doi: 10.1021/es00011a024

Beller, H. R., and Spormann, A. (1997). Anaerobic activation of toluene and *o*-xylene by addition to fumarate in denitrifying strain T. *J. Bacteriol.* 179, 670–676.

Beller, H. R., Kane, S. R., Legler, T. C., and Alvarez, P. J. J. (2002). A real-time polymerase chain reaction method for monitoring anaerobic, hydrocarbon-degrading bacteria based on a catabolic gene. *Environ. Sci. Technol.* 36, 3977–3984. doi: 10.1021/es025556w

Beller, H. R., Kane, S. R., Legler, T. C., McKelvie, J. R., Sherwood-Lollar, B., Pearson, F., et al. (2008). Comparative assessments of benzene, toluene, and xylene natural attenuation by quantitative polymerase chain reaction analysis of a catabolic gene, signature metabolites, and compound-specific isotope analysis. *Environ. Sci. Technol.* 42, 6065–6072. doi: 10.1021/es8009666

Biegert, T., Fuchs, G., and Heider, J. (1996). Evidence that anaerobic oxidation of toluene in the denitrifying bacterium *Thauera aromatica* is initiated by formation of benzylsuccinate from toluene and fumarate. *Eur. J. Biochem.* 238, 661–668. doi: 10.1111/j.1432-1033.1996.0661w.x

Bombach, P., Richnow, H. H., Kastner, M., and Rischer, A. (2010). Current approaches for the assessment of *in situ* biodegradation. *Appl. Environ. Microbiol.* 86, 839–852. doi: 10.1007/s00253-010-2461-2

Bregnard, T. P., Haner, A., Hohener, P., and Zeyer, J. (1997). Anaerobic degradation of pristane in nitrate-reducing microcosms and enrichment cultures. *Appl. Environ. Microbiol.* 63, 2077–2081.

Callaghan, A. V. (2012). Metabolomic investigations of anaerobic hydrocarbon-impacted environments. *Curr. Opin. Biotechnol.* doi: 10.1016/j.copbio.2012.08.012. [Epub ahead of print].

Callaghan, A. V., Davidova, I. A., Savage-Ashlock, K., Parisi, V. A., Gieg, L. M., Suflita, J. M., et al. (2010). Diversity of benzyl- and alkylsuccinate synthase genes in hydrocarbon-impacted environments and enrichment cultures. *Environ. Sci. Technol.* 44, 7287–7294. doi: 10.1021/es1002023

Callaghan, A. V., Gieg, L. M., Kropp, K. G., Suflita, J. M., and Young, L. Y. (2006). Comparison of mechanisms of alkane metabolism under sulfate-reducing conditions among two bacterial isolates and a bacterial consortium. *Appl. Environ. Microbiol.* 72, 4274–4282. doi: 10.1128/AEM.02896-05

Callaghan, A. V., Tierney, M., Phelps, C. D., and Young, L. Y. (2009). Anaerobic biodegradation of n-hexadecane by a nitrate-reducing consortium. *Appl. Environ. Microbiol.* 75, 1339–1344. doi: 10.1128/AEM.02491-08

Callaghan, A. V., Wawrik, B., Ní Chadhain, S. M., Young, L. Y., and Zylstra, G. J. (2008). Anaerobic alkane-degrading strain AK-01 contains two alkylsuccinate synthase genes. *Biochem. Biophys. Res. Commun.* 366, 142–148. doi: 10.1016/j.bbrc.2007.11.094

Callbeck, C. M., Dong, X., Chatterjee, I., Agrawal, A., Caffrey, S. M., Sensen, C., et al. (2011). Microbial community succession in a bioreactor modeling a souring low temperature oil reservoir subjected to nitrate injection. *Appl. Microbiol. Biotech.* 91, 799–810. doi: 10.1007/s00253-011-3287-2

Carey, F. A. (2007). *Organic Chemistry, 7th Edn*. New York, NY: McGraw-Hill Science, 1312.

Cheng, L., Rui, J., Li, Q., Zhang, H., and Lu, Y. (2013). Enrichment and dynamics of novel syntrophs in a methanogenic hexadecane-degrading culture from a Chinese oilfield. *FEMS Microbiol. Ecol.* 83, 757–766. doi: 10.1111/1574-6941.12031

Cozzarelli, I. M., Herman, J. S., and Baedecker, M. J. (1995). Fate of microbial metabolites of hydrocarbons in a coastal plain aquifer: the role of electron acceptors. *Environ. Sci. Technol.* 29, 458–469. doi: 10.1021/es00002a023

Cravo-Laureau, C., Grossi, V., Raphel, D., Matheron, R., and Hirschler-Rea, A. (2005). Anaerobic *n*-alkane metabolism by a sulfate-reducing bacterium, *Desulfatibacillum aliphaticovorans* strain CV2803^T. *Appl. Environ. Microbiol.* 71, 3458–3467. doi: 10.1128/AEM.71.7.3458-3467.2005

Davidova, I. A., Gieg, L. M., Nanny, M., Kropp, K. G., and Suflita, J. M. (2005). Stable isotopic studies of *n*-alkane metabolism by a sulfate-reducing bacterial enrichment culture. *Appl. Environ. Microbiol.* 71, 8174–8182. doi: 10.1128/AEM.71.12.8174-8182.2005

Duncan, K. E., Gieg, L. M., Parisi, V. A., Tanner, R. S., Tringe, S. G., Bristow, J., et al. (2009). Biocorrosive thermophilic microbial communities in Alaskan North Slope oil facilities. *Environ. Sci. Technol.* 43, 7977–7984. doi: 10.1021/es9013932

Foght, J. (2008). Anaerobic biodegradation of aromatic hydrocarbons: pathways and prospects. *J. Mol. Microbiol. Biotechnol.* 15, 93–120. doi: 10.1159/000121324

Formolo, M. J., Salacup, J. M., Petsch, S. T., Martini, A. M., and Nusslein, K. (2008). A new model linking atmospheric methane sources to Pleistocene glaciation via methanogenesis in sedimentary basins. *Geology* 36, 139–142.

Frey, P. A. (2001). Radical mechanisms of enzymatic catalysis. *Ann. Rev. Biochem.* 70, 121–148. doi: 10.1146/annurev.biochem.70.1.121

Gieg, L. M., Alumbaugh, R. E., Field, J. A., Jones, J., Istok, J. D., and Suflita, J. M. (2009). Assessing *in situ* rates of anaerobic hydrocarbon bioremediation. *Microb. Biotechnol.* 2, 222–233. doi: 10.1111/j.1751-7915.2008.00081.x

Gieg, L. M., Davidova, I. A., Duncan, K. E., and Suflita, J. M. (2010). Methanogenesis, sulfate reduction and crude oil biodegradation in hot Alaskan oilfields. *Environ. Microbiol.* 12, 3074–3086. doi: 10.1111/j.1462-2920.2010.02282.x

Gieg, L. M., Duncan, K. E., and Suflita, J. M. (2008). Bioenergy production via microbial conversion of residual oil to natural gas. *Appl. Environ. Microbiol.* 74, 3022–3029. doi: 10.1128/AEM.00119-08

Gieg, L. M., and Suflita, J. M. (2002). Detection of anaerobic metabolites of saturated and aromatic hydrocarbons in petroleum-contaminated aquifers. *Environ. Sci. Technol.* 36, 3755–3762.

Gieg, L. M., and Suflita, J. M. (2005). "Metabolic indicators of anaerobic hydrocarbon biodegradation in petroleum-laden environments," in *Petroleum Microbiology.* eds B. Ollivier, and M. Magot (Washington DC: ASM Press), 337–356.

Gray, N. D., Sherry, A., Hubert, C., Dolfing, J., and Head, I. M. (2010). Methanogenic degradation of petroleum hydrocarbons in subsurface environments: remediation, heavy oil formation, and energy recovery. *Adv. Appl. Microbiol.* 72, 137–161. doi: 10.1016/S0065-2164(10)72005-0

Griebler, C., Safinowski, M., Vieth, A., Richnow, H. H., and Meckenstock, R. U. (2004). Combined stable carbon isotope analysis and specific metabolites determination for assessing is situ degradation of aromatic hydrocarbons in a tar oil-contaminated aquifer. *Environ. Sci. Technol.* 38, 617–631.

Grossi, V., Raphel, D., Hirschler-Rea, A., Gilewicz, M., Mouzdahir, A., Bertrand, J.-C., et al. (2000). Anaerobic biodegradation of pristane by a marine sedimentary bacterial and/or archaeal community. *Org. Geochem.* 31, 769–772. doi: 10.1016/S0146-6380(00)00060-7

Grundmann, O., Behrends, A., Rabus, R., Amann, J., Halder, T., Heider, J., et al. (2008). Genes encoding the candidate enzyme encoding for anaerobic activation of *n*-alkanes in the denitrifying bacterium, strain HxN1. *Environ. Microbiol.* 10, 376–385. doi: 10.1111/j.1462-2920.2007.01458.x

Head, I. M., Larter, S. R., Gray, N. D., Sherry, A., Adams, J. J., Aitken, C. M., et al. (2010). "Hydrocarbon biodegradation in petroleum reservoirs," in *Handbook of Hydrocarbon and Lipid Microbiology*, ed T. M. Timmis (Berlin: Springer-Verlag), 3098–3109.

Heath, J. S., Koblis, K., and Sager, S. L. (1993). Review of chemical, physical, and toxicologic properties of components of total petroleum hydrocarbons. *J. Soil Contam.* 2, 1–25.

Hsieh, M., Philp, R. P., and del Rio, J. C. (2000). Characterization of high molecular weight biomarkers in crude oils. *Org. Geochem.* 31, 1581–1588.

Huang, H., and Larter, S. R. (2005). "Biodegradation of petroleum in subsurface geological reservoirs," in *Petroleum Microbiology*, eds B. Ollivier and M. Magot (Washington, DC: ASM Press), 91–121.

Hunt, J. M. (1996). *Petroleum Geochemistry and Geology, 2nd Edn*. New York, NY: W. H. Freeman and Company.

Jack, T. R., Lee, E., and Mueller, J. (1985). "Anaerobic gas production from crude oil," in *Microbes and Oil Recovery: International Bioresources Journal,* Vol. 1, eds J. E. Zajic and E. C. Donaldson (El Paso, TX: Bioresources Publications), 167–180.

Jeon, C. O., and Madsen, E. L. (2012). *in situ* microbial metabolism of aromatic-hydrocarbon environmental pollutants. *Curr. Opin. Biotechnol.* doi: 10.1016/j.copbio.2012.09.001. [Epub ahead of print].

Jobelius, C., Ruth, B., Griebler, C., Meckenstock, R. U., Hollender, J., Reineke, A., et al. (2011). Metabolites indicate hot spots of biodegradation and biogeochemical gradients in a high-resolution monitoring well. *Environ. Sci. Technol.* 45, 474–481. doi: 10.1021/es1030867

Jones, D. M., Head, I. A., Gray, N. D., Adams, J. J., Rowan, A. K., Aitken, C. M., et al. (2008). Crude oil biodegradation via methanogenesis in subsurface petroleum reservoirs. *Nature* 451, 176–180. doi: 10.1038/nature06484

Kimes, N. E., Callaghan, A. V., Aktas, D. F., Smith, W. L., Sunner, J., Golding, B. T., et al. (2013). Metagenomic analysis and metabolite profiling of deep-sea sediments from the Gulf of Mexico following the Deepwater Horizon oil spill. *Front. Microbiol.* 4:50. doi: 10.3389/fmicb.2013.00050

Kniemeyer, O., Musat, F., Sievert, S. M., Knittel, K., Wilkes, H., Blumenberg, M., et al. (2007). Anaerobic oxidation of short-chain hydrocarbons by marine sulphate-reducing bacteria. *Nature* 449, 898–902. doi: 10.1038/nature06200

Kropp, K. G., Davidova, I. A., and Suflita, J. M. (2000). Anaerobic oxidation of *n*-dodecane by an addition reaction in a sulfate-reducing bacterial enrichment culture. *Appl. Environ. Microbiol.* 66, 5393–5398. doi: 10.1128/AEM.66.12.5393-5398.2000

Kunst, L., and Samuels, L. (2009). Plant cuticles shine: advances in wax biosynthesis and export. *Curr. Opin. Plant Biol.* 12, 721–727. doi: 10.1016/j.pbi.2009.09.009

Lambo, A. J., Noke, K., Larter, S. R., and Voordouw, G. (2008). Competitive, microbially-mediated reduction of nitrate with sulfide and aromatic oil components in a low-temperature, western Canadian oil reservoir. *Environ. Sci. Technol.* 42, 8941–8946.

Li, W., Wang, L.-Y., Duan, R.-Y., Liu, J.-F., Gu, J.-D., and Mu, B.-Z. (2012). Microbial community characteristics of petroleum reservoir production water amended with *n*-alkanes and incubated under nitrate-, sulfate-reducing and methanogenic conditions. *Int. Biodeter. Biodeg.* 69, 87–96. doi: 10.1016/j.ibiod.2012.01.005

Maltoni, C., Ciliberti, A., Cotti, G., Conti, B., and Belpoggi, F. (1989). Benzene, an experimental multipotential carcinogen: results of the long-term bioassays performed at the Bologna Institute of Oncology. *Environ. Health Perspect.* 82, 109–124.

Mbadinga, S. M., Wang, L.-Y., Zhou, L., Liu, J.-F., Gu, J.-D., and Mu, B.-Z. (2011). Microbial communities involved in anaerobic degradation of alkanes. *Int. Biodeter. Biodeg.* 65, 1–13. doi: 10.1016/j.ibiod.2010.11.009

Morasch, B., Hunkeler, D., Zopfi, J., Temime, B., and Hohener, P. (2011). Intrinsic biodegradation potential of aromatic hydrocarbons in an alluvial aquifer—potentials and limits of signature metabolite analysis and two stable isotope-based techniques. *Water Res.* 45, 4459–4469. doi: 10.1016/j.watres.2011.05.040

Muller, F. M. (1957). On methane fermentation of higher alkanes. *Antonie Van Leeuwenhoek* 23, 369–384. doi: 10.1007/BF02545890

Musat, F., Wilkes, H., Behrends, A., Woebken, D., and Widdel, F. (2010). Microbial nitrate-dependent cyclohexane degradation coupled with anaerobic ammonium oxidation. *ISME J.* 4, 1290–1301. doi: 10.1038/ismej.2010.50

Nascarella, M. A., Kostecki, P. T., Calabrese, E. J., and Click, D. (2002). "AEHS's 2001 survey of states' soil and groundwater cleanup standards," in *Contaminated Soil, Sediment, and Water* (January/February), 15–68.

National Research Council (NRC). (1993). *In Situ Bioremediation: When Does it Work?* Washington, DC: National Academy Press.

Oka, A. R., Phelps, C. D., Zhu, X., Saber, D. L., and Young, L. Y. (2011). Dual biomarkers of anaerobic hydrocarbon degradation in historically contaminated groundwater. *Environ. Sci. Technol.* 45, 3407–3414. doi: 10.1021/es103859t

Orem, W. H., Tatu, C. A., Lerch, H. E., Rice, C. A., Bartos, T. T., Bates, A. L., et al. (2007). Organic compounds in produced waters from coalbed natural gas wells in the Powder River Basin, Wyoming, USA. *Appl. Geochem.* 22, 2240–2256.

Parisi, V. A., Brubaker, G. R., Zenker, M. J., Prince, R. C., Gieg, L. M., da Silva, M. L. B., et al. (2009). Field metabolomics and laboratory assessments of anaerobic intrinsic bioremediation of hydrocarbons at a petroleum-contaminated site. *Microb. Biotechnol.* 2, 202–212. doi: 10.1111/j.1751-7915.2009.00077.x

Rabus, R., Jarling, R., Lahme, S., Kuhner, S., Heider, J., Widdel, F., et al. (2011). Co-metabolic conversion of toluene in anaerobic *n*-alkane-degrading bacteria. *Environ. Microbiol.* 13, 2576–2586. doi: 10.1111/j.1462-2920.2011.02529.x

Rabus, R., Wilkes, H., Behrends, A., Armstroff, A., Fischer, T., Pierik, A. J., et al. (2001). Anaerobic initial reaction of *n*-alkanes in a denitrifying bacterium: evidence for (1-methylpentyl)succinate as initial product and for involvement of an organic radical in *n*-hexane metabolism. *J. Bacteriol.* 183, 1707–1715. doi: 10.1128/JB.183.5.1707-1715.2001

Reddy, C. M., Arey, J. S., Seewald, J. S., Sylva, S., Lemkau, K. L., Nelson, R. K., et al. (2012). Composition and fate of gas and oil released to the water column during the Deepwater Horizon oil spill. *Proc. Natl. Acad. Sci. U.S.A.* 109, 20229–20234. doi: 10.1073/pnas.1101242108

Rios-Hernandez, L. A., Gieg, L. M., and Suflita, J. M. (2003). Biodegradation of an alicyclic hydrocarbon by a sulfate-reducing enrichment from a gas condensate-contaminated aquifer. *Appl. Environ. Microbiol.* 69, 434–443. doi: 10.1128/AEM.69.1.434-443.2003

Ritchie, G. D., Still, K. R., Alexander, W. K., Nordholm, A. F., Wilson, C. L., Rossi, J. 3rd., et al. (2001). A review of the neurotoxicity risk of selected hydrocarbon fuels. *J. Toxicol. Environ. Health* 4(Pt. B), 223–312. doi: 10.1080/10937400118874

Rojo, F. (2009). Degradation of alkanes by bacteria. *Environ. Microbiol.* 11, 2477–2490. doi: 10.1111/j.1462-2920.2009.01948.x

Rowland, S. J., West, C. E., Scarlett, A. G., Jones, D., and Frank, R. A. (2011). Identification of individual tetra− and pentacyclic naphthenic acids in oil sands process water by comprehensive two−dimensional gas chromatography/mass spectrometry. *Rapid Commun. Mass Spectrom.* 25, 1198–1204. doi: 10.1002/rcm.4977

Savage, K. N., Krumholz, L. R., Gieg, L. M., Parisi, V. A., Suflita, J. M., Allen, J., et al. (2010). Biodegradation of low-molecular-weight alkanes under mesophilic sulfate-reducing conditions: metabolic intermediates and community patterns. *FEMS Microbiol. Ecol.* 72, 485–495. doi: 10.1111/j.1574-6941.2010.00866.x

Siddique, T., Fedorak, P. M., and Foght, J. M. (2006). Biodegradation of short-chain *n*-alkanes in oil sands tailings ponds under methanogenic conditions. *Environ. Sci. Technol.* 40, 5459–5464. doi: 10.1021/es200649t

Siddique, T., Penner, T., Semple, K., and Foght, J. M. (2011). Anaerobic biodegradation of longer chain *n*-alkanes coupled to methane production in oil sands tailings. *Environ. Sci. Technol.* 45, 5892–5899. doi: 10.1021/es200649t

So, C. M., Phelps, C. D., and Young, L. Y. (2003). Anaerobic transformation of alkanes to fatty acids by a sulfate-reducing bacterium, strain Hxd3. *Appl. Environ. Microbiol.* 69, 3892–3900. doi: 10.1128/AEM.69.7.3892-3900.2003

Strąpoć, D., Mastalerz, M., Dawson, K., Macaladay, J. L., Callaghan, A. V., Wawrik, B., et al. (2011). Biogeochemistry of microbial coalbed methane. *Annu. Rev. Earth Planet. Sci.* 39, 617–656.

Thauer, R. K., and Shima, S. (2008). Methane as fuel for anaerobic microorganisms. *Ann. N.Y. Acad. Sci.* 1125, 158–170. doi: 10.1196/annals.1419.000

Thom, C., Gilley, D. C., Hooper, J., and Esch, H. E. (2007). The scent of the waggle dance. *PLoS Biol.* 5:e228. doi: 10.1371/journal.pbio.0050228

von Netzer, F., Pilloni, G., Kleindienst, S., Krueger, M., Knittel, K., Grundger, T., et al. (2013). Enhanced gene detection assays for fumarate-adding enzymes allow uncovering anaerobic hydrocarbon degraders in terrestrial and marine systems. *Appl. Environ. Microbiol.* 79, 543–552. doi: 10.1128/AEM.02362-12

Voordouw, G., Grigoryan, A. A., Lambo, A., Lin, S., Park, H. S., Jack, T. R., et al. (2009). Sulfide remediation by pulsed injection of nitrate into a low temperature Canadian heavy oil reservoir. *Environ. Sci. Technol.* 43, 9512–9518. doi: 10.1021/es902211j

Wawrik, B., Mendivelso, M., Parisi, V. A., Suflita, J. M., Davidova, I. A., Marks, C. R., et al. (2012). Field and laboratory studies on the bioconversion of coal to methane in the San Juan Basin. *FEMS Microbiol. Ecol.* 81, 26–42. doi: 10.1111/j.1574-6941.2011.01272.x

Weiss, J. V., and Cozzarelli, I. M. (2008). Biodegradation in contaminated aquifers: incorporating microbial/molecular methods. *Ground Water* 46, 305–322. doi: 10.1111/j.1745-6584.2007.00409.x

Widdel, F., and Grundmann, O. (2010). "Biochemistry of the anaerobic degradation of non-methane alkanes," in *Handbook of Hydrocarbon and Lipid Microbiology,* ed K. N. Timmis (Berlin: Springer-Verlag), 909–924.

Wilkes, H., Kuhner, S., Bolm, C., Fischer, T., Classen, A., Widdel, F., et al. (2003). Formation of *n*-alkane- and cycloalkane-derived organic acids during anaerobic growth of a denitrifying bacterium with crude oil. *Org. Geochem.* 34, 1313–1323.

Wilkes, H., Rabus, R., Fischer, T., Armstroff, A., Behrends, A., and Widdel, F. (2002). Anaerobic degradation of *n*-hexane in a denitrifying bacterium: further degradation of the initial intermediate (1-methylpentyl)succinate via C-skeleton rearrangement. *Arch. Microbiol.* 177, 235–243. doi: 10.1007/s00203-001-0381-3

Winderl, C., Schaefer, S., and Lueders, T. (2007). Detection of anaerobic toluene and hydrocarbon degraders in contaminated aquifers using benzylsuccinate synthase (bssA) genes as a functional marker. *Environ. Microbiol.* 9, 1035–1046. doi: 10.1111/j.1462-2920.2006.01230.x

Zedelius, J., Rabus, R., Grundmann, O., Werner, I., Brodkorb, D., Schreiber, F., et al. (2011). Alkane degradation under anoxic conditions by a nitrate-reducing bacterium with possible involvement of the electron acceptor in substrate activation. *Environ. Microbiol. Rep.* 3, 125–135. doi: 10.1111/j.1758-2229.2010.00198.x

Zengler, K., Richnow, H. H., Rossello-Mora, R., Michaelis, W., and Widdel, F. (1999). Methane formation from long-chain alkanes by anaerobic microorganisms. *Nature* 401, 266–269. doi: 10.1038/45777

Zhou, L., Li, K.-P., Mbadinga, S. M., Yang, S.-Z., Gu, J.-D., and Mu, B.-Z. (2012). Analyses of *n*-alkanes degrading community dynamics of a high-temperature methanogenic consortium enriched from production water of a petroleum reservoir by a combination of molecular techniques. *Exotoxicology* 21, 1680–1691. doi: 10.1007/s10646-012-0949-5

ZoBell, C. E. (1946). Action of microorganisms on hydrocarbons. *Bacteriol. Rev.* 10, 1–49.

Conflict of Interest Statement: The authors declare that the research was conducted in the absence of any commercial or financial relationships that could be construed as a potential conflict of interest.

Received: 02 January 2013; accepted: 17 May 2013; published online: 04 June 2013.

Citation: Agrawal A and Gieg LM (2013) In situ detection of anaerobic alkane metabolites in subsurface environments. Front. Microbiol. ***4****:140. doi: 10.3389/fmicb.2013.00140*

This article was submitted to Frontiers in Microbiological Chemistry, a specialty of Frontiers in Microbiology.

frontiers in
MICROBIOLOGY

ORIGINAL RESEARCH ARTICLE
published: 15 February 2013
doi: 10.3389/fmicb.2013.00024

Targeting of insect epicuticular lipids by the entomopathogenic fungus *Beauveria bassiana*: hydrocarbon oxidation within the context of a host-pathogen interaction

Nicolás Pedrini[1], Almudena Ortiz-Urquiza[2], Carla Huarte-Bonnet[1], Shizhu Zhang[2,3] and Nemat O. Keyhani[2]*

[1] *Facultad de Ciencias Médicas, Instituto de Investigaciones Bioquímicas de La Plata (CCT La Plata CONICET-UNLP), La Plata, Argentina*
[2] *Department of Microbiology and Cell Science, University of Florida, Gainesville, FL, USA*
[3] *Jiangsu Key Laboratory for Microbes and Functional Genomics, Jiangsu Engineering and Technology Research Center for Microbiology, College of Life Sciences, Nanjing Normal University, Nanjing, China*

Edited by:
Rachel N. Austin, Bates College, USA

Reviewed by:
Rachel N. Austin, Bates College, USA
Alan A. DiSpirito, Ohio State University, USA

Correspondence:
Nemat O. Keyhani, Department of Microbiology and Cell Science, University of Florida, Gainesville, FL 32611, USA.
e-mail: keyhani@ufl.edu

Broad host range entomopathogenic fungi such as *Beauveria bassiana* attack insect hosts via attachment to cuticular substrata and the production of enzymes for the degradation and penetration of insect cuticle. The outermost epicuticular layer consists of a complex mixture of non-polar lipids including hydrocarbons, fatty acids, and wax esters. Long chain hydrocarbons are major components of the outer waxy layer of diverse insect species, where they serve to protect against desiccation and microbial parasites, and as recognition molecules or as a platform for semiochemicals. Insect pathogenic fungi have evolved mechanisms for overcoming this barrier, likely with sets of lipid degrading enzymes with overlapping substrate specificities. Alkanes and fatty acids are substrates for a specific subset of fungal cytochrome P450 monooxygenases involved in insect hydrocarbon degradation. These enzymes activate alkanes by terminal oxidation to alcohols, which are further oxidized by alcohol and aldehyde dehydrogenases, whose products can enter β-oxidation pathways. *B. bassiana* contains at least 83 genes coding for cytochrome P450s (CYP), a subset of which are involved in hydrocarbon oxidation, and several of which represent new CYP subfamilies/families. Expression data indicated differential induction by alkanes and insect lipids and four CYP proteins have been partially characterized after heterologous expression in yeast. Gene knockouts revealed a phenotype for only one (*cyp52X1*) out of six genes examined to date. CYP52X1 oxidizes long chain fatty acids and participates in the degradation of specific epicuticular lipid components needed for breaching the insect waxy layer. Examining the hydrocarbon oxidizing CYP repertoire of pathogens involved in insect epicuticle degradation can lead to the characterization of enzymes with novel substrate specificities. Pathogen targeting may also represent an important co-evolutionary process regarding insect cuticular hydrocarbon synthesis.

Keywords: *B. basiana*, entomopathogenic fungi, epicuticle, hydrocarbon degradation, cytochrome P450, host-pathogen coevolution

INTRODUCTION

Insect cuticles are a significant source of hydrocarbons in terrestrial ecosystems and remediation and turnover of these compounds is critical for the maintenance and flux of normal carbon cycles. Yeasts and filamentous fungi are known to degrade *n*-alkanes and although significant portions of the biochemical pathways regarding alkane catabolism have been described, much remains obscure. The insect epicuticle or waxy layer represents the first barrier to environmental threats including external compounds such as chemical and biological pesticides. This thin layer on the outer surface of the insect is comprised of a complex mixture of lipids that include abundant amounts of straight-chain and methyl-branched, saturated and unsaturated hydrocarbons.

Pathogenicity to invertebrates is represented by primitive fungi and is postulated to have arisen simultaneously with the emergence of insects approximately 500 million years ago (Berbee and Taylor, 2001). The ancient Chinese noted the lethal effects of fungi on silkworms and cicadas more than 2 millennia ago (Roberts and Humber, 1981) and Augustino Bassi in the 1830s used strains of *Beauveria (bassi)ana* as a model for his germ theory of disease in animals (Steinhaus, 1956). Due to their dispersal within most major fungal taxonomic groups, fungal-insect pathogens represent lifestyle adaptations that have likely evolved numerous times (Khachatourians, 1996; Goettel et al., 2000). *B. bassiana* has an exceptionally broad host range and is being studied for use as a biological control for a diverse range of insects (**Figure 1**). This

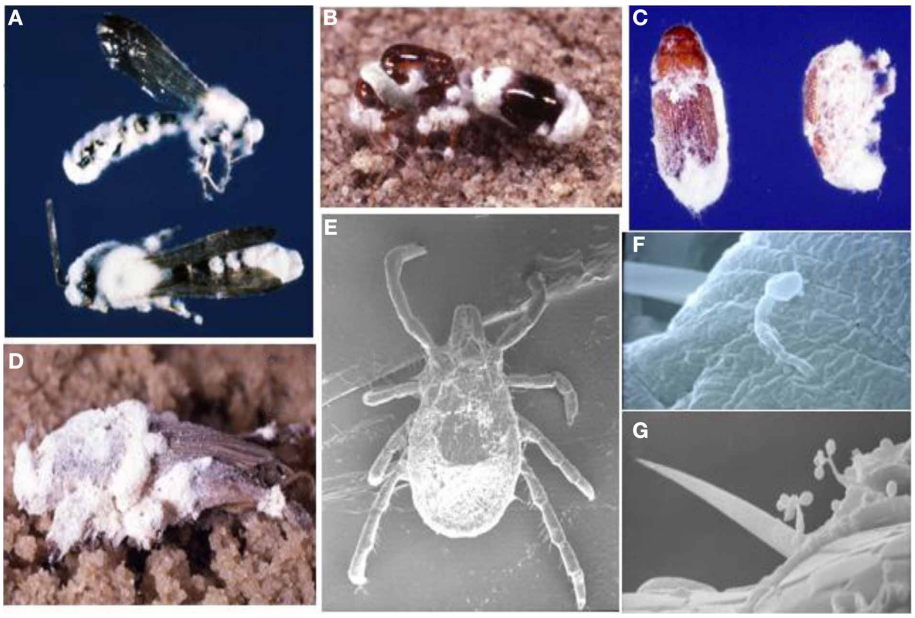

FIGURE 1 | *B. bassiana* has an exceptionally broad host range that spans across Arthropoda classes, from insects including; wasps (A), fire ants (B), bark beetles (C), and mole crickets (D) to arachnids such as mites and ticks (E). Cuticle penetration **(F)** and conidiogenesis from host cadaver **(G)** are also illustrated. (Images courtesy of D. Boucias and N. O. Keyhani).

host range includes insects that act as disease vectors and nuisance pests, crop pests, and even ecologically hazardous, invading pests, with recent studies highlighting the potential of entomopathogenic fungi as agents in combating the spread of malaria by controlling mosquito populations and in protecting agricultural crops from marauding locusts (Inglis et al., 2001; Kirkland et al., 2004b; Scholte et al., 2005; Fan et al., 2012a,b).

B. bassiana is a facultative saprophyte that belongs to the Hypocrealean order within the Ascomycota, and has evolved sophisticated mechanisms for penetrating the formidable barrier that constitutes the insect/arthropod exoskeleton or integument (Ferron, 1981; Binnington and Retnakaran, 1991; St Leger, 1991; Clarkson and Charnley, 1996). Interspersed within the cuticle barrier are biochemical components such as toxic lipids and phenols, enzyme inhibitors, proteins, and other defensive compounds that entomopathogens must overcome for successful virulence (Hackman, 1984; Renobales et al., 1991; Anderson et al., 1995). Pathogens must cope with hydrophobic barriers, electrostatic charges, low relative humidity, low or sequestered nutrient levels, endogenous microbial flora, and cross-linked proteins that contribute to a stiff cuticle (St Leger, 1991). Successful pathogenic fungi must also thwart infection-induced responses such as melanization and hemocyte activation (Pendland et al., 1993; Riley, 1997). The overall process of arthropod infection by pathogenic fungi involves many steps (Charnley and St Leger, 1991; Holder and Keyhani, 2005; Lewis et al., 2009; Wanchoo et al., 2009) that include complex systems for (1) finding (likely via passive mechanisms) the appropriate insect host(s), (2) adhering to the exoskeletal substrata, (3) evading host defenses, (4) penetrating and degrading the cuticle, (5) transporting to the cytoplasm and catabolizing necessary nutrients (carbon/nitrogen, external products of the degradation), and (6) dispersing from the catabolized host(s). Infection involves the production of specialized infection structures (appressoria), penetration of the cuticle and surrounding tissues by elongating hyphae (reaching the hemolymph), and the production of single celled hyphal bodies or blastospores within the hemolymph that are able to evade the host immune cells (Hung and Boucias, 1992; Pendland et al., 1993; Kurtti and Keyhani, 2008; Bidochka et al., 2010).

Progress has been made in uncovering some of the molecular and biochemical determinants of *B. bassiana* virulence. These include descriptions of suites of hydrolases, including proteases, lipases, and phosphatases and the production of numerous toxic metabolites such as beauvericins, oosporein, and oxalic acid. However, little is known concerning the degradation and/or penetration of the initial barrier that must be overcome for successful infection to occur, in particular the hydrocarbons that constitute the insect epicuticle or waxy layer.

BIOSYNTHESIS OF INSECT HYDROCARBONS

Insect cuticular lipids are comprised of a diverse array of compounds with much variation in content and composition (Blomquist and Dillwith, 1985; Lockey, 1988; Buckner, 1993; Nelson and Blomquist, 1995) (**Figure 2**). This variation extends to the different life stages (adults, nymphs, larvae) and larval instars of each insect. The composition of surface lipids has profound consequences impacting ecological and behavioral aspects of the insect. Aside from acting as a barrier to desiccation and potential microbial pathogens, surface hydrocarbons contribute to numerous biochemical, physiological, and semiochemical (behavior and signaling) functions. These include roles as species, nest mate, and caste recognition cues and as

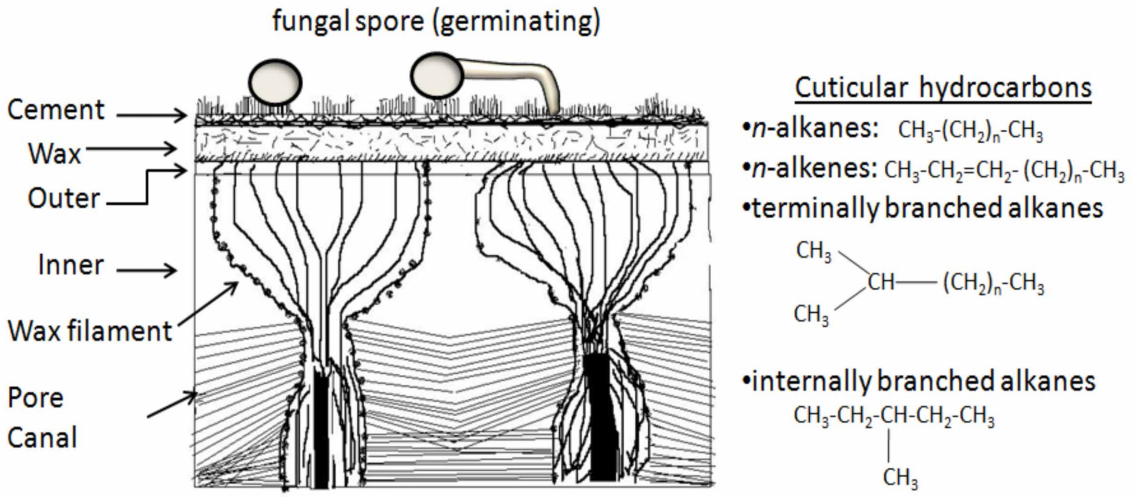

FIGURE 2 | Initial aspects of the fungal-insect interaction: the insect cuticle and its hydrocarbon contents. Image adapted from (Noble-Nesbitt, 1991). The inner, outer, wax, cement, and bloom layers are often considered as the epicuticle, with the pore canals, that transverse the exo-, plus the meso-, and endocuticle portions (not shown in figure) comprising the procuticle.

a reservoir for a suite of pheromones responsible for sexual attraction, epideictic (insect display behavior), territorial markers, alarm, recruitment, chemical defense, and thermoregulation (Blomquist et al., 1987; Singer, 1998; Howard and Blomquist, 2005). Additional roles involve predator–prey and parasitoid-host interactions, mimicry and camouflage (Howard, 1993; Dettner and Liepert, 1994). Cuticular lipids include compounds with antifungal activity and components toxic to entomopathogenic fungi (Koidsumi, 1957; Smith and Grula, 1982; Saito and Aoki, 1983; Golebiowski et al., 2008). Hydrocarbons, mainly *n*-alkanes, alkenes and methyl-branched chains, are the most common epicuticular lipids. In insects, hydrocarbon are synthesized from fatty acids via an elongation-dexcarboxylation pathway which comprises (1) elongation of fatty acyl-CoAs, (2) fatty acids reduction to aldehydes by acyl-CoA reductases, and (3) conversion of fatty aldehydes to alka(e)nes with one less carbon, in an oxidative descarbonylation process catalyzed by cytochrome P450 enzymes (Blomquist et al., 1987, 1993; Nelson, 1993; Qiu et al., 2012). Cuticular hydrocarbons appear to be synthesized in oenocytes, large specialized cells rich in endoplasmic reticulum (ER) and mitochondria. Depending upon the insect species, oenocytes can be found within the epidermis, the peripheral (subcuticular) fat body or the hemocoel (Schal et al., 1998; Bagnères and Blomquist, 2010). Significant aspects of the export and deposition of hydrocarbons on the insect surface remain obscure particularly since it appears that certain parts of the insect do not synthesize hydrocarbons. It is known, however, that some hydrocarbons are transported after synthesis (presumably in the oenocytes) likely via the hemolymph to sites of deposition by reusable lipoproteins known as lipophorins, which shuttle the hydrocarbons among tissues without entering cells (Chino and Kitazawa, 1981; Van Heusden et al., 1991). Several hemolymph lipophorins have been characterized which are capable of binding newly synthesized hydrocarbons from oenocytes to the epicuticle (Gu et al., 1995; Schal et al., 1998). However, as mentioned, the mechanism of uptake, crossing of the integument, and deposition and/or assembly on the epicuticle remains unknown (Schal et al., 1998; Bagnères and Blomquist, 2010).

DEGRADATION OF INSECT EPICUTICLULAR HYDROCARBONS BY ENTOMOPATHOGENIC FUNGI

The initial interaction between the fungal infectious propagule, i.e., spores, conidia, or blastospores, and the insect host occurs at the level of the insect epicuticle. It is likely that insect pathogenic microbes such as *B. bassiana* are able to recognize, assimilate and/or alter specific hydrocarbons, which in turn can impact the behavior and ecology of the insect host. Thus, an intriguing corollary to the pathogen-insect interaction is that the action of the fungus via enzymatic modification/degradation of insect cuticular compounds can have a dramatic effect on insect behavior. For instance, by degrading specific pheromones, behaviors such as grooming or nest mate recognition can be modified. Either the host or the pathogen could exploit these effects, i.e., target insects may detect infected individuals as foreign and quarantine/eliminate them (benefiting the host) or induction of behaviors such as enhanced grooming might act as a means for increased dissemination of the pathogen (although grooming typically helps eliminates microbes).

As described above, hydrocarbons, especially *n*-alkanes, *n*-alkenes, and methyl-branched chains, represent one of the major components of the epicuticle and have been extensively studied (Blomquist and Dillwith, 1985; Blomquist et al., 1987; Lockey, 1988). Insect hosts for examining fungal mediated alkane degradation include the grasshoppers, *Schistocerca americana* (Drury) and *Melanoplus sanguinipes* (Fabricius). The alkane component of the surface lipids of *S. americana* ranges from 25 to 35% of the total hydrocarbons present, covering chain lengths from C_{23}–C_{35}. Odd chain hydrocarbons predominate, with the major

components being C_{25}, C_{27}, C_{29}, C_{31}, and C_{33} (Lockey and Oraha, 1990; Espelie et al., 1994). Similar values have been reported for the surface lipid composition of *M. sanguinipes* with C_{27} and C_{29} predominating, but also including C_{23} (Gibbs et al., 1990; Gibbs and Mousseau, 1994). *B. bassiana* can grow on most of these alkanes as a sole source of carbon.

Alternations in hydrocarbon content during fungal infection of various insects have been noted (Lecuona et al., 1991; Jarrold et al., 2007). Differences in the hydrocarbon content of the waxy layer can have profound effects on fungal pathogenesis. Some hydrocarbons inhibit spore germination, while others stimulate germination and growth (Smith and Grula, 1982; Saito and Aoki, 1983). Cuticular hydrocarbons can also promote (Boucias and Pendland, 1984; Boucias et al., 1988) or inhibit (Lord and Howard, 2004) fungal attachment to cuticle, and specific components may act as chemical inducers for the production of penetrant germ tubes on hosts (Kerwin, 1984; Latge et al., 1987). Spore germination and hyphal growth on insect lipids using pathogenic and non-pathogenic *Beauveria* strains toward the European common cockchafer (*Melolontha melolontha* L.) revealed inhibition of growth of the non-pathogenic strain by cuticular pentane extracts derived from the cockchafer, whereas no inhibition of growth of the pathogenic strains was observed (Lecuona et al., 1997). Pentane extracts of two closely related tick species, one highly susceptible to *B. bassiana* (*Amblyomma maculatum* Koch) and the other somewhat resistant to fungal infection (*A. americanum* L.), revealed inhibition of fungal germination in the case of *A. americanum* but good growth on the *A. maculatum* extracts (Kirkland et al., 2004a). *B. bassiana* has been shown to utilize several insect hydrocarbons including aliphatic and methyl branched alkanes (Napolitano and Juarez, 1997). C_{28} and C_{24} alkanes were degraded by *B. bassiana* mainly into free fatty acids, phospholipids, and acylglycerols, with alkane grown cells producing *n*-decane as a volatile organic compound as a by-product of the β-oxidation reactions (Crespo et al., 2000, 2008). Similarly, the major components of the larvae of the blood-sucking bug *Triatoma infestans* Klug (an important vector of human disease causing microbes) epicuticle includes C_{29}, C_{31}, and C_{33} are able to promote *B. bassiana* growth (Napolitano and Juarez, 1997). Radiolabeled hydrocarbons have been used to investigate the catabolic pathways of alkane degradation in *B. bassiana*, and these data support a degradative pathway involving β-oxidation by a cytochrome P450 enzyme system, followed by peroxisome mediated successive transformations to yield the appropriate fatty acyl CoA as further described below (Pedrini et al., 2006, 2007). Alkane growth has been linked to increased virulence, with *B. bassiana* cells grown on alkane containing media displaying a dramatic 2–4-fold increase in mortality against the bean weevil *Acanthoscelides obtectus*, when compared to cells grown on glucose (Crespo et al., 2002). These data indicate that *B. bassiana* mediated alkane degradation represents a key metabolic pathway that is linked to the entomopathogenic nature of the fungus.

n-ALKANE ASSIMILATION IN FUNGI

Little is known concerning how alkanes are taken up and transferred into cells by fungi. Active transport appears to be involved and *n*-alkane uptake experiments performed in *Cladosporium resinae* in the presence of metabolic uncouplers indicate that the uptake of alkanes in fungi comprises (1) passive adsorption to the outer cell surface where long hair-like structures are formed upon alkane binding, also seen in alkane-grown *Candida tropicalis* and *B. bassiana* cells (Kappeli et al., 1984; Juárez et al., 2004) and (2) an energy-requiring transfer of the unmodified alkane into the cytosol (Lindley and Heydeman, 1986). Typically, after binding the cell surface, *n*-alkanes are solubilized in order of increasing molecular weight (Goma et al., 1973; Reddy et al., 1982; Cameotra et al., 1983; Lindley and Heydeman, 1986). Subsequently, these alkanes are shuttled into the cell inside of membrane-bound vesicles likely by a process of pycnocytosis (Meisel et al., 1973; Cooney et al., 1980; Lindley and Heydeman, 1986). Although unclear, the role of these membrane-bound vesicles is thought to provide continuous input of alkanes while avoiding the potential toxicity of insoluble alkanes floating in the cytosol (Lindley and Heydeman, 1986).

Many fungi have developed metabolic systems to assimilate *n*-alkanes as carbon sources via the activities of cytochrome P450 mono-oxygenases (**Figure 3**) (Lindley, 1995; Van Beilen et al., 2003; Singh, 2006; Rojo, 2010). However, while much is known about these enzymes in *n*-alkane assimilating yeasts, such as *Candida maltosa* and *Yarrowia lipolytica*, their orthologs in filamentous fungi have not yet received adequate attention. In yeasts cytochrome P450ALKs (alkanes), belonging to the CYP52 family (Nelson, 2009), are thought to catabolize *n*-alkanes. Where examined, in yeasts, the pathway starts with terminal hydroxylation of alkanes to fatty alcohols by P450ALKs in the ER, and further oxidation to fatty aldehydes either by the fatty alcohol dehydrogenase (FADH) in the ER or by fatty alcohol oxidase (FAOD) in the peroxisome. Whether in the ER or peroxisome, fatty aldehydes are oxidized by fatty aldehyde dehydrogenases (FALDHs) to fatty acids that are further activated by acyl-CoA synthetases (ACS I and/or ACS II). The activated fatty acids are then utilized in membranes or storage lipids, or degraded in the peroxisome via β-oxidation to yield acetyl-CoA (Fickers et al., 2005). Similarly, in filamentous fungi, the hydroxylation of the terminal methyl group of *n*-alkanes is carried out in the ER by (specific) cytochromes P450s that are coupled to general NADPH-cytochrome P450 reductases. The resultant fatty alcohol can also be catabolized to activate fatty acid in the mitochondrion in addition to ER and peroxisome. The activated fatty acids are catabolized to acetyl-CoA by β-oxidation in the peroxisome and/or the mitochondrion (**Figure 4**).

In both yeast and filamentous fungi, although there has been little examination of the central pathways of alkane metabolism, it is considered to involve a predominantly amphibolic tricarboxylic acid cycle with high glyoxylate bypass activity and gluconeogenesis. Such a metabolic pathway results in highly reduced co-enzyme and acetyl-CoA production, with the latter compound feeding anabolic pathways. Alternate pathways include diterminal or subterminal oxidation of alkanes whose products are ultimately assimilated via β-oxidation reactions, where in the latter case a mixture of secondary alcohols can be formed which are first metabolized to yield the corresponding primary alcohols (which then undergo dehydrogenation) and organic acids (**Figure 4**).

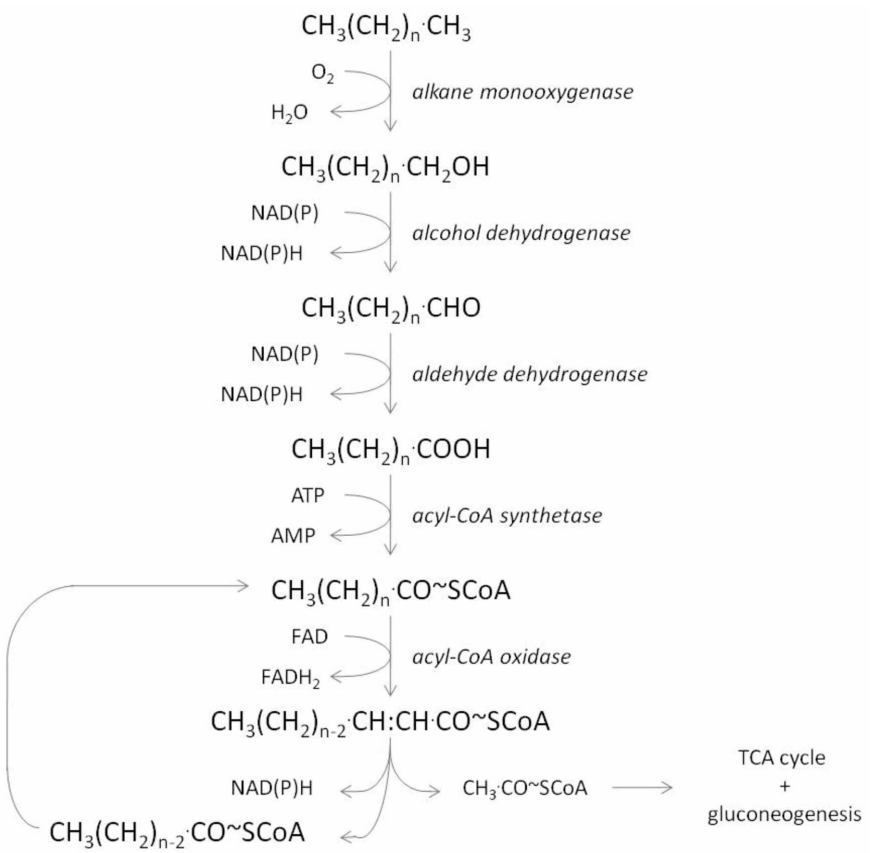

FIGURE 3 | Proposed main catabolic pathway for alkane degradation.

There remain, however, many unanswered biochemical questions regarding *n*-alkane assimilation by fungi.

ALKANE CATABOLIC PATHWAY AND CYTOCHROME P450s IN *B. bassiana*

B. bassiana is likely to contain novel enzymes due to the diverse nature and large chain lengths of the hydrocarbon constituents of the insect waxy layer. In the pre-genomic era we identified several genes implicated in alkane degradation in *B. bassiana*, by exploring our EST dataset (Cho et al., 2006a,b). These included eight cytochrome P450 genes (CYP) encoding enzymes with putative specificity for alkanes (Pedrini et al., 2010), four catalases, and long chain alcohol and aldehyde dehydrogenases (**Table 1**). Overall, we have identified at least 12 additional P450 genes (for a total of at least 20 P450 genes in *B. bassiana*) in EST dataset with substrates specificities for a range of compounds besides alkanes. The recent release of *B bassiana* complete genome (Xiao et al., 2012) has permitted the extension of this list of genes as follows; 77 CYP genes with families and subfamilies assigned, five catalases and at least 22 alcohol dehydrogenases and 11 aldehyde dehydrogenases.

From genome analyses, fungi have a large diversity in P450 content. Yeasts such as *S. cerevisiae*, *C. albicans*, and *Y. lipolytica* contain 3, 10, and 17 identified P450 ORFs, respectively. Filamentous fungi such as *Neurospora crassa*, *Magnaporthe grisea*, and *Fusarium oxysporum*, contain 43, 139, and 170 putative P450 enzymes, respectively, and the basidiomycetes, *Phanerochaete chrysosporium* and the brown rot fungus, *Postia placenta* contain 145 and 353, P450 ORFs, respectively (Source: Fungal Cytochrome P450 DataBase). Other insect pathogens, such *as Metarhizium robertsii* and *M. acridum*, have 123 and 100 CYP genes, respectively (Gao et al., 2011). Thus from genomic analyses, fungi and plants appear to contain the largest complements of CYP genes, probably due to the diversity of both primary and secondary metabolism, and xenobiotic transformation and detoxification pathways.

Within the P450 superfamily, genes are assigned into families and subfamilies based mainly on amino acid sequence identity. Genes are assigned to families when they share greater than 40% amino acid identity with reference sequences and are assigned to subfamilies when they are more than 55% identical (Nelson et al., 1996). A higher order for grouping P450 genes, called the clan, has been proposed and applied to studies of P450s from different Kingdoms. The introduction of clan categories attempts to group genes based on robust phylogenetic relationships. Genes within a clan likely diverged from a common ancestor gene (Nelson, 1999) and may share common functions (Nelson, 1998). In fungi, few phylogenetic studies using P450s have been reported. In the

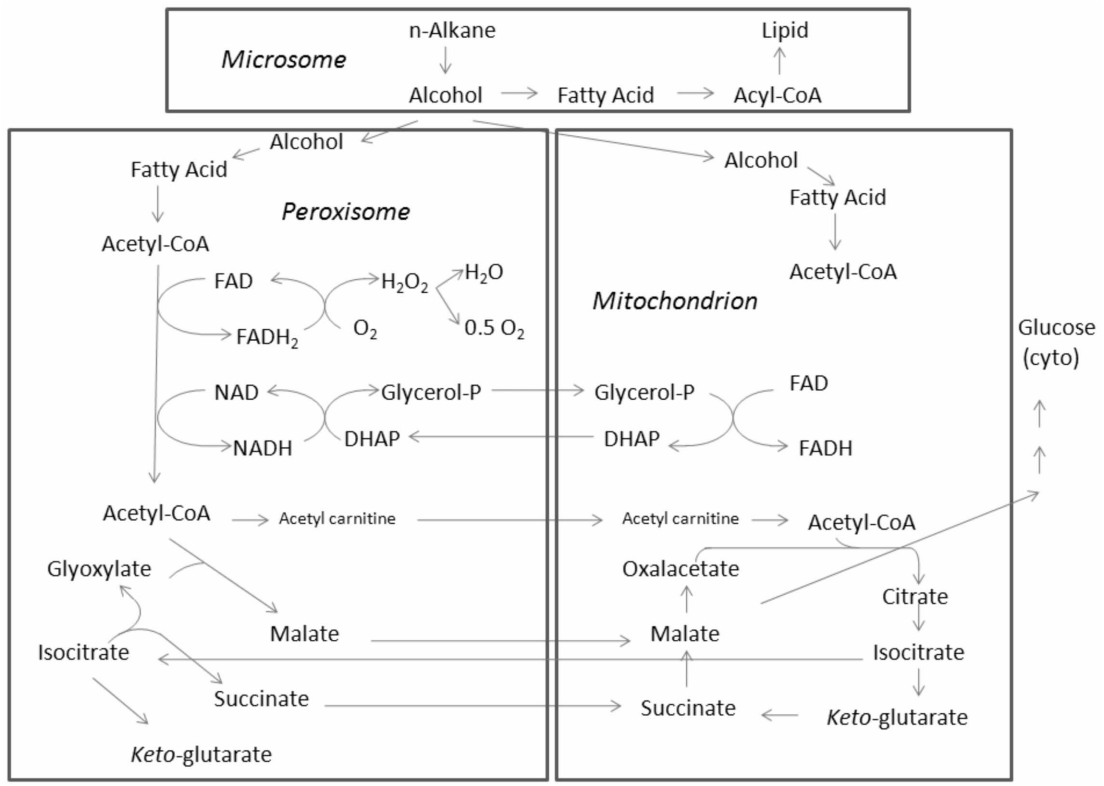

FIGURE 4 | Sub-cellular distribution of hydrocarbon catabolic enzymes.

basidiomycete *P. chrysosporium*, 12 CYP families were classified into 11 clans (Doddapaneni et al., 2005), whereas the sum of the four ascomycetes *Aspergillus nidulans*, *N. crassa*, *F. graminearum*, and *M. grisea* has a total of 376 P450 genes that were assigned to 168 families clustered into 115 clans (in average 42 families and 29 clans per species) (Deng et al., 2007). The availability of the *B. bassiana* genome has contributed to the further annotation of the diversity of fungal P450s; from our analysis at least 15 sequences represent the founding members of a new cytochrome P450 family (20% of total P450s), and 21 genes (27%) appear to represent the first members of new subfamilies (**Table 2**).

Genome mining of *B. bassiana* indicates the presence of two clans that represent 45.5% of total P450 genes: CYP52 and CYP53 clans (**Table 2**). The CYP52 family, part of the CYP52 clan, was originally identified in alkane assimilating yeast, and identified to have a role in terminal hydroxylation of *n*-alkanes and fatty acids. This clan includes the highest gene number per family in *B. bassiana*, with five genes in each of the families CYP52 and CYP584 (the CYP584 family is part of the CYP52 clan). Two genes, belonging to the CYP52 family, have been (partially) characterized in *B. bassiana*, with evidence that they participate in both hydrocarbon and insect lipid degradation (Pedrini et al., 2010; Zhang et al., 2012). However, BbCYP584Q1 showed little to no induction in any of the alkane growth conditions examined (Pedrini et al., 2010). Other members of this clan (BbCYP539B5 and BbCYP655C1) are induced in the presence of C_{16}, C_{20}, C_{24}, C_{28}, and *T. infestans* lipid extract carbon sources (Pedrini et al., 2010). A phylogenetic analysis of the CYP52 clan revealed that these genes fall into discrete clusters (**Figure 5**). The significant divergence in amino acid sequence observed may indicate substrates beyond alkanes and/or likely reflects distinct biological roles for subsets of these proteins. The CYP53 family was first described as including benzoate 4-hydroxylases in *A. niger* and *Rhodotorula minuta*. *B. bassiana* has several candidate genes that fall within the CYP53 clan (**Figure 6**). Amongst these, BbCYP53A26, is induced in the presence of various hydrocarbons and insect lipids (Pedrini et al., 2010), suggesting that this fungus employs a differentiated strategy for hydrocarbon-assimilation using a variety of enzyme classes. However, not all identified cytochromes may be directly involved in lipid assimilation. For example, *B. bassiana* CYP655C1 (CYP52 clan) expression was strongly induced by hydrocarbons and insect lipids, but it appears to be involved in tenellin synthesis (with aromatic intermediates) (Doddapaneni et al., 2005), indicating that lipid may act as signals for the biosynthesis of select fungal secondary metabolites. In the basidiomycete, *P. chrysosporium*, seven members belonging to the CYP63 family have been identified which all can be classified under the CYP52 clan. All seven genes showed transcriptional induction with alkanes, mono-aromatic and polycyclic aromatic hydrocarbons, and also alkyl-substituted aromatics compounds (Yadav et al., 2006).

Table 1 | Candidate genes involved in alkane degradation identified in the *B. bassiana* EST dataset.

Gene (accession No.)	Putative function	Gene knockout available?	Phenotype	References
CYP52(X1) (GU566074)	Lipid oxidation	Yes	Decreased virulence in insect topical assays/no effect in intrahemoceol injection assays	Zhang et al., 2012
CYP655(C1) (AM409327)	Lipid oxidation	Yes	No phenotype detected thus far	This study
CYP5337(A1) (GU566075)	Lipid oxidation	Yes	No phenotype detected thus far	This study
CYP52(G11) (GU566076)	Lipid oxidation	Yes	No phenotype detected thus far	This study
CYP539(B5) (GU566077)	Lipid oxidation	No	–	–
CYP617(N1) (GU566078)	Lipid oxidation	Yes	No phenotype detected thus far	This study
CYP53(A26) (GU566079)	Lipid oxidation	Yes	No phenotype detected thus far	This study
CYP584(Q1) (GU566080)	Lipid oxidation	No	–	–
catA (spore-specific)		Yes	Decreased virulence, thermotolerance and UV resistance. Not tested for alkane degradation	Wang et al., 2012
catB (secreted)	H_2O_2 scavenging	Yes	Not tested for alkane degradation	Wang et al., 2012
catP (peroxisomal)	β-oxidation pathway	Yes	Decreased virulence. Not tested for alkane degradation	Wang et al., 2012
catC (cytoplasmic)	H_2O_2 scavenging	Yes	Not tested for alkane degradation	Wang et al., 2012
catD (secreted peroxidase/catalase)	H_2O_2 scavenging	Yes	Decreased virulence and UV resistance. Not tested for alkane degradation	Wang et al., 2012
Acyl CoA oxidase	β-oxidation pathway	No	N/A	N/A
3-oxoacyl carrier protein reductase	Biosurfactants synthesis/transport	No	N/A	N/A
ADH-2 FALDH	Long-chain alcohol and aldehyde dehydrogenase	No	N/A	N/A

CYTOCHROME P450 EXPRESSION IN *B. bassiana*

The expression pattern of eight *B. bassiana* cytochrome P450 enzymes has been examined under a variety of conditions (Pedrini et al., 2010). Cells grown in minimal media containing either C_{16}, C_{24}, or C_{28} as the sole source of carbon showed significant induction of several of the cytochrome P450 genes by growth on specific alkanes as compared to glucose grown cells. Of the set of *B. bassiana* cytochrome p450 examined, enzymes belonging to the families CYP52(X1) and CYP617(N1) showed only slight to moderate induction in the alkanes tested. In contrast, Bb-CYP655(C1) and Bb-CYP52(G11) were induced >200-fold in all alkanes tested (C_{16}, C_{24}, and C_{28}), with Bb-CYP655(C1) displaying maximal induction by C_{24}. Bb-CYP5337(A1) showed slight induction when grown on C_{16} and C_{24}, but >200-fold when grown on C_{28}, indicating that it may be important for oxidation of longer chain length alkanes. Bb-CYP53(A26) displayed only minor induction when grown on C_{16}, but >200-fold by C_{24} and C_{28}. Bb-CYP584(Q1) displayed only minor to moderate induction when grown on C_{16} and C_{28}, but >200-fold by C_{24}. These data support a model indicating the presence and importance of a suite of P450 enzymes with overlapping but distinct substrate and expression specificities, particularly since P450s are well-known to be induced by their substrates (Montellano, 2005).

Thus far, the expression patterns of these P450s have only been examined after fungal growth on insect-derived lipids from the blood-sucking bug, *T. infestans* (Pedrini et al., 2010). Similar to what was observed for the pure alkanes, three distinct induction profiles were noted: Bb-CYP655(C1) and CYP617(N1) were highly induced (>200-fold), Bb-CYP52(X1), CYP5337(A1), and CYP53(A26) were moderately induced (>30-fold), and Bb-CYP539(B5), CYP52(G1), and CYP584(Q1) displayed low to no induction, i.e., 12-fold, 4-fold, and no induction, respectively when grown in *T. infestans* cuticular lipid extracts. Since the content and structure of hydrocarbons and lipids shows considerable variation not only between diverse insect but sometimes between the various life stages of a particular insect, it is intriguing to hypothesize that hydrocarbon assimilating cytochrome P450s may act as partial specificity factors, helping to account for the broad host range of entomopathogenic fungi such as *B. bassiana*. Thus, such an idea would predict that individual members of *B. bassiana* P450 (lipid assimilating) repertoire would differentially contribute to the pathogenic process depending upon insect target. Further examination of the expression profiles of the P450s after growth on different insects would help shed light on this issue. In addition, knowledge concerning the contributions and/or importance of individual P450s to the ability of the fungus in targeting specific insects could be used to manipulate, i.e., increase, the virulence of the fungus toward those targets, e.g., by increasing the expression levels of critical P450s.

GENETIC DISSECTION OF THE ALKANE PATHWAY: CYTOCHROME P450s

To date, the role of a single cytochrome P450, Bb-CYP52(X1) has been investigated genetically in *B. bassiana* (Zhang et al., 2012). A targeted gene knockout mutant of Bb-CYP52(X1) did not display any noticeable growth defects on any substrates tested including

Table 2 | Cytochrome P450 monooxygenase genes (CYP) in *B. bassiana*.

CYP clan	CYP family	CYP subfamily
CYP 54	CYP 503	B1
CYP 504	CYP 504	A6, B10, E1, E5
CYP 505	CYP 505	A1 (CYPOR), A2, D4
nd	CYP 5060	A1
CYP 531	CYP 5080	B3
CYP 56	CYP 5099	A1
CYP 51	CYP 51	F1, F2
CYP 52	CYP 52	X1, T1, G6, G8, G11
nd	CYP 5202	A1
CYP 526	CYP 526	H1
nd	CYP 5262	A3
CYP528 (kr)/53 (dn)	CYP 528	A4
nd	CYP 5280	A1P
nd	CYP 5282	A1
nd	CYP 5293	A1, A2
CYP 53	CYP 53	A11, A26
nd	CYP 5337	A1
CYP 534	CYP 534	C2
CYP 537 (kr)/53 (dn)	CYP 537	A4
CYP 52	CYP 539	B1, B5
CYP 540	CYP 540	B16
CYP 505	CYP 541	A2
CYP 58 (kr)/53 (dn)	CYP 542	B1, B2, B3
CYP 548 (kr)/53 (dn)	CYP 548	A5
CYP 58	CYP 551	C1
CYP 56	CYP 56	C1
CYP 65 (kr)/53 (dn)	CYP 561	D2P
CYP 507 (kr)/53 (dn)	CYP 570	A1, H1, E2,
CYP 578	CYP 578	A2
CYP 58	CYP 58	A3
CYP 52	CYP 584	D4, E2, E7, G1, Q1
CYP 59	CYP 586	B1
nd	CYP 6001	C8
nd	CYP 6003	A1
nd	CYP 6004	A2
CYP 61	CYP 61	A1
CYP 547	CYP 617	A1, A2, N1
CYP 533	CYP 620	C2, D1
CYP 533	CYP 621	A2
CYP 559	CYP 623	C1
CYP 578 (kr)/53 (dn)	CYP 625	A1
nd (kr)/53 (dn)	CYP 628	A2
CYP 639	CYP 639	A3
CYP 645	CYP 645	A1
CYP 65	CYP 65	A1, T7
CYP 52	CYP 655	C1
CYP 550	CYP 660	A2
CYP 68	CYP 68	N1
CYP 58 (kr)/53 (dn)	CYP 682	H1, N1
CYP 58 (kr)/53 (dn)	CYP 684	A2, B2
	Total	77
	New CYP family	15 (19.5%)
	New CYP subfamily	21 (27.3%)

The genes with experimental evidence of involvement in both hydrocarbon and insect lipid degradation are underlined.

Source: Xiao et al. (2012). Kr, It was generated via the implemented pipeline in the Fungal Cytochrome P450 Database; dn, Nelson's curation; nd, not determined (neither by kr nor dn).

alkanes ranging from C_9–C_{28}, fatty acids, e.g., oleic, linoleic, stearic, palmitic, myristic, and lauric acids, or in media containing olive oil. Intriguingly, neither wild type nor the mutant strain was able to grow on pelargonic acid. A grasshopper wing assay in which fungal spores are deposited onto dissected wings and germination/fungal growth was measured, however, revealed a difference between the wild type and ΔBb-CYP52(X1) strains. Germination of the mutant strain on the grasshopper wings was 50% lower than the wild type or complemented mutant strains, the latter representing a mutant strain in which the wild type gene was retransformed into the fungus under control of its endogenous promoter. Perhaps the most interesting results dealt with the virulence of the mutant strain in insect bioassays. As previously mentioned, *B. bassiana* infects target host via (random) attachment to the cuticle, followed by germination, hyphal growth along the surface, and penetration through the cuticle into the insect hemocoel. Topical application of fungal conidia (spores) represents that "natural" route of infection, and experiments performed using the Greater Waxmoth, *Galleria mellonella*, indicated a 25–50% reduction in virulence (time to kill, LT_{50}value) in the ΔBb-CYP52(X1) strain as compared to the wild type and complemented strains. Cuticle penetration can be bypassed, however, by directly injecting the fungal cells into the insect hemoceol. In such experiments, i.e., intrahemoceol injection assays, the mutant strain was as virulent as the wild type parent. These data support a hypothesis that certain cytochrome P450 enzymes are important for cuticle penetration events, presumably via assimilation or detoxification of cuticular substrate for the enzyme, but that these P450s are not required for post-penetration events once the cuticle has been breached. An important piece of the puzzle, however, remains obscure, namely, since P450s are ER-derived membrane bound proteins, how are their (cuticular) substrates accessed and/or transported to the proteins?

We have also constructed targeted gene knockouts of the six out of eight of the other identified cytochrome P450 enzymes implicated in insect hydrocarbon degradation (**Table 1**). However, to date, no phenotype with respect to growth or germination on lipids or virulence has been noted for any of these mutants (data not shown). These results may not be too surprising for several reasons. First, due to the potential redundancy and/or (partial) overlapping substrates specificities of these enzymes single gene knockout like we have constructed may not display any noticeable phenotypes. This has been also

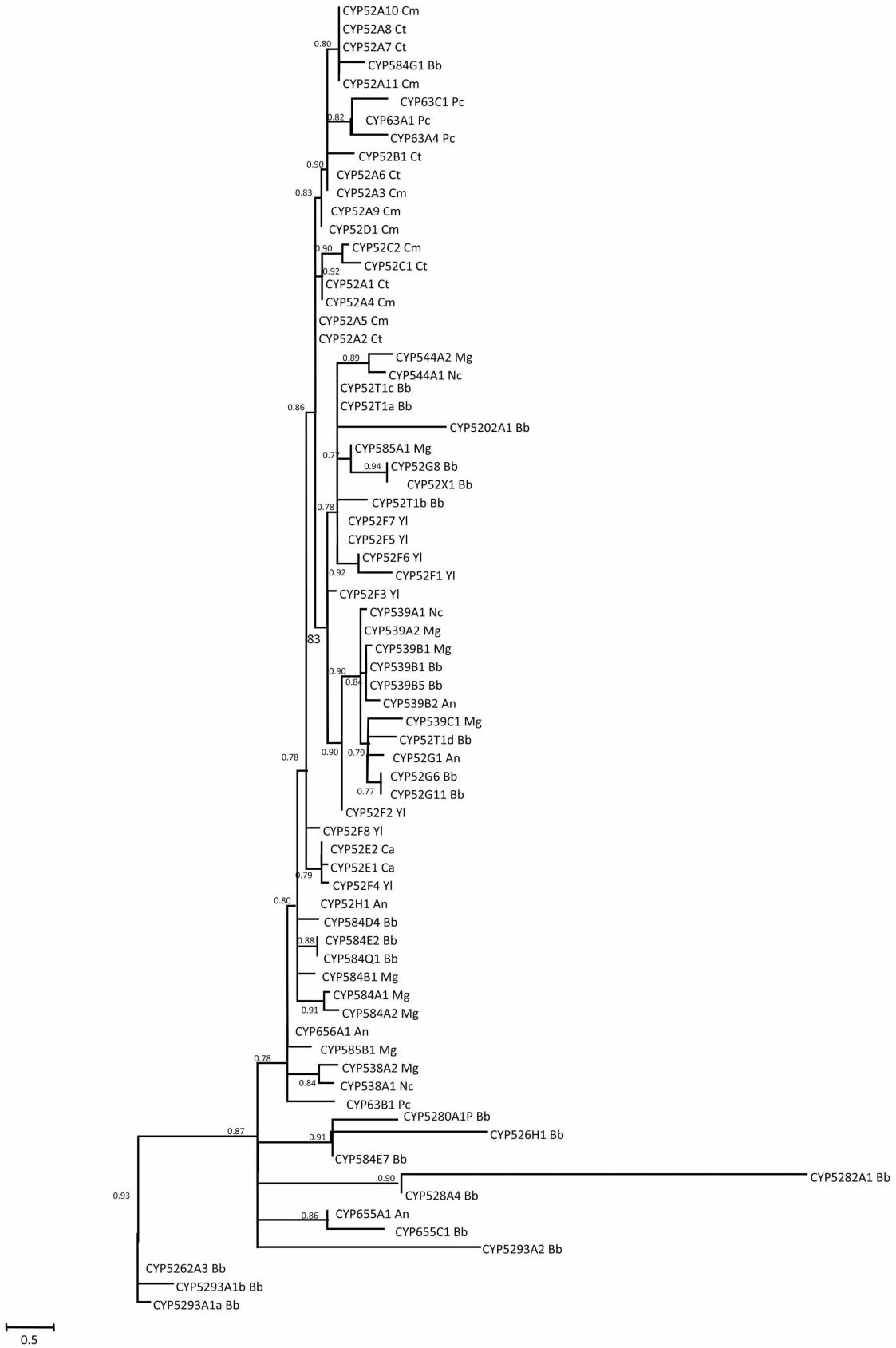

FIGURE 5 | Continued

FIGURE 5 | Maximum likelihood phylogenetic tree of clan 52 cytochrome P450s. The putative conserved domains for each protein were picked up from the conserved domain database (CDD) (Marchler-Bauer et al., 2011), and aligned using MUSCLE. The multiple sequence alignment was cured with Gblocks. PhylML was used to build the tree. All the analyses were performed at the online platform Phylogeny.fr (Dereeper et al., 2008, 2010). Numbers at nodes indicate SH-like branch support. Scale bar indicates number of amino acid substitutions per site. Amino acid substitution model John Taylor Thornton (JTT).

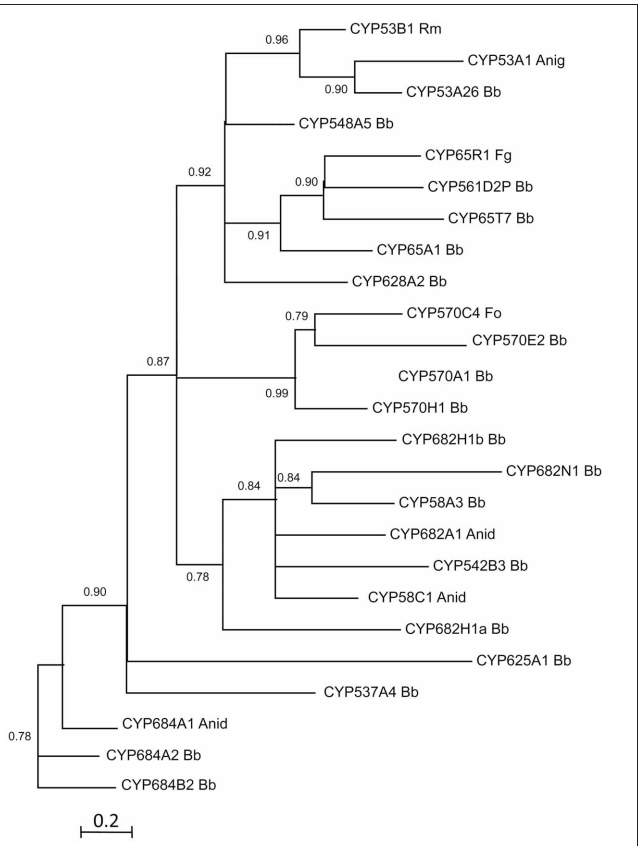

FIGURE 6 | Maximum likelihood phylogenetic tree of clan 53 cytochrome P450s.

observed in *Y. lipolytica*, where the abundance of paralog genes encoding for alkane degradation proteins, makes it difficult to unravel the function and the physiological substrate(s) of individual alkane degradation proteins (Takai et al., 2012). Second, the virulence of these strains have only been examined with respect to a single insect target (*G. mellonella*), it is possible that some of these enzymes may have substrates found on other targets not present on *G. mellonella*. Thus, assaying a diversity of target insects may reveal differential contributions of various P450s to the pathogenic process toward specific insects. If properly demonstrated, this would support the idea that P450s can act as insect target specificity factors, contributing to the broad host range nature of *B. bassiana*.

BIOCHEMICAL CHARACTERIZATION OF *B. bassiana* CYTOCHROME P450s

B. bassiana CYP52(X1) has been expressed in a yeast (*Saccharomyces cerevisiae*) heterologous expression system and its activity examined in yeast-derived microsomal extracts (Zhang et al., 2012). This yeast system has been optimized for expression of cytochrome P450s and contains elevated amounts of the needed companion reductase for activity (Pompon et al., 1996). Intriguingly, although a low spin heme spectrum was detected in yeast microsomes isolated from expression-induced cells harboring the Bbcyp52x1 plasmid construct, no CO difference spectral shift, a tell-tale biophysical signal for cytochrome P450 content, was observed. The (ER-derived) microsomes, however, displayed NADPH-dependent oxidation of a number of substrates under conditions in which no activity was detected in control microsomes derived from wild type yeast cells or cells transformed with an empty vector. Use of radiolabeled lauric and oleic acids followed by GC/MS analysis confirmed CYP52X1 mediated NADPH-dependent regioselective addition of a terminal hydroxyl to both substrates. TLC analysis of reaction products using a variety of other fatty acid substrates revealed that CYP52X1 displayed highest activity against C12:0, C14:0, and epoxy stearic acid, 4–8-fold lower activity against C16:0, C18:1, and C18:2, and little to no activity toward C9:0 and C18:0 (Zhang et al., 2012).

Additional *B. bassiana* proteins, namely, CYP5337A1, CYP617N1, CYP53A26, and CYP584Q1 have also been expressed in the same yeast system. These constructs contained N-terminal his-tags which have been used for partial purification using immobilized metal ion chromatography (Ni^{2+} IMAC) (**Figure 7**). Of the proteins examined thus far, only CYP53A26 showed a CO spectrum corresponding to the oxidized protein, including a peak at 426 nm and a small shoulder at 450 nm (**Figure 7**). The rest of the proteins showed no CO difference spectral shift when dithionite was added (data not shown). Poor or atypical CO spectra have been reported for a number of cytochrome P450s including some plant P450s that have weak affinity for CO (Lau et al., 1993), and P450 19A1 (human aromatase) which does not bind CO (Harada, 1998; Gartner et al., 2001). Our data suggest that the number of P450s with atypical CO spectra is greater than what is currently thought.

FATTY ALCOHOL AND ALDEHYDE DEHYDROGENASES

Upon terminal hydroxylation of alkanes to fatty alcohols by P450ALKs, fatty alcohol and aldehyde dehydrogenases (FADHs and FALDHs) oxidize the fatty alcohols to fatty aldehydes and fatty acid, respectively. There have been few reports examining fungal very long chain alcohol and aldehyde dehydrogenases, and little is known concerning their potential role in the oxidation of the fatty alcohol products of P450 activity. Dehydrogenases, however, are considered to yield the fatty acids that feed into the β-oxidation pathway. Fatty alcohol dehydrogenases (FADHs) are mainly linked to the biosynthesis of mannitol, an important intracellular carbohydrate factor that participates in stress tolerance

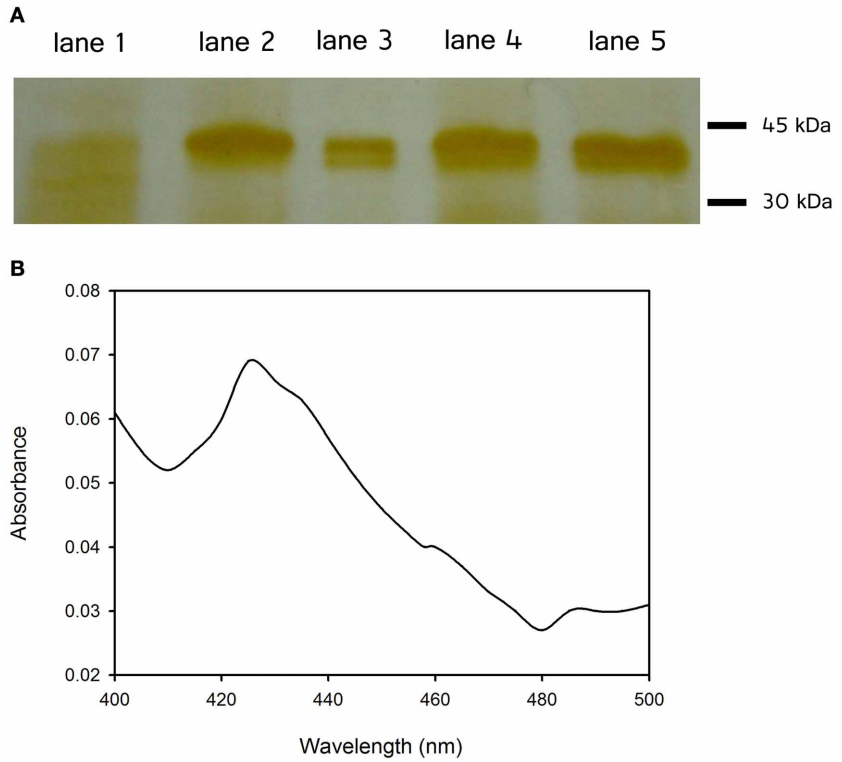

FIGURE 7 | (A) SDS–PAGE of partial purified proteins using immobilized metal ion chromatography (Ni^{2+} IMAC): vector without insert (lane 1), CYP52X1 (lane 2), CYP5337A1 (lane 3), CYP617N1 (lane 4), and CYP53A26 (lane 5). Examined proteins were expressed in the yeast *Saccharomyces cerevisiae* WAT11. The cells were transformed with the lithium acetate method (Ito et al., 1983) for microsome isolation purposes. Proteins were solubilized with 10% w/v sodium cholate and loaded onto the column. **(B)** CO difference spectrum of CYP53A26: Sodium dithionite and CO were added to the purified protein, and absorbance between 400 and 500 nm was measured.

and has even been linked to virulence in certain fungal pathogens. *M. anisopliae* has 17 zinc-containing alcohol dehydrogenases (Gao et al., 2011). FALDHs, responsible for the oxidation of various aldehydes to their corresponding carboxylic acids are widely distributed in filamentous fungi. Although little empirical data is currently available, it is postulated that in entomopathogenic fungi specific FALDHs may exist with substrate specificity for the aldehydes present or generated during cuticular hydrocarbon assimilation. Two *M. anisopliae* FALDHs have thus far been examined in relation with cuticle degradation, and these have been shown to be up-regulated in when the fungus is grown in the presence of insect cuticles as compared to growth in sugar-rich media (Freimoser et al., 2005). It is likely therefore that the observed induction of these genes in the presence of insect cuticle is a consequence of the availability of aldehydes resulting from the oxidation of cuticular hydrocarbons.

In the *Aspergillus nidulans* ethanol utilization pathway, FALDH and FADH are co-regulated, at the transcription level, via the *alc* regulon (Flipphi et al., 2001). Aside from ethanol and acetaldehyde, other inducers of the *alc* system including amino acids and other aliphatic alcohols have been identified. However, it is thought that the real physiological inducers are aldehydes, and that the other examined compounds are first converted to their corresponding aldehydes in order to act as inducers (Flipphi et al., 2001). Analysis of the promoter region of the FALDH *ald1* of the mycorrhizal fungus *Tricholoma vaccinum* revealed the presence of five putative stress response elements (STREs) (Asiimwe et al., 2012). These elements have also been detected in the promoters of several *B. bassiana* CYP genes (Pedrini et al., 2010), suggesting common induction/regulatory compounds and pathways function to co-regulate FALDH, FADH, and CYP activities. It should be noted that alternative pathways also exist; the alkane-assimilating yeast *C. maltosa* is able to catalyze the production of a cascade of mono-oxidation products followed by di-terminal oxidation of substrates to yield α-ω acids. These reactions can be catalyzed by a single P450 enzyme and include both alcohol and aldehyde intermediates but do not use the corresponding dehydrogenases (Scheller et al., 1998). Although no evidence exists for such pathways in *B. bassiana*, at this time they cannot be excluded.

Feeding of hydrocarbon assimilation products into central metabolic pathways (**Figure 4**) may also contribute to the *B. bassiana* pathogenic lifecycle. Isocitrate lyase (ICL) and malate synthase (MLS) are not only up-regulated during growth on two-carbon compounds including acetate and ethanol, but also during growth in insect hemoplymph (Padilla-Guerrero et al., 2011). In *M. anisopliae*, *icl* is up-regulated during the initial infection stage of appressoria formation as well as during late host growth events when the fungi are engulfed by insect heamocytes,

highlighting the contribution of the glyoxylate cycle in pathogenesis (Padilla-Guerrero et al., 2011). Production of metabolic acids by entomopathogenic fungi, potentially resulting from cuticular hydrocarbon recognition and assimilation cues, can also directly participate in insect virulence; and citrate, formate, and oxalate have been shown to contribute to *B. bas*siana virulence (Bidochka and Khachatourians, 1991; Kirkland et al., 2005). Oxalate production in particular contributes to pathogenesis via acidification of host tissues, sequestration of metal ion such as calcium, magnesium, manganese, and iron and could inhibit or disrupt host defense responses (Kirkland et al., 2005).

CATALASES

Fatty acids are completely catabolized through β-oxidation. Peroxisomal proliferation together with a marked induction of the β-oxidation system has been related to alkane-growth adaptation in *B. bassiana* (Crespo et al., 2000). The typical peroxisomal marker enzyme is catalase, a hemoprotein that decomposes excess H_2O_2 produced by β-oxidation. Peroxisomal catalase induction was observed in alkane-grown *B. bassiana*, a high increment in the catalase activity (14-fold) was measured in these fungi compared with control cultures grown in complete medium (Pedrini et al., 2006). Catalase activity was also detected in the cytosolic fraction of *B. bassiana*, although this isoform was not induced in the same culture condition (Pedrini et al., 2006). Catalase induction was proposed as a simple biochemical marker to follow the course of fungal growth adaptation in insect-like hydrocarbons and was correlated with enhance virulence parameters (i.e., lower LC_{50} and/or LT_{50}) (Crespo et al., 2002; Pedrini et al., 2007, 2009).

The catalase family of *B. bassiana* consists of at least five genes designed as; catA (spore-specific), catB (secreted), catP (peroxisomal), catC (cytoplasmic), and catD (secreted peroxidase/catalase). The functions of these genes and their protein products have been studied via generation of single targeted gene disruption mutant strains (Wang et al., 2012). CatB appeared to account for the predominant catalase activity produced by the fungus with ΔcatB mutants displaying ∼90% decrease in total catalase activity, however ΔcatP mutants were reported to results in ∼55% decrease in total catalase activity, suggesting negative pleiotropic effects between certain catalases. Intriguingly, ΔcatB (and ΔcatC) mutants displayed only minor phenotypic effects, which the authors explain by the observation of up-regulation of the other catalases in these mutants and hence potential functional redundancy. If correct, it is unclear, however, how this would explain the low (∼10% of wild-type) activity seen in the ΔcatB mutant. ΔcatA strains were more theromosensitive than the wild type parent, showed a ∼50% decrease in UV-B resistance, decreased virulence in insect bioassays, and conidial sensitivity to H_2O_2 although colony growth in the presence of H_2O_2 was essentially unaffected. ΔcatD strains were unaffected in thermal stability and oxidative stress in general, but did display reduced UV-B tolerance and virulence in insect bioassays. Deletion of the peroxisomal catalase (catP), the enzyme most likely to be involved in hydrocarbon assimilation pathways, resulted in increased sensitivity to oxidative stress both on the conidial germination level and during colony (vegetative) growth. ΔcatP mutants were essentially unaffected in thermal sensitivity and UV-B tolerance, but displayed ∼50% decrease in virulence (LT_{50}) indicating that it is an important enzyme involved in the pathogenic process (Wang et al., 2012). Although alkane and hydrocarbon assimilation in the catP (or other catalase) mutants has not yet been examined, these data suggest that peroxisomal catalases might be crucial factors for adaptation to oxidative stress generated during fungal growth on insect alkanes and other hydrocarbons.

INSECT CUTICULAR HYDROCARBONS SYNTHESIS AND FUNGAL HYDROCARBON ASSIMILATION—AN EXAMPLE OF "RED QUEEN" CO-EVOLUTION?

The co-evolutionary arms race between a pathogen and its target host has been referred to as the "Red-Queen Hypothesis," and is taken from Lewis Carroll's Through the Looking Glass, where in the Red Queen's race "it takes all the running you can do, to keep in the same place" (Van Valen, 1973). The hypothesis is that target hosts evolve mechanisms for resistance against pathogens, and that pathogens, in turn, evolve mechanisms for surmounting the evolving host defenses. Could insect cuticular hydrocarbon synthesis be under a Red Queen selection mechanism? It is undoubtable that the insect epicuticle layer, with its complexity of hydrocarbons serves as a means for protection against abiotic stress, e.g., desiccation, heat, and even potentially UV irradiation, and that this layer serves as a platform for semiochemicals involved in insect communication and signaling. It is also clear that many of the hydrocarbons present in the epicuticle have antimicrobial properties and suppress the growth of microbes. Antimicrobial mechanisms may be passive in that these hydrocarbons are poor substrates for most microbes and that they can effectively sequester nutrients from scavenging and/or attacking parasites. However, there is ample evidence for the existence of chemically diverse species-specific antimicrobial compounds targeted for secretion to the insect epicuticle. Both such molecules must be overcome for successful pathogenesis to occur. Specific antimicrobial compounds would require detoxification and/or remediation that occur via enzymatic inactivation and/or efflux or sequestration of such molecules via multidrug-efflux systems. In this respects *B. bassiana* displays a high level of resistance to many antifungal compounds and genomic analyses has revealed a large set of detoxifying enzymes as well as efflux transporters. Insect epicuticles, however, often contain significant amounts of long chain hydrocarbons, whose purpose regarding abiotic stress and/or semiochemicals potential are obscure. However, long(er) chain hydrocarbons become increasingly difficult for microbes to assimilate and can directly inhibit the growth of many bacteria and fungi. As elongation reactions in insect hydrocarbon biosynthesis typically add two-carbons to the growing chain, from a biochemical and physiological stand-point, increasing chain length and secreting/transporting the products to the epicuticle represents a facile mechanism to thwart the growth of potential pathogens. Successful pathogens, in turn must develop mechanisms for bypassing and/or degrading the ever-growing hydrocarbon chain lengths. In short, could fungal pathogens help explain the diversity and chain length of insect hydrocarbons on the one hand, and the evolution of specific enzymes (cytochrome P450s) and pathways to assimilate these lipids on the other? It should be noted that to date, there is little empirical evidence

to support this idea, however, such a hypothesis does make certain predictions and can help explain certain phenomena. First, one would predict that insects that make longer chain hydrocarbons that *B. bassiana* cannot assimilate would be more resistant to fungal infection or vice versa that insects which display resistance to *B. bassiana* do so because of epicuticular lipid content, in particular by synthesizing longer and/or branched-chain hydrocarbons. Second, epicuticular hydrocarbon content may explain strain variation and sub-specificity seen between different fungal isolates. Finally, it is known that even amongst some (*B. bassiana*) susceptible insect species certain developmental stages (instars) are more resistant than others. Since epicuticular hydrocarbons are known to vary between such developmental stages, one could predict that these differences may help account for the variation in pathogen susceptibility observed.

CONCLUDING REMARKS

The lipid-rich insect epicuticle represents the first barrier against, and mediates the initial interaction with, microbial pathogens. Targeting of this layer by the entomopathogenic fungus *Beauveria bassiana* occurs within the context of a host-pathogen interaction. Aspects of the biochemical basis for fungal mediated hydrocarbon oxidation and assimilation have been uncovered. Genomic, genetic, and biochemical data indicate that the fungus contains a repertoire of cytochrome P450 enzymes, likely with over-lapping specificities, along with attendant downstream pathways, that act to assimilate insect hydrocarbons. There remain, however, many unanswered questions and significant aspects of the fungal-epicuticle interaction remains obscure. The substrate specificities of only one *B. bassiana* cytochrome P450 has been examined, and questions concerning the uptake and transport of hydrocarbons into the fungus have yet to be adequately addressed. The idea that epicuticular hydrocarbon synthesis and fungal assimilation of these compounds may represent a co-evolutionary race needs empirical support. Further research aimed toward examining these and other questions can yield novel insights into the biochemistry of hydrocarbon degradation as well as into the ecology and evolution of the interaction between fungal entomopathogens and their insect hosts, and can impact practical applications of fungi in biological control of insects and/or exploitation of the fungal hydrocarbon pathways in biotechnological applications.

MATERIALS AND METHODS

CHEMICAL REAGENTS AND CULTIVATION OF FUNGI

Beauveria bassiana (ATCC 90517) was routinely grown on potato dextrose agar (PDA) or Czapek-Dox plates. Plates were incubated at 26°C for 10–15 days and aerial conidia were harvested by flooding the plate with sterile distilled water. Conidial suspensions were filtered through a single layer of Miracloth and final spore concentrations were determined by direct count using a hemocytometer. The *S. cereviseae* WAT11 strain was used for heterologous expression of *B. bassiana* cytochrome P450s. Yeast cells were grown at 30°C in Difco Yeast Nitrogen Base medium without amino acids (YNB-aa, 6.7 g/L) containing glucose or galactose at 2%(w/v) with supplements as indicated. Chemical reagents were obtained from either Fischer Scientific or Sigma-Aldrich chemicals unless otherwise noted. Phosphinothricin was purchased from Gold Biotech or purified in the lab from the herbicide Finale (AgrEvo, Montvale, NJ) as described (Metzenberg et al., 2000).

NUCLEIC ACID MANIPULATIONS AND CONSTRUCTION OF *B. bassiana* CYTOCHROME P450 KNOCKOUT STRAINS

All primer sequences for the nucleic acid manipulations, RT-PCR, Southern blot probe generation, and yeast expression vector construction are listed in **Table 3**. To generate the vector for construction of the cytochrome P450 knockout strains in *B. bassiana* via homologous recombination, fragments for each gene (see **Table 1** for list of P450s and accession numbers) were amplified from genomic DNA using the primer pairs as listed in **Table 3**. PCR products was cloned into the pCR2.1-TOPO blunt-end vector (Invitrogen) generating pTOPO-*Bbcyp450xxx* clones for each gene. Long-range deletion inverse PCR using the primer pair for each gene (**Table 3**) were then used to produce linear fragments lacking 50–200 bp of internal sequence for each gene using the respective pTOPO-*Bbcyp450* plasmid of each gene as template. The generated linear DNA was then blunt-end ligated to a PCR product corresponding to the herbicide resistance gene (*bar*) cassette amplified from pBAR-GPE (Sweigard et al., 1997) using primer pair pBARF and pBARR. The integrity of each resultant gene replacement plasmid designated as pKO-*Bbcyp450xxx*, was confirmed by PCR and sequencing. Preparation of competent cells, transformation, and screening of recombinant clones was performed as described using a PEG-LiAc mediated protocol (Zhang et al., 2010; Fan et al., 2011). The transformation mixture (0.25–0.5 ml) was plated onto Czapek-Dox medium containing 200 mg/ml phosphinothricin, 0.01% bromocresol purple, pH 6.3, in 150 mm diameter Petri dishes overlaid with a sheet of sterilized cellophane. Genomic DNA was isolated as described (Liu et al., 2000). Putative *B. bassiana* gene knockout clones were screened and verified by PCR analysis using primers designed to each *Bbcyp450* gene (**Table 3**). PCR reactions were performed using the following protocol: 95°C for 3 min, followed by 35 cycles of denaturation at 95°C for 30 s, annealing at 56°C for 30 s, and extension at 72°C for 1 min. Transformants were confirmed by PCR and RT-PCR using primers as listed in **Table 3**.

GROWTH AND GRASSHOPPER WING GERMINATION ASSAYS

Fungal growth experiments of various hydrocarbons were performed as follows; fungal spores were harvested from PDA plates directly into sterile distilled water and were washed twice with the same solution; the suspension was then adjusted to 10^7–10^8 conidia ml^{-1} after counting using a hemocytometer. Spore suspensions (5–10 μl) were then placed into the middle of microtiter agar plates (24- or 48-well). For 24-well plates, each well contained 1 ml MM in Noble agar overlaid with the desired alkane (0.1 ml of a10% hydrocarbon stock solution in hexane) as a carbon source. Substrates tested included the following alkanes (0.1%); C_9, C_{10}, C_{12}, C_{14}, C_{16}, C_{18}, C_{24}, and C_{28}. Grasshopper wings sterilized using 37% H_2O_2 were immersed in a conidial suspension in water at a concentration of 1×10^6spores/ml for 20 s, and placed on 0.7% water agar. After incubation for 18 h, the germinated conidia were counted under a light microscope.

Table 3 | Primers used in this study.

Name	Sequence (5′ to 3′)	Use
pBARF	GTCGACAGAAGATGATATTGAAGG	KO strain construction
pBARR	TCATCAGATCTCGGTGACGGGCAGG	KO strain construction
CYP5337A1 KNOCKOUT		
P4F	GTGTGCGTGATCCAGAGCTCTGC	KO strain construction
P4R	GCACCAAGTTTCGAGACTGGGACAT	KO strain construction
P4KOF	ACTTACGACCTATGCAGATGCGC	KO strain construction
P4KOR	GTTGGCTTGTATGGGATTACGCC	KO strain construction
P4RTPCRF	CACATTGTTGTACGCGGTACTTTGC	KO screening
P4RTPCRR	TATGGTCCGGATGCAATGGAGTGG	KO screening
CYP52G11 KNOCKOUT		
P5F	CGCTCACTGCTATCCTCATCGGC	KO strain construction
P5R	CAGAACAGCGATAACGTGACGAGCT	KO strain construction
P5KOF	CAAGGGCGGCTGGGAATATCTC	KO strain construction
P5KOR	TTCTCGTAGCCGCCAAAGGTCT	KO strain construction
P5RTPCRF	CTCCTCAACGTCCTCCTCGCCGG	KO screening
P5RTPCRR	GAGGAGTCGGGCGAGGACGTAAC	KO screening
CYP617N1 KNOCKOUT		
P7F	GAAAGCCCCAACGAAGGCCTGAT	KO strain construction
P7R	GAAGTTGCCCGGTCCCTTGTCAA	KO strain construction
P7KOF	GGACAAGTCTCTTCTTGACGAAAGCA	KO strain construction
P7KOR	ATTGGTCGCATTCTTGCCGCC	KO strain construction
P7RTPCRF	TGGGATTGGTGCCGTGGGCAA	KO screening
P7RTPCRR	CCTGTATGCACATTTCCATTCCGCC	KO screening
CYP53A26 KNOCKOUT		
P8F	CCGTCATTGTCCCGAGCCAAGAA	KO strain construction
P8R	TGGCAACGGATGCAAAGACCAAGAC	KO strain construction
P8KOF	CTGGACGCCGTCATTCCCGAG	KO strain construction
P8KOR	CGGGTTCTCGATTCGGCTCTTG	KO strain construction
P8RTPCRF	ATTCGGCATGTTGGCGAGTGGTAT	KO screening
P8RTPCRR	AGGTCGGCACGCTCAAGACGGT	KO screening
CYP655C1 KNOCKOUT		
Ep(2)F	GCCTCACGCAACTACTCAGCCTTTCATC	KO strain construction
Ep(2)R	CGCAGACTCATTCTGGACCATCATTTG	KO strain construction
Ep(2)KOF	CAAACTATGGCGGCTACCGGT	KO strain construction
Ep(2)KOR	GTCGTGAGCTAGGAATCTGCGCA	KO strain construction
Ep(2)RTPCRF	CTCCTAGACAGCGTGAGCCTCCCAT	KO screening
Ep(2)RTPCRR	GGTGCTGCCTGATGGGCTCGAC	KO screening
CYP5337A1 EXPRESSION		
EP(4)F	GGATTAATAATGGCGCTCACTGCTATCCT	
EP(4)R	GGGTTAATTTAGTGGTGGTGGTGGTGG TGGACAGCCTCGTGCAGGCGGAC	
CYP617N1 EXPRESSION		
EP(7)F	GGATTAATAATGGCCGTGGTTGAGCTC	
EP(7)R	GGGTTAATTTAGTGGTGGTGGTGGTGGT GTCGCCTAGCCAGTGCATCTC	
CYP53A26 EXPRESSION		
EP(8)F	GGATTAATAATGGCTCTCGGCCAACTT GCC	
EP(8)R	GGGTTAATTTAGTGGTGGTGGTGGTGGT GTTGCAGCTTTTCTTCTGCATTCTG	
ActinF	TTGGTGCGAAACTTCAGCGTCTAGTC	RT-PCR
ActinR	TCCAGCAAATGTGGATCTCCAAGCAG	

(Continued)

HETEROLOGOUS EXPRESSION OF *B. bassiana* CYTOCHROME P450s IN YEAST

The coding region of CYP5337A1, CYP617N1, CYP53A26, and CYP584Q1 genes were cloned from a *B. bassiana* cDNA library by PCR using primer pairs as listed in **Table 3**. The resultant PCR product corresponding to each gene was designed to contain an 18 bp (6 amino acid) histidine tag and the products were cloned into pYeDP60 under the control of a GAL1 promoter. The sequence integrity of plasmid inserts were confirmed by sequencing and plasmids were then transformed into *S. cerevisiae* WAT11, a yeast strain engineered and optimized for cytochrome P450 expression, using a lithium acetate protocol (Pompon et al., 1996). Transformants were selected on YNB w/o amino acids, 2% glucose and auxotrophic supplements and the expression strain designated as *Sc-Bbcyp5337a1*, *Sc-Bbcyp617N1*, *Sc-Bbcyp53a26*, and *Sc-Bbcyp584q1*, respectively.

Yeast cultures were grown and heterologous expression of each CYP (CYP5337A1, CYP617N1, CYP53A26, and CYP584Q1) was induced as described in Pompon et al. (Pompon et al., 1996) from one isolated transformed colony. Briefly, after growth, cells were harvested by centrifugation and manually broken with glass beads (0.45 mm diameter) in 50 mM Tris-HCl buffer (pH 7.5) containing 1 mM EDTA and 600 mM sorbitol. The homogenate was centrifuged for 10 min at 10,000 g. The resulting supernatant was centrifuged for 1 h at 100,000 g. The pellet consisting of

microsomal membranes was resuspended in 50 mMTris-HCl (pH 7.4), 1 mM EDTA and 30% (v/v) glycerol with a Potter-Elvehjem homogenizer and stored at −30°C. The volume of resuspension buffer is proportional to the weight of yeast pellet: microsomes extracted from 6 g of yeast are resuspended in 3 ml of buffer. All procedures for microsomal preparation were carried out at 0–4°C. Western blots were performed using standard protocols. Mouse anti-His monoclonal antibodies were obtained from Invitrogen.

CYP SOLUBILIZATION AND PARTIAL PURIFICATION

Microsomal fractions were treated with 10% (w/v) sodium cholate solution (final concentration 1% w/v) for 30 min at 4°C, in order to solubilize proteins from membranes. After ultracentrifugation (100,000 g, 60 min, 4°C) supernatants were loaded onto Ni-NTA columns and purified by immobilized metal-ion affinity chromatography (IMAC) following standards protocols. Eluted fractions were analyzed by SDS–PAGE. Fractions containing the tagged protein were pooled, concentrated, and assayed for P450 content.

MEASUREMENT OF REDUCED CARBON MONOXIDE (CO) DIFFERENCE SPECTRA

The reduced CO difference spectra were measured in an Ultrospec 2100 pro spectrophotometer (Biochrom Ltd., Cambridge, UK) as described (Schenkman and Jansson, 2006), with minimal modifications. Briefly, samples were diluted to 1 mg ml^{-1} protein, CO was slowly burbled into the cuvet for about 30 s, and a few milligrams of sodium dithionite were added. After stirring and waiting 1 min, the difference spectrum was recorded between 400 and 500 nm. Protein concentrations were determined by the Pierce bicinchoninic acid microassay, using bovine serum albumin as standard.

ACKNOWLEDGMENTS

This work was supported in part by an NSF grant IOS-1121392 to Nemat O. Keyhani. Almudena Ortiz-Urquiza was supported in part by a Fellowship from the Spanish Ministry of Education (EX2010-1098). This work was also supported in part by grants from ANPCyT (PICT 2008 0802) and CONICET (PIP 0237) to Nicolás Pedrini.

REFERENCES

Anderson, S. O., Hojrup, P., and Roepstorff, P. (1995). Insect cuticular proteins. *Insect Biochem. Mol. Biol.* 25, 153–176.

Asiimwe, T., Krause, K., Schlunk, I., and Kothe, E. (2012). Modulation of ethanol stress tolerance by aldehyde dehydrogenase in the mycorrhizal fungus *Tricholoma vaccinum*. *Mycorrhiza* 22, 1–14.

Bagnères, A. G., and Blomquist, G. J. (2010). "Site of synthesis, mechanism of transport and selective deposition of hydrocarbons," in *Insect Hydrocarbons: Biology, Biochemistry and Chemical Ecology,* eds G. J. Blomquist and A. G. Bagnères (New York, NY: Cambridge University Press), 75–99.

Berbee, M. L., and Taylor, J. W. (2001). "Fungal molecular evolution: gene trees and geologic time," in *The Mycota VII Part, B,* eds McLaughlin, McLaughlin, and Lemke (Berlin Heidelberg: Springer-Verlag), 229–245.

Bidochka, M. J., Clark, D. C., Lewis, M. W., and Keyhani, N. O. (2010). Could insect phagocytic avoidance by entomogenous fungi have evolved via selection against soil amoeboid predators? *Microbiology* 156, 2164–2171.

Bidochka, M. J., and Khachatourians, G. G. (1991). The implication of metabolic acids produced by *Beauveria bassiana* in pathogenesis of the migratory grasshopper, *Melanoplus sanguinipes*. *J. Invertebr. Pathol.* 58, 106–117.

Binnington, K., and Retnakaran, A. (1991). *Physiology of the Insect Epidermis.* Melbourne: CSIRO Publications.

Blomquist, G. J., and Dillwith, J. W. (1985). "Cuticular lipids," in *Comprehensive Insect Physiology, Biochemistry, and Pharmacology,* eds G. A. Kerkut and L. I. Gilbert (Oxford: Pergamon Press), 117–154.

Blomquist, G. J., Nelson, D. R., and Derenobales, M. (1987). Chemistry, biochemistry, and physiology of insect cuticular lipids. *Arch. Insect Biochem. Physiol.* 6, 227–265.

Blomquist, G. J., Tillman-Wall, J. A., Guo, L., Quilici, D. R., Gu, P., and Schal, C. (1993). "Hydrocarbon and hydrocarbon-derived sex pheromones in insects," in *Biochemistry and Endocrine Regulation,* eds D. W. Stanley-Samuelson and D. R. Nelson (Lincoln, NE: University of Nebraska Press), 317–351.

Boucias, D. G., and Pendland, J. C. (1984). Nutritional requirements for conidial germination of several host range pathotypes of the entomopathogenic fungus *Nomuraea rileyi*. *J. Invertebr. Pathol.* 43, 288–292.

Boucias, D. G., Pendland, J. C., and Latge, J. P. (1988). Nonspecific factors involved in attachment of entomopathogenic Deuteromycetes to host insect cuticle. *Appl. Environ. Microbiol.* 54, 1795–1805.

Buckner, J. S. (1993). "Cuticular polar lipids of insects," in *Insect Lipids: Chemistry, Biochemistry and Biology,* eds D. W. Stanley-Samuelson and D. R. Nelson (Lincoln, NE: University of Nebraska Press), 227–270.

Cameotra, S. S., Singh, H. D., Hazarika, A. K., and Baruah, J. N. (1983). Mode of uptake of insoluble solid substrates by microorganisms 2. Uptake of solid normal-alkanes by yeast and bacterial species. *Biotechnol. Bioeng.* 25, 2945–2956.

Charnley, A. K., and St Leger, R. (1991). "The role of cuticle degrading enzymes in fungal pathogenesis of insects," in *The Fungal Spore and Disease Initiation,* eds G. T. Cole and H. C. Hoch (New York, NY: Plenum Press), 267–286.

Chino, H., and Kitazawa, K. (1981). Diacylglycerol-carrying lipoprotein of hemolymph of the locust and some insects. *J. Lipid Res.* 22, 1042–1052.

Cho, E. M., Boucias, D., and Keyhani, N. O. (2006a). EST analysis of cDNA libraries from the entomopathogenic fungus *Beauveria (Cordyceps) bassiana*. II. Fungal cells sporulating on chitin and producing oosporein. *Microbiology* 152, 2855–2864.

Cho, E. M., Liu, L., Farmerie, W., and Keyhani, N. O. (2006b). EST analysis of cDNA libraries from the entomopathogenic fungus *Beauveria* (*Cordyceps*) *bassiana*. I. Evidence for stage-specific gene expression in aerial conidia, in vitro blastospores and submerged conidia. *Microbiology* 152, 2843–2854.

Clarkson, J. M., and Charnley, A. K. (1996). New insights into the mechanisms of fungal pathogenesis in insects. *Trends Microbiol.* 4, 197–203.

Cooney, J. J., Siporin, C., and Smucker, R. A. (1980). Physiological and cytological responses to hyd rocarbons by the hydrocarbon-using fungus *Cladosporium resinae*. *Botanica Marina* 23, 227–232.

Crespo, R., Juarez, M. P., and Cafferata, L. F. R. (2000). Biochemical interaction between entomopathogenous fungi and their insect-host-like hydrocarbons. *Mycologia* 92, 528–536.

Crespo, R., Juarez, M. P., Dal Bello, G. M., Padin, S., Fernandez, G. C., and Pedrini, N. (2002). Increased mortality of *Acanthoscelides obtectus* by alkane-grown *Beauveria bassiana*. *Biocontrol* 47, 685–696.

Crespo, R., Pedrini, N., Juarez, M. P., and Dal Bello, G. M. (2008). Volatile organic compounds released by the entomopathogenic fungus *Beauveria bassiana*. *Microbiol. Res.* 163, 148–151.

Deng, J., Carbone, I., and Dean, R. A. (2007). The evolutionary history of Cytochrome P450 genes in four filamentous Ascomycetes. *BMC Evol. Biol.* 7:30. doi: 10.1186/1471-2148-7-30

Dereeper, A., Audic, S., Claverie, J.-M., and Blanc, G. (2010). BLAST-EXPLORER helps you building datasets for phylogenetic analysis. *BMC Evol. Biol.* 10:8. doi: 10.1186/1471-2148-10-8

Dereeper, A., Guignon, V., Blanc, G., Audic, S., Buffet, S., Chevenet, F., et al. (2008). Phylogeny.fr: robust phylogenetic analysis for the non-specialist. *Nucleic Acids Res.* 36, 465–469.

Dettner, K., and Liepert, C. (1994). Chemical mimicry and camouflage. *Annu. Rev. Entomol.* 39, 129–154.

Doddapaneni, H., Chakraborty, R., and Yadav, J. S. (2005). Genome-wide structural and evolutionary analysis of the P450 monooxygenase genes (P450ome) in the white rot fungus Phanerochaete chrysosporium: evidence for gene duplications and extensive gene clustering. *BMC Genomics* 6:92. doi: 10.1186/1471-2164-6-92

Espelie, K., Chapman, R. F., and Sword, G. A. (1994). Variation in the surface lipids of the grasshopper, *Schistocerca americana* (Drury). *Biochem. Syst. Ecol.* 22, 563–575.

Fan, Y., Borovsky, D., Hawkings, C., Ortiz-Urquiza, A., and Keyhani, N. O. (2012a). Exploiting host molecules to augment mycoinsecticide virulence. *Nat. Biotechnol.* 30, 35–37.

Fan, Y., Pereira, R. M., Kilic, E., Casella, G., and Keyhani, N. O. (2012b). Pyrokinin beta-neuropeptide affects necrophoretic behavior in fire ants (*S. invicta*), and expression of beta-NP in a mycoinsecticide increases its virulence. *PLoS ONE* 7:e26924. doi: 10.1371/journal.pone.0026924

Fan, Y., Zhang, S., Kruer, N., and Keyhani, N. O. (2011). High-throughput insertion mutagenesis and functional screening in the entomopathogenic fungus *Beauveria bassiana*. *J. Invertebr. Pathol.* 106, 274–279.

Ferron, P. (1981). "Pest control by the fungi Beauveria and Metarhizium," in *Microbial Control of Pests and Plant Diseases 1970-1980,* ed H. D. Burges (New York, NY: Academic Press), 465–482.

Fickers, P., Benetti, P. H., Wache, Y., Marty, A., Mauersberger, S., Smit, M. S., et al. (2005). Hydrophobic substrate utilisation by the yeast *Yarrowia lipolytica*, and its potential applications. *Fems Yeast Res.* 5, 527–543.

Flipphi, M., Mathieu, M., Cirpus, I., Panozzo, C., and Felenbok, B. (2001). Regulation of the aldehyde dehydrogenase gene (aldA) and its role in the control of the coinducer level necessary for induction of the ethanol utilization pathway in *Aspergillus nidulans*. *J. Biol. Chem.* 276, 6950–6958.

Freimoser, F. M., Hu, G., and St. Leger, R. J. (2005). Variation in gene expression patterns as the insect pathogen *Metarhizium anisopliae* adapts to different host cuticles or nutrient deprivation *in vitro*. *Microbiology* 151, 361–371.

Gao, Q., Jin, K., Ying, S.-H., Zhang, Y., Xiao, G., Shang, Y., et al. (2011). Genome sequencing and comparative transcriptomics of the model entomopathogenic fungi *Metarhizium anisopliae* and *M. acridum*. *PLoS Genetics* 7:e1001264. doi: 10.1371/journal.pgen.1001264

Gartner, C. A., Thompson, S. J., Rettie, A. E., and Nelson, S. D. (2001). Human aromatase in high yield and purity by perfusion chromatography and its characterization by difference spectroscopy and mass spectrometry. *Protein Expr. Purif.* 22, 443–454.

Gibbs, A., and Mousseau, T. A. (1994). Thermal acclimation and genetic variation in cuticular lipids of the lesser migratory grasshopper (*Melanoplus sanguinipes*) - effects of lipid composition on biophysical properties. *Physiol. Zool.* 67, 1523–1543.

Gibbs, A., Mousseau, T. A., Dingle, H., and Crowe, J. H. (1990). Genetic and acclimatory variation in cuticle lipids of grasshoppers, *Melanoplus sanguinipes*. *Am. Zool.* 30, A33–A33.

Goettel, M. S., Inglis, G. D., and Wraight, S. P. (2000). "Fungi," in *Field Manual of Techniques in Invertebrate Pathology,* eds L. A. Lacey and H. K. Kaya (Netherlands: Kluwer Academic), 255–282.

Golebiowski, M., Malinski, E., Bogus, M. I., Kumirska, J., and Stepnowski, P. (2008). The cuticular fatty acids of *Calliphora vicina*, *Dendrolimus pini* and *Galleria mellonella* larvae and their role in resistance to fungal infection. *Insect Biochem. Mol. Biol.* 38, 619–627.

Goma, G., Pareilleux, A., and Durand, G. (1973). Cinetique de degradation des hydrocarbures par *Candida lipolytica*. *Arch. Mikrobiol.* 88, 97–109.

Gu, X., Quilici, D., Juarez, P., Blomquist, G. J., and Schal, C. (1995). Biosynthesis of hydrocarbons and contact sex pheromone and their transport by lipophorin in females of the German cockroach (*Blattella germanica*). *J. Insect Physiol.* 41, 257–267.

Hackman, R. H. (1984). "Cuticle: biochemistry," in *Biology of the Integument,* eds J. Bereiter-Hahn, A. G. Mateltsy, and K. S. Richards (Berlin: Springer-Verlag), 583–610.

Harada, N. (1998). Novel properties of human placental aromatase as cytochrome P450. Purification and characterization of a unique form of aromatase. *J. Biochem.* 103, 106–113.

Holder, D. J., and Keyhani, N. O. (2005). Adhesion of the entomopathogenic fungus *Beauveria (Cordyceps) bassiana* to substrata. *Appl. Environ. Microbiol.* 71, 5260–5266.

Howard, R. W. (1993). "Cuticular hydrocarbons and chemical communication," in *Insect Lipids: Chemistry, Biochemistry and Biology,* eds D. R. Stanley-Samuelson and D. R. Nelson (Lincoln, NE: University of Nebraska Press), 179–226.

Howard, R. W., and Blomquist, G. J. (2005). Ecological, behavioral, and biochemical aspects of insect hydrocarbons. *Annu. Rev. Entomol.* 50, 371–393.

Hung, C. Y., and Boucias, D. G. (1992). Influence of *Beauveria bassiana* on the cellular defense response of the *Beet Armyworm*, *Spodoptera exigua*. *J. Invertebr. Pathol.* 60, 152–158.

Inglis, G. D., Goettel, M. S., Butt, T. M., and Strasser, H. (2001). "Use of hyphomycetous fungi for managing insect pests," in *Field Manual of Techniques in Invertebrate Pathology,* eds L. A. Lacey and H. K. Kaya (Netherlands: Kluwer Academic), 651–679.

Ito, H., Fukuda, Y., Murata, K., and Kimura, A. (1983). Transformation of intact yeast cells treated with alkali cations. *J. Bacterol.* 153, 163–168.

Jarrold, S. L., Moore, D., Potter, U., and Charnley, A. K. (2007). The contribution of surface waxes to pre-penetration growth of an entomopathogenic fungus on host cuticle. *Mycol. Res.* 111, 240–249.

Juárez, M. P., Pedrini, N., Crespo, R., (2004). "Mycoinsecticides against Chagas disease vectors: biochemistry involved in insect host hydrocarbon degradation," in *Multidisciplinarity for Parasites, Vectors and Parasitic Diseases*, ed S. Mas-Comas (Bologna: Monduzzi Editore), 137–142.

Kappeli, O., Walther, P., Mueller, M., and Fiechter, A. (1984). Structure of the cell-surface of the yeast *Candida tropicalis* and its relation to hydrocarbon transport. *Arch. Microbiol.* 138, 279–282.

Kerwin, J. L. (1984). Fatty acid regulation of the germination of *Erynia variabilis* conidia on adults and puparia of the lesser housefly, *Fannia canicularis*. *Can. J. Microbiol.* 30, 158–161.

Khachatourians, G. G. (1996). "Biochemistry and Molecular Biology of Entomopathogenic Fungi," in *The Mycota VI: Human and Animal Relationships,* eds D. H. Howard and J. D. Miller (Berlin, Heidelberg: Springer-Verlag), 331–363.

Kirkland, B. H., Cho, E. M., and Keyhani, N. O. (2004a). Differential susceptibility of *Amblyomma maculatum* and *Amblyomma americanum* (Acari: Ixodidea) to the entomopathogenic fungi *Beauveria bassiana* and *Metarhizium anisopliae*. *Biol. Control* 31, 414–421.

Kirkland, B. H., Westwood, G. S., and Keyhani, N. O. (2004b). Pathogenicity of entomopathogenic fungi *Beauveria bassiana* and *Metarhizium anisopliae* to Ixodidae tick species *Dermacentor variabilis*, *Rhipicephalus sanguineus*, and *Ixodes scapularis*. *J. Med. Entomol.* 41, 705–711.

Kirkland, B. H., Eisa, A., and Keyhani, N. O. (2005). Oxalic acid as a fungal acaracidal virulence factor. *J. Med. Entomol.* 42, 346–351.

Koidsumi, K. (1957). Antifungal action of cuticular lipids in insects. *J. Insect Physiol.* 1, 40–51.

Kurtti, T. J., and Keyhani, N. O. (2008). Intracellular infection of tick cell lines by the entomopathogenic fungus *Metarhizium anisopliae*. *Microbiology* 154, 1700–1709.

Latge, J. P., Sampedro, L., Brey, P., and Diaquin, M. (1987). Aggressiveness of *Conidiobolus obscurus* against the pea aphid - influence of cuticular extracts on ballistospore germination of aggressive and nonaggressive Strains. *J. Gen. Microbiol.* 133, 1987–1997.

Lau, S. M., Harder, P. A., and O'Keefe, D. P. (1993). Low carbon monoxide affinity allene oxide synthase is the predominant cytochrome P450 in many plant tissues. *Biochemistry* 32, 1945–1950.

Lecuona, R., Clement, J. L., Riba, G., Joulie, C., and Juarez, P. (1997). Spore germination and hyphal growth of *Beauveria* sp on insect lipids. *J. Econ. Entomol.* 90, 119–123.

Lecuona, R., Riba, G., Cassier, P., and Clement, J. L. (1991). Alterations of insect epicuticular hydrocarbons during infection with *Beauveria bassiana* or *B.* brongniartii. *J. Invertebr. Pathol.* 58, 10–18.

Lewis, M. W., Robalino, I. V., and Keyhani, N. O. (2009). Uptake of the fluorescent probe FM4-64 by hyphae and haemolymph-derived *in vivo* hyphal bodies of the entomopathogenic fungus

Beauveria bassiana. *Microbiology* 155, 3110–3120.

Lindley, N. D. (1995). Bioconversion and biodegradation of aliphatic-hydrocarbons. *Can. J. Bot.* 73, S1034–S1042.

Lindley, N. D., and Heydeman, M. T. (1986). The uptake of normal-alkanes from alkane mixtures during growth of the hydrocarbon-utilizing fungus *Cladosporium resinae*. *Appl. Microbiol. Biotechnol.* 23, 384–388.

Liu, D., Coloe, S., Baird, R., and Pedersen, J. (2000). Rapid mini-preparation of fungal DNA for PCR. *J. Clin. Microbiol.* 38, 471–471.

Lockey, K. H. (1988). Lipids of the insect cuticle - origin, composition and function. *Comp. Biochem. Physiol. B Biochem. Mol. Biol.* 89, 595–645.

Lockey, K. H., and Oraha, V. S. (1990). Cuticular lipids of adult *Locusta migratoria* migratoriodes (R and F), *Schistocerca gregaria* (Forskal) (Acrididae) and Other Orthopteran Species.2. Hydrocarbons. *Comp. Biochem. Physiol. B Biochem. Mol. Biol.* 95, 721–744.

Lord, J. C., and Howard, R. W. (2004). A proposed role for the cuticular fatty amides of *Liposcelis bostrychophila* (Psocoptera: Liposcelidae) in preventing adhesion of entomopathogenic fungi with dry-conidia. *Mycopathologia* 158, 211–217.

Marchler-Bauer, A., Lu, S., Anderson, J. B., Chitsaz, F., Derbyshire, M. K., Deweese-Scott, C., et al. (2011). CDD: a conserved domain database for the functional annotation of proteins. *Nucleic Acids Res.* 39, D225–D229.

Meisel, M. N., Medvedeva, G. A., Kozlova, T. M., Domoshnikova, N. A., Zaikina, A. I., and Fedoseeva, G. E. (1973). "Regularities of penetration into yeast cells of higher fatty acids and hydrocarbons, their intracellular migration and concentration," in *Proceedings of the 3rd International Specilized Symposium on Yeast,* eds H. Suomalainen and C. Waller (Helsinki: Otaniemi), 149–168.

Metzenberg, R. L., Jacobson, D. J., and Bertrand, H. (2000). Making the selective agent for the *Bar* plasmids, phosphinothricin (glufosinate) affordable for routine use. *Fungal Genet. Newsl.* 47, 79–80.

Montellano, P. R. O. D. (ed.). (2005). *Cytochrome P450: Structure, Mechanism, and Biochemistry.* New York, NY: Kluwer Academic/Plenum.

Napolitano, R., and Juarez, M. P. (1997). Entomopathogenous fungi degrade epicuticular hydrocarbons of *Triatoma infestans*. *Arch. Biochem. Biophys.* 344, 208–214.

Nelson, D. R. (1993). "Methyl-branched lipids in insects," in *Insect lipids: Chemistry, Biochemistry and Biolgy,* eds D. W. Stanley-Samuelson and D. R. Nelson (Lincoln, NE: University of Nebraska Press), 271–315.

Nelson, D. R., Koymans, L., Kamataki, T., Stegeman, J. J., Feyereisen, R., Waxman, D. J., et al. (1996). P450 superfamily: update on new sequences, gene mapping, accession numbers and nomenclature. *Pharmacogenetics* 6, 1–42.

Nelson, D. R. (1998). Metazoan cytochrome P450 evolution. *Comp. Biochem. Physiol. C Pharmacol. Toxicol. Endocrinol.* 121, 15–22.

Nelson, D. R. (1999). Cytochrome P450 and the individuality of species. *Arch. Biochem. Biophys.* 369, 1–10.

Nelson, D. R. (2009). The cytochrome P450 homepage. *Hum. Genomics* 4, 59–65.

Nelson, D. R., and Blomquist, G. J. (1995). "Insect Waxes," in *Waxes: Chemistry, Molecular Biology, and Functions,* ed R. J. Hamilton (Dundee: The Oily Press, Ltd.), 1–90.

Noble-Nesbitt, J. I. E. (1991). "Cuticular permeability and its control," in *Physiology of the Insect Epidermis,* eds K. Binnington and A. Retnakaran (Melbourne: CSIRO), 252–283.

Padilla-Guerrero, I. E., Barelli, L., Gonzalez-Hernandez, G. A., Torres-Guzman, J. C., and Bidochka, M. J. (2011). Flexible metabolism in *Metarhizium anisopliae* and *Beauveria bassiana*: role of the glyoxylate cycle during insect pathogenesis. *Microbiology* 157, 199–208.

Pedrini, N., Crespo, R., and Juarez, M. P. (2007). Biochemistry of insect epicuticle degradation by entomopathogenic fungi. *Comp. Biochem. Physiol. C Toxicol. Pharmacol.* 146, 124–137.

Pedrini, N., Juárez, M., Crespo, R., and De Alaniz, M. (2006). Clues on the role of *Beauveria bassiana* catalases in alkane degradation events. *Mycologia* 98, 528–534.

Pedrini, N., Mijailovsky, S. J., Girotti, J. R., Stariolo, R., Cardozo, R. M., Gentile, A., et al. (2009). Control of pyrethroid-resistant chagas disease vectors with entomopathogenic fungi. *PLoS Negl. Trop. Dis.* 3:e434. doi: 10.1371/journal.pntd.0000434

Pedrini, N., Zhang, S., Juárez, M., and Keyhani, N. O. (2010). Molecular characterization and expression analysis of a suite of cytochrome P450 enzymes implicated in insect hydrocarbon degradation in the entomopathogenic fungus *Beauveria bassiana*. *Microbiology* 156, 2549–2557.

Pendland, J. C., Hung, S. Y., and Boucias, D. G. (1993). Evasion of host defense by *in vivo*-produced protoplast-like cells of the insect mycopathogen *Beauveria bassiana*. *J. Bacteriol.* 175, 5962–5969.

Pompon, D., Louerat, B., Bronine, A., and Urban, P. (1996). Yeast expression of animal and plant P450s in optimized redox environments. *Cytochrome* P450(Pt B 272), 51–64.

Qiu, Y., Tittiger, C., Wicker-Thomas, C., Le Goff, G., Young, S., Wajnberg, E., et al. (2012). An insect-specific P450 oxidative decarbonylase for cuticular hydrocarbon biosynthesis. *Proc. Natl. Acad. Sci. U.S.A.* 109, 14858–14863.

Reddy, P., Singh, H., Roy, P., and Baruah, J. (1982). Predominant role of hydrocarbon solubilization in the microbial uptake of hydrocarbons. *Biotechnol. Bioeng.* 24, 1241–1269.

Renobales, M., Nelson, D. R., and Blomquist, G. J. (1991). "Cuticular Lipids," in *Physiology of the Insect Epidermis,* eds K. Binnington and A. Retnakaran (Melbourne: CSIRO Publications), 240–251.

Riley, P. A. (1997). Melanin. *In.t J. Biochem. Cell Biol.* 29, 1235–1239.

Roberts, D. W., and Humber, R. A. (1981). "Entomogenous Fungi," in *Biology of Conidial Fungi,* eds G. T. Cole and B. Kendrick (New York, NY: Academic Press), 201–236.

Rojo, F. (2010). "Enzymes for aerobic degradation of alkanes," in *Handbook of Hydrocarbon and Lipid Microbiology,* ed K. N. Timmis (Berlin Heidelberg: Springer-Verlag), 781–797.

Saito, T., and Aoki, J. (1983). Toxicity of free fatty acids on the larval surfaces of 2 Lepidopterous insects towards *Beauveria bassiana* (Bals) Vuill and *Paecilomyces fumoso-roseus* (Wize) Brown Et Smith (Deuteromycetes, Moniliales). *Appl. Entomol. Zool.* 18, 225–233.

Schal, C., Sevala, V. L., Young, H. P., and Bachmann, J. A. S. (1998). Sites of synthesis and transport pathways of insect hydrocarbons: cuticle and ovary as target tissues. *Am. Zool.* 38, 382–393.

Scheller, U., Zimmer, T., Becher, D., Schauer, F., and Schunck, W. H. (1998). Oxygenation cascade in conversion of n-alkanes to alpha, omega-dioic acids catalyzed by cytochrome p450 52A3. *J. Biol. Chem.* 273, 32528–32534.

Schenkman, J. B., and Jansson, I. (2006). "Spectral analyses of cytochromes P450," in *Methods in Molecular Biology: Cytochrome P450 Protocols,* eds I. R. Phillips and E. A. Shepard (New Jersey, NJ: Humana Press), 11–18.

Scholte, E. J., Ng'habi, K., Kihonda, J., Takken, W., Paaijmans, K., Abdulla, S., et al. (2005). An entomopathogenic fungus for control of adult African malaria mosquitoes. *Science* 308, 1641–1642.

Singer, T. L. (1998). Roles of hydrocarbons in the recognition systems of insects. *Am. Zool.* 38, 394–405.

Singh, H. (2006). "Fungal metabolism of petroleum hydrocarbons," in *Mycoremediation: Fungal Bioremediation* (Hoboken, NJ: John Wiley and Sons), 115–148.

Smith, R. J., and Grula, E. A. (1982). Toxic components on the larval surface of the Corn-Earworm (*Heliothis zea*) and their effects on germination and growth of *Beauveria bassiana*. *J. Invertebr. Pathol.* 39, 15–22.

Steinhaus, E. A. (1956). Microbial control-The emergence of an idea: a brief history of insect pathology through the nineteenth century. *Hilgardia* 26, 107–160.

St Leger, R. (1991). "Integument as a Barrier to Microbial Infections," in *Physiology of the Insect Epidermis,* eds K. Binnington and A. Retnakaran (Melbourne: CSIRO Publications), 284–306.

Sweigard, J., Chumley, F., Carroll, A., Farrall, L., and Valent, B. (1997). A series of vectors for fungal transformation. *Fungal Genet. Newsl.* 44, 52–53.

Takai, H., Iwama, R., Kobayashi, S., Horiuchi, H., Fukuda, R., and Ohta, A. (2012). Construction and characterization of a *Yarrowia lipolytica* mutant lacking genes encoding cytochromes P450 subfamily 52. *Fungal Genet. Biol.* 49, 58–64.

Van Beilen, J. B., Li, Z., Duetz, W. A., Smits, T. H. M., and Witholt, B. (2003). Diversity of alkane hydroxylase systems in the environment. *Oil Gas Sci. Technol.* 58, 427–440.

Van Heusden, M. C., Van Der Horst, D. J., Ka-Wooya, J. K., and Law, J. H. (1991). *In vivo* and *in vitro* loading of lipid by artificially lipid-depleted lipophorins: evidence for the role of lipophorin as a reusable lipid shuttle. *J. Lipid Res.* 32, 1789–1794.

Van Valen, L. (1973). A new evolutionary law. *Evol. Theory* 1, 1–30.

Wanchoo, A., Lewis, M. W., and Keyhani, N. O. (2009). Lectin mapping reveals stage-specific display of surface carbohydrates in *in vitro* and haemolymph-derived cells of the entomopathogenic fungus *Beauveria bassiana*. *Microbiology* 155, 3121–3133.

Wang, Z.-L., Zhang, L.-B., Ying, S.-H., and Feng, M.-G. (2012). Catalases play differentiated roles in the adaptation of a fungal entomopathogen to environmental stresses. *Environ. Microbiol.* 15, 409–418.

Xiao, G., Ying, S.-H., Zheng, P., Wang, Z.-L., Zhang, S., Xie, X.-Q., et al. (2012). Genomic perspectives on the evolution of fungal entomopathogenicity in *Beauveria bassiana*. *Sci. Rep.* 2, 483.

Yadav, J. S., Doddapaneni, H., and Subramanian, V. (2006). P450ome of the white rot fungus Phanerochaete chrysosporium: structure, evolution and regulation of expression of genomic P450 clusters. *Biochem. Soc. Trans.* 34, 1165–1169.

Zhang, S., Fan, Y., Xia, Y. X., and Keyhani, N. O. (2010). Sulfonylurea resistance as a new selectable marker for the entomopathogenic fungus *Beauveria bassiana*. *Appl. Microbiol. Biotechnol.* 87, 1151–1156.

Zhang, S., Widemann, E., Bernard, G., Lesot, A., Pinot, F., Pedrini, N., et al. (2012). CYP52X1, representing new cytochrome P450 subfamily, displays fatty acid hydroxylase activity and contributes to virulence and growth on insect cuticular substrates in entomopathogenicfungus *Beauveria bassiana*. *J. Biol. Chem.* 287, 13477–13486.

Conflict of Interest Statement: The authors declare that the research was conducted in the absence of any commercial or financial relationships that could be construed as a potential conflict of interest.

Received: 13 December 2012; paper pending published: 04 January 2013; accepted: 30 January 2013; published online: 15 February 2013.

*Citation: Pedrini N, Ortiz-Urquiza A, Huarte-Bonnet C, Zhang S and Keyhani NO (2013) Targeting of insect epicuticular lipids by the entomopathogenic fungus Beauveria bassiana: hydrocarbon oxidation within the context of a host-pathogen interaction. Front. Microbio. **4**:24. doi: 10.3389/fmicb.2013.00024*

This article was submitted to Frontiers in Microbiological Chemistry, a specialty of Frontiers in Microbiology.

frontiers in
MICROBIOLOGY

REVIEW ARTICLE
published: 10 October 2013
doi: 10.3389/fmicb.2013.00302

The *bamA* gene for anaerobic ring fission is widely distributed in the environment

Abigail W. Porter and Lily Y. Young*

Department of Environmental Science, School of Biological and Environmental Sciences, Rutgers University, New Brunswick, NJ, USA

Edited by:
Amy V. Callaghan, University of Oklahoma, USA

Reviewed by:
Rachel Narehood Austin, Bates College, USA
Lisa Gieg, University of Calgary, Canada

****Correspondence:***
Lily Y. Young, Department of Environmental Science, School of Biological and Environmental Sciences, Rutgers University, 59 Dudley Road, New Brunswick, NJ 08901, USA
e-mail: lyoung@aesop.rutgers.edu

Benzoyl-CoA is the signature central metabolite associated with the anaerobic metabolism of a diverse range of compounds such as humic acid, lignin, amino acids, and industrial chemicals. Aromatic chemicals with different upstream degradation pathways all funnel into the downstream benzoyl-CoA pathway. Different genes encoding enzymes of the benzoyl-CoA pathway could be used as biomarkers for the anaerobic benzoyl-CoA pathway, however, the ring opening hydrolase, encoded by the *bamA* gene, is ideal because it is detected under a range of respiratory conditions, including under denitrifying, iron-reducing, sulfate-reducing, and fermentative conditions. This work evaluated DNA samples from six diverse environments for the presence of the *bamA* gene, and had positive results for every sample. Individual *bamA* gene clones from these sites were compared to published genome sequences. The clone sequences were distributed amongst the genome sequences, although there were clone sequences from two of the analyzed sites that formed a unique clade. Clone sequences were then grouped by site and analyzed with a functional operational taxonomic unit based clustering program to compare the *bamA* gene diversity of these sites to that of several locations reported in the literature. The results showed that the sequence diversity of the sites separated into two clusters, but there was no clear trend that could be related to the site characteristics. Interestingly, two pristine freshwater sites formed a subgroup within one of the larger clusters. Thus far the *bamA* gene has only been examined within the context of contaminated environments, however, this study demonstrates that the *bamA* gene is also detected in uncontaminated sites. The widespread presence of the *bamA* gene in diverse environments suggests that the anaerobic benzoyl-CoA pathway plays an important role in the global carbon cycle that has thus far been understudied.

Keywords: anaerobic benzoyl-CoA pathway, *bamA* gene, 6-oxocylcohex-1-ene-1-carbonyl-CoA hydrolase, monoaromatic degradation, anaerobic hydrocarbon biodegradation

INTRODUCTION

Aromatic compounds are commonly found in the environment as components in petroleum, industrial contaminants, amino acids, or as humic acids and lignins. Due to the stability of the aromatic ring, these chemicals can be recalcitrant in the environment. Under aerobic conditions, molecular oxygen is incorporated into the aromatic structure by oxygenase enzymes. In the absence of oxygen, therefore, anaerobes have had to evolve different strategies in order to attack these aromatic rings and utilize the available carbon. While anaerobic monoaromatic compound degradation can be initiated in a number of different ways, the signature central metabolite for these pathways is benzoyl-CoA. Under anaerobic conditions, benzoyl-CoA degradation involves an initial systematic reduction of the benzene ring (**Figure 1**, structures II and III), followed by the hydrolysis of 6-oxocyclohex-1-ene-1-carbonyl-CoA (**Figure 1**, structure IV) to 3-hydroxypimelyl-CoA (**Figure 1**, structure V) by 6-oxocyclohex-1-ene-1-carbonyl-CoA hydrolase. This latter enzyme is encoded by the *bamA* gene and its homologs *oah* and *bzdY*, which were previously described in *Thauera aromatica* (Laempe et al., 1999) and *Azoarcus* strain CIB (López Barragán et al., 2004), respectively. These enzymes have the same function, but differ in their genetic nomenclature.

In contrast to the benzoyl-CoA reductase, which differs in obligate and facultative anaerobes (Boll and Fuchs, 1995; Peters et al., 2004; Hosoda et al., 2005; Song and Ward, 2005; Wischgoll et al., 2005), the *bamA* gene has been reported to be present in isolates growing under a range of redox conditions (Butler et al., 2007; McInerney et al., 2007; Kuntze et al., 2008; for review, see Carmona et al., 2009). Since regions of the *bamA* gene are highly conserved in a variety of different organisms that are known to utilize the benzoyl-CoA pathway, it is an ideal candidate for use as a molecular biomarker for anaerobic aromatic hydrocarbon biodegradation (Kuntze et al., 2008). In addition, focusing on the *bamA* gene has the further benefit of indicating that the aromatic ring has been anaerobically cleaved, whereas the upstream reactions do not confer ring fission information.

Reports in the literature have suggested the potential usefulness of using a genetic biomarker based on the benzoyl-CoA pathway for benzene, toluene, and xylene (BTX) or other aromatic contaminants (Hosoda et al., 2005; Song and Ward, 2005; Kuntze et al.,

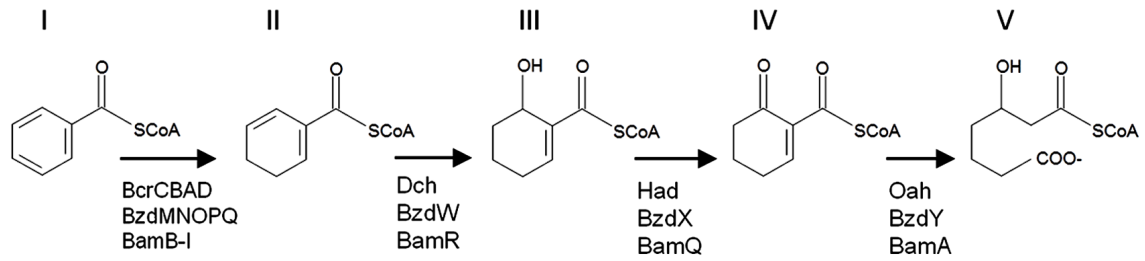

FIGURE 1 | A comparison of the benzoyl-CoA downstream metabolic pathways. Benzoyl-CoA (I) is dearomatized to cyclohexa-1,5-diene-1-carbonyl-CoA (II). For *Thauera*, *Azoarcus*, and *Geobacter* the metabolites include 6-hydroxycyclohex-1-ene-1-carbonyl-CoA (III), 6-oxocyclohex-1-ene-1-carbonyl-CoA (IV), and result in 3-hydroxypimelyl-CoA (V). The corresponding enzymes are indicated below the arrows in the pathway. The pathway is modified from Carmona et al. (2009).

2011; Staats et al., 2011; Li et al., 2012; Sun et al., 2013) yet this pathway is not exclusive to contaminants. There are other aromatic compounds that are found in or released into the environment, including vanillin, *p*-cresol, phenol, aniline, and phenylalanine that are also metabolized via benzoyl-CoA (Harwood et al., 1998).

The *bamA* gene has thus far been examined only in the context of BTX contamination. It has been used as a molecular biomarker in the laboratory to examine the functional microbial diversity in *p*-xylene degrading marine enrichments (Higashioka et al., 2011), in benzoate- and toluene-degrading denitrifying freshwater enrichments (Li et al., 2012), and in sulfate-reducing, denitrifying, and methanogenic toluene-degrading microcosms (Sun et al., 2013). While the *bamA* gene has been identified in some aromatic compound-degrading isolates, there are a very limited number of studies in which the *bamA* gene has been used as an environmental biomarker. These include environmental surveys of benzene-contaminated aquifer samples (Kuntze et al., 2011), benzene-contaminated landfill leachate (Staats et al., 2011), and crude oil-contaminated mangrove sediment (Andrade et al., 2012).

The *bamA* gene has not yet been widely detected in the environment because it has only been evaluated under very limited conditions. We hypothesize that since the *bamA* gene is specific for a common anaerobic pathway that is would also be key to the downstream metabolism of other types of aromatic compounds, including naturally occurring substrates, and thus be present in uncontaminated sites. This study used culture-independent techniques to examine the *bamA* gene diversity in DNA extracts from a range of environments and habitats, both with and without aromatic hydrocarbon contaminants, to examine the range of environments in which this gene could be detected as a proxy for the presence of the anaerobic benzoyl-CoA pathway.

MATERIALS AND METHODS

DNA EXTRACTIONS

DNA was extracted from a variety of environments and sample types as described in **Table 1**. Specifically, DNA was extracted from 0.5 g sediment samples from sites in New Jersey, USA, and from 1 g of estuarine and marine sediments from Massachusetts, USA, using a PowerSoil DNA Extraction Kit (Mo Bio Laboratories, Carlsbad, CA) as per the manufacturer's instructions. Approximately 300 ml groundwater samples from Six Mile Run and Crosswicks Creek were filtered through a 0.45 μm filter, which was cut into six pieces and extracted using an UltraClean Soil DNA Extraction Kit (Mo Bio Laboratories) with modifications to the manufacturer's instructions as previously described (Barringer et al., 2010).

A conserved 300 base pair region of the *bamA* gene was targeted with PCR primers BamA SP9F (5′ CAG TAC AAY TCC TAC ACV ACB G 3′) and BamA ASP1R (5′ CMA TGC CGA TYT CCT GRC 3′) as previously described by Kuntze et al. (2008). Each 20 μl reaction included 10 mg bovine serum albumin (New England Biolabs, Ipswich, MA, USA), 40 pmol forward and reverse primers, 0.5 mM $MgCl_2$, 0.2 mM dNTPs, and 1 U REDTaq DNA polymerase. The reaction conditions were 5 min at 94°C, followed by 35 cycles of denaturation at 94°C for 30 s, annealing at 59°C for 45 s, and elongation at 72°C for 60 s, and concluded at 72°C for 10 min. All reaction components were from Sigma-Aldrich (St. Louis, MO, USA) unless otherwise indicated.

An arsenic-reducing isolate, Strain MPA-C3, was used as a negative control in the PCR assay. This strain was isolated in our laboratory and had demonstrated anaerobic benzoate-degrading activity, although genome analysis has shown that it does not contain a *bamA* homolog (Mumford et al., 2013). Strain MPA-C3 was grown in anaerobic freshwater minimal medium (Mumford et al., 2012) with 2 mM NaH_2AsO_4 as the terminal electron acceptor and 2 mM sodium acetate as the electron donor. DNA was extracted from 1 ml of log phase culture using the Mo Bio UltraClean DNA extraction kit, according to the manufacturer's instruction (Mumford et al., 2013).

The *bamA* gene diversity was further explored in DNA samples from Six Mile Run, Crosswicks Creek, anaerobic digester sludge, and a peat bog by cloning the gene into pGEM-T Easy (Promega, Madison, WI, USA). The Eel Pond and Wild Harbor

Table 1 | Sites that have tested positive for the *bamA* gene grouped by the states in which the sites are located.

Location	Sample type	Site description	Available electron acceptors	Reference
New Jersey				
Crosswicks Creek	Groundwater	Agricultural impact	Fe^{3+}	Barringer et al. (2010)
Joint Meetings of Essex and Union Counties Wastewater Treatment Facility	Digester sludge	Anaerobic digester	CO_2	Crawford et al. (1995)
Mashipacong Bogs Preserve	Sediment	Pristine peat bog	CO_2	This study
Six Mile Run	Groundwater	No contamination	Fe^{3+}	This study
Massachusetts				
Eel Pond	Sediment	Estuarine harbor with frequent boat activity	SO_4^{2-}	This study
Wild Harbor	Sediment	Historic petroleum contamination	SO_4^{2-}	Teal et al. (1978); Culbertson et al. (2007)

The type of sample used in the DNA extraction is indicated, as is the site description which includes potential chemical inputs.

bamA gene PCR products were cloned into an Invitrogen TOPO TA cloning vector (Life Technologies, Grand Island, NY, USA). We randomly selected 38 Eel Pond, 42 Wild Harbor, 8 Crosswicks Creek, 6 Six Mile Run, 6 anaerobic digester, and 13 peat bog clones for nucleotide sequencing (Genewiz, Plainfield, NJ, USA).

PREDICTED AMINO ACID SEQUENCE ANALYSIS

Predicted amino acid sequences were aligned with ClustalX (Larkin et al., 2007) with BamA hydrolase amino acid sequences from genome sequences and biochemically characterized isolates that have demonstrated anaerobic aromatic hydrocarbon degradation activity. Using ClustalX, we generated a bootstrapped neighbor-joined tree, using 1000 iterations, with methyl-6-ketocyclohex-1-ene-1-carbonyl-CoA hydrolase (accession number CCH23022.1) as the outgroup.

Functional operational taxonomic unit (OTU) analyses with the Mothur software package (Schloss et al., 2009) were used to compare site-dependent diversity. The analysis included the clones described above with sequences that had been deposited in GenBank from environmental analyses of 192 clones from Banisveld Landfill (Staats et al., 2011), 6 clones from Hansemann Aquifer (Kuntze et al., 2011), and 9 clones from Gneisenau Aquifer (Kuntze et al., 2011).

NUCLEOTIDE SEQUENCES

Nucleotide sequences were deposited in GenBank under accession numbers KF170933–KF171005.

RESULTS

All the DNA extracts from the diverse environmental habitats listed in **Table 1** tested positive for the *bamA* gene. These sites included Crosswicks Creek and Six Mile Run, both of which are uncontaminated, iron rich environments, as well as methanogenic sites including sediment from a pristine bog and sludge from an anaerobic digester. Additionally, two petroleum-contaminated sites Wild Harbor and Eel Pond, which are marine and estuarine, respectively, also contained the *bamA* gene. We cloned and sequenced random clones from these environments.

To compare these new *bamA* gene sequences with those previously reported in the literature, we constructed a neighbor-joined tree of predicted amino acid sequences from characterized anaerobic aromatic hydrocarbon-degrading isolates and genome sequences, in addition to our environmental clones, as shown in **Figure 2**. There were three major clades. Clade-1 grouped the BamA amino acid sequences from *Rhodomicrobium vannielii* with the previously established grouping of *Geobacter/Magnetospirillum/Thauera* (Staats et al., 2011). More specifically, this clade also included the Oah amino acid sequence from *T. aromatica* (accession number CAA12245), which clustered closely with sequences from two other *Thauera* isolates. The *T. aromatica* Oah amino acid sequence shared 82% identity with the *Geobacter bemidjiensis* Bem BamA amino acid sequence (accession number YP_002138257) over the 100 residue region analyzed in this study. As with the sequences from *Thauera* isolates, the BamA amino acid sequences from *Geobacter* genomes clustered together to form a separate grouping within Clade-1, although this grouping also included sequences from our Crosswicks Creek and Six Mile Run groundwater samples (**Figure 2**, Clade-1).

Interestingly, we found that Clade-2 (**Figure 2**) was almost exclusively composed of clones from marine environments Eel Pond and Wild Harbor, with a single clone sequence from the peat bog DNA extract. The sequences in Clade-2 did not cluster with any known characterized isolates or genome sequences, although this may be due to the limited number of BamA hydrolase sequences available. Wild Harbor clone sequences were found exclusively in Clades 2 and 3, whereas the clones from Eel Pond were distributed throughout the dendrogram.

The third clade contained the *Syntrophus* and *Azoarcus* groups (Clade-3A and Clade-3B, respectively). The *Azoarcus* group included the *Azoarcus* strain CIB BzdY (accession number AAQ08817) amino acid sequence, which also clustered closely with the BamA amino acid sequence from other *Azoarcus* isolates

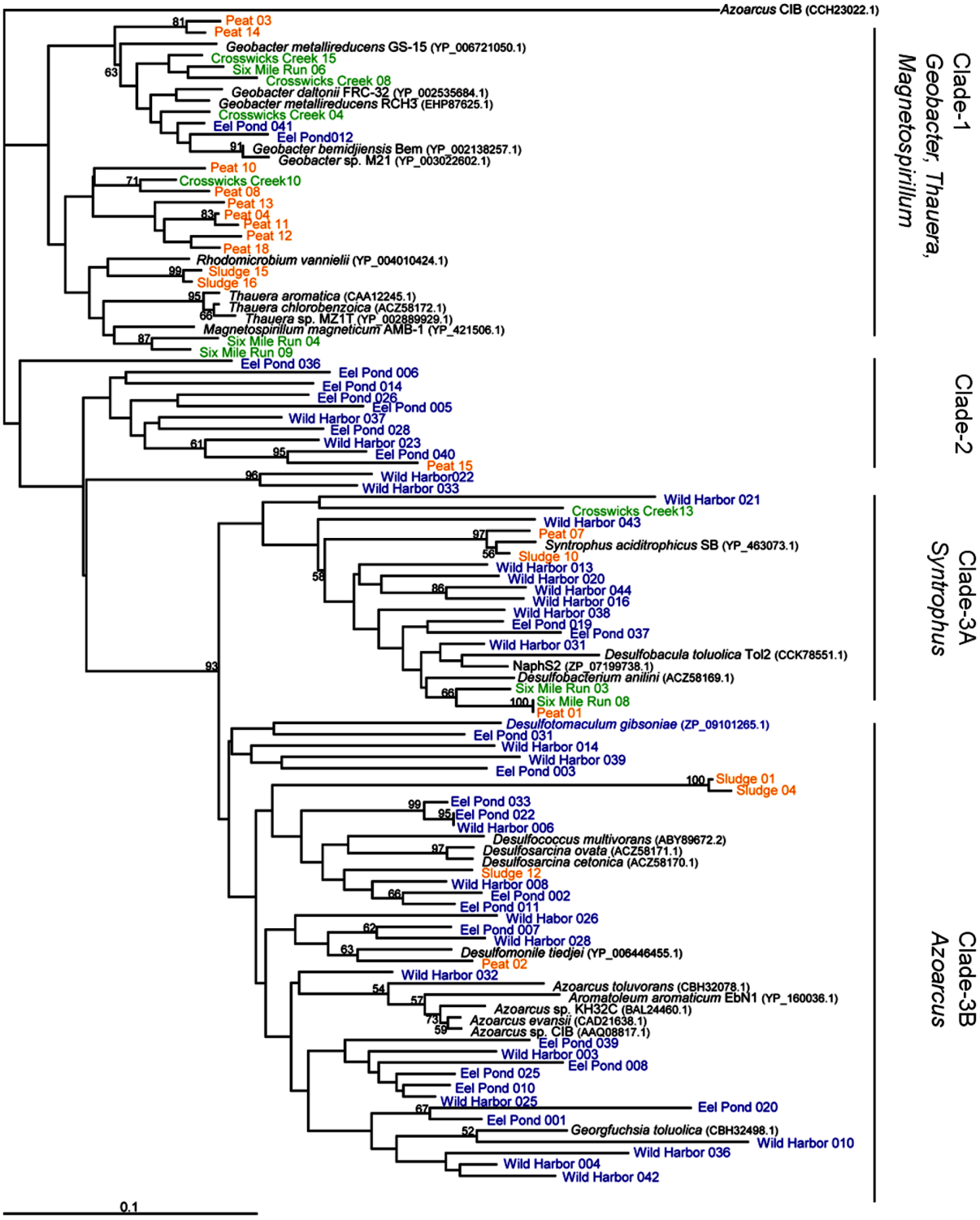

FIGURE 2 | BamA amino acid sequence from characterized isolates, genome sequences, and environmental clones. This is a neighbor-joining tree based on a 97 amino acid sequence alignment and rooted to *Azoarcus* sp. CIB methyl-6-ketocyclohex-1-ene-1-carbonyl-CoA hydrolase. Bootstrap values are given for 1000 replicate trees, and the values greater than 50% are indicated. Clones in blue indicate marine sediment DNA extracts (Eel Pond and Wild Harbor), green indicates groundwater samples (Crosswicks Creek and Six Mile Run), and orange represents methanogenic sites (anaerobic digester and peat bog). Clade-1 contains genome sequences from *Geobacter*, *Magnetospirillum*, and *Thauera* sp. Clade-2 is unique to this study and only contains sequences from Eel Pond and Wild Harbor. Clade-3 has representatives from the *Syntrophus* (Clade-3A) and *Azoarcus* (Clade-3B) isolates, along with a several sulfate-reducing microorganisms.

(**Figure 2**). The *G. bemidjiensis* Bem BamA sequence from above and the *Azoarcus* strain CIB BzdY amino acid sequence shared 70% identity for the 100 residue region analyzed in this study, which further illustrates the differences between clades. Clade-3 also included a number sequences from sulfate-reducing organisms, such as *Desulfobacterium anilini*, *Desulfobacula toluolica* tol2, and NaphS2, that were distributed in both Clade-3A and Clade-3B. Wild Harbor and Eel Pond clones were present in both Clade-3A and Clade-3B as well, as were clones from the anaerobic digester and peat bog DNA samples. The BamA hydrolase sequences from Crosswicks Creek and Six Mile Run groundwater samples were found only in Clade-3A.

We then used a different approach to examine the total *bamA* gene diversity within each site. In addition to our clone sequences, we also included sequence data from published environmental studies of Hansemann Aquifer and Gneisenau Aquifer, two benzene-contaminated freshwater locations, and Banisveld Landfill leachate, which was also a freshwater site contaminated with BTX chemicals (Kuntze et al., 2011; Staats et al., 2011). The diversity within each site was compared utilizing a functional OTU-based cluster analysis of the predicted amino acid sequences described above using Mothur software (Schloss et al., 2009). All of the sequences used here were from environmental DNA extracts and were not from laboratory cultures. **Figure 3** illustrates the differences in diversity across the different sites and shows that the sites were divided into two groups. This data set cannot be compared with the data set used in **Figure 2** in which individual sequences are compared to each other, as **Figure 3** shows the relationship between sites based on the diversity of the total sequences from each site.

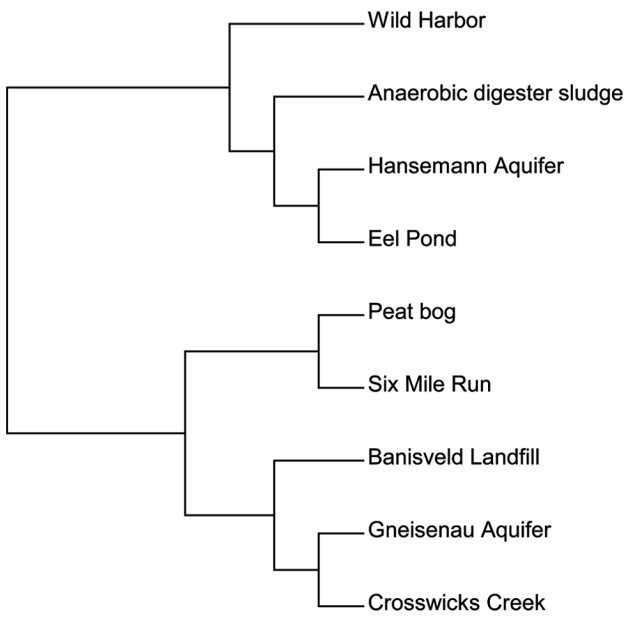

FIGURE 3 | A functional OTU-based cluster analysis of environmental samples based on location. Amino acid sequences from all published culture-independent surveys were compared over an 81 amino acid region of the BamA hydrolase. Sites were compared using mothur software (Schloss et al., 2009) with a 95% cutoff.

The first group in **Figure 3** contained one cluster of BamA hydrolase sequences from sites that included Wild Harbor, anaerobic digester sludge, Hansemann Aquifer, and Eel Pond. Both Wild Harbor and Eel Pond were sites that have had long-term petroleum contamination, while the Hansemann Aquifer had benzene contamination (Kuntze et al., 2011). The anaerobic digester sludge likely contained other types of aromatic compounds and was not limited to petroleum hydrocarbon contamination. The second group was further divided into two different clusters. The first cluster grouped the total sequences from the peat bog and Six Mile Run groundwater clones together, both of which are clean sites and neither of which have petroleum contamination. Interestingly, these two sites are distinct from the second clustering of sequences from Banisveld Landfill leachate, the Gneisenau Aquifer, and Crosswicks Creek, although Gneisenau Aquifer and Crosswicks Creek shared more total sequence similarity to each other than to Banisveld Landfill sequences. While the Banisveld Landfill and Gneisenau Aquifer were reported to have benzene contamination (Kuntze et al., 2011; Staats et al., 2011), Crosswicks Creek was influenced by agricultural activity (Barringer et al., 2010). Based on our analysis of a limited number of clones from environmental samples, there is evidence of *bamA* gene diversity in the environment. Although there does not appear to be a clear pattern with respect to the total sequence diversity at the site level that can be attributed to the type of possible organic substrates at the site, it is interesting that the sequences from the peat bog and Six Mile Run, both uncontaminated freshwater sites, clustered separately.

DISCUSSION

Our analysis of the individual BamA hydrolase amino acid sequence diversity is based upon environmental clones from our laboratory and from the limited number of characterized anaerobic aromatic hydrocarbon-degrading isolates. We did not include other environmental clones or enrichment culture sequences from other studies in **Figure 2**, as there was no clear association between the BamA amino acid sequence and metabolic activity from these complex samples. The results suggest that to some degree there is an association between some individual BamA hydrolase amino acid sequences and the sample site characteristics. For example, Crosswicks Creek clones are found mainly in Clade-1, which is in agreement with published work that detected measurable iron at the site and identified 16S rRNA gene clones with high similarity to *Geobacter* sp. Ply1 (Mumford et al., 2012). The peat bog and anaerobic digester clone sequences originated from methanogenic environments and are predominately found in Clade-1 (**Figure 2**). There are sequences, nonetheless, from these clones that are also found in Clade-3 and cluster near *Syntrophus aciditrophicus*, a fermenting benzoate-degrading organism (McInerney et al., 2007). *Syntrophus*-like organisms have been previously identified in anaerobic digester sludge (Shin et al., 2010).

The majority of the Eel Pond and Wild Harbor sequences are in Clade-2 and Clade-3 (see **Figure 2**). In addition, Clade-3A and Clade-3B both contain BamA hydrolase sequences from genome sequences of sulfate-reducing microorganisms. The clustering of

sequences from Eel Pond and Wild Harbor is not unexpected given that they are both coastal marine sites with abundant sulfate that would be found in seawater, and thus support sulfate reducers. The wider distribution of the Eel Pond sequences (Clade-1,-2, and -3), however, differ from the somewhat more narrow distribution of Wild Harbor sequences. Sun et al. (2013) suggested a correlation between the *bamA* gene sequence and the terminal electron acceptor that was supplied in their microcosm study. That does appear to be the case for the BamA hydrolase sequences from isolates, since the sequences from a particular genus clustered together as previously reported (Kuntze et al., 2008, 2011; Staats et al., 2011). Given the small number of BamA hydrolase sequences available from isolated organisms with available genomes, however, it is difficult to say with confidence that the clone sequences are derived from a specific group within our samples.

In addition to examining the individual clone sequences, we completed a different analysis in which the sequences were grouped by site and the differences in total BamA hydrolase amino acid sequence diversity were examined to see if there was a trend between the study sites and the BamA hydrolase diversity. We included published environmental sequences, although we chose to focus only on the sites with publicly available sequences that did not originate from laboratory cultures (Kuntze et al., 2011; Staats et al., 2011). While there have been studies that examined *bamA* gene diversity in enrichments or microcosms, the culturing process would have favored specific organisms that were able to utilize the exogenous substrate and thus would not provide an accurate picture of the *bamA* gene sequences that were present at the site from which the inocula came (Higashioka et al., 2011; Li et al., 2012; Sun et al., 2013). Our intent was to study BamA hydrolase diversity in the natural habitat without culturing or enrichment. The results of site-based diversity comparisons suggest that there were not differences in diversity with respect to type of sites and potentially available organic substrates. For example, both Eel Pond and Wild Harbor are marine sites with historical petroleum contamination. While the total sequences from these two associated together in the same large clustering, the Eel Pond sequence diversity was more similar to that of the benzene-contaminated freshwater Gneisenau Aquifer than to Wild Harbor sequences. Similarly, benzene-contaminated freshwater sites (Banisveld Landfill, Gneisenau Aquifer, and Hansemann Aquifer) were present in both clusters. In contrast, it is interesting that the total sequences from the peat bog and Six Mile Run, both uncontaminated freshwater sites, appear to cluster separately from the other sites. It should be noted, however, that the data presented here are from a limited number of clones in addition to only three sites in the literature from which data were available. The number of available sequences was less than 50 for all of our sites, the Gneisenau Aquifer, and the Hansemann Aquifer (Kuntze et al., 2011), although there were nearly 200 sequences from the Banisveld Landfill (Staats et al., 2011). Expanding the number of sample sites and increasing the sequence coverage with next generation sequencing techniques could potentially yield a more complete assessment of *bamA* gene diversity in the environment by capturing the less abundant sequences that might be overlooked in cloning experiments.

A large number of naturally occurring aromatic compounds, including amino acids, humic acid, plant phenolics, and lignin metabolites, are metabolized through the anaerobic benzoyl-CoA pathway, therefore the benzoyl-CoA pathway must play an important role in global anaerobic aromatic hydrocarbon metabolism. We detected the *bamA* gene in petroleum-contaminated marine sediments, uncontaminated groundwater, anaerobic digester sludge, and peat bog sediment, suggesting that the benzoyl-CoA pathway is common in the environment. Our findings are in agreement with a previous study (Sun et al., 2013) that detected the *bamA* gene in toluene amended microcosms from diverse inocula, including contaminated sediment and soil, anaerobic digester sludge, aerobic digester sludge, and uncontaminated soil. More specifically, the data reported here demonstrates that the BamA hydrolase is a common feature for the downstream metabolism of the key benzoyl-CoA pathway in anaerobic environments. This, however, does not necessarily relate to contaminant presence, but rather could be the contribution of natural aromatic inputs such as lignin and humic acid. For example, lignin metabolites identified in methanogenic enrichment cultures include cinnamic, vanillic, syringic, and ferulic acids (Colberg and Young, 1985), which would also be metabolized through the benzoyl-CoA pathway. Since the *bamA* gene has not yet been studied in the context of natural aromatic substrates, future work should utilize a quantitative approach, such as qPCR, to elucidate the naturally occurring abundance of the *bamA* gene in the environment.

The *bamA* gene is a biomarker for the anaerobic benzoyl-CoA pathway, and more broadly anaerobic aromatic hydrocarbon degradation, that we detected in both contaminated and pristine environments. In addition, the *bamA* gene could be used as a tool for examining sites that contain chemicals with either unknown or multiple mechanisms by which the substrate is anaerobically transformed to benzoyl-CoA. There is great diversity in the mechanisms used in the initial steps of anaerobic aromatic compound degradation that occur prior to benzoyl-CoA formation. For example, L-phenylalanine degradation requires an amino transferase to form phenylpyruvate, which further undergoes a series of steps including decarboxylation, and results in the ultimate formation of benzoyl-CoA (Schneider et al., 1997). In contrast, it has been widely reported that toluene degradation occurs through a fumarate addition mechanism, which results in benzylsuccinate as an intermediate prior to benzoyl-CoA formation (Evans et al., 1992; Biegert et al., 1996). On the other hand, the activation mechanism for anaerobic benzene degradation is less clear as three different mechanisms have been reported. One is methylation to form toluene, which is then metabolized via fumarate addition to benzylsuccinate (Ulrich et al., 2005). Secondly, benzene can undergo hydroxylation to form phenol, which can be further transformed to benzoate and subsequently benzoyl-CoA (Caldwell and Suflita, 2000; Chakraborty and Coates, 2005). Finally, direct carboxylation of benzene to benzoate has also been reported (Phelps et al., 2001; Kunapuli et al., 2008; Abu Laban et al., 2010). As a result, the *bamA* gene has been targeted, and consistently detected, in benzene-contaminated sites (Kuntze et al., 2011; Staats et al., 2011; Andrade et al., 2012). The *bamA* gene has demonstrated usefulness when used in conjunction with biomarkers for other genes in the benzoyl-CoA pathway (Kuntze et al., 2011) or with

molecular probes for specific degradation steps that occur prior to benzoyl-CoA formation, such as the *bssA* gene which is key in toluene degradation (Staats et al., 2011; Andrade et al., 2012; Sun et al., 2013).

The anaerobic degradation of aromatic hydrocarbons, however, is more important than just with respect to contaminants. The cycling of carbon in anoxic environments is critical to the global carbon cycle but it receives less attention than in its oxic counterpart. To better utilize the *bamA* gene as a biomarker for anaerobic aromatic compound degradation through the benzoyl-CoA pathway, however, a more comprehensive set of data are needed for anaerobic degradation of naturally occurring aromatic compounds such as plant phenolics, humics, and lignin. Whether there are *bamA* gene differences for anthropogenic or natural aromatic substrates has yet to be determined. Nonetheless, evidence thus far, indicates that the *bamA* gene in the benzoyl-CoA pathway is central to anaerobic aromatic ring fission in a variety of environments and by extension is a key component in the global carbon cycle.

ACKNOWLEDGMENTS

We wish to thank Sarah Wolfson for contributing Eel Pond and Wild Harbor *bamA* gene clone sequences, Adam Mumford for providing DNA extracts and sediment samples, Maria Rivera for anaerobic digester samples, and Katie Della Terza for peat bog samples.

REFERENCES

Abu Laban, N., Selesi, D., Rattei, T., Tischler, P., and Meckenstock, R. U. (2010). Identification of enzymes involved in anaerobic benzene degradation by a strictly anaerobic iron-reducing enrichment culture. *Environ. Microbiol.* 12, 2783–2796.

Andrade, L. L., Leite, D., Ferreira, E., Ferreira, L., Paula, G. R., Maguire, M., et al. (2012). Microbial diversity and anaerobic hydrocarbon degradation potential in an oil-contaminated mangrove sediment. *BMC Microbiol.* 12:186. doi: 10.1186/1471-2180-12-186

Barringer, J. L., Mumford, A., Young, L. Y., Reilly, P. A., Bonin, J. L., and Rosman, R. (2010). Pathways for arsenic from sediments to groundwater to streams: biogeochemical processes in the Inner Coastal Plain, New Jersey, USA. *Water Res.* 44, 5532–5544. doi: 10.1016/j.watres.2010.05.047

Biegert, T., Fuchs, G., and Heider, J. (1996). Evidence that anaerobic oxidation of toluene in the denitrifying bacterium *Thauera aromatica* is initiated by formation of benzylsuccinate from toluene and fumarate. *Eur. J. Biochem.* 238, 661–668. doi: 10.1111/j.1432-1033.1996.0661w.x

Boll, M., and Fuchs, G. (1995). Benzoyl-coenzyme A reductase (dearomatizing), a key enzyme of anaerobic aromatic metabolism. *Eur. J. Biochem.* 234, 921–933. doi: 10.1111/j.1432-1033.1995.921_a.x

Butler, J. E., He, Q., Nevin, K. P., He, Z., Zhou, J., and Lovley, D. R. (2007). Genomic and microarray analysis of aromatics degradation in *Geobacter metallireducens* and comparison to a *Geobacter* isolate from a contaminated field site. *BMC Genomics* 8:180. doi: 10.1186/1471-2164-8-180

Caldwell, M. E., and Suflita, J. M. (2000). Detection of phenol and benzoate as intermediates of anaerobic benzene biodegradation under different terminal electron-accepting conditions. *Environ. Sci. Technol.* 34, 1216–1220. doi: 10.1021/es990849j

Carmona, M., Zamarro, M. T., Blázquez, B., Durante-Rodríguez, G., Juárez, J. F., Valderrama, J. A., et al. (2009). Anaerobic catabolism of aromatic compounds: a genetic and genomic view. *Microbiol. Mol. Biol. Rev.* 73, 71–133. doi: 10.1128/MMBR.00021-08

Chakraborty, R., and Coates, J. D. (2005). Hydroxylation and carboxylation - two crucial steps of anaerobic benzene degradation by *Dechloromonas* strain RCB. *Appl. Environ. Microbiol.* 71, 5427–5432. doi: 10.1128/AEM.71.9.5427-5432.2005

Colberg, P. J., and Young, L. Y. (1985). Aromatic and volatile acid intermediates observed during anaerobic metabolism of lignin-derived oligomers. *Appl. Environ. Microbiol.* 49, 350–358.

Crawford, D. W., Bonnevie, N. L., and Wenning, R. J. (1995). Sources of pollution and sediment contamination in Newark Bay, New Jersey. *Ecotoxicol. Environ. Saf.* 30, 85–100. doi: 10.1006/eesa.1995.1010

Culbertson, J. B., Valiela, I., Peacock, E. E., Reddy, C. M., Carter, A., and VanderKruik, R. (2007). Long-term biological effects of petroleum residues on fiddler crabs in salt marshes. *Mar. Pollut. Bull.* 54, 955–962. doi: 10.1016/j.marpolbul.2007.02.015

Evans, P. J., Ling, W., Goldschmidt, B., Ritter, E. R., and Young, L. Y. (1992). Metabolites formed during anaerobic transformation of toluene and *o*-xylene and their proposed relationship to the initial steps of toluene mineralization. *Appl. Environ. Microbiol.* 58, 496–501.

Harwood, C. S., Burchhardt, G., Herrmann, H., and Fuchs, G. (1998). Anaerobic metabolism of aromatic compounds via the benzoyl-CoA pathway. *FEMS Microbiol. Rev.* 22, 439–458. doi: 10.1111/j.1574-6976.1998.tb00380.x

Higashioka, Y., Kojima, H., and Fukui, M. (2011). Temperature-dependent differences in community structure of bacteria involved in degradation of petroleum hydrocarbons under sulfate-reducing conditions. *J. Appl. Microbiol.* 110, 314–322. doi: 10.1111/j.1365-2672.2010.04886.x

Hosoda, A., Kasai, Y., Hamamura, N., Takahata, Y., and Watanabe, K. (2005). Development of a PCR method for the detection and quantification of benzoyl-CoA reductase genes and its application to monitored natural attenuation. *Biodegradation* 16, 591–601. doi: 10.1007/s10532-005-0826-5

Kunapuli, U., Griebler, C., Beller, H. R., and Meckenstock, R. U. (2008). Identification of intermediates formed during anaerobic benzene degradation by an iron-reducing enrichment culture. *Environ. Microbiol.* 10, 1703–1712. doi: 10.1111/j.1462-2920.2008.01588.x

Kuntze, K., Shinoda, Y., Moutakki, H., McInerney, M. J., Vogt, C., Richnow, H.-H., et al. (2008). 6-Oxocyclohex-1-ene-1-carbonyl-coenzyme A hydrolases from obligately anaerobic bacteria: characterization and identification of its gene as a functional marker for aromatic compounds degrading anaerobes. *Environ. Microbiol.* 10, 1547–1556. doi: 10.1111/j.1462-2920.2008.01570.x

Kuntze, K., Vogt, C., Richnow, H.-H., and Boll, M. (2011). Combined application of PCR-based functional assays for the detection of aromatic compound-degrading anaerobes. *Appl. Environ. Microbiol.* 77, 5056–5061. doi: 10.1128/AEM.00335-11

Laempe, D., Jahn, M., and Fuchs, G. (1999). 6-Hydroxycyclohex-1-ene-1-carbonyl-CoA dehydrogenase and 6-oxocyclohex-1-ene-1-carbonyl-CoA hydrolase, enzymes of the benzoyl-CoA pathway of anaerobic aromatic metabolism in the denitrifying bacterium *Thauera aromatica*. *Eur. J. Biochem.* 263, 420–429. doi: 10.1046/j.1432-1327.1999.00504.x

Larkin, M. A., Blackshields, G., Brown, N. P., Chenna, R., McGettigan, P. A., McWilliam, H., et al. (2007). Clustal W and Clustal X version 2.0. *Bioinformatics* 23, 2947–2948. doi: 10.1093/bioinformatics/btm404

Li, Y.-N., Porter, A. W., Mumford, A., Zhao, X.-H., and Young, L. Y. (2012). Bacterial community structure and *bamA* gene diversity in anaerobic degradation of toluene and benzoate under denitrifying conditions. *J. Appl. Microbiol.* 112, 269–279. doi: 10.1111/j.1365-2672.2011.05213.x

López Barragán, M. J., Carmona, M., Zamarro, M. T., Thiele, B., Boll, M., Fuchs, G., et al. (2004). The *bzd* gene cluster, coding for anaerobic benzoate catabolism, in *Azoarcus* sp. strain CIB. *J. Bacteriol.* 186, 5762–5774. doi: 10.1128/JB.186.17.5762-5774.2004

McInerney, M. J., Rohlin, L., Mouttaki, H., Kim, U., Krupp, R. S., Rios-Hernandez, L., et al. (2007). The genome of *Syntrophus aciditrophicus*: life at the thermodynamic limit of microbial growth. *Proc. Natl. Acad. Sci. U.S.A.* 104, 7600–7605. doi: 10.1073/pnas.0610456104

Mumford, A. C., Barringer, J. L., Benzel, W. M., Reilly, P. A., and Young, L. Y. (2012). Microbial transformations of arsenic: mobilization from glauconitic sediments to water. *Water Res.* 46, 2859–2868. doi: 10.1016/j.watres.2012.02.044

Mumford, A. C., Yee, N., and Young, L. Y. (2013). Precipitation of alacranite (As8S9) by a novel As(V)-respiring anaerobe strain MPA-C3. *Environ. Microbiol.* doi: 10.1111/1462-2920.12136 [Epub ahead of print].

Peters, F., Rother, M., and Boll, M. (2004). Selenocysteine-containing proteins in anaerobic benzoate metabolism of

Desulfococcus multivorans. *J. Bacteriol.* 186, 2156–2163. doi: 10.1128/JB.186.7.2156-2163.2004

Phelps, C. D., Zhang, X., and Young, L. Y. (2001). Use of stable isotopes to identify benzoate as a metabolite of benzene degradation in a sulphidogenic consortium. *Environ. Microbiol.* 3, 600–604. doi: 10.1046/j.1462-2920.2001.00228.x

Schloss, P., Westcott, S., Ryabin, T., Hall, J., Hartmann, M., Hollister, E., et al. (2009). Introducing mothur: open-source, platform-independent, community-supported software for describing and comparing microbial communities. *Appl. Environ. Microbiol.* 75, 7537–7534. doi: 10.1128/AEM.01541-09

Schneider, S., Mohamed, M. E., and Fuchs, G. (1997). Anaerobic metabolism of L-phenylalanine via benzoyl-CoA in the denitrifying bacterium *Thauera aromatica*. *Arch. Microbiol.* 168, 310–320. doi: 10.1007/s002030050504

Shin, S. G., Lee, S., Lee, C., Hwang, K., and Hwang, S. (2010). Qualitative and quantitative assessment of microbial community in batch anaerobic digestion of secondary sludge. *Bioresour. Technol.* 101, 9461–9470. doi: 10.1016/j.biortech.2010.07.081

Song, B., and Ward, B. B. (2005). Genetic diversity of benzoyl coenzyme A reductase genes detected in denitrifying isolates and estuarine sediment communities. *Appl. Environ. Microbiol.* 71, 2036–2045. doi: 10.1128/AEM.71.4.2036-2045.2005

Staats, M., Braster, M., and Röling, W. F. M. (2011). Molecular diversity and distribution of aromatic hydrocarbon-degrading anaerobes across a landfill leachate plume. *Environ. Microbiol.* 13, 1216–1227. doi: 10.1111/j.1462-2920.2010.02421.x

Sun, W., Sun, X., and Cupples, A. M. (2013). Presence, diversity and enumeration of functional genes (*bssA* and *bamA*) relating to toluene degradation across a range of redox conditions and inoculum sources. *Biodegradation* doi: 10.1007/s10532-013-9651–9654

Teal, J. M., Burns, K., and Farrington, J. (1978). Analyses of aromatic hydrocarbons in intertidal sediments resulting from two spills of No. 2 fuel oil in Buzzards Bay, Massachusetts. *J. Fish. Res. Board Can.* 35, 510–520. doi: 10.1139/f78-095

Ulrich, A. C., Beller, H. R., and Edwards, E. A. (2005). Metabolites detected during biodegradation of 13C6-benzene in nitrate-reducing and methanogenic enrichment cultures. *Environ. Sci. Technol.* 39, 6681–6691. doi: 10.1021/es050294u

Wischgoll, S., Heintz, D., Peters, F., Erxleben, A., Sarnighausen, E., Reski, R., et al. (2005). Gene clusters involved in anaerobic benzoate degradation of *Geobacter metallireducens*. *Mol. Microbiol.* 58, 1238–1252. doi: 10.1111/j.1365-2958.2005.04909.x

Conflict of Interest Statement: The authors declare that the research was conducted in the absence of any commercial or financial relationships that could be construed as a potential conflict of interest.

Received: 31 December 2012; accepted: 19 September 2013; published online: 10 October 2013.

*Citation: Porter AW and Young LY (2013) The bamA gene for anaerobic ring fission is widely distributed in the environment. Front. Microbiol. **4**:302. doi: 10.3389/fmicb.2013.00302*

This article was submitted to Microbiological Chemistry, a section of the journal Frontiers in Microbiology.

frontiers in
MICROBIOLOGY

ORIGINAL RESEARCH ARTICLE
published: 15 March 2013
doi: 10.3389/fmicb.2013.00050

Metagenomic analysis and metabolite profiling of deep-sea sediments from the Gulf of Mexico following the Deepwater Horizon oil spill

Nikole E. Kimes[1†], Amy V. Callaghan[2], Deniz F. Aktas[2,3], Whitney L. Smith[2,3], Jan Sunner[2,3], Bernard T. Golding[4], Marta Drozdowska[4], Terry C. Hazen[5,6,7,8], Joseph M. Suflita[2,3] and Pamela J. Morris[1]*

[1] Baruch Marine Field Laboratory, Belle W. Baruch Institute for Marine and Coastal Sciences, University of South Carolina, Georgetown, SC, USA
[2] Department of Microbiology and Plant Biology, University of Oklahoma, Norman, OK, USA
[3] Institute for Energy and the Environment, University of Oklahoma, Norman, OK, USA
[4] School of Chemistry, Newcastle University, Newcastle upon Tyne, UK
[5] Department of Civil and Environmental Engineering, University of Tennessee, Knoxville, TN, USA
[6] Department of Microbiology, University of Tennessee, Knoxville, TN, USA
[7] Department of Earth and Planetary Sciences, University of Tennessee, Knoxville, TN, USA
[8] Ecology Department, Lawrence Berkeley National Laboratory, Berkeley, CA, USA

Edited by:
Rachel Narehood Austin, Bates College, USA

Reviewed by:
John Senko, The University of Akron, USA
John W. Moreau, University of Melbourne, Australia

***Correspondence:**
Pamela J. Morris, Baruch Marine Field Laboratory, Belle W. Baruch Institute for Marine and Coastal Sciences, University of South Carolina, PO BOX 1630, Georgetown, SC 29442, USA. e-mail: pjmorris@belle.baruch.sc.edu

†Present address:
Nikole E. Kimes, Evolutionary Genomics Group, División de Microbiología, Universidad Miguel Hernández, San Juan, Alicante, Spain.

Marine subsurface environments such as deep-sea sediments, house abundant and diverse microbial communities that are believed to influence large-scale geochemical processes. These processes include the biotransformation and mineralization of numerous petroleum constituents. Thus, microbial communities in the Gulf of Mexico are thought to be responsible for the intrinsic bioremediation of crude oil released by the Deepwater Horizon (DWH) oil spill. While hydrocarbon contamination is known to enrich for aerobic, oil-degrading bacteria in deep-seawater habitats, relatively little is known about the response of communities in deep-sea sediments, where low oxygen levels may hinder such a response. Here, we examined the hypothesis that increased hydrocarbon exposure results in an altered sediment microbial community structure that reflects the prospects for oil biodegradation under the prevailing conditions. We explore this hypothesis using metagenomic analysis and metabolite profiling of deep-sea sediment samples following the DWH oil spill. The presence of aerobic microbial communities and associated functional genes was consistent among all samples, whereas, a greater number of Deltaproteobacteria and anaerobic functional genes were found in sediments closest to the DWH blowout site. Metabolite profiling also revealed a greater number of putative metabolites in sediments surrounding the blowout zone relative to a background site located 127 km away. The mass spectral analysis of the putative metabolites revealed that alkylsuccinates remained below detection levels, but a homologous series of benzylsuccinates (with carbon chain lengths from 5 to 10) could be detected. Our findings suggest that increased exposure to hydrocarbons enriches for Deltaproteobacteria, which are known to be capable of anaerobic hydrocarbon metabolism. We also provide evidence for an active microbial community metabolizing aromatic hydrocarbons in deep-sea sediments of the Gulf of Mexico.

Keywords: Deepwater Horizon, metagenomics, metabolomics, oil-degradation

INTRODUCTION

The Deepwater Horizon (DWH) blowout resulted in the largest marine US oil spill to date, in which 4.1 million barrels of crude oil flowed into the depths (∼1500 m) of the Gulf of Mexico (Operational Science Advisory Team, 2010). Although an estimated 78% of the oil was depleted through either human intervention or natural means by August 2010 (Ramseur, 2010), the fate of the remaining 22% was uncertain. Evidence subsequently showed that both oil (Hazen et al., 2010; Mason et al., 2012) and gas (Kessler et al., 2011) persisted in the Gulf of Mexico water column, affecting deep-sea (>1000 m) microbial communities that potentially facilitate the biodegradation of residual hydrocarbons. Much less is known about the impact of anthropogenic hydrocarbons on the microbial communities of deep-sea sediments. Although much of the hydrocarbons from sub-sea oil spills and natural seeps may rise to the surface, there are water-soluble components in oil as well as hydrocarbons adhering to solid particulates that can settle in deep-sea sediments (Ramseur, 2010). After the 1979 Ixtoc I oil spill, for example, in which over three million barrels of oil flowed into the Gulf of Mexico, it is estimated that 25% of the oil was transported to the sea floor (Jernelov and Linden, 1981).

The deep-sea biosphere, including deep-sea sediments, is both one of the largest and one of the most understudied ecosystems on earth (Jørgensen, 2011). Although the global estimates

of prokaryotic biomass supported by deep-subsurface sediments are lower than originally thought, regional variation supports the presence of abundant and diverse sub-seafloor microbial communities in continental shelf areas, such as the Gulf of Mexico (Kallmeyer et al., 2012). This is especially true for the more surficial sediment communities, such as those utilized in this study. Evidence suggests that these deep-sea sediment communities support diverse metabolic activities (D'Hondt et al., 2004, 2009), including evidence of hydrocarbon degradation in microbial communities associated with cold water hydrocarbon seeps located in the Gulf of Mexico (Joye et al., 2004; Lloyd et al., 2006, 2010; Orcutt et al., 2010). As a result, it has been suggested that the microbial communities in the Gulf of Mexico deep-sea sediment would play a role in the biodegradation of persistent oil components following the DWH blowout. Despite numerous advances pertaining to individual microorganisms capable of metabolizing hydrocarbon compounds (Seth-Smith, 2010) and community responses to natural hydrocarbon seeps (Lloyd et al., 2010; Orcutt et al., 2010), little is known about the microbial capacity for oil-degradation within deep-sea sediment communities under the circumstances presented by the DWH spill, including the extreme depth (~1500 m) and the sudden hydrocarbon exposure.

To gain a better understanding of the sediment-associated microbial response to the DWH oil spill, deep-sea sediment cores were collected by a Lawrence Berkeley National Laboratory (LBNL) team aboard the R/V Gyre in the area surrounding the DWH oil spill between September 19 and October 10, 2010. Preliminary chemical analysis revealed that the cores closest to the DWH spill contained high levels of polycyclic aromatic hydrocarbons (PAHs; >24,000 μg/kg) compared to distant cores (~50 μg/kg), confirming a greater exposure of the resident microflora to aromatic hydrocarbons near the DWH well (Operational Science Advisory Team, 2010). Although it is likely that the DWH oil spill contributed to the higher PAH levels observed, other sources that could have influenced these levels include natural seeps located near the DWH site and drilling fluids.

In this study, we hypothesized that increased hydrocarbon exposure results in the alteration of microbial community structure, such that it reflects the selection for organisms capable of the anaerobic metabolism of petroleum constituents. We performed metagenomic sequencing on three of the deep-sea sediment samples collected by LBNL (described above) and compared our results to a Gulf of Mexico deep-subsurface sediment metagenomic library sequenced prior to the DWH oil spill (Biddle et al., 2011). To complement the metagenomic analysis, metabolic profiling was used to detect homologous series of putative signature metabolites associated with anaerobic hydrocarbon biodegradation. Our data indicated significant differences among the microbial communities examined in this study compared to those detected prior to the DWH oil spill. Moreover, the metabolite profiling revealed significantly more putative metabolites in the two samples closest to the DWH site relative to the more distant background site. These findings were consistent with the metagenomic data showing an increase in the number of functional genes associated with anaerobic hydrocarbon degradation in samples closest to the DWH.

MATERIALS AND METHODS

SAMPLE COLLECTION

Deep-sea sediment cores were collected by LBNL from the area surrounding the DWH oil spill in the Gulf of Mexico during six cruises by the R/V Gyre from September 16 to October 20, 2010 (Operational Science Advisory Team, 2010). An OSIL Mega corer (Bowers and Connelly) was used to collect deep-sea sediment cores, and overlying water was siphoned off using a portable peristaltic pump. The capped sediment cores were frozen at −80°C and shipped on dry ice to the LBNL where the cores were sectioned while frozen. The three cores utilized in this study were designated SE-20101017-GY-D040S-BC-315 (GoM315); SE-20101017-GY-D031S-BC-278 (GoM278); and SE-20100921-GY-FFMT4-BC-023 (GoM023). GoM315 and GoM278 were located near the DWH well (0.5 and 2.7 km, respectively), while GoM023 was located at a distance of 127 km from the DWH well (**Figure 1**). One-half of each core (GoM315, GoM278, and GoM023), approximately 5″ diameter and 1″ thick, was sent on dry ice to the University of South Carolina Baruch Marine Field Laboratory in Georgetown, SC, USA. Upon arrival they were further subsectioned in half using sterile razorblades in a biosafety hood. One half was used for DNA extraction and metagenomic analysis, while the other half was sent on dry ice to the University of Oklahoma (Norman, OK, USA) for metabolomic analysis.

DNA EXTRACTION

Inside a biosafety hood, a sterile razor blade was used to cut a 3–4 g wedge from each of the three frozen cores (GoM315, GoM278, and GoM023). Community DNA was extracted from each core using a PowerMax® Soil DNA Isolation kit (Mo Bio Laboratories, Inc., Carlsbad, CA, USA) according to the manufacturer's instructions. The resulting DNA (~ 2 μg) from each sample was purified and concentrated via ethanol precipitation. The quality and quantity of the DNA were assessed via gel electrophoresis on a 2% agar gel with a 1 kb ladder and spectrophotometer analysis.

METAGENOMIC SEQUENCING AND ANALYSIS

Approximately 1 μg DNA (per core sample) was sent to Engencore (University of South Carolina, Columbia, SC, USA), where high-throughput sequencing was performed using the Roche 454 FLX pyrosequencing platform. The sequencing results were recorded as SFF files and uploaded to the MetaGenome Rapid Annotation Subsystems Technology (MG-RAST) server for analysis (Meyer et al., 2008). Each file underwent quality control (QC), which included quality filtering (removing sequences with ≥5 ambiguous base pairs), length filtering (removing sequences with a length ≥2 standard deviations from the mean), and dereplication (removing similar sequences that are artifacts of shotgun sequencing). Organism and functional identifications were made using a BLAT [Basic Local Alignment Search Tool (BLAST)-like alignment tool] search of the integrative MG-RAST M5NR database, which is a non-redundant protein database that combines sequences from multiple common sources. All identifications were made using a maximum e-value of 1e-5, a minimum identity cutoff of 50%, and a minimum alignment length of 50 bp. The hierarchical clustering/heat map comparisons were constructed in MG-RAST using dendrograms based on abundance counts for

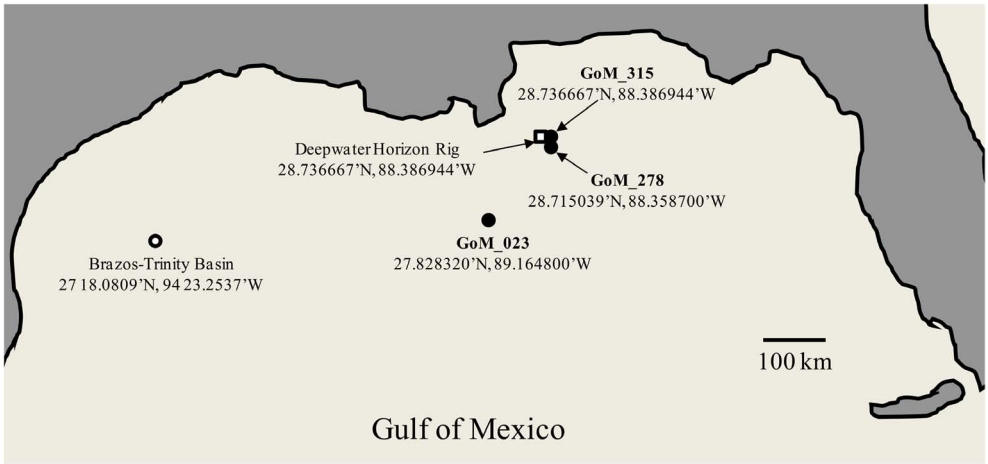

FIGURE 1 | Map of the Gulf of Mexico sampling sites. Open square – DWH rig; filled circle – sampling sites from the current study; open circle – BT Basin sampling site from Biddle et al. (2011). The Peru Margin (PM) sampling sites used for comparison are described in Biddle et al. (2008).

each category examined. Similarity/dissimilarity was determined using a Euclidean distance metric, and the resulting distance matrix was combined with ward-based clustering to produce dendrograms. Diversity indices for species richness and diversity estimates were calculated using EstimateS software (Colwell, 2006). Circular recruitment plots were created through the comparison of each metagenomic library to the whole genomes of reference organisms (Refseq genomes only) using a maximum e-value of 1e − 5 and a log10 abundance scale. Three organisms of interest were investigated: *Alcanivorax borkumensis* SK2 (Yakimov et al., 1998; Schneiker et al., 2006; dos Santos et al., 2010), an aerobic gammaproteobacterium that utilizes oil hydrocarbons as its exclusive source of carbon and energy and is often the most dominant bacterium in oil-polluted marine systems (Harayama et al., 1999; Kasai et al., 2001; Hara et al., 2003; Yakimov et al., 2005), *Desulfatibacillum alkenivorans* AK-01, a sulfate-reducing, *n*-alkane and *n*-alkene utilizing Deltaproteobacterium (So and Young, 1999; Callaghan et al., 2012), and *Geobacter metallireducens* GS-15, a metal-reducing, aromatic hydrocarbon utilizer within the *Deltaproteobacteria* (Lovley et al., 1993).

PCR AMPLIFICATION OF FUNCTIONAL GENES

Sediment DNA from GoM315, GoM278, GoM023 was also interrogated with nine primer set combinations specific to *assA* and/or *bssA* (Callaghan et al., 2010). The *assA* and *bssA* genes encode the catalytic subunits of the anaerobic glycyl radical enzymes, alkylsuccinate synthase (ASS; also known as methylalkylsuccinate synthase, MAS; Callaghan et al., 2008; Grundmann et al., 2008) and benzylsuccinate synthase (BSS; Leuthner et al., 1998), respectively. Polymerase chain reaction (PCR) SuperMix (2X Dreamtaq, Fermentas) was used to set up 50-μL reactions containing 25 μL of 2X Dreamtaq mastermix, 0.4 μM of each primer, 5 μL of betaine (5 M stock), and 10 ng of DNA template. A modified touchdown PCR method (Muyzer et al., 1993) was used to minimize unspecific amplification. The cycling program was as follows: 95°C for 4 min followed by 2 cycles at each annealing temperature (i.e., 95°C for 1 min, 63–52°C for 1 min, 72°C for 2 min), 19 cycles at the plateau annealing temperature (53°C), and a final extension step at 72°C for 10 min.

CONSTRUCTION AND PHYLOGENETIC ANALYSIS OF *assA* AND *bssA* CLONE LIBRARIES

Polymerase chain reaction products were purified using the Qiaquick purification kit (Qiagen) and cloned into either pCRII or pCRII-TOPO vector (Invitrogen, Carlsbad, CA, USA) following the manufacturer's instructions. For each PCR product, colonies were picked into individual wells of two 96-well microtiter plates and grown overnight. Inserts of the correct size were sequenced using the M13R priming site. After sequencing, reads were trimmed to remove vector and primer sequences before further analysis. Sequences from each respective library were assembled into operational taxonomic units (OTUs) of ≥97% sequence identity using Lasergene 7.2 (DNASTAR Inc., Madison, WI, USA). The *assA*/*bssA* OTUs were aligned with *assA* and *bssA* genes from described strains for which complete sequences were available and the best BLAST matches National Center for Biotechnology Information (NCBI). Neighbor-joining trees were constructed in MEGA4 (Kumar et al., 2008) using the Tajima–Nei distance method, with pairwise deletion and performing 10,000 bootstrap replicates. The glycyl radical enzyme, pyruvate formate lyase (PFL), served as the outgroup. The DNA sequences of GoM *assA* and *bssA* OTUs were deposited in GenBank under the accession numbers JX135105 through JX135128.

METABOLOMIC EXTRACTIONS AND ANALYSIS

Approximately 25 g of each core sample was thawed in 20 mL of double-distilled sterile water and then acidified with 10 N HCl until the pH was ≤2. Each sample was mixed with 100 mL of ethyl acetate and stirred overnight. The water phase was removed and the ethyl acetate solution was dried over anhydrous Na_2SO_4, concentrated by rotary evaporation to approximately 2 mL and

reduced further under a stream of N_2 to a volume of 100 μL. Half of the extract was derivatized and analyzed by GC/MS as described previously (Aktas et al., 2010). The other half was analyzed by LC/MS with an Agilent 1290 UPLC and an Agilent 6538 Accurate-Mass Q-TOF with a dual electrospray ionization (ESI) ion source. A 5-μL volume of each concentrated ethyl acetate solution was introduced to a ZORBAX SB-C18 column (2.1 mm × 100 mm, 1.8 μm). A gradient method was used for the separation (0–3 min 15% acetonitrile, 3–25 min linear gradient to 95% acetonitrile in water). The flow rate was 0.4 mL/min, and the temperature of the drying gas was maintained at 325°C. The data were analyzed using the Agilent B.04.00 MassHunter Qualitative Analysis software. A positive identification of key metabolites, such as alkylsuccinates, alkylmalonates, alkylbenzylsuccinates, and alkanoic acids, required that these were observed with the correct mass (±1 ppm), as well as with the retention times and MS/MS spectra observed for standard compounds.

RESULTS

In total, we sequenced 191.6 Mb from three deep-sea sediment samples collected after the DWH blowout (**Table 1**), which included two sediment cores (GoM315 and GoM278) within 3 km of the DWH rig and one (GoM023) 127 km away (**Figure 1**). Post QC, 125.8 Mb were designated as high-quality sequences (252,082 individual reads), resulting in an average of 84,023 individual reads (average length of 491 bp/read) per deep-sea sediment core (**Table 1**).

Table 1 | Data from the three GoM metagenomic libraries described in this study.

Features	GoM315	GoM278	GoM023
Distance from Deepwater Horizon blowout (km)	0.5	2.7	127.9
Depth below sea-level (m)	1,464	1,500	1,614
Basepairs sequenced prior to QC (Mb)	68.7	60.7	62.2
Individual reads prior to QC	144,700	127,356	122,703
Average length of reads prior to QC (bp)	474	476	506
Basepairs sequenced post QC (Mb)	43.9	38.8	41.1
Individual reads post QC	91,717	80,841	79,524
Average length of reads post QC (bp)	478	479	517
Prokaryotes	72,845	64,997	70,415
Eukaryotes	2,056	1,750	2,376
Viruses	268	372	74
Functional classifications (subsystems database)	59,175	52,599	55,130
Alpha diversity (species-level analysis)	1003.4	981.6	908.7
Chao 1 estimate ± SD (genus-level analysis)	593 ± 6.4	562 ± 2.6	582 ± 4.6
Shannon index (genus-level analysis)	5.64	5.55	5.55

PHYLOGENETIC CLASSIFICATION

The MG-RAST classification tool revealed that at the domain level, all three samples had similar distributions. Bacteria (97–95%) dominated, while the archaea (4.2–2.2%) and eukaryotes (0.8–0.6%) contributed substantially less to the sediment communities. Differences among the three samples were observed when examined at the phylum level (**Figure 2**). The archaea associated with the deep-sea sediment cores were predominantly Euryarchaeota, Thaumarchaeota, and Crenarchaeota (**Figure 2A**). The Euryarchaeota dominated (65%) in the sample closest to the DWH rig (GoM315), but the same taxon and the Thaumarchaeota were equally represented (45%) at GoM278. The Thaumarchaeota dominated (55%) in the sample most distant from the spill site (GoM023).

Within the bacterial domain (**Figure 2B**), Proteobacteria dominated (60–65%) all three sediment cores, followed by Firmicutes in GoM315 (9%), Bacteroidetes in GoM278 (11%), and Actinobacteria in GoM023 (7%). The eukaryotic sequences represented 21 phyla from the Animalia, Fungi, Plantae, and Protista kingdoms. The Animalia phyla Arthropoda (e.g., crab and shrimp) and Chordata (e.g., fish and sharks) increased in abundance as the distance from the DWH rig increased, while the Cnidaria (e.g., corals and sponges) and Nematoda (e.g., roundworms) phyla were found only at greater abundance in the two sediment cores closest to the DWH rig. Although the number of viruses was relatively low (0.17–0.01%), a greater number of viruses were associated with the two samples located nearest the DWH rig (GoM315 and GoM278) compared to the sample furthest away (**Table 1**). Alpha diversity values calculated using annotated species-level distribution increased as the distance to the DWH rig lessened. However, other diversity indices revealed similar levels of both species in richness and diversity among the samples (**Table 1**).

The Proteobacteria associated with each sample were examined more closely in order to evaluate the potential for both aerobic and anaerobic oil biodegradation (**Figure 3**), since numerous Proteobacteria spp. are known to utilize petroleum hydrocarbons (Atlas, 1981; Widdel et al., 2010). The Gammaproteobacteria was the most diverse class with the *Shewanella*, *Marinobacter*, and *Pseudomonas* genera being the most common. Although the Gammaproteobacteria were similarly distributed (∼33%), the distributions of both the Alphaproteobacteria and Deltaproteobacteria varied among the three deep-sea sediment samples (**Figure 3A**). The Alphaproteobacteria, predominantly the Rhizobiales and Rhodobacterales orders (**Figure 3B**), contributed to the highest percentage (37%) of Proteobacteria spp. in the sample furthest from the DWH rig (GoM023), while the two closer samples (GoM315 and GoM278) contained 30 and 26%, respectively. Greater numbers of sequences associated with GoM023 were detected in numerous Alphaproteobacteria genera, including *Rhizobium*, *Sinorhizobium*, *Bradyrhizobium*, *Roseobacter*, *Roseovarius*, and *Rhodobacter*. Deltaproteobacterial distributions revealed a wider range than the Gamma- and Alphaproteobacteria, one in which the two sediment cores closest to the DWH rig (GoM315

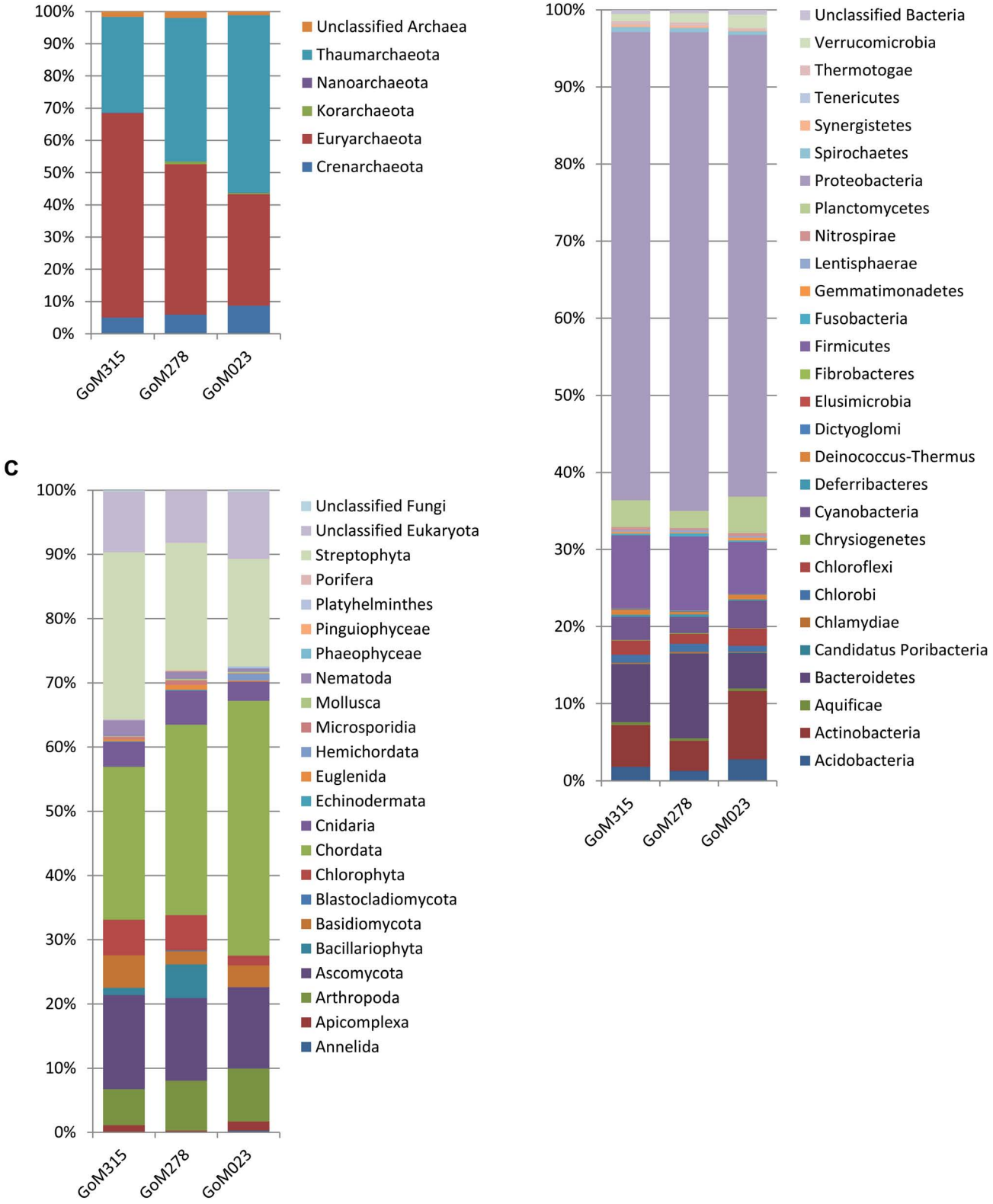

FIGURE 2 | Phylum-level organism classifications reveal differences among the three metagenomes sequenced in this study. (A) Archaea; **(B)** bacteria; and **(C)** eukaryotes.

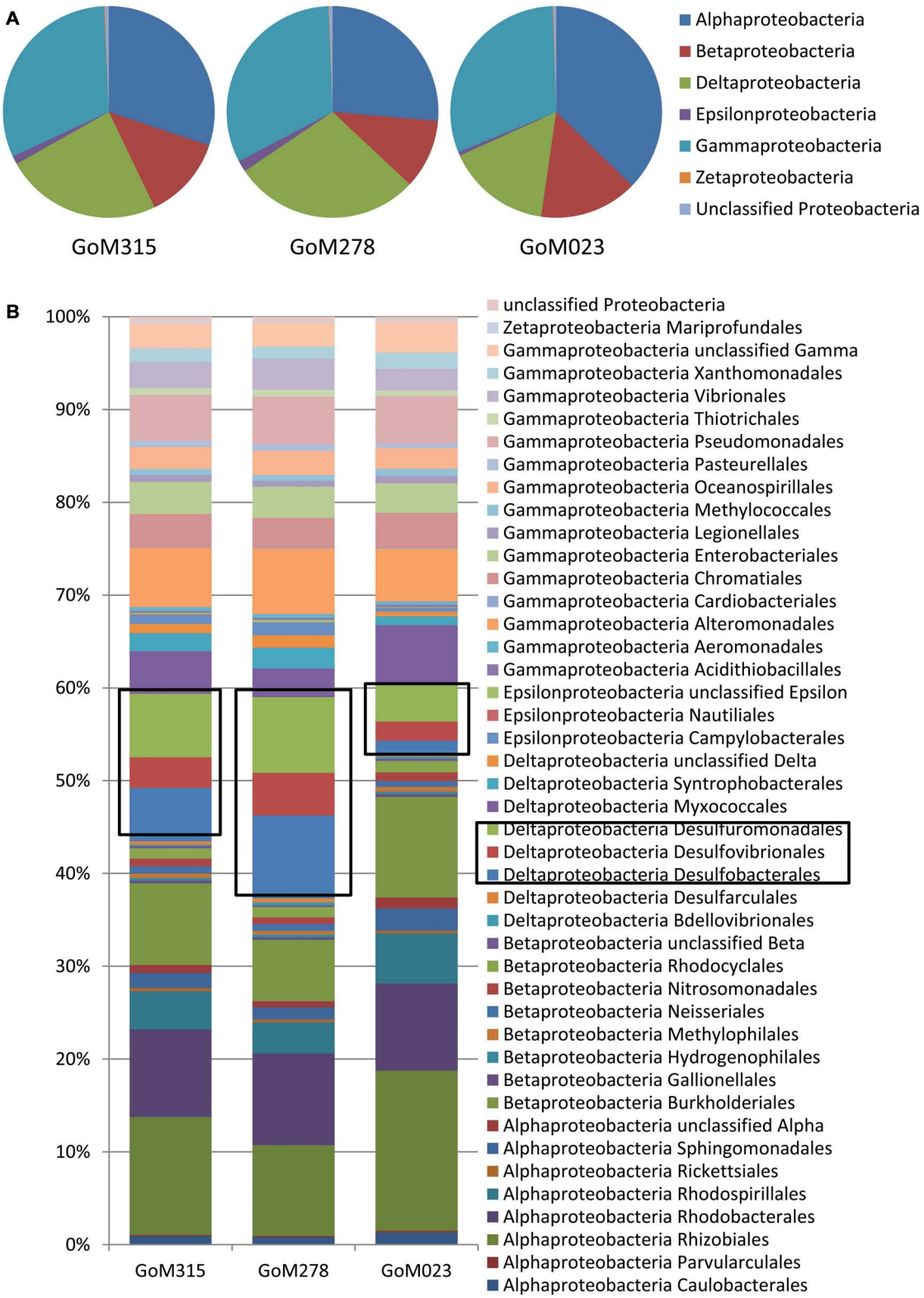

FIGURE 3 | Differences are observed among the sites closest to the DWH rig and the site located over a 100 km away when examining more of the Proteobacteria. (A) Proteobacteria classes associated with each of the three sites reveals a decrease in the Deltaproteobacteria at the far site GoM023; **(B)** Proteobacteria order-level classifications identify Desulfobacterales, Desulfovibrionales, and Desulfuromonaldes as the major contributors to the difference observed.

and GoM278) exhibited higher levels (26 and 30%, respectively), while the furthest core (GoM023) exhibited only 16% Deltaproteobacteria (**Figure 3A**). No single organism accounted for the shift in Deltaproteobacteria communities, rather a myriad of genera in the Desulfobacterales (e.g., *Desulfatibacillum*, *Desulfobacterium*, and *Desulfococcus*), Desulfovibrionales (e.g., *Desulfovibrio*), and Desulfuromonadales (e.g., *Geobacter*, and *Desulfomonas*) orders displayed higher levels in the GoM315 and GoM278 samples (**Figure 3B**).

RECRUITMENT PLOTS

Recruitment plots, comparing sequences from each metagenomic library to the genomes of specific organisms, supported the presence of known hydrocarbon-utilizing Proteobacteria (**Table 2**). The analysis revealed a total of 169, 857, and 547 sequences, respectively, matching to features of the *Alcanivorax borkumensis* SK2 genome (Proteobacteria, Gammaproteobacteria, Oceanospirillales, Alcanivoracaceae; Yakimov et al., 1998; Schneiker et al., 2006), the *Desulfatibacillum alkenivorans* AK-01 genome (Proteobacteria, Deltaproteobacteria, Desulfobacterales, Desulfobacteraceae; So and Young, 1999; Callaghan et al., 2012), and the *G. metallireducens* GS-15 genome (Proteobacteria, Deltaproteobacteria, Desulfuromonadales, Geobacteraceae; Lovley et al., 1993) in all three deep-sea sediment samples. Interestingly, matches to the aerobic hydrocarbon degrader, *Alcanivorax borkumensis* SK2 (51–61 sequence hits), remained consistent among all three samples; whereas, the comparison to the two anaerobic hydrocarbon degraders, *Desulfatibacillum alkenivorans* AK-01 (97–426 sequence hits) and *G. metallireducens* GS-15 (92–278 sequence hits), revealed a greater number of sequence matches to the two samples (GoM315 and GoM278) closest to the DWH well (**Figure 4**). Similarly, sequences recruited to *Desulfococcus oleovorans* Hxd3 (**Table 2**), a model sulfate-reducing alkane/alkene utilizer, in all three samples; however, GoM315 and GoM278 recruited a greater number of sequences (256 and 332, respectively) compared to GoM023 (79).

FUNCTIONAL GENE ANALYSIS

All three samples revealed a similar functional blueprint at the broadest level of classification (**Figure 5A**). Genes coding for clustering-based subsystems (15–16%), amino acid and derivatives (9.2–9.3%), miscellaneous (8.2–9.5%), carbohydrates (8.8%), and protein metabolism (7.4–8.7%) represented the five most abundant categories when classified using the SEED database (**Figure 5A**). Analysis using COG classifications revealed a similar functional distribution, with the majority of sequences assigned to metabolism (45–46%), followed by cellular processes and signaling (19–21%), information storage and processing (17–18%), and poorly characterized categories (15–18%). There was genetic evidence in all three samples for the potential degradation of oil compounds, including genes vital to both the aerobic (e.g., mono- and dioxygenases) and anaerobic degradation (e.g., *bss* and benzoyl-CoA reductase) of compounds such as butyrate, benzoate, toluene, and alkanoic acids (Table S1 in Supplementary Material). Functional analysis of the "metabolism of aromatic compounds" subsystem provided additional evidence of a greater potential for anaerobic metabolism in the two samples nearest the DWH rig compared to the more distant sample (**Figure 5B**). GoM315 (located 0.5 km from the DWH rig) exhibited the highest percentage (15%) of anaerobic degradation genes for aromatic compounds, while GoM023 (located 128 km from the DWH rig) exhibited the lowest (9.9%). Notably, the metagenomics data revealed *bssA* in GoM315 only, the sample closest to the DWH well, and the complete complement (subunits D–G) of benzoyl-CoA reductase genes (Egland et al., 1997) was detected in GoM315 and GoM278, but not GoM023, the site farthest from the DWH well.

CLONE LIBRARIES

Functional gene libraries supported the metagenomic analysis and also suggested a greater genetic potential for anaerobic hydrocarbon degradation at the two sites near the DWH well, with respect to the *assA* and *bssA* genes. The *assA* and *bssA* genes encode the catalytic subunits of the glycyl radical enzymes, ASS, MAS; Callaghan et al., 2008; Grundmann et al., 2008) and BSS; Leuthner et al., 1998), respectively. Based on previous studies, ASS/MAS presumably catalyzes the addition of *n*-alkanes to fumarate (Callaghan et al., 2008; Grundmann et al., 2008) to form methylalkylsuccinic acids (for review see Widdel and Grundmann, 2010), whereas BSS catalyzes the addition of aromatic hydrocarbons to fumarate to yield benzylsuccinic acids and benzylsuccinate derivatives (for review see Boll and Heider, 2010). Both *assA* and *bssA* have been used as biomarkers, in conjunction with metabolite profiling, as evidence of *in situ* aliphatic and aromatic hydrocarbon degradation (Beller et al., 2008; Callaghan et al., 2010; Yagi et al., 2010; Oka et al., 2011; Wawrik et al., 2012). Of the nine primer sets tested (Callaghan et al., 2010), primer set 2 (specific to *bssA*) yielded four *bssA* OTUs in GoM278 sediment and four *bssA* OTUs in GoM315 sediment (**Figure 6**). Primer set 7 (specific to *assA*) yielded eight *assA* OTUs in GoM278 and eight *assA* OTUs in GoM315 (**Figure 7**). A comparison of the *bssA* and *assA* OTU sequences revealed that there are unique and shared OTUs between the two sites. Sequence identities ranged from 68.8 to 100% and 63.7 to 100% for *bssA* and *assA*, respectively. Based on BlastX and BlastN, the GoM *bssA* clone sequences were similar to those from uncultured bacteria as well as to *bssA* in *Thauera aromatica* K172 and *Azoarcus* sp. T (Table S2 in Supplementary Material). Based on BlastX and BlastN, the GoM *assA* clone sequences were similar to those from uncultured bacteria, as well as to *masD* in "*Aromatoleum*" sp. HxN1 (Table S2 in Supplementary Material). The *assA* and *bssA* genes were not detected in sediment collected from the background site, GoM023, under the PCR conditions and primers tested in this study.

METABOLITE PROFILING

We specifically looked for the presence of alkylsuccinate derivatives that were presumed metabolites formed by the addition of hydrocarbon substrates across the double bond of fumarate (Biegert et al., 1996; Kropp et al., 2000; Elshahed et al., 2001; Gieg and Suflita, 2005). For example, the presence of benzyl- or alkylsuccinic acids indicates the anaerobic metabolic decay of alkylated aromatic or *n*-alkane hydrocarbons, respectively (Davidova et al.,

Table 2 | Top ranked recruitment results for each of the GoM deep-sea sediment metagenomic libraries.

	Recruited genome	Rank	Number of sequences	Number of features	Features in genome	Genome coverage (%)
GoM315	*Desulfobacterium autotrophicum* HRM2	1	464	428	4943	8.66
	"Candidatus" Solibacter usitatus Ellin6076	2	397	300	7826	3.83
	Desulfatibacillum alkenivorans AK-01	3	334	288	5252	5.48
	Nitrosopumilus maritimus SCM1	4	268	223	1796	12.42
	Desulfococcus oleovorans Hxd3	5	256	227	3265	6.95
	Rhodopirellula baltica SH 1	7	211	193	7325	2.63
	Desulfotalea psychrophila LSv54	12	185	169	3234	5.23
	Haliangium ochraceum DSM14365	15	174	155	6719	2.31
	Cenarchaeum symbiosium A	34	122	111	2017	5.5
	Archaeoglobus fulgidus DSM4304	>300	20	18	2420	0.74
GoM278	*Desulfobacterium autotrophicum* HRM2	1	746	593	4943	12
	Desulfatibacillum alkenivorans AK-01	2	426	362	5252	6.89
	Nitrosopumilus maritimus SCM1	3	358	294	1796	16.37
	Desulfococcus oleovorans Hxd3	4	332	288	3265	8.82
	Desulfotalea psychrophila LSv54	5	256	221	3234	6.83
	"Candidatus" Solibacter usitatus Ellin6076	7	218	189	7826	2.42
	Cenarchaeum symbiosium A	10	187	165	2017	8.18
	Haliangium ochraceum DSM14365	20	134	123	6719	1.83
	Rhodopirellula baltica SH 1	22	124	124	7325	1.69
	Archaeoglobus fulgidus DSM4304	>300	33	31	2420	1.28
GoM023	*Nitrosopumilus maritimus* SCM1	1	713	520	1796	28.95
	"Candidatus" Solibacter usitatus Ellin6076	2	564	410	7826	5.24
	Cenarchaeum symbiosium A	3	373	296	2017	14.68
	Haliangium ochraceum DSM14365	4	290	242	6719	3.6
	Rhodopirellula baltica SH 1	5	279	243	7325	3.32
	Desulfatibacillum alkenivorans AK-01	58	97	81	5252	1.54
	Desulfococcus oleovorans Hxd3	79	81	74	3265	2.27
	Desulfobacterium autotrophicum HRM2	102	72	70	4943	1.42
	Desulfotalea psychrophila LSv54	>200	39	37	3234	1.14
	Archaeoglobus fulgidus DSM4304	>300	16	14	2420	0.58

2005; Duncan et al., 2009; Parisi et al., 2009). Straight chain alkanes and alkenes with carbon lengths from C11 to C14 and from C13 to C22, respectively, were detected using GC/MS in the two sites closest to the spill site (GoM278 and GoM315). A few branched alkanes and alkenes were also observed. *n*-Alkane and *n*-alkene hydrocarbons were not detected in the background sample (GoM023). With GC/MS, alkanoic acids in GoM278 (2.7 km) with lengths between C14 and C18 were detected, whereas the lengths ranged from C7 to C22 in GoM315 (0.5 km). Alkylsuccinate or alkylmalonate metabolites typically associated with the anaerobic biodegradation of *n*-alkanes via "fumarate addition" were below detection levels in all samples. However, putative benzylsuccinates were identified in the samples, based on their metastable fragmentation pattern of ≈5% loss of CO_2 and no detectable loss of H_2O in MS mode. The highest abundances were observed for C16 to C19 benzylsuccinates (**Figure 8**), and their abundances were also three times higher in GoM315 (0.5 km) than in the other two samples. The presence of benzylsuccinates is consistent with the detection of *bssA* genotypes. Benzoate, a central metabolite of both aerobic and anaerobic hydrocarbon metabolism, was also detected in the two samples closest to the spill site.

COMPARATIVE METAGENOMICS

Comparison of our metagenomic data to that of two other deep-sea metagenomes revealed a number of interesting differences. The first metagenomic study examined deep-subsurface sediment cores (PM01*, PM01, PM50) from the nutrient-rich area of the Peru Margin (Biddle et al., 2008), while the second examined an oligotrophic subsurface sediment core from the Gulf of

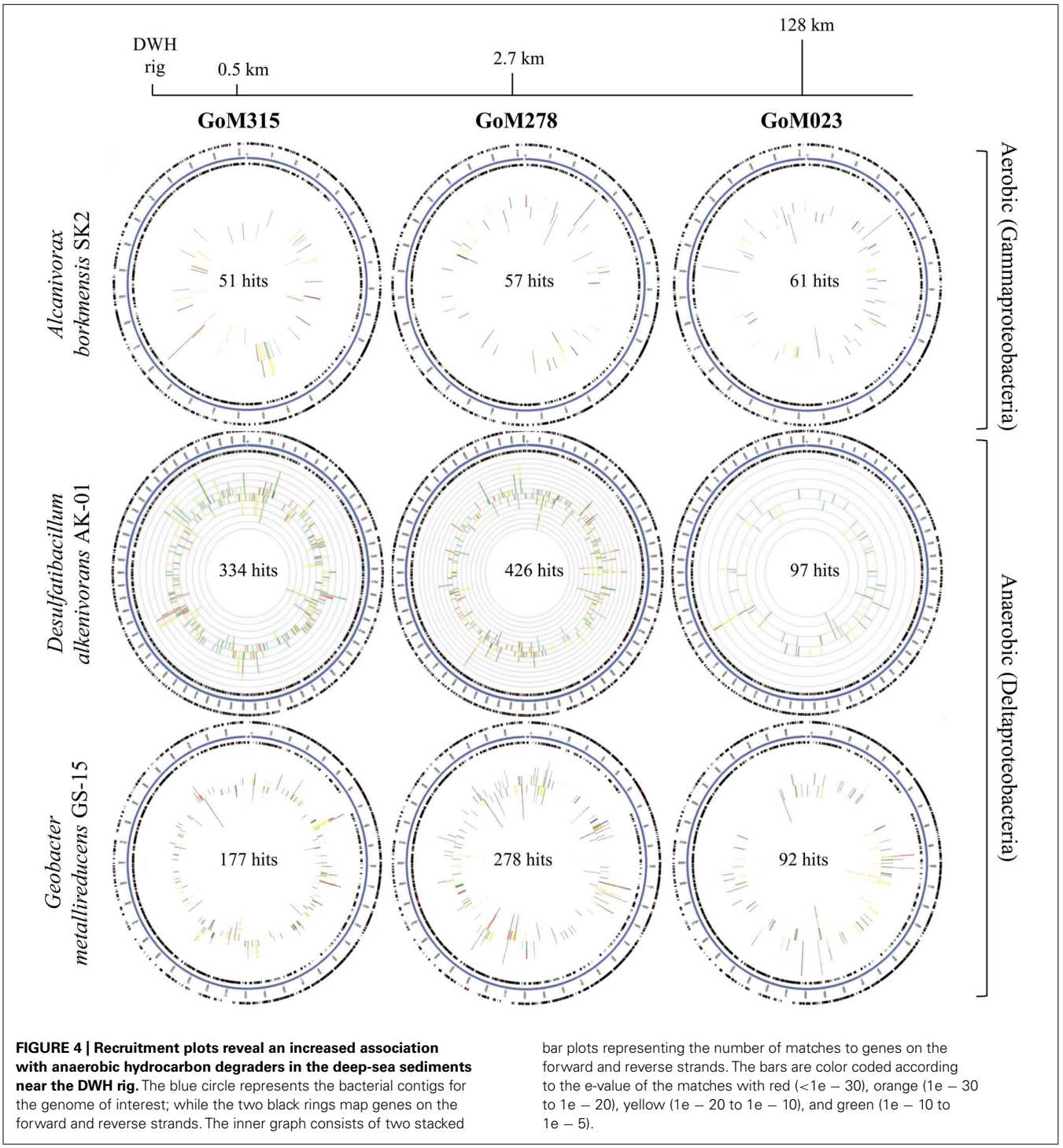

FIGURE 4 | Recruitment plots reveal an increased association with anaerobic hydrocarbon degraders in the deep-sea sediments near the DWH rig. The blue circle represents the bacterial contigs for the genome of interest; while the two black rings map genes on the forward and reverse strands. The inner graph consists of two stacked bar plots representing the number of matches to genes on the forward and reverse strands. The bars are color coded according to the e-value of the matches with red (<1e − 30), orange (1e − 30 to 1e − 20), yellow (1e − 20 to 1e − 10), and green (1e − 10 to 1e − 5).

Mexico (BT Basin) prior to the DWH blowout (Biddle et al., 2011). In both studies the samples were subsurface sediments collected at a depth of two meters or greater, whereas the samples collected in this study were surficial samples collected at the interface between the water and the sediment. Distributions of organisms at the domain level were slightly different between the Peru Margin/BT Basin samples and our GoM samples, with the former harboring a greater percentage of archaea (18.1–8.6% compared to 2.9–3.3%) and eukaryotes (17.7–5.8% compared to 2.6–3.3%). At the phylum level, the Peru Margin and BT Basin data revealed a different picture from this study with a more even distribution of Proteobacteria and Firmicutes, followed by Euryarchaeota and Chloroflexi (**Figure 9A**). Although the functional gene patterns were similar among the three studies, sequences associated with the "metabolism of aromatic compounds" category were more abundant in all three of

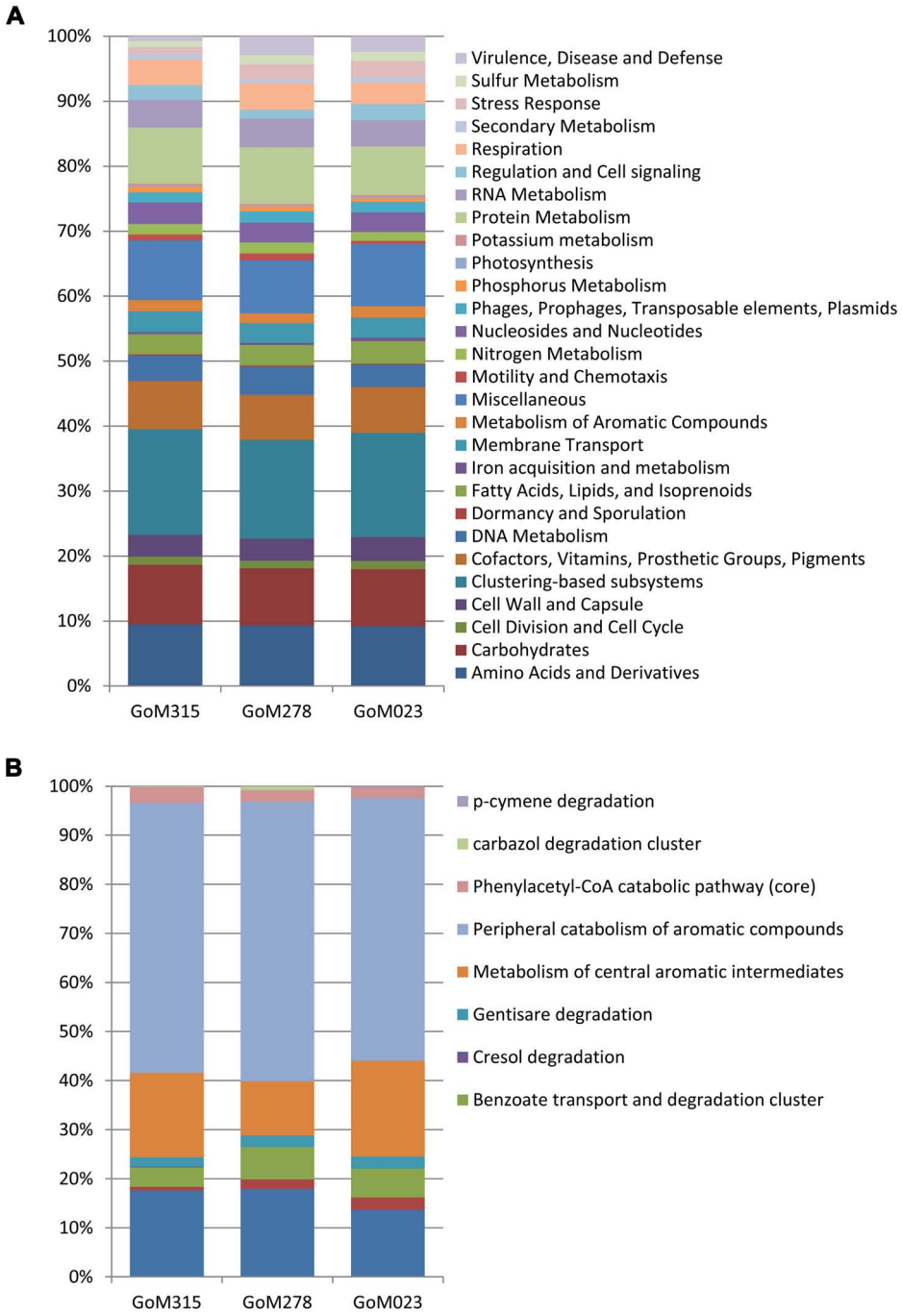

FIGURE 5 | Functional classifications of the metagenomic sequences. (A) Similar functional fingerprints are observed at the broadest subsystem classification. **(B)** Functional genes associated with the "metabolism of aromatic compounds" reveal a decreased association with "anaerobic degradation in aromatic compounds" in GoM023.

our samples (1.4–1.9%) following the DWH oil spill compared to the BT Basin (0.5%) level evaluated prior to the spill (**Figure 9B**). Hierarchical clustering analysis, based on subsystem functional classification, revealed geographical separation between the Peru Margin and Gulf of Mexico samples (**Figure 10A**). Within the Gulf of Mexico cluster, the BT Basin clustered separately from GoM023, GoM278, and GoM315. Furthermore, GoM315 and GoM278, the samples located relatively close to the DWH rig, clustered separately from GoM023, the sample furthest from the DWH rig. A similar pattern of separation was visualized using principal component analysis (**Figure 10B**) with the organism classifications.

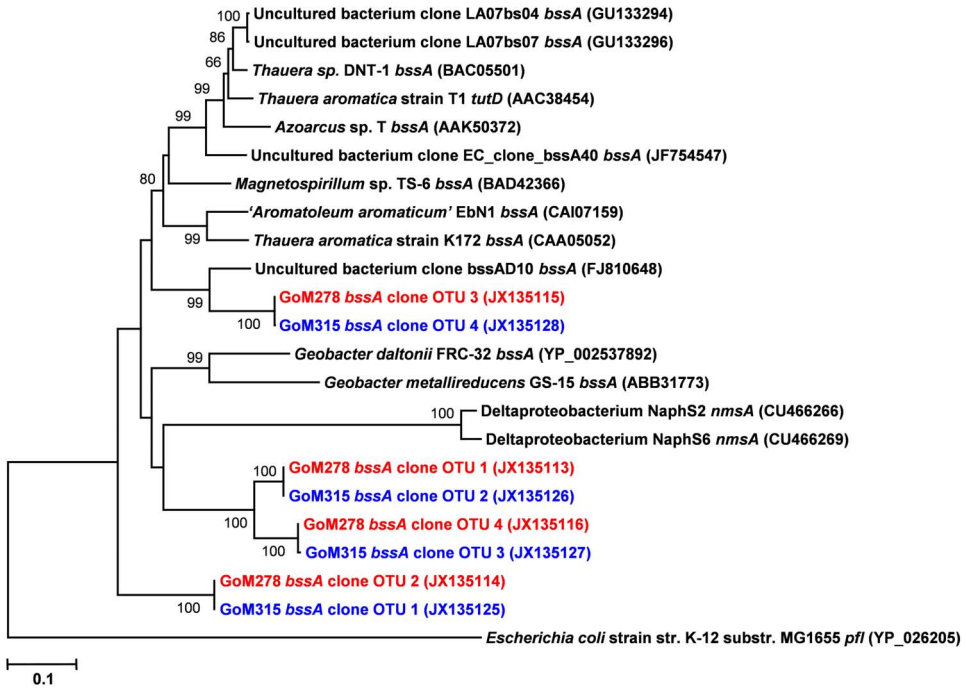

FIGURE 6 | Neighbor-joining dendrogram of *bssA* clone sequences obtained from GoM sediments (GoM278 – red; GoM315 – blue) compared to *bssA* sequences of reference strains and BLAST matches. The tree was constructed using the Tajima–Nei distance method (scale bar), with pairwise deletion and performing 10,000 bootstrap replicates. Bootstrap values below 65 are not shown. pyruvate formate lyase (*pfl*) served as the outgroup. Numbers in parentheses represent NCBI GenBank accession numbers. *bss*, benzylsuccinate synthase; *tut*, toluene-utilizing (i.e., benzylsuccinate synthase); *nms*, naphthylmethylsuccinate synthase.

DISCUSSION

In this study, we present three new metagenomic data sets from deep-sea sediments of the Gulf of Mexico following the DWH oil spill. Due to logistical and political circumstances surrounding the DWH oil spill, three samples were the extent of which we were able to obtain. These data, however, present a unique opportunity to examine deep-sea sediments following a massive anthropogenic hydrocarbon loading event and triples the number of metagenomic datasets previously available (one metagenome; Biddle et al., 2011) for deep-sea subsurface sediments in the Gulf of Mexico. Although the lack of replication makes it difficult to draw wide conclusions regarding the effects of hydrocarbon exposure on microbial community composition and activity, these metagenomes provide important data to make baseline observations that will need to be examined more thoroughly in future studies.

Two previous deep-sea metagenomic studies resulted in the suggestion that there is a core metagenomic structure for deep-sea sediments, composed of four main microbial groups (Euryarchaeota, Proteobacteria, Firmicutes, and Chloroflexi) that can vary depending on specific parameters, such as depth, organic carbon content, and geography (Biddle et al., 2008; Biddle et al., 2011). These four microbial taxa were also detected in GoM sediment samples in the present work; however, they do not constitute the four major groups detected in this report (Proteobacteria, Bacteroidetes, Firmicutes, and Actinobacteria). Despite similarities to the microbial communities described previously (Biddle et al., 2008; Biddle et al., 2011), our cross-study comparisons via hierarchical clustering and principal component analyses reveal a distinct separation between the Peru Margin communities (Biddle et al., 2008) and both Gulf of Mexico communities (Biddle et al., 2011, and current report). This is of particular interest, since the two previous studies were subsurface samples, compared to our surficial samples. A metagenomic fosmid library of deep-sea sediments from the organic-rich Qiongdongnan Basin in the South China Sea (Hu et al., 2010) revealed a community structure that was more similar to this study than to those of the Biddle et al. (2008, 2011) studies. These data suggest the possibility that organic carbon content is more relevant to microbial community structure than geography. Hu et al. (2010) detected Proteobacteria as the dominant (~43%) bacterial phylum, and Deltaproteobacteria as the most abundant class within this phylum. KEGG analysis of the fosmid ends also revealed genes associated with the biodegradation pathways of numerous xenobiotics including, but not limited to dichloroethane, benzoate, biphenyl, ethylbenzene, fluorene, naphthalene, anthracene, styrene, tetrachloroethene, and gamma-hexachlorocyclohexane. The detection of genes related to the biodegradation of xenobiotic compounds in their study and ours supports the premise that deep-sea sediment microbial communities have the potential to metabolize a diverse array of organic compounds, including many that are found in oil.

Numerous bacterial species have evolved the ability to metabolize aliphatic (e.g., alkanes and alkenes) and aromatic hydrocarbons (e.g., mono- and polynuclear), with the most rapid

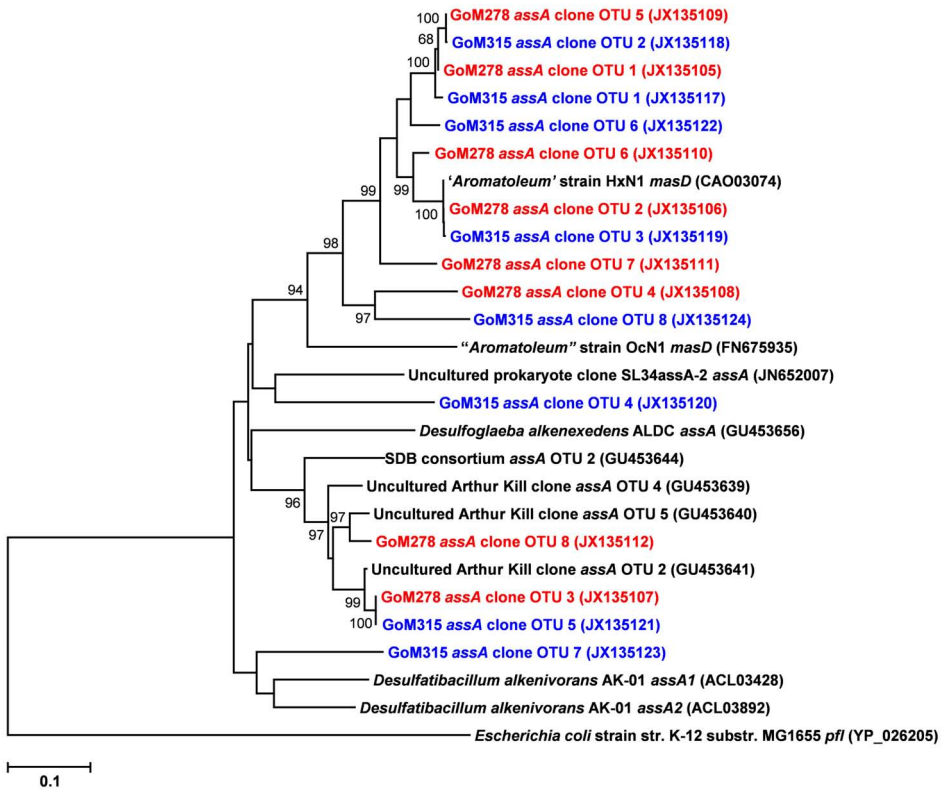

FIGURE 7 | Neighbor-joining dendrogram of *assA* clone sequences obtained from GoM sediments (GoM278 – red; GoM315 – blue) compared to *assA*/*masD* sequences of reference strains and BLAST matches. The tree was constructed using the Tajima–Nei distance method (scale bar), with pairwise deletion and performing 10,000 bootstrap replicates. Bootstrap values below 65 are not shown. Pyruvate formate lyase (*pfl*) served as the outgroup. Numbers in parentheses represent NCBI GenBank accession numbers. *ass*, alkylsuccinate synthase; *mas*, methylalkylsuccinate synthase.

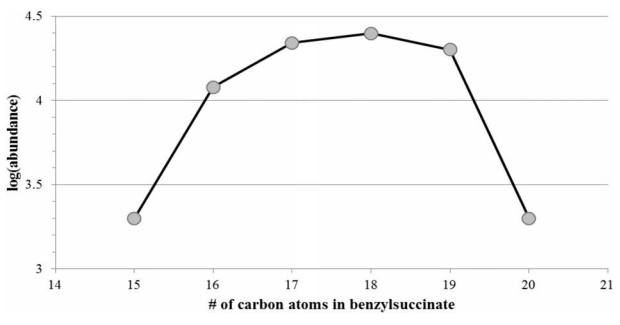

FIGURE 8 | Logarithm of abundance of benzyl succinates in the sample GoM315.

and complete degradation achieved through aerobic processes (Fritsche and Hofrichter, 2008). The majority of characterized oil-degraders within marine systems are aerobic members of the Alpha- and Gammaproteobacteria (for reviews see Head et al., 2006; Kim and Kwon, 2010) that use mono- and dioxygenases to initiate degradation (Haddock, 2010; Rojo, 2010). This includes *Alcanivorax borkumensis*, a ubiquitous gammaproteobacterium in marine environments, which is known to utilize aliphatic hydrocarbons (Yakimov et al., 1998; Schneiker et al., 2006; dos Santos et al., 2010). Following the DWH blow out, *Oceanospirillales* was shown to be the dominant bacterial orders associated with the resulting deepwater (∼1100 m) oil plume (i.e., more than 90% of the sequences were classified as *Oceanospirillales*, predominantly from one monophylectic lineage(Hazen et al., 2010). Our metagenomic analysis revealed the presence, in all three deep-sea sediment libraries, of bacteria belonging to the broader *Oceanospirillales* order, including 51–61 sequences specifically recruited to the *Alcanivorax borkumensis* genome in each sample (**Figure 4**). The abundance of *Oceanospirillales*, however, was relatively low (< 2% of bacterial sequences) compared to those found in the deep water oil plume (Hazen et al., 2010; Mason et al., 2012). GoM315, GoM278, and GoM023 exhibited similar levels of *Oceanospirillales* spp. (1.5, 1.7, and 1.4% of bacterial sequences, respectively) and Gammaproteobacteria in general (19, 20, and 19% of bacterial sequences, respectively), showing no correlation to the hydrocarbon levels associated with each sample. Alphaproteobacteria associated with aerobic oil-degradation were also found at very low abundances with similar levels across the deep-sea sediment samples, including *Roseovarius* spp. and *Maricaulis* spp. (<0.5 and <0.3% of bacterial species, respectively). Nonetheless, mono- and dioxygenases were present in all three samples. These data indicate that the potential for aerobic degradation is present in these samples, albeit at much lower levels than

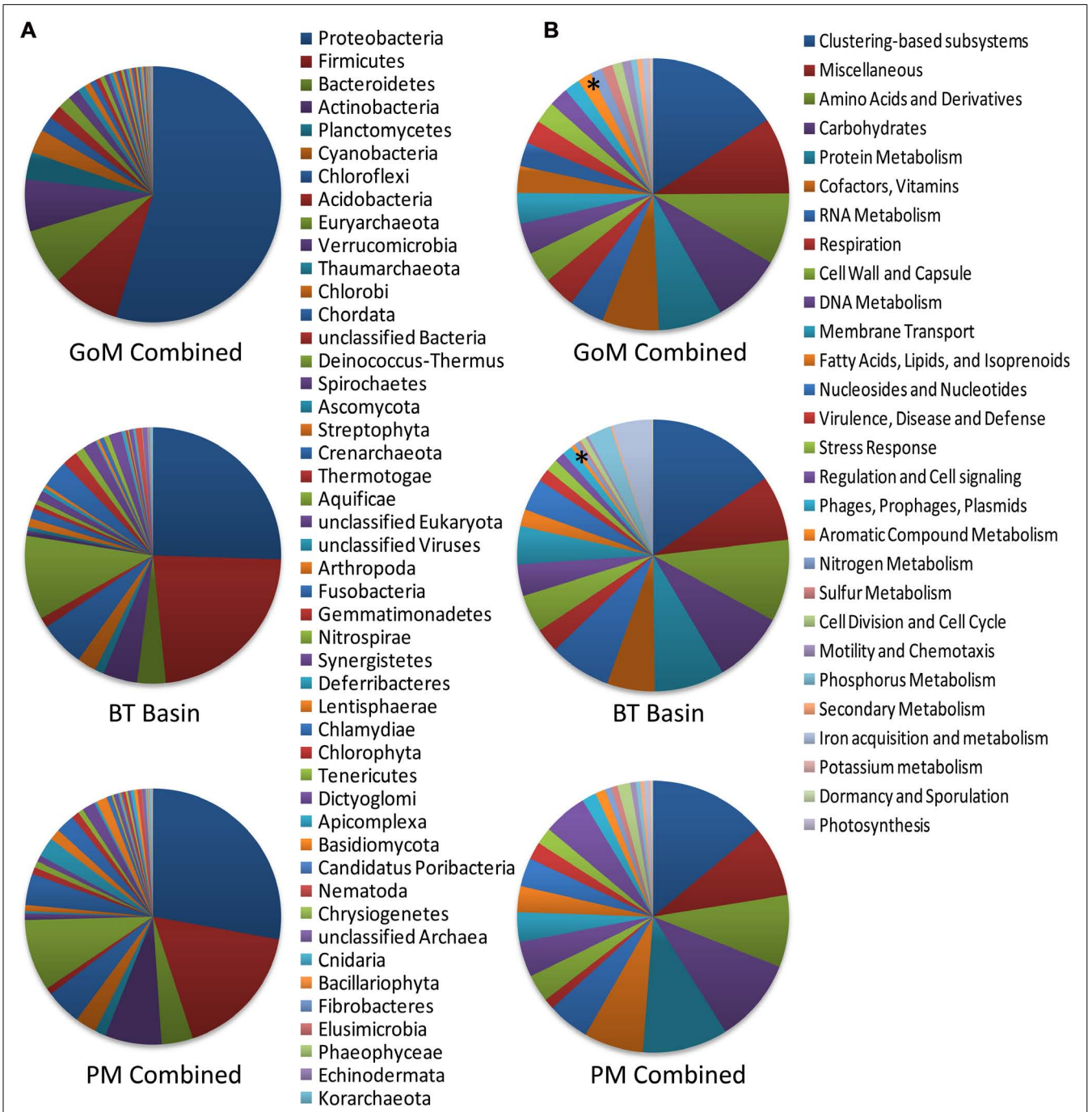

FIGURE 9 | Phylogenetic and functional comparison of deep-sea sediment metagenomes across three studies. (A) Phylogenetic comparison at the phylum level reveals differences among this study and the two previously performed by Biddle et al. (2008, 2011). **(B)** Functional comparison of the broadest level of subsystem classifications reveals a more similar pattern between the three studies. Asterisk "*" denotes the "aromatic compound metabolism" category; GoM combined, represents the collective data from GoM315, GoM278, and GoM023; PM combined, represents the collective data from PM01*, PM01, and PM50. The BT basin represents a single metagenome.

observed in the water column (Hazen et al., 2010; Mason et al., 2012), and that the level of hydrocarbon exposure did not significantly impact this potential. One potential explanation for this is that the hydrocarbons susceptible to aerobic degradation were depleted rapidly in the water column, either by dispersants or by the quick responding bacterial blooms of aerobic hydrocarbon-degrading microorganisms (Hazen et al., 2010; Kessler et al., 2011). As a result, the hydrocarbon loading that occurred in the deep-sea sediments may not have promoted the growth of microorganisms capable of aerobic hydrocarbon degradation, but rather that of

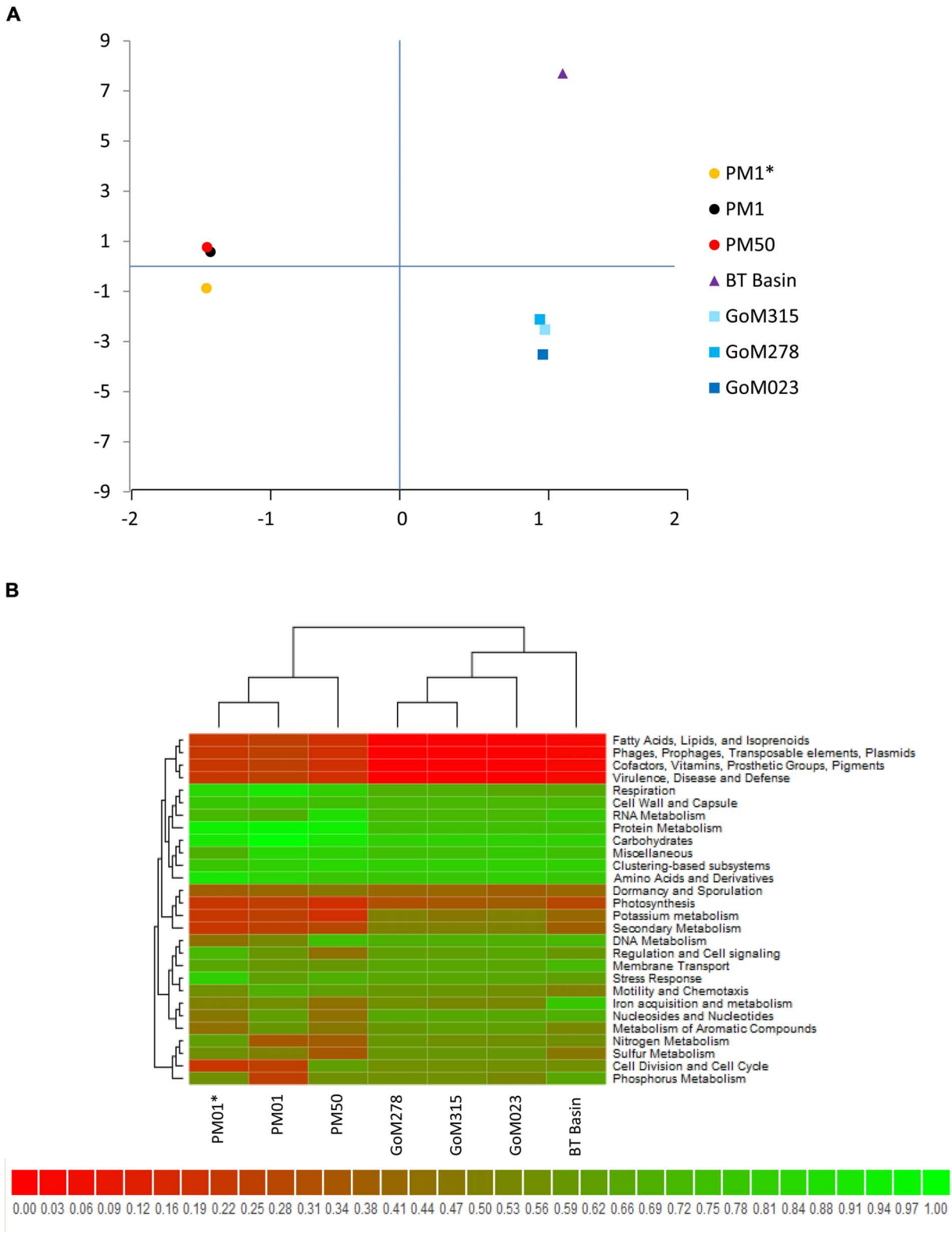

FIGURE 10 | Cross-study comparisons of deep-sea metagenomes. **(A)** Principal component analysis using organism classifications (species-level) from the current study as well as those from two studies (Biddle et al., 2008, 2011) reveals clear geographic separation, in addition to a second component of separation that is currently unknown. **(B)** Hierarchical clustering combined with heat mapping based on subsystem classifications reveals similar partitioning among the three studies compared.

microorganisms capable of degrading the remaining recalcitrant hydrocarbons that require anaerobic processing. It is also possible, however, that we sampled at a time when the community was just beginning to shift to reflect the increasing importance of anaerobic microbes. Future work involving time series samples and/or the analysis of aerobic metabolites will be necessary to provide further insights.

Anaerobic biodegradation of hydrocarbons is an important biogeochemical process in a variety of deep-subsurface environments (Aitken et al., 2004; Jones et al., 2007; Wawrik et al., 2012). Studies during the last two decades have highlighted the ability of anaerobic microorganisms to metabolize a variety of hydrocarbons, including *n*-alkanes, *n*-alkenes, alicyclic hydrocarbons, and mono- and polycyclic aromatic compounds (for reviews see Boll and Heider, 2010; Widdel and Grundmann, 2010; Widdel et al., 2010). To date, the most well-characterized anaerobic mechanism for hydrocarbon activation and degradation is via addition of the hydrocarbon to the double bond of fumarate ("fumarate addition") catalyzed by glycyl radical enzymes (for reviews see Boll and Heider, 2010; Widdel and Grundmann, 2010). Deltaproteobacteria, in particular, have been implicated in "fumarate addition" of both aromatic and aliphatic hydrocarbons (Widdel et al., 2010). In this study, metagenomic analysis revealed an increase in the percentage of bacterial sequences that represent Deltaproteobacteria associated with the sediment cores closest to the DWH well, where there were higher levels of PAHs (Operational Science Advisory Team, 2010) and detectable levels of alkanes and alkenes. It should be noted that the increase in Deltaproteobacteria is potentially an indirect effect of the increased dead biomass from the oil spill, which cannot be ruled out by this study. In any case, recruitment plots demonstrated that 857 and 547 of the metagenomic sequences mapped onto the Deltaproteobacterial genomes of *Desulfatibacillum alkenivorans* AK-01 and *G. metallireducens* GS-15, respectively. The increases in Deltaproteobacteria were also concurrent with an increase in functional genes involved in the anaerobic degradation of hydrocarbons, such as BSS, acetyl-CoA acetyltransferase and benzoyl-CoA reductase. These results suggest that the microbial response to anthropogenic hydrocarbon loading may mirror aspects of microbial communities associated with Gulf of Mexico natural seeps, where Deltaproteobacteria play a dominant role in their biogeochemical activity, including anaerobic hydrocarbon degradation (Lloyd et al., 2010; Orcutt et al., 2010). Most likely, however, the specific genus-level lineages of Deltaproteobacteria will be dependent on the hydrocarbon source present, since the natural gas-rich seeps contain specialized deltaproteobacterial groups for anaerobic methane utilization that are unlikely to thrive in sediments with more recalcitrant oil remnants.

Clone libraries of *assA* and *bssA* supported the metagenomic analysis. Both genotypes were detected in sediments near the DWH well (GoM278 and GoM315), but not at the unimpacted site (GoM023). The presence of *assA* and *bssA* suggests the potential for both aliphatic and aromatic hydrocarbon activation via "fumarate addition." Although *assA* genotypes were detected in sediments from GoM278 and GoM315, alkylsuccinates were not detected in these samples. However, this should not be interpreted as conclusive evidence that aliphatic substrates were not being metabolized. The requisite metabolites are usually in low abundance (typically nM) and transitory and could have easily been further metabolized or been below method detection limits. The alkanoic acid compounds detected in the GoM samples could have been formed via multiple biological pathways, including aerobic and anaerobic transformation of aliphatic hydrocarbons, but they are not highly diagnostic. Despite the non-detection of alkylsuccinates, both *bssA* genotypes *and* the putative benzylsuccinate metabolites were detected in the two sediment cores closest to the spill site, suggesting *in situ* anaerobic biodegradation of alkylbenzenes. This is consistent with the increased number of genes related to "aromatic metabolism" detected in the corresponding sediments via metagenomic analysis. Benzoate was also detected in GoM278 and GoM315 sediments, suggesting further transformation of the benzylsuccinate derivatives of monoaromatic hydrocarbons (Beller and Spormann, 1997; Leuthner et al., 1998). However, benzoate can be formed during the metabolism of a wide variety of aromatic compounds under aerobic *and* anaerobic conditions.

Overall, this study took an interdisciplinary approach of investigating the phylogenetic composition and functional potential of Gulf of Mexico deep-sea sediment communities following the DWH oil spill. Based on metagenomic analyses, functional gene clone libraries, and metabolite profiling, the data herein suggest that the presence of PAHs, alkanes, and alkenes may influence the microbial community through the enrichment of Deltaproteobacteria capable of anaerobic hydrocarbon metabolism. This evidence suggests that the microbial communities exposed to anthropogenic hydrocarbon loading in the Gulf of Mexico deep-sea sediments likely impacted the bioremediation of the DWH oil spill through anaerobic degradation, which has been previously overlooked. The integrated approach used herein augments other efforts to deduce the fate of the oil spilled in the DWH incident and to assess the impact of the spill on the indigenous microbial communities.

ACKNOWLEDGMENTS

We would like to thank the following individuals at LBNL that were instrumental in collecting, preserving, and aseptically sectioning the deep-sea sediment cores: Sharon Borglin, Yvette Piceno, Dominique Joyner, Janet Jansson, and Olivia Mason. We would also like to thank Andreas Teske for his thoughtful comments and critical review of the manuscript. This study was supported by the National Science Foundation (MCB-1049411) and (MCB-1049409) to PJM and JMS, respectively, by the program SPP 1319 of the Deutsche Forschungsgemeinschaft (grant to BTG in support of MD), and also in part by an NSF grant (MCB-0921265) to AVC. BTG and MD also thank the EPSRC Mass Spectrometry Service at the University of Wales (Swansea) for mass spectrometric analyses.

SUPPLEMENTARY MATERIAL

The Supplementary Material for this article can be found online at: http://www.frontiersin.org/Microbiological_Chemistry/10.3389/fmicb.2013.00050/abstract

REFERENCES

Aitken, C. M., Jones, D. M., and Larter, S. R. (2004). Anaerobic hydrocarbon biodegradation in deep subsurface oil reservoirs. *Nature* 431, 291–294.

Aktas, D. F., Lee, J. S., Little, B. J., Ray, R. I., Davidova, I. A., and Lyles, C. N. (2010). Anaerobic metabolism of biodiesel and its impact on metal corrosion. *Energ. Fuels* 24, 2924–2928.

Atlas, R. M. (1981). Microbial degradation of petroleum hydrocarbons: an environmental perspective. *Microbiol. Rev.* 45, 180–209.

Beller, H. R., Kane, S. R., Legler, T. C., McKelvie, J. R., Lollar, B. S., Pearson, F., et al. (2008). Comparative assessments of benzene, toluene, and xylene natural attenuation by quantitative polymerase chain reaction analysis of a catabolic gene, signature metabolites, and compound-specific isotope analysis. *Environ. Sci. Technol.* 42, 6065–6072.

Beller, H. R., and Spormann, A. M. (1997). Anaerobic activation of toluene and o-xylene by addition to fumarate in denitrifying strain T. *J. Bacteriol.* 179, 670–676.

Biddle, J. F., Fitz-Gibbon, S., Schuster, S. C., Brenchley, J. E., and House, C. H. (2008). Metagenomic signatures of the Peru Margin subseafloor biosphere show a genetically distinct environment. *Proc. Natl. Acad. Sci. U.S.A.* 105, 10583–10588.

Biddle, J. F., White, J. R., Teske, A. P., and House, C. H. (2011). Metagenomics of the subsurface Brazos-Trinity Basin (IODP site 1320): comparison with other sediment and pyrosequenced metagenomes. *ISME J.* 5, 1038–1046.

Biegert, T., Fuchs, G., and Heider, J. (1996). Evidence that anaerobic oxidation of toluene in the denitrifying bacterium *Thauera aromatica* is initiated by formation of benzylsuccinate from toluene and fumarate. *Euro. J. Biochem.* 238, 661–668.

Boll, M., and Heider, J. (2010). "Anaerobic degradation of hydrocarbons: mechanisms of C–H-bond activation in the absence of oxygen," in *Handbook of Hydrocarbon and Lipid Microbiology,* eds K. Timmis, T. Mcgenity, J. Van Der Meer, and V. De Lorenzo (Berlin: Springer-Verlag), 1011–1024.

Callaghan, A. V., Davidova, I. A., Savage-Ashlock, K., Parisi, V. A., Gieg, L. M., Suflita, J. M., et al. (2010). Diversity of benzyl- and alkylsuccinate synthase genes in hydrocarbon-impacted environments and enrichment cultures. *Environ. Sci. Technol.* 44, 7287–7294.

Callaghan, A. V., Morris, B. E. L., Pereira, I. A. C., McInerney, M. J., Austin, R. N., Groves, J. T., et al. (2012). The genome sequence of *Desulfatibacillum alkenivorans* AK-01: a blueprint for anaerobic alkane oxidation. *Environ. Microbiol.* 14, 101–113.

Callaghan, A. V., Wawrik, B., Ní Chadhain, S. M., Young, L. Y., and Zylstra, G. J. (2008). Anaerobic alkane-degrading strain AK-01 contains two alkylsuccinate synthase genes. *Biochem. Biophys. Res. Commun.* 366, 142–148.

Colwell, R. K. (2006). *EstimateS: Statistical Estimation of Species Richness and Shared Species for Samples*, Version 8. Available at: http://purl.oclc.org/estimates

Davidova, I. A., Gieg, L. M., Nanny, M., Kropp, K. G., and Suflita, J. M. (2005). Stable isotopic studies of n-alkane metabolism by a sulfate-reducing bacterial enrichment culture. *Appl. Environ. Microbiol.* 71, 8174–8182.

D'Hondt, S., Jørgensen, B. B., Miller, D. J., Batzke, A., Blake, R., Cragg, B. A., et al. (2004). Distributions of microbial activities in deep subseafloor sediments. *Science* 306, 2216–2221.

D'Hondt, S., Spivack, A. J., Pockalny, R., Ferdelman, T. G., Fischer, J. P., Kallmeyer, J., et al. (2009). Subseafloor sedimentary life in the South Pacific Gyre. *Proc. Natl. Acad. Sci. U.S.A.* 106, 11651–11656.

dos Santos, V., Sabirova, J., Timmis, K., Yakimov, M., and Golyshin, P. (2010). "*Alcanivorax borkumensis*," in *Handbook of Hydrocarbon and Lipid Microbiology*, eds K. Timmis, T. Mcgenity, J. Van Der Meer, and V. De Lorenzo.(Berlin: Springer-Verlag), 1011–1024.

Duncan, K. E., Gieg, L. M., Parisi, V. A., Tanner, R. S., Tringe, S. G., Bristow, J., et al. (2009). Biocorrosive thermophilic microbial communities in Alaskan North Slope oil facilities. *Environ. Sci. Technol.* 43, 7977–7984.

Egland, P. G., Pelletier, D. A., Dispensa, M., Gibson, J., and Harwood, C. S. (1997). A cluster of bacterial genes for anaerobic benzene ring biodegradation. *Proc. Nat. Acad. Sci. U.S.A.* 94, 6484–6489.

Elshahed, M. S., Gieg, L. M., McInerney, M. J., and Suflita, J. M. (2001). Signature metabolites attesting to the in situ attenuation of alkylbenzenes in anaerobic environments. *Environ. Sci. Technol.* 35, 682–689.

Fritsche, W., and Hofrichter, M. (2008). "Aerobic degradation by microorganisms," in *Biotechnology: Environmental Processes II*, Vol. 11b, 2nd Edn, eds H. J. Rehm and G. Reed (Weinheim: Wiley-VCH Verlag GmbH), 146–164.

Gieg, L. M., and Suflita, J. M. (2005). "Metabolic indicators of anaerobic hydrocarbon biodegradation in petroleum-laden environments," in *Petroleum Microbiology*, eds B. Ollivier, and M. Magot (Washington, DC: ASM Press), 356–371.

Grundmann, O., Behrends, A., Rabus, R., Amann, J., Halder, T., Heider, J., et al. (2008). Genes encoding the candidate enzyme for anaerobic activation of n-alkanes in the denitrifying bacterium, strain HxN1. *Environ. Microbiol.* 10, 376–385.

Haddock, J. D. (2010). "Aerobic degradation of aromatic hydrocarbons: enzyme structures and catalytic mechanisms," in *Handbook of Hydrocarbon and Lipid Microbiology,* eds K. Timmis, T. Mcgenity, J. Van Der Meer, and V. De Lorenzo (Berlin: Springer-Verlag), 1057–1069.

Hara, A., Syutsubo, K., and Harayama, S. (2003). *Alcanivorax* which prevails in oil-contaminated seawater exhibits broad substrate specificity for alkane degradation. *Environ. Microbiol.* 5, 746–753.

Harayama, S., Kishira, H., Kasai, Y., and Shutsubo, K. (1999). Petroleum biodegradation in marine environments. *J. Mol. Microbiol. Biotechnol.* 1, 63–70.

Hazen, T. C., Dubinsky, E. A., Desantis, T. Z., Andersen, G. L., Piceno, Y. M., Singh, N., et al. (2010). Deep-sea oil plume enriches indigenous oil-degrading bacteria. *Science* 330, 204–208.

Head, I. M., Jones, D. M., and Röling, W. F. M. (2006). Marine microorganisms make a meal of oil. *Nat. Rev. Microbiol.* 4, 173–182.

Hu, Y., Fu, C., Yin, Y., Cheng, G., Lei, F., Yang, X., et al. (2010). Construction and preliminary analysis of a deep-sea sediment metagenomic fosmid library from Qiongdongnan Basin, South China Sea. *Mar. Biotechnol.* 12, 719–727.

Jernelov, A., and Linden, O. (1981). Ixtoc I: a case study of the world's largest oil spill. *Ambio* 10, 299–306.

Jones, D., Head, I., Gray, N., Adams, J., Rowan, A., Aitken, C., et al. (2007). Crude-oil biodegradation via methanogenesis in subsurface petroleum reservoirs. *Nature* 451, 176–180.

Jørgensen, B. B. (2011). Deep subseafloor microbial cells on physiological standby. *Proc. Natl. Acad. Sci. U.S.A.* 108, 18193–18194.

Joye, S. B., Boetius, A., Orcutt, B. N., Montoya, J. P., Schulz, H. N., Erickson, M. J., et al. (2004). The anaerobic oxidation of methane and sulfate reduction in sediments from Gulf of Mexico cold seeps. *Chem. Geol.* 205, 219–238.

Kallmeyer, J., Pockalny, R., Adhikari, R. R., Smith, D. C., and D'Hondt, S. (2012). Global distribution of microbial abundance and biomass in subseafloor sediment. *Proc. Natl. Acad. Sci. U.S.A.* 109, 16213–16216.

Kasai, Y., Kishira, H., Syutsubo, K., and Harayama, S. (2001). Molecular detection of marine bacterial populations on beaches contaminated by the Nakhodka tanker oil-spill accident. *Environ. Microbiol.* 3, 246–255.

Kessler, J. D., Valentine, D. L., Redmond, M. C., Du, M., Chan, E. W., Mendes, S. D., et al. (2011). A persistent oxygen anomaly reveals the fate of spilled methane in the deep Gulf of Mexico. *Science* 331, 312–315.

Kim, S., and Kwon, K. (2010). "Marine, hydrocarbon-degrading Alphaproteobacteria," in *Handbook of Hydrocarbon and Lipid Microbiology,* eds K. Timmis, T. Mcgenity, J. Van Der Meer, and V. De Lorenzo (Berlin: Springer-Verlag), 1707–1714.

Kropp, K. G., Davidova, I. A., and Suflita, J. M. (2000). Anaerobic oxidation of n-dodecane by an addition reaction in a sulfate-reducing bacterial enrichment culture. *Appl. Environ. Microbiol.* 66, 5393–5398.

Kumar, S., Nei, M., Dudley, J., and Tamura, K. (2008). MEGA: a biologist-centric software for evolutionary analysis of DNA and protein sequences. *Brief. Bioinform.* 9, 299–306.

Leuthner, B., Leutwein, C., Schulz, H., Hörth, P., Haehnel, W., Schiltz, E., et al. (1998). Biochemical and genetical characterization of benzylsuccinate synthase from *Thauera aromatica*: a new glycyl radical enzyme catalyzing the first step in anaerobic toluene metabolism. *Mol. Microbiol.* 28, 615–628.

Lloyd, K. G., Albert, D. B., Biddle, J. F., Chanton, J. P., Pizarro, O., and Teske, A. (2010). Spatial structure and activity of sedimentary microbial communities underlying a *Beggiatoa* spp. mat in a Gulf of Mexico hydrocarbon seep. *PLoS ONE* 5:e8738. doi: 10.1371/journal.pone.0008738

Lloyd, K. G., Lapham, L., and Teske, A. (2006). An anaerobic methane-oxidizing community of ANME-1b archaea in hypersaline Gulf of Mexico sediments. *Appl. Environ. Microbiol.* 72, 7218–7230.

Lovley, D. R., Giovannoni, S. J., White, D. C., Champine, J. E., Phillips, E. J. P., Gorby, Y. A., et al. (1993). Geobacter metallireducens gen. nov. sp. nov.,

a microorganism capable of coupling the complete oxidation of organic compounds to the reduction of iron and other metals. *Arch. Microbiol.* 159, 336–344.

Mason, O. U., Hazen, T. C., Borglin, S., Chain, P. S. G., Dubinsky, E. A., Fortney, J. L., et al. (2012). Metagenome, metatranscriptome and single-cell sequencing reveal microbial response to Deepwater Horizon oil spill. *ISME J.* 6, 1715–1727.

Meyer, F., Paarmann, D., D'souza, M., Olson, R., Glass, E. M., Kubal, M., et al. (2008). The metagenomics RAST server – a public resource for the automatic phylogenetic and functional analysis of metagenomes. *BMC Bioinformatics* 9:386. doi: 10.1186/1471-2105-9-386

Muyzer, G., De Waal, E. C., and Uitterlinden, A. G. (1993). Profiling of complex microbial populations by denaturing gradient gel electrophoresis analysis of polymerase chain reaction-amplified genes coding for 16S rRNA. *Appl. Environ. Microbiol.* 59, 695–700.

Oka, A. R., Phelps, C. D., Zhu, X., Saber, D. L., and Young, L. (2011). Dual biomarkers of anaerobic hydrocarbon degradation in historically contaminated groundwater. *Environ. Sci. Technol.* 45, 3407–3414.

Operational Science Advisory Team. (2010). *Summary Report for Sub-Sea and Sub-Surface Oil and Dispersant Detection: Sampling and Monitoring. December* 17, 2010.

Orcutt, B. N., Joye, S. B., Kleindienst, S., Knittel, K., Ramette, A., Reitz, A., et al. (2010). Impact of natural oil and higher hydrocarbons on microbial diversity, distribution, and activity in Gulf of Mexico cold-seep sediments. *Deep Sea Res. Part 2 Top. Stud. Oceanogr.* 57, 2008–2021.

Parisi, V. A., Brubaker, G. R., Zenker, M. J., Prince, R. C., Gieg, L. M., Da Silva, M. L. B., et al. (2009). Field metabolomics and laboratory assessments of anaerobic intrinsic bioremediation of hydrocarbons at a petroleum-contaminated site. *Microb. Biotechnol.* 2, 202–212.

Ramseur, J. L. (2010). *Deepwater Horizon Oil Spill: the Fate of the Oil*. Washington, DC: Congressional Research Service.

Rojo, F. (2010). "Enzymes for aerobic degradation of alkanes," in *Handbook of Hydrocarbon and Lipid Microbiology*, eds K. Timmis, T. Mcgenity, J. Van Der Meer, and V. De Lorenzo (Berlin: Springer-Verlag), 781–797.

Schneiker, S., Martins Dos Santos, V., Bartels, D., Bekel, T., Brecht, M., Buhrmester, J., et al. (2006). Genome sequence of the ubiquitous hydrocarbondegrading marine bacterium *Alcanivorax borkumensis*. *Nat. Biotechnol.* 24, 997–1004.

Seth-Smith, H. (2010). 'Slick' operations. *Nat. Rev. Microbiol.* 8, 538.

So, C. M., and Young, L. (1999). Isolation and characterization of a sulfate-reducing bacterium that anaerobically degrades alkanes. *Appl. Environ. Microbiol.* 65, 2969–2976.

Wawrik, B., Mendivelso, M., Parisi, V. A., Suflita, J. M., Davidova, I. A., Marks, C. R., et al. (2012). Field and laboratory studies on the bioconversion of coal to methane in the San Juan Basin. *FEMS Microbiol. Ecol.* 81, 26–42.

Widdel, F., and Grundmann, O. (2010). "Biochemistry of the anaerobic degradation of non-methane alkanes," in *Handbook of Hydrocarbon and Lipid Microbiology*, eds K. Timmis, T. Mcgenity, J. Van Der Meer, and V. De Lorenzo (Berlin: Springer-Verlag), 909–924.

Widdel, F., Knittel, K., and Galushko, A. (2010). "Anaerobic hydrocarbon-degrading microorganisms: an overview," in *Handbook of Hydrocarbon and Lipid Microbiology*, eds K. Timmis, T. Mcgenity, J. Van Der Meer and V. De Lorenzo (Berlin: Springer-Verlag), 1997–2021.

Yagi, J. M., Suflita, J. M., Gieg, L. M., DeRito, C. M., Jeon, C. O., and Madsen, E. L. (2010). Subsurface cycling of nitrogen and anaerobic aromatic hydrocarbon biodegradation revealed by nucleic acid and metabolic biomarkers. *Appl. Environ. Microbiol.* 76, 3124–3134.

Yakimov, M. M., Denaro, R., Genovese, M., Cappello, S., D'Auria, G., and Chernikova, T. N., et al. (2005). Natural microbial diversity in superficial sediments of Milazzo Harbor (Sicily) and community successions during microcosm enrichment with various hydrocarbons. *Environ. Microbiol.* 7, 1426-1441.

Yakimov, M. M., Golyshin, P. N., Lang, S., Moore, E. R. B., Abraham, W. R., Lünsdorf, H., et al. (1998). *Alcanivorax borkumensis* gen. nov., sp. nov., a new, hydrocarbon-degrading and surfactant-producing marine bacterium. *Int. J. Syst. Bacteriol.* 48, 339–348.

Conflict of Interest Statement: The authors declare that the research was conducted in the absence of any commercial or financial relationships that could be construed as a potential conflict of interest.

Received: 17 December 2012; accepted: 21 February 2013; published online: 15 March 2013.

Citation: Kimes NE, Callaghan AV, Aktas DF, Smith WL, Sunner J, Golding BT, Drozdowska M, Hazen TC, Suflita JM and Morris PJ (2013) Metagenomic analysis and metabolite profiling of deep-sea sediments from the Gulf of Mexico following the Deepwater Horizon oil spill. Front. Microbiol. ***4****:50. doi: 10.3389/fmicb.2013.00050*

This article was submitted to Frontiers in Microbiological Chemistry, a specialty of Frontiers in Microbiology.

frontiers in
MICROBIOLOGY

ORIGINAL RESEARCH ARTICLE
published: 10 May 2013
doi: 10.3389/fmicb.2013.00109

Identity and mechanisms of alkane-oxidizing metalloenzymes from deep-sea hydrothermal vents

Erin M. Bertrand[1,2], Ramaydalis Keddis[3,4], John T. Groves[5], Costantino Vetriani[3,4] and Rachel Narehood Austin[1]*

[1] *Department of Chemistry, Bates College, Lewiston, ME, USA*
[2] *Microbial and Environmental Genomics, J. Craig Venter Institute, San Diego, CA, USA*
[3] *Department of Biochemistry and Microbiology, Rutgers University, New Brunswick, NJ, USA*
[4] *Institute of Marine and Coastal Sciences, Rutgers University, New Brunswick, NJ, USA*
[5] *Department of Chemistry, Princeton University, Princeton, NJ, USA*

Edited by:
Amy V. Callaghan, University of Oklahoma, USA

Reviewed by:
Eric Boyd, Montana State University, USA
John W. Moreau, University of Melbourne, Australia

****Correspondence:***
Rachel Narehood Austin, Department of Chemistry, Bates College, 5 Andrews Rd., Lewiston, 04240 ME, USA.
e-mail: raustin@bates.edu

Six aerobic alkanotrophs (organism that can metabolize alkanes as their sole carbon source) isolated from deep-sea hydrothermal vents were characterized using the radical clock substrate norcarane to determine the metalloenzyme and reaction mechanism used to oxidize alkanes. The organisms studied were *Alcanivorax* sp. strains EPR7 and MAR14, *Marinobacter* sp. strain EPR21, *Nocardioides* sp. strains EPR26w, EPR28w, and *Parvibaculum hydrocarbonoclasticum* strain EPR92. Each organism was able to grow on *n*-alkanes as the sole carbon source and therefore must express genes encoding an alkane-oxidizing enzyme. Results from the oxidation of the radical-clock diagnostic substrate norcarane demonstrated that five of the six organisms (EPR7, MAR14, EPR21, EPR26w, and EPR28w) used an alkane hydroxylase functionally similar to AlkB to catalyze the oxidation of medium-chain alkanes, while the sixth organism (EPR92) used an alkane-oxidizing cytochrome P450 (CYP)-like protein to catalyze the oxidation. DNA sequencing indicated that EPR7 and EPR21 possess genes encoding AlkB proteins, while sequencing results from EPR92 confirmed the presence of a gene encoding CYP-like alkane hydroxylase, consistent with the results from the norcarane experiments.

Keywords: alkanotrophs, hydrocarbon oxidation, deep-sea hydrothermal vents, alkanes, alkane hydroxylases

INTRODUCTION

The microbial transformation of alkanes, saturated energy-rich hydrocarbons, is significant for a number of reasons (Das and Chandran, 2011). Alkanes are a major constituent of petroleum and natural gas and are a primary energy source for human society. Alkanes are toxic to some microorganisms and a source of energy and carbon for others, including, perhaps, ancient organisms from which life arose (Kobayashi and Yanagawa, 2002). The selective activation of carbon-hydrogen bonds, necessary for microbial alkane transformation, is one of the most energetically difficult processes accomplished in nature (Borovik, 2011). Understanding biological alkane activation could yield insight into new methods for industrial production of valuable materials and improve our understanding of molecular level processes underpinning the global carbon cycle (Bosetti et al., 1992; Shilov and Shul'pin, 1997; Baik et al., 2003; Groves, 2006; Que and Tolman, 2008).

Alkanes originate from a variety of sources, the largest of which are biogenic (McCollom, 2013). These biogenic sources include thermogenesis, the geochemical processing of decaying plant and algal matter, as well as direct production by living organisms (Volkman, 2006). There are also abiotic sources of alkanes (Parson et al., 1995; Sherwood Lollar et al., 2002). Methane and other low molecular weight alkanes are produced abiogenically through water-rock interactions under conditions of high temperature and pressure and are discharged through fractures in places like hard rock mines and oceanic thermal vents (Lancet and Anders, 1970; Parson et al., 1995; Sherwood Lollar et al., 2002). In hydrothermal systems, abiotic synthesis of hydrocarbons may involve Fisher-Tropsch reactions and the serpentinization of ultramafic rocks (Lancet and Anders, 1970; Berndt et al., 1996; McCollom et al., 1999). In general, abiotic synthesis is thought to contribute relatively small amounts of alkanes to the global stock, though it may be a significant source in geothermal environments (Sherwood Lollar et al., 2002; Proskurowski et al., 2008). There have been some suggestions that such abiogenically produced hydrocarbons could have played a role in the origin and evolution of early life (Martin et al., 2008).

Alkane oxidation has evolved in a variety of organisms both as a strategy for hydrocarbon detoxification and to harness the carbon and energy stored in alkanes (Hanson and Thomas, 1996; Van Beilen et al., 2003; Van Beilen and Enrico, 2005; Hakemian and Rosenzweig, 2007). Hydrocarbonoclastic bacteria are those that can utilize hydrocarbons as their sole source of carbon and energy. In surface waters, they have been identified as

members of the genera *Alcanivorax, Marinobacter, Cycloclasticus, Neptunomonas, Oleiphilus, Oleispira,* and *Planococcus* (Harayama et al., 1999; Yakimov et al., 2004; Wang and Shao, 2012b; Viggor et al., 2013). Members of the *Parvibaculum* species may be involved in the global cycling of alkanes, as well as other anthropogenic pollutants (Schleheck et al., 2011). Though aerobic alkane metabolism involves many steps (Van Beilen et al., 2003) the initial oxidation, which involves breaking a strong non-polar C–H bond, is the chemically most challenging and intriguing (Marquez-Rocha et al., 2005; Nakano et al., 2011; Al-Awadhi et al., 2012; Sun et al., 2012).

Eight different families of aerobic alkane-oxidizing enzymes have been identified in marine bacteria (Austin and Groves, 2011). Methane is oxidized primarily by particulate methane monooxygenase (pMMO), encoded by the *pmo* genes (Hanson and Thomas, 1996; Hakemian and Rosenzweig, 2007; Rosenzweig, 2011) although soluble methane monooygenase (sMMO) has been shown to be functional in a few instances (Hakemian and Rosenzweig, 2007). Propane (pMO) and butane monooxygenases (bMO) have both been identified in microorganisms that can metabolize short chain alkanes (Sluis et al., 2002; Arp et al., 2007; Cooley et al., 2009; Redmond et al., 2010). Medium chain (C_5–C_{22}) alkanes are oxidized by particulate alkane hydroxylases (pAHs, e.g., AlkB) and/or cytochrome P450/CYP153 enzymes (Smits et al., 1999, 2002; Van Beilen et al., 2006; Van Beilen and Funhoff, 2007). Recently, a flavin-binding monoxygenase, encoded by the *almA* gene, has been shown to be involved in the metabolism of long chain *n*-alkanes of C_{32} and longer (Throne-Holst et al., 2006, 2007; Wang and Shao, 2012a). Another flavin-binding monooxygenase, LadA, has also been identified (Li et al., 2008). Information about the active site structures of these enzymes and their presumed mechanisms has been recently reviewed (Austin and Groves, 2011).

Though biotic alkane hydroxylation occurs in a wide range of environments (Das and Chandran, 2011), the implications of alkane hydroxylase activity in deep-sea hydrothermal vents are of particular interest. Deep-sea hydrothermal vents are found at sites of seafloor spreading at mid-ocean ridges as well as at other tectonically active regions, such as hot spot volcanoes and back-arc spreading centers (Simoneit, 1993; Van Dover, 2000). Some hydrothermal vent fluids contain high to moderate amounts of hydrocarbons, including *n*-alkanes (Whelan and Hunt, 1983; Whelan et al., 1988; Simoneit, 1993; Higashihara et al., 1997). For instance, medium-chain *n*-alkanes (between *n*-C_{13} and *n*-C_{21}), were found to be 100 to 400 times more concentrated in warm fluids venting from fissures in basalt on the East Pacific Rise (EPR) than in the surrounding seawater (Brault et al., 1988). Furthermore, more recent studies revealed the presence of hydrocarbons derived from thermogenic processes in higher temperature portions of the subsurface reaction zone in geothermal systems off the coast of New Zealand and on the Juan de Fuca Ridge (Botz et al., 2002; Cruse and Seewald, 2006).

These hydrothermal fluids are generally highly reducing and anoxic, but when they mix with colder, oxygenated water, steep thermal and redox gradients are generated (Perner et al., 2012). These gradients are exploited by microbes and support complex ecosystems surrounding hydrothermal vents. The oxidation of methane and other short chain alkanes is an important metabolism in vent environments and has been shown to aid in supporting higher trophic levels (Fujiwara et al., 2000). The anaerobic oxidation of methane in vent sediments it has been shown to be a powerful driver of carbon cycling (Wankel et al., 2012). Sulfate-reducing bacteria from sediments in the Gulf of Mexico and Guaymas Basin have been shown to anaerobically oxidize short alkanes (Kniemeyer et al., 2007). Additionally, *pmo* transcripts were found to be abundant in vent plumes and deep water sites, suggesting that methane oxidation is important in the aerated water column as well (Lesniewski et al., 2012). However, while organisms that oxidize mid or long -chain ($>C_6$) alkanes have been isolated from hydrothermal vent environments, including both plume water and sediments, our knowledge of the diversity and ecological role of $>C_6$ alkane oxidizers in these environments remains limited (Bazylinski et al., 1989; Rosario-Passapera et al., 2012). Given that marine microbes are less well-characterized than their terrestrial counterparts, it is possible that new enzymes and possibly even new chemical approaches to converting alkanes to alcohols may be found in vent environments (Harayama et al., 1999; Harayama and Hara, 2004).

In this paper we examine the reaction mechanisms of alkane hydroxylation in six different bacteria isolated from deep-sea vents that were able to grow on mid-chain (C_8–C_{16}) alkanes as their sole carbon source, using a diagnostic substrate, bicyclo[4.1.0]heptane (norcarane). Enzymatic oxidation of norcarane generates different products depending on the reaction mechanism employed by the enzyme. As such, norcarane oxidation studies are able to functionally distinguish between AlkB and cytochromes P450 (CYP) in purified enzymes as well as in whole-cell bioassays and it is described as a "diagnostic substrate" for this reason (Rozhkova-Novosad et al., 2007).

Norcarane can be hydroxylated in three different ways; each creates a different distribution of oxidized products (Austin et al., 2000). Homolytic bond cleavage creates a substrate-based radical intermediate, while heterolytic bond cleavage creates a carbon-centered cationic intermediate. When homolytic bond cleavage at the carbon α to the cyclopropyl group occurs, a carbon radical is generated. This enables the three-membered carbon ring to open, relieving ring strain. The norcarane ring opens with an internal rearrangement rate of $2 \times 10^8\ s^{-1}$ (Austin et al., 2000, 2006). Internal molecular rearrangement occurs while the enzyme is carrying out the next step in the catalytic cycle, the "rebound step" where "OH." combines with the substrate radical to form an alcohol. The rate of this enzyme-specific step is termed the "rebound rate." The rebound rate can be calculated from the ratio of the concentration of unrearranged alcohol products (at the 2-position only) generated during oxidation to the concentration of rearranged products multiplied by the intramolecular rearrangement rate for the molecule itself (Equation 1). The average lifetime of the substrate radical is given by the reciprocal of the rebound rate. Using this approach, norcarane has yielded valuable information about enzyme active site structure and function for cytochrome P450 enzymes (Auclair et al., 2002), alkane monooxygenase AlkB (Austin et al., 2000; Cooper et al., 2012; Naing et al., 2013), xylene monooxygenase(Austin et al., 2003),

toluene monooxygenase (Moe et al., 2004) as well as soluble methane monooxygenase (Brazeau et al., 2001).

Equation 1. Enzyme rebound rate constant and radical lifetime.

$$k_{\text{rebound rate constant}} = k_{\text{rearrangement}} \left(\frac{[\text{ring closed}]}{[\text{ring opened}]} \right)$$

$$\text{radical lifetime} = \frac{1}{k_{\text{rebound}}}$$

In this work, we hypothesized that norcarane would be a substrate for these novel organisms and that identifying the products formed from its transformation would provide a means to provisionally identify the enzymes being used for alkane oxidation by vent bacteria. Our results show that both CYP and AlkB-like enzymes are functional proteins that contribute to alkane-oxidation in deep-sea hydrothermal vent bacterial isolates, suggesting that these metalloenzymes may be of importance in hydrothermal vent ecosystems.

MATERIALS AND METHODS

CHEMICALS

Chemicals and solvents were purchased from Sigma–Aldrich Corp. (St. Louis, MO) or BioRad (Hercules, CA). The diagnostic substrate bicyclo [4.1.0] heptane (norcarane), was synthesized and purified following published procedures (Smith and Simmons, 1973). Product standards were characterized on a Bruker Advance™ 400 MHz Nuclear Magnetic Resonance (NMR) Spectrometer at ambient temperature.

ORGANISMS

Hydrothermal fluids were collected from diffuse flow deep-sea vents located on the EPR and the Mid-Atlantic Ridge (MAR). The fluids were collected using titanium samplers operated by the manipulator of the Deep-Submergence Vehicle *Alvin*. In the laboratory, 1 ml aliquots of fluid were inoculated into 10 ml of Artificial Sea Water Minimal Medium (ASW MM) (Crespo-Medina et al., 2009). Each tube was then supplemented with dodecane ($C_{12}H_{26}$) in the vapor phase as the only carbon and energy source and was incubated at various temperatures (**Table 1**). Pure cultures were isolated by successive transfers of single colonies on ASW MM/dodecane solidified with Noble agar (Sigma). Once the isolation of pure cultures was completed, the ability of the isolates to grow in complex Artificial Sea Water Medium (ASW; l^{-1}: NaCl, 24 g; KCl, 0.7 g; MgCl, 7.0 g, yeast extract, 3.0 g; peptone, 2.5 g) was tested. All six hydrothermal vent isolates were able to grow in complex ASW medium. However, for the purpose of the experiments described here, the six hydrothermal vent isolates (EPR7, EPR21, EPR26w, EPR28w, MAR14, EPR92) were grown aerobically on alkanes as the sole carbon

Table 1 | Characteristics of hydrothermal vent isolates.

Isolate	EPR7	EPR21	ERP26w, 28w	MAR14	EPR92
Temp range (°C)	37–45	28–37	28–30	28–30	20–40
Genus of closest characterized relative (16S rRNA gene accession No; Sequence identity)	*Alcanivorax dieselolei* (EF647617; 99%)	*Marinobacter* sp. (AY196982; 99%)	*Nocardioides* sp. (HM222686; 99%)	*Alcanivorax borkumensis* (NR074890; 99%)	*Parvibaculum hydrocarbonoclasticum* DSM 23209[a], (GU574708; 100%)
Type of sample, vent site, location	Diffuse flow vent, Mk119, East Pacific Rise (EPR), 9° N, 104° W	Diffuse flow vent, Mk119, EPR, 9° N, 104° W	Diffuse flow vent, Mk119, EPR, 9° N, 104° W	Diffuse flow vent, Lucky Strike, Mid-Atlantic Ridge (MAR), 37° N, 32° W	Diffuse flow vent EPR, Tica, 9° N, 104° W
Collection date	May 1999	May 1999	May 1999	July 2001	April 2004
Depth of vent site	2500 m	2500 m, 1 m above source	2500 m, 1 m above source	1700 m	2513 m
Culture T (°C)	37°C	37°C	28–30°C	28–30°C	35°C
Ability to grow in complex ASW medium	Yes	Yes	Yes	Yes	Yes
n-alkane substrate tested	Octane, dodecane, hexadecane	Dodecane	Dodecane	Dodecane	Octane, dodecane, hexadecane
Detection of the gene for *n*-alkane oxidation	*alkB*	*alkB*	ND	ND	*cyp*

[a] *Described in Rosario-Passapera et al. (2012).*

"ND" denotes no data available.

source in ASW MM at the appropriate temperature (**Table 1**) at 300 rpm for up to 1 week, subcultured into fresh media and then were allowed to grow to an optical density (OD) near 0.1. The diagnostic substrate was then introduced in the vapor phase (30–50 μL in 50 mL) to the growing cultures via a hanging bulb apparatus, as previously described (Bertrand et al., 2005). An OD of 0.1 was chosen for metabolic analysis because cultures at this density were in exponential growth phase (data not shown). The cultures were incubated at their appropriate temperatures at 300 rpm for 4–18 h.

In all cases, after the incubation was completed, the supernatant, composed of growth media and compounds produced in cellular metabolism, was collected by centrifugation (8000×g, 15 min), extracted three times with ethyl acetate, concentrated, and the products assayed directly by GC-MS. Control experiments in which all the reaction components were added to the media except for the organisms, were also done to control for abiotic substrate oxidation.

MASS SPECTROMETRY

GC-MS analyses were performed on an Agilent 689N Network GC system with a 6890N Series Injector and 5973N Network Mass selective detector with a HP-5MS crosslinked 5% PH ME Siloxane capillary column (dimensions of 30 m × 0.25 mm × 0.25 μm). Various methods were utilized, but generally the injection temperature was 225°C, and the initial oven temperature was 50°C. Both split and splitless injections were done to optimize peak shape and product detection respectively. The typical GC method ramped the oven to a final temperature of 220°C with a ramp rate of 10°C/min. Authentic products were synthesized and their retention times and fragmentation patterns compared to those of the identified peaks in the GC-MS spectra.

DNA ISOLATION, PCR AND PHYLOGENETIC ANALYSES

Genomic DNA was extracted from cells collected by centrifugation using the UltraClean™ Microbial DNA isolation kit, according to the manufacturer's instructions (MoBio Laboratories). The 16S rRNA, *alkB*, and *cyp153* genes were selectively amplified from the genomic DNA by PCR, sequenced and subjected to phylogenetic analyses as described previously (Vetriani et al., 2004; Crespo-Medina et al., 2009; Pérez-Rodríguez et al., 2010; Rosario-Passapera et al., 2012).

RESULTS

CHARACTERIZATION OF HYDROCARBONOCLASTIC BACTERIA

Phylogenetic analysis of the 16S rRNA gene of the six alkane-oxidizing bacteria used in this study placed them in three different taxonomic groups. **Figure 1** shows a 16S rRNA gene-based tree illustrating these relationships. Strains EPR 7, MAR14, and EPR21 are *Gammaproteobacteria* of the genus *Alcanivorax* (EPR7 and MAR14) and *Marinobacter* (EPR21), EPR 26w and 28w are *Actinobacteria* related to the *Nocardioides* and strain EPR92 is an *Alphaproteobacterium* that has been recently described as a new species of the genus *Parvibaculum*, *P. hydrocarbonoclasticum* (Rosario-Passapera et al., 2012). **Table 1** summarizes the main characteristics of the bacteria used in this study. PCR amplification of the genes putatively involved in the oxidation of *n*-alkanes in three of the six strains used in this study showed that *Alcanivorax* sp. strain EPR7 and *Marinobacter* sp. strain EPR21 encoded for the AlkB alkane hydroxylase, while *P. hydrocarbonoclasticum* strain EPR92 encoded for CYP (Rosario-Passapera et al., 2012). **Figure 2** shows a phylogenetic tree inferred from AlkB amino acid sequences that shows the position of the alkane hydroxylase from strains EPR7 and EPR21 relative to closely related enzymes.

MECHANISTIC STUDIES

Figure 3 describes products formed during enzymatic oxidation of norcarane, which are used here to characterize alkane oxidation mechanisms in strains EPR7, EPR21, EPR26w, EPR28w, MAR14, and EPR92. **Figure 4** shows the calculated radical lifetime determined from the oxidation of norcarane by these strains, demonstrating that EPR7, 21, 26w, 28w, and MAR14 are all using AlkB-like enzymes to oxidize alkanes. This is clear from the substantial amount of rearranged alcohols detected with these assays (radical lifetimes of 3.9, 4.8, 2.4, 2.4, and 4.6 ns respectively), which is the signature for the AlkB enzyme (Austin et al., 2000, 2008; Bertrand et al., 2005; Cooper et al., 2012; Naing et al., 2013). DNA analysis, described in section "Characterization of Hydrocarbonoclastic Bacteria," confirms that EPR7 and EPR21 contain an *alkB* gene. EPR92, in contrast, is using a CYP-like enzyme to oxidize alkanes, as evidenced by the minuscule amount of rearranged alcohols, which leads to a very short radical lifetime (50 ps), characteristic of all CYPs that have been examined (Austin et al., 2006). DNA analysis, described above, confirms that EPR92 has a *cyp* gene. Chromatograms for GC-MS analysis of EPR92 and EPR21-catalyzed oxidation of norcarane are provided in **Figures 5** and **6**. The insert in **Figure 6** shows the fragmentation pattern for the radical ring-opened product (structure 1 in **Figure 3**).

DISCUSSION

Our study reveals two main findings. First, we describe some of the first medium-chain alkane-oxidizing mesophilic bacterial isolates from hydrothermal vent environments, suggesting that alkane oxidation could be an important component of microbial metabolism in diffuse flow vent environments. Second, we identify the enzymes responsible for this activity as well-characterized AlkB and CYP-like enzymes, suggesting that the mechanisms responsible for medium-chain alkane oxidation in the surface ocean and other environments are also active in extreme environments.

While the occurrence of petroleum hydrocarbons in deep-sea geothermal environments has been documented for over 20 years (e.g., Brault et al., 1988; Didyk and Simoneit, 1989), most of the studies on microbial oxidation of hydrocarbons in these environments are focused on short-chain alkanes (C_1–C_4; Wankel et al., 2010, 2012). Hence, our knowledge of the taxonomic, physiological, and metabolic diversity of mid-chain (C_6–C_{16}) or long-chain ($>C_{16}$) alkane-oxidizing bacteria in deep-sea geothermal environments remains very limited. An early study of microbial oxidation of hexadecane and naphthalene by bacteria isolated from deep-sea hydrothermal sediments revealed activity under aerobic

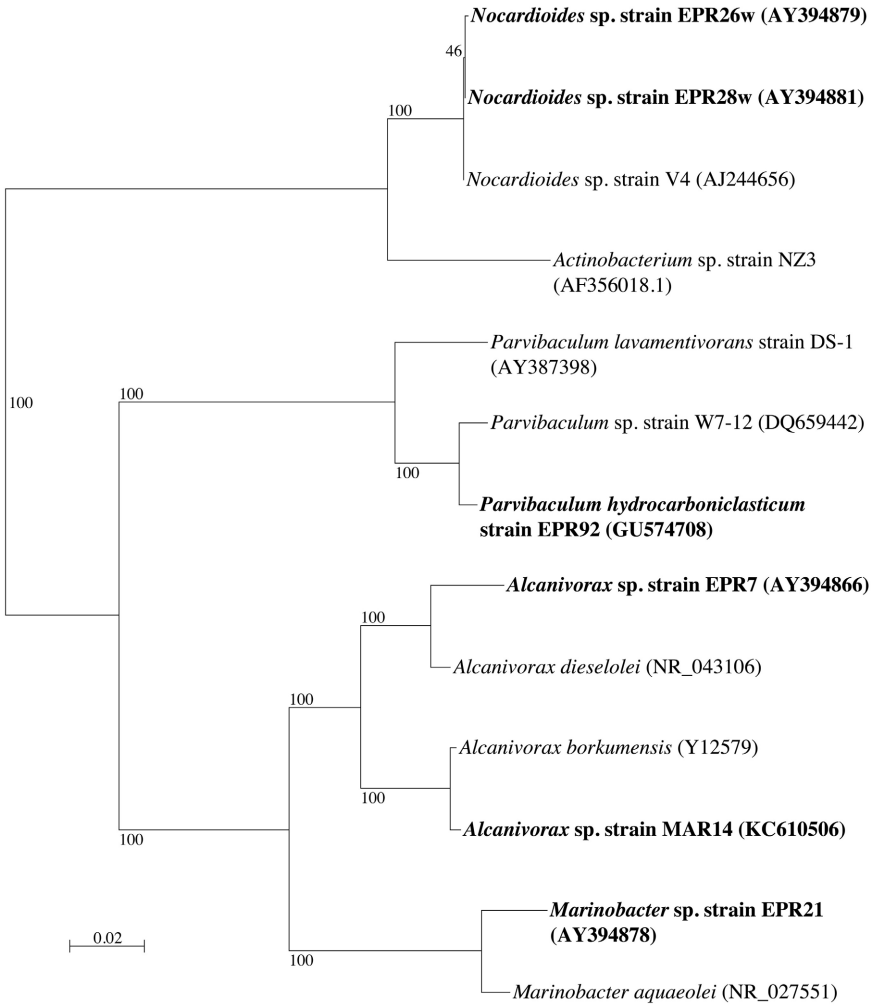

FIGURE 1 | Neighbor-joining phylogenetic tree inferred from 16S rRNA gene sequences, showing the position of the six deep-sea hydrothermal vent strains (in boldface) used in this study. The tree was constructed using Phylo_Win. Bootstrap values based on 100 replications are shown as percentages at branch nodes. Bar indicates 2% estimated substitution. Accession numbers for all strains are given in parentheses.

and mesophilic conditions (Bazylinski et al., 1989). However, neither the organisms, nor the enzymes, responsible for the oxidation of these hydrocarbons were identified in this study. More recently, the description of two mesophilic *Proteobacteria* isolated from deep-sea hydrothermal vents and capable of growth on *n*-alkanes as their sole carbon source was reported (Crespo-Medina et al., 2009; Rosario-Passapera et al., 2012). Furthermore, aerobic, hydrocarbonoclastic bacteria were isolated from deep-sea sediments collected in the Atlantic Ocean (depth: 3542 m) and in the Mediterranean Sea (depth: 2400 m). The isolates obtained in these studies were related to known genera of marine bacteria, including *Alcanivorax, Marinobacter,* and *Halomonas* spp., among others (Wang et al., 2008; Tapilatu et al., 2010). Finally, two recent culture-independent surveys of the genes encoding for the alkane hydroxylase, *alkb*, revealed the presence of these genes in bacteria from sediments collected from depths of 100–400 m and 5724 m, respectively (Xu et al., 2008; Wasmund et al., 2009). However, to our knowledge, our study is the first to probe mechanisms of alkane-oxidizing metalloenzymes from aerobic, hydrocarbonoclastic bacteria from deep-sea hydrothermal vents.

Here we also report the identification and mechanisms of the alkane-hydroxylases from of six strains of aerobic, mesophilic, hydrocarbonoclastic bacteria isolated from deep-sea hydrothermal vents. The six vent organisms belong to the genera *Alcanivorax* (EPR7 and MAR14), *Marinobacter*, (EPR21), *Nocardioides* (EPR26w and 28w) and the previously described *P. hydrocarbonoclasticum* EPR92 (Rosario-Passapera et al., 2012). We demonstrate that both AlkB and CYP are functional in these organisms, which is consistent with their taxonomic assignments and previous work describing these enzyme classes in bacteria from other environments. The apparent trend toward enzyme redundancy in each class of alkane-oxidizing enzymes, including this study, is notable. Implications for this redundancy are discussed below.

While different classes of enzymes exist that oxidize methane, propane and butane, medium chain (C_5–C_{22}) alkanes, and long

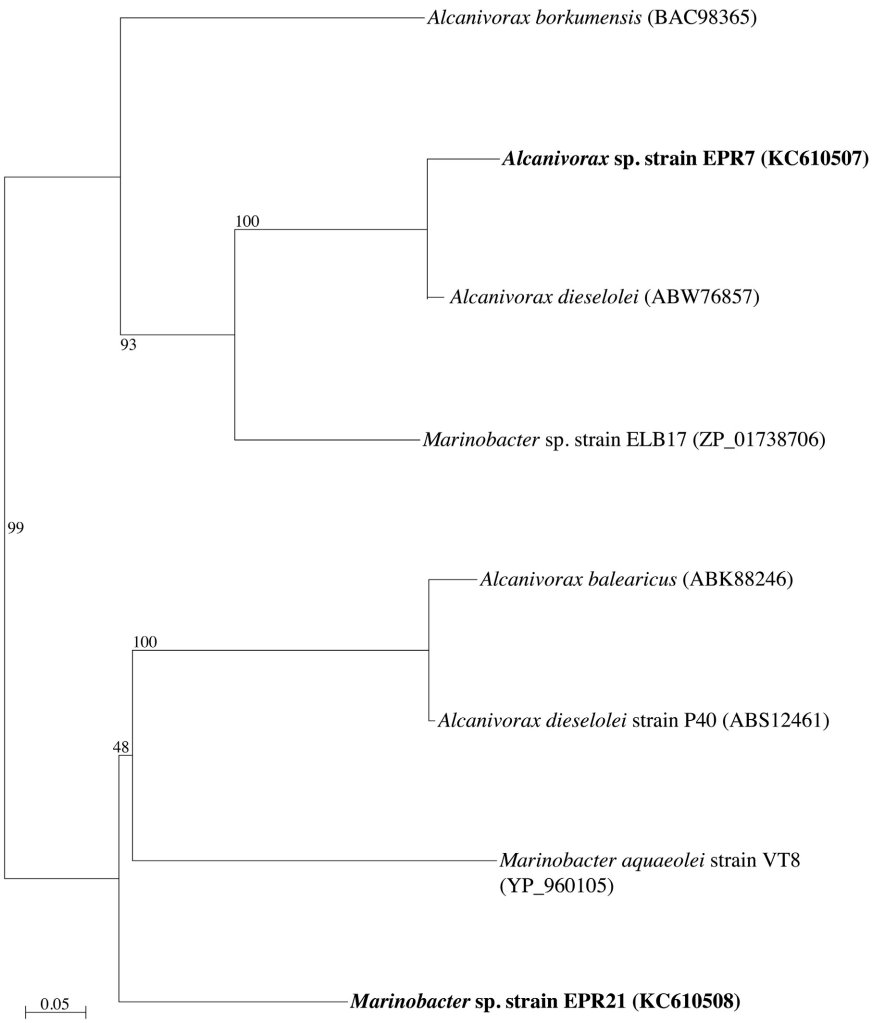

FIGURE 2 | Neighbor-joining phylogenetic tree inferred from amino acid sequences deduced from the nucleotide sequence of a fragment of the *alkB* gene (encoding for the alkane hydroxylase), showing the position of *Alcanivorax* sp. strain EPR7 and *Marinobacter* sp. strain EPR21 (in boldface). The tree was constructed using Phylo_Win. Bootstrap values based on 100 replications are shown as percentages at branch nodes. Bar indicates 5% estimated substitutions.

chain alkanes, there seems to be redundancy in most of these classes. For example, both pMMO and sMMO oxidize methane, there are both particulate and soluble propane and bMO, AlkB, and CYP both oxidize medium chain alkanes, and LadA and AlmA both oxidize long chain alkanes (Austin and Groves, 2011). Some hydrocarbonoclastic organisms appear to express only one kind of alkane-oxidizing enzyme, although they may have multiple genes encoding different isozymes of the same enzyme that could enable them to oxidize alkanes of different chain lengths (Whyte et al., 2002; Van Beilen et al., 2006; Lo Piccolo et al., 2011; Nie et al., 2013). Other organisms contain multiple different alkane-oxidizing genes (e.g., both *cyp* and *alkb*) and may express them simultaneously (Ishikawa et al., 2004; Schneiker et al., 2006; Hakemian and Rosenzweig, 2007; Liu et al., 2011; Lo Piccolo et al., 2011; Nie et al., 2013). The reason for the redundancy in microbial alkane oxidizing enzymes is not clear, nor is it clear what factors control their expression.

Possible factors that contribute to this redundancy include metal availability and subcellular enzyme localizations. Many of these alkane-degrading enzymes require metals for catalysis and their expression can be a function of metal availability. sMMO, for example, is only expressed under copper-limiting conditions (Hakemian and Rosenzweig, 2007). Butane and propane monooxygenases come in both a soluble diiron form and a particulate copper-containing form as well (Austin and Groves, 2011). AlkB and CYP are both iron containing enzymes, but AlkB requires two iron atoms for activity while CYP only one (Shanklin et al., 1997; Van Beilen et al., 2006). Additionally, in most cases of alkane oxidizing enzyme redundancy, one enzyme is a membrane-spanning enzyme (pMMO, particulate butane and propane monooxygenase, AlkB) while the other enzyme in the class is soluble (sMMO, soluble butane and propane monooxygeanse, CYP). It seems possible that there is an as of yet undescribed functional reason to

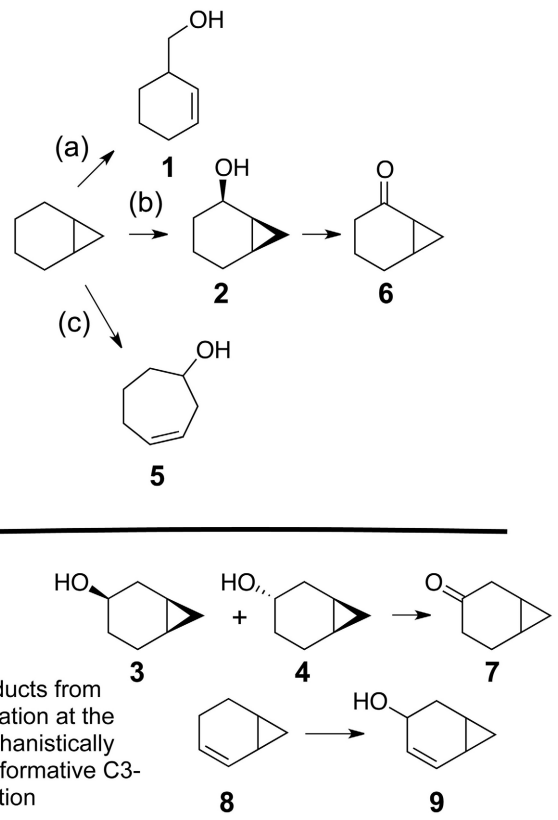

FIGURE 3 | Possible products from the oxidation of norcarane. **(a)** radical pathway **(b)** insertion pathway or pathway of short lived radical **(c)** cationic pathway. **1–9** represent specific compounds that can be formed from the oxidation of norcarane.

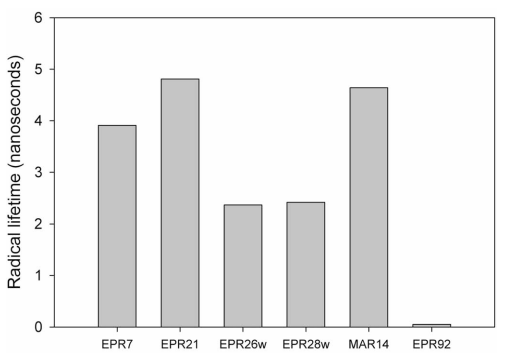

FIGURE 4 | Measured radical lifetimes for hydrothermal vent isolates EPR7, EPR21, EPR26w, EPR28w, MAR14, and EPR 92 using norcarane as the radical clock substrate.

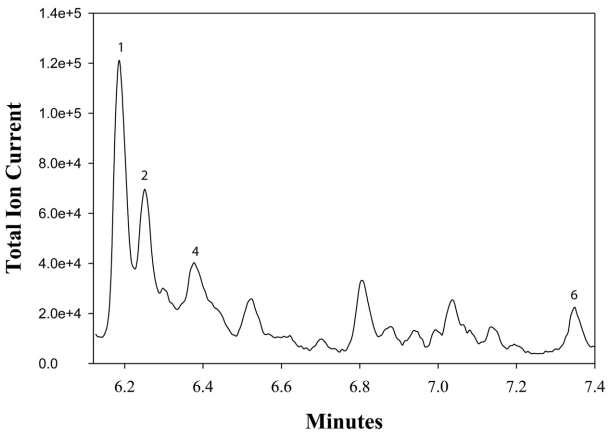

FIGURE 5 | A chromatogram of norcarane hydroxylation products, as metabolized by strain EPR21. Norcarane was introduced in the vapor phase, and the cells were then incubated for 10 h. Products are identified in **Figure 3**.

maintain a membrane bound versus soluble enzyme or vice versa.

Since all of the organisms studied here are mesophilic alkane degraders isolated in the same manner from similar environments, it suggests they may fill similar ecological roles. Yet our study shows that they use two distinct enzymes to accomplish the same task. Under the experimental conditions employed here, only EPR92 expresses CYP (consistent with the presence of only this enzyme in its genome and in the complete genome sequence of its close relative, *P. lavamentivorans*), while all of the other organisms express AlkB-like hydroxylases (regardless of whether they have multiple enzyme systems, which is not yet known). Whether the iron quota differences that would result from expressing a diiron protein (AlkB) vs. a single-iron heme protein (CYP) is significant to a hydrocarbonoclastic organism in low iron/high alkane environments is not clear. In the case of deep-sea vents, however, iron should not be a limiting factor since vent plumes appear to be a source of iron to the global ocean (Noble et al., 2012). Slightly different substrate ranges might explain the coexistence of both enzymes in the same environment, as EPR92 grew well on octane while the other organisms were all grown on dodecane, although a detailed characterization of the substrate ranges of the specific enzymes in these organisms has not been done. CYP and AlkB enzymes are known to have very similar substrate ranges. However, AlkB and CYP enzyme classes have multiple isoforms, each with the ability to oxidize only a limited range of alkanes (Whyte et al., 2002; Van Beilen et al., 2005; Naing et al., 2013; Nie et al., 2013).

We studied the alkane-oxidizing behavior of six organisms isolated from deep-sea vents and did not find evidence for a novel alkane oxygenase reaction mechanism, since, as shown in **Figure 7**, all six isolates generated norcarane profiles that were entirely consistent with expression of either AlkB or CYP. We thus report that the two enzymes thought to be responsible for catalyzing the hydroxylation of medium-chain alkanes in surface waters, AlkB and CYP (Wang et al., 2010a), are likely employed for alkane oxidation in organisms isolated from deep-sea vents. Since the organisms studied in this report are closely related to strains isolated from different marine environments (**Figure 1**), it is not surprising that they encode functionally similar enzymes to those isolated from other environments. Given that it is theoretically possible that unknown alkane hydroxylases may function with

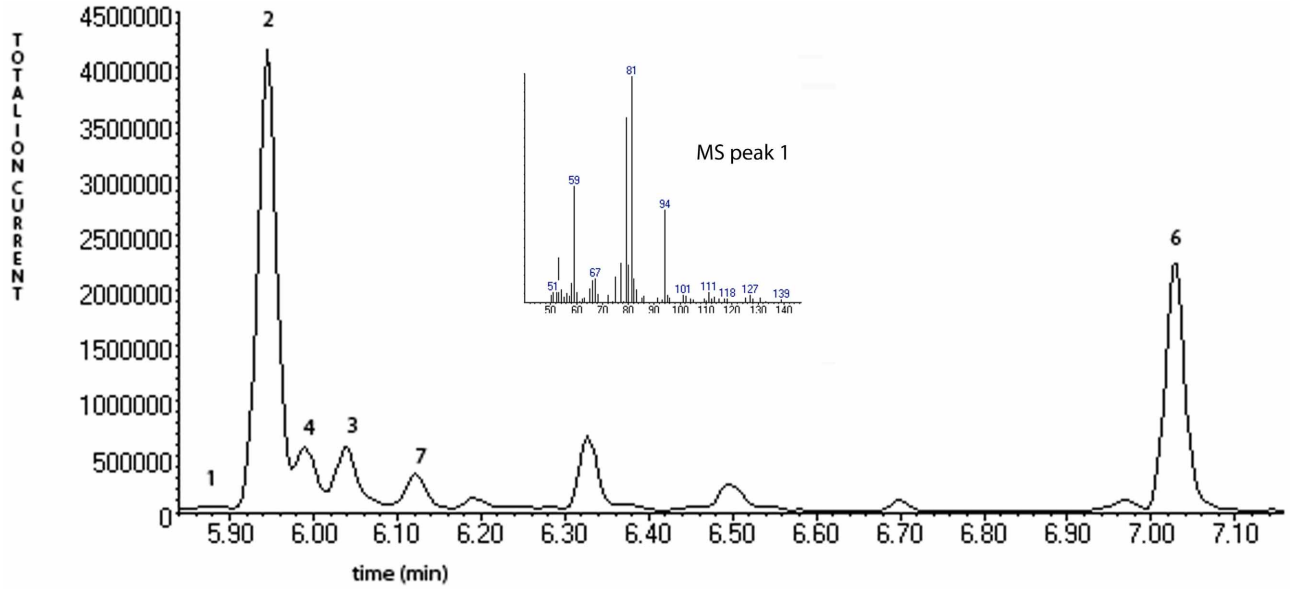

FIGURE 6 | A chromatogram of norcarane hydroxylation products, as generated by strain EPR92. Products are identified in **Figure 3**. The inset shows the fragmentation pattern for peak 3, characteristic of the ring-opened radical product (**1** in **Figure 3**).

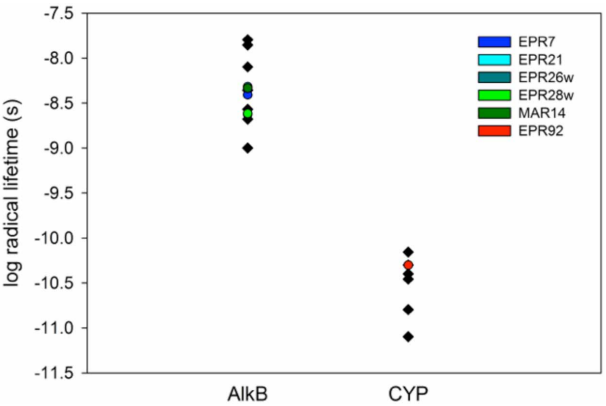

FIGURE 7 | Log of the radical lifetime for a series of AlkB and CYP-containing organisms. Data points given in black were previously described (Rozhkova-Novosad et al., 2007). Entries marked in color are from this work. EPR7, 21, 26w, 28w, and MAR14 clearly cluster with AlkB containing organisms while EPR92 displays a CYP-like radical lifetime.

similar reaction mechanisms to AlkB or CYP, these results alone do not entirely rule out the possibility of an unidentified alkane hydroxylase in these organisms. However, considering the characteristic patterns observed here (**Figure 7**), the PCR confirmation, and the ubiquity of similar organisms in other environments where AlkB and CYP are known to be abundant, we find this an extremely unlikely possibility.

This study supports the notion that alkane oxidation may be an important metabolism in diffuse flow vent environments and that this alkane oxidation is supported, at least in part, by well characterized iron-containing metalloenzymes. These are among the first documented cases of alkane-oxidizing enzymes from deep-sea hydrothermal vents. It remains unclear whether the deep-sea vent alkane hydroxylation via AlkB and CYP reported here is widespread. Future efforts should confirm such activity *in situ*. Environmental transcriptomics and proteomics studies coupled with *in-situ* activity assays would offer such evidence. This, coupled with geochemical profiles of alkane availability in vent environments, would additionally allow for an evaluation of what percentage of vent microbial activity is supported by heterotrophic growth on alkanes, and important consideration since microbial life in vent environments support rich, unique ecosystems. Given that alkane oxidizing organisms encoding AlkB and CYP enzymes have been identified in oceanic surface waters (Wang et al., 2010a,b), it remains to be seen whether alkane oxidation is of elevated importance in vent environments over deep water or surface water marine sites. In order to evaluate this, future studies should compare hydrocarbon availability and the diversity and abundance of known metal- and flavin-containing alkane hydroxylases between deep water, vent plume, vent sediment and shallow marine water.

ACKNOWLEDGMENTS

Support of this research by the National Institutes of Health (NIH 2R15GM072506 to Rachel Narehood Austin) is gratefully acknowledged. Support of this research by the National Science Foundation (CHE-0616633 and CHE-1148597 to John T. Groves: OCE-0327353, MCB-0456676 and OCE-1136451 to Costantino Vetriani and ANT-1103503 to Erin M. Bertrand) is gratefully acknowledged. A grant from NSF to establish an Environmental Molecular Science Institute initially supported the work of John T. Groves, Erin M. Bertrand, Costantino Vetriani, and Rachel Narehood Austin.

REFERENCES

Al-Awadhi, H., Sdashti, N., Kansour, M., Sorkoh, N., and Radwan, S. (2012). Hydrocarbon-utilizing bacteria associated with biofouling materials from offshore waters of the Arabian Gulf. *Int. Biodeterior. Biodegradation* 69, 10–16.

Arp, D. J., Dubbels, B. L., and Sayavedra-Soto, L. A. (2007). Butane monooxygenase of *Pseudomonas butanovora*. *Microbiology* 153, 1808–1816.

Auclair, K., Hu, Z., Little, D. M., Ortiz De Montellano, P. R., and Groves, J. T. (2002). Revisiting the mechanism of P450 enzymes with the radical clocks norcarane and spiro[2, 5]octane. *J. Am. Chem. Soc.* 124, 6020–6027.

Austin, R. N., Buzzi, K., Kim, E., Zylstra, G., and Groves, J. T. (2003). Xylene Monooxygenase, a membrane-spanning non-heme diiron enzyme that hydroxylates hydrocarbons via a substrate radical intermediate. *J. Biol. Inorg. Chem.* 8, 733–740.

Austin, R. N., Chang, H.-K., Zylstra, G., and Groves, J. T. (2000). The non-heme diiron alkane monooxygenase of *Pseudomonas oleovorans* (AlkB) hydroxylates via a substrate radical intermediate. *J. Am. Chem. Soc.* 122, 11747–11748.

Austin, R. N., Deng, D., Jiang, Y., Luddy, K., Van Beilen, J. B., Ortiz De Montellano, P. R., et al. (2006). The diagnostic substrate bicyclohexane reveals a radical mechanism for bacterial Cytochrome P450 in whole cells. *Angew. Chemie. Int. Ed. Engl.* 45, 8192–8194.

Austin, R. N., and Groves, J. T. (2011). Alkane-oxidizing metalloenzymes in the carbon cycle. *Metallomics* 3, 775–787.

Austin, R. N., Luddy, K., Erickson, K., Pender-Cudlip, M., Bertrand, E. M., Deng, D., et al. (2008). Cage escape competes with geminate recombination during alkane hydroxylation by the diiron oxygenase AlkB. *Angew. Chemie. Int. Ed. Engl.* 47, 5232–5234.

Baik, M.-H., Newcomb, M., Friesner, R., and Lippard, S. J. (2003). Mechanistic studies on the hydroxylation of methane by methane monooxygenase. *Chem. Rev.* 103, 2385–2419.

Bazylinski, D. A., Wirsen, C. O., and Jannasch, H. W. (1989). Microbial utilization of naturally occurring hydrocarbons at the guaymas basic hydrothermal vent site. *Appl. Environ. Microbiol.* 55, 2832–2836.

Berndt, M. E., Allen, D. E., and Seyfried, W. E. (1996). Reduction of CO_2 during serpentinization of olivine at 300 degrees C and 500 bar. *Geology* 24, 351–354.

Bertrand, E. M., Sakai, R., Rozhkova-Novosad, E. A., Moe, L. A., Fox, B. G., Groves, J. T., et al. (2005). Reaction mechanisms of non-heme diiron hydroxylases characterized in whole cell. *J. Inorg. Biochem.* 99, 1998–2006.

Borovik, A. S. (2011). Role of metal-oxo complexes in the cleavage of C-H bonds. *Chem. Soc. Rev.* 40, 1870–1874.

Bosetti, A., Van Beilen, J. B., Preusting, H., Lageveen, R. G., and Witholt, B. (1992). Production of primary aliphatic alcohols with a recombinant *Pseudomonas* strain, encoding the alkane hydroxylase enzyme system. *Enzyme Microb. Technol.* 14, 702–708.

Botz, R., Wehner, H., Schmitt, W., Worthington, T. J., Schmidt, M., and Stoffers, P. (2002). Thermogenic hydrocarbons from the offshore Calypso hydrothermal field, Bay of Plenty, New Zealand. *Chem. Geol.* 186, 235–248.

Brault, M., Simoneit, B. R. T., Marty, J. C., and Saliot, A. (1988). Hydrocarbons in waters and particulate material from hydrothermal environments at the East pacific Rise, 13°N. *Org. Geochem.* 12, 209–219.

Brazeau, B. J., Austin, R. N., Tarr, C., Groves, J. T., and Lipscomb, J. D. (2001). Intermediate Q from soluble Methane Monooxygenase (sMMO) hydroxylates the mechanistic substrate probe norcarane: evidence for a stepwise reaction. *J. Am. Chem. Soc.* 123, 11831–11837.

Cooley, R. B., Bottomley, P. J., and Arp, D. J. (2009). Growth of a non-methanotroph on natural gas: ignoring the obvious to focus on the obscure. *Environ. Microbiol. Rep.* 1, 408–413.

Cooper, H. L. R., Mishra, G., Huang, X., Pender-Cudlip, M., Austin, R. N., Shanklin, J., et al. (2012). Parallel and competitive pathways for substrate desaturation, hydroxylation, and radical rearrangement by the non-heme diiron hydroxylase Alkb. *J. Am. Chem. Soc.* 134, 20365–20375.

Crespo-Medina, M., Chatziefthimiou, A., Cruz-Matos, R., Perez-Rodriguez, I., Barkay, T., Lutz, R. A., et al. (2009). *Salinisphaera hydrothermalis* sp. nov., a mesophilic, halotolerant, facultatively autotrophic, thiosulfate-oxidizing gammaproteobacterium from deep-sea hydrothermal vents, and emended description of the genus Salinisphaera. *Int. J. Syst. Evol. Microbiol.* 59, 1497–1503.

Cruse, A. M., and Seewald, J. S. (2006). Geochemistry of low-molecular weight hydrocarbons in hydrothermal fluids from Middle Valley, northern Juan de Fuca Ridge. *Geochim. Cosmochimica Acta* 70, 2073–2092.

Das, N., and Chandran, P. (2011). Microbial degradation of petroleum hydrocarbon contaminants: an overview. *Biotechnol. Res. Int.* 2011, 1–13.

Didyk, B. M., and Simoneit, B. R. T. (1989). Hydrothermal oil of guaymas basin and implications for petroleum formation. *Science* 342, 65–69.

Fujiwara, Y., Takai, K., Uematsu, K., Tsuchida, S., Hunt, J. C., and Hashimoto, J. (2000). Phylogenetic characterization of endosymbionts in three hydrothermal vent mussels: influence on host distributions. *Mar. Ecol. Prog. Ser.* 208, 147–155.

Groves, J. T. (2006). High valent iron in chemical and biological oxidations. *J. Inorg. Biochem.* 100, 434–437.

Hakemian, A. S., and Rosenzweig, A. C. (2007). The biochemistry of methane oxidation. *Annu. Rev. Biochem.* 76, 223–241.

Hanson, R. S. H., and Thomas, E. (1996). Methanotrophic bacteria. *Microbiol. Rev.* 60, 439–471.

Harayama, S., Kishira, H., Kasai, Y., and Shutsubo, K. (1999). Petroleum biodegradation in marine environments. *J. Mol. Microbiol. Biotechnol.* 1, 63–70.

Harayama, S. K. Y., and Hara, A. (2004). Microbial communities in oil-contaminated seawater. *Curr. Opin. Biotech.* 15, 205–214.

Higashihara, M., Igari, S.-I., Maekawa, T., Noda, T., Sakata, S., Asada, N., et al. (1997). C5+ hydrocarbons in fumatolic gases from the Kakkonda (Takinoue) geothermal area, Japan. *Geochem. J.* 31, 63–73.

Ishikawa, J., Yamashita, A., Mikami, Y., Hoshino, Y., Kurita, H., Hotta, K., et al. (2004). The complete genomic sequence of *Nocaradia farcinica* IFM. *Proc. Natl. Acad. Sci. U.S.A.* 101, 14925–14930.

Kniemeyer, O., Musat, F., Sievert, S. M., Knittel, K., Wilkes, H., Blumenberg, M., et al. (2007). Anaerobic oxidation of short-chain hydrocarbons by marine sulphate-reducing bacteriua. *Nature* 449, 898–901.

Kobayashi, K., and Yanagawa, H. (2002). "Submarine hydrothermal vents as possible sites of the origin of life," in *Biological Systems under Extreme Conditions*, eds Y. S. Tanigushi and H. Ludwig (Berlin: Springer), 221–238.

Lancet, H. S., and Anders, E. (1970). Carbon isotope fractionation in the Fisher-Tropsch synthesis of methane. *Science* 170, 980–982.

Lesniewski, R. A., Jain, S., Anantharaman, K., Schloss, P. D., and Dick, G. J. (2012). The metatranscriptome of a deep-sea hydrothermal plume is dominated by water column methanotrophs and lithotrophs. *ISME J.* 6, 2257–2268.

Li, L., Liu, X., Yang, W., Xu, F., Wang, W., Feng, L., et al. (2008). Crystal structure of long-chain alkane monooxygenase (LadA) in complex with coenzyme FMN: unveiling the long-chain alkane hydroxylase. *J. Mol. Biol.* 376, 453–465.

Liu, C., Wang, W., Wu, Y., Zhou, Z., Lai, Q., and Shao, Z. (2011). Multiple alkane hydroxylase systems in a marine alkane degrader, Alcanivorax dieseloei B-5. *Environ. Microbiol.* 13, 1168–1178.

Lo Piccolo, L., De Pasquale, C., Fodale, R., Puglia, A. M., and Quatrini, P. (2011). Involvement of an alkane hydroxylase system of *Gordonia* sp. strain SoCg in degradation of solid n-alkanes. *Appl. Environ. Microbiol.* 77, 1204–1213.

Marquez-Rocha, F. J., Olmos-Soto, J., Rosano-Hernadez, M. C., and Muriel-Garcia, M. (2005). Determination of the hydrocarbon-degrading metabolic capabilities of tropical bacterial isolates. *Int. Biodeterior. Biodegradation* 55, 17–23.

Martin, W., Baross, J., Kelley, D., and Russell, M. J. (2008). Hydrothermal vents and the origiin of life. *Nat. Rev. Microbiol.* 6, 805–814.

McCollom, T. M. (2013). Laboratory simulations of abiotic hydrocarbon formation in earth's deep subsurface. *Rev. Mineral. Geochem.* 75, 467–494.

McCollom, T. M., Ritter, G., and Simoneit, B. R. (1999). Lipid synthesis under hydrothermal conditions by Fischer-Tropsch-type reactions. *Orig. Life Evol. Biosph.* 29, 153–166.

Moe, L. A., Hu, Z., Deng, D., Austin, R. N., Groves, J. T., and Fox, B. G. (2004). Remarkable aliphatic hydroxylation by diiron enzyme Toluene 4-Monooxygenase in reactions with radical/cation diagnostic probes norcarane, 1, 1-Dimethylcyclopropane, and 1, 1-diethylcyclopropane. *Biochemistry* 43, 15688–15701.

Naing, S.-H., Parvez, S., Pender-Cudlip, M., Groves, J. T., and Austin,

R. N. (2013). Substrate specificity and reaction mechanism of purified alkane hydroxylase (AlkB) from the hydrocarbonoclastus bacterium *Alcanivorax borkumensis*. *J. Inorg. Biochem.* 121, 46–52.

Nakano, M., Kihara, M., Iehata, S., Tanaka, R., Maeda, H., and Yoshikawa, T. (2011). Wax ester-like compounds as biosurfactants produced by Dietzia maris from n-alkane as a sole carbon source. *J. Basic. Microbiol.* 51, 490–498.

Nie, Y., Liang, J.-L., Fang, H., Tang, Y.-Q., and Wu, X.-L. (2013). Characterization of a CYP153 alkane hydroxylase gene in a Gram-positive *Dietzia* sp. DQ12-45-1b and its "team role" with *alkW1* in alkane degradation. *Appl. Microbiol. Biotechnol.* doi: 10.1007/s00253-013-4821-1. [Epub ahead of print].

Noble, A. E., Lamborg, C. H., Ohnemus, D. C., Lam, P. J., Goepfert, T. J., Measures, C. I., et al. (2012). Basin-scale inputs of cobalt, iron, and manganese from the Benguela-Angola front to the South Atlantic Ocean. *Limnol. Oceanogr.* 57, 989–1010.

Parson, L. M., Walker, C. L., and Dixon, D. R. (1995). "Hydrothermal vents and processes," in *Hydrothermal Vents and Processes,* eds C. L. Walker, L. M., Parson, and D. R. Dixon (London: Geologic Society), 1–3.

Pérez-Rodríguez, I., Ricci, J., Voordeckers, J. W., Starovoytov, V., and Vetriani, C. (2010). *Nautilia nitratireducens* sp. nov, a thermophilic, anaerobic, chemosynthetic, nitrate-ammonifying bacterium isolated from a deep-sea hydrothermal vent on the East Pacific Rise. *Int. J. Syst. Evol. Microbiol.* 60, 1182–1186.

Perner, M., Gonnella, G., Hourdez, S., Bohnke, S., Kurtz, S., and Girguis, P. R. (2012). *In situ* chemistry and microbial community compositions in five deep-sea hydrothermal fluid samples from Irina II in the Logatchev field. *Environ. Microbiol.* 15, 1551–1560.

Proskurowski, G., Lilley, M. D., Seewald, J. S., Fruh-Green, G. L., Olson, E. J., Lupton, J. E., et al. (2008). Abiogenic hydrocarbon production at lost city hydrothermal field. *Science* 319, 604–606.

Que, L. J., and Tolman, W. B. (2008). Biologically inspired oxidation catalysis. *Nature* 455, 333–340.

Redmond, M. C., Valentine, D. L., and Sessions, A. L. (2010). Identification of novel methane-, ethane-, and propane-oxidizing bacteria at marine hydrocarbon seeps by stable isotope probing. *Appl. Environ. Microbiol.* 76, 6412–6422.

Rosario-Passapera, R., Cruz-Matos, R., Wong, R., Lutz, R. A., Starovoytov, V., and Vetriani, C. (2012). *Parvibaculum hydrocarbonoclasticus* sp. nov., a mesophilic, alkane-oxidizing alphaproteobacterium isolated from a deep-sea hydrothermal vent on the East Pacific Rise. *Int. J. Syst. Evol. Microbiol.* 62, 2921–2926.

Rosenzweig, A. C. (2011). "Particulate methane monooxygenase," in *Handbook of Metalloproteins*, Vols. 4 and 5. ed A. Messerschmidt (Chichester, UK: John Wiley & Sons), 615–622. [originally published online September 2008].

Rozhkova-Novosad, E. A., Chae, J.-C., Zylstra, G. J., Bertrand, E. M., Alexander-Ozinskas, M., Deng, D., et al. (2007). Profiling mechanisms of alkane hydroxylase activity *in vivo* using the diagnostic substrate norcarane. *Chem. Biol.* 14, 165–172.

Schleheck, D., Weiss, M., Pitluck, S., Bruce, D., Land, M., Han, S., et al. (2011). Complete genome sequence of *Parvibaculum lavamentivorans* type strain (DS-1). *Stand. Genomic Sci.* 5, 298–310.

Schneiker, S., Martins Dos Santos, V. A., Bartels, D., Bekel, T., Brecht, M., Burhmester, J., et al. (2006). Genome sequence of the ubiquitous hydrocarbon-degrading marine bacterium *Alcanivorax borkumensis*. *Nat. Biotech.* 24, 997–1004.

Shanklin, J., Achim, C., Schmidt, H., Fox, B. G., and Munck, E. (1997). Mossbauer studies of alkane omega-hydroxylase: evidence for a diiron cluster in an integral-membrane enzyme. *Proc. Natl. Acad. Sci. U.S.A.* 94, 2981–2986.

Sherwood Lollar, S., Westgate, T. D., Ward, J. A., Slater, G. F., and Lacrampe-Couloume, G. (2002). Abiogenic formation of alkanes in the Earth's crust as a minor source for global hydrocarbon reservoirs. *Nature* 416, 522–524.

Shilov, A. E., and Shul'pin, G. B. (1997). Activation of C-H bonds by metal complexes. *Chem. Rev.* 97, 2879–2932.

Simoneit, B. R. T. (1993). "Hydrothermal alteration of organic matter in marine and terrestrial systems," in *Organic Geochemistry*, eds M. H. Engel and S. A. Macko (New York, NY: Plenum Press), 397–418.

Sluis, M., Sayavedra-Soto, L., and Arp, D. (2002). Molecular analysis of the soluble butane monooxygenase from "*Pseudomonas butanovora*." *Microbiology* 148, 3617–3629.

Smith, R. D., and Simmons, H. E. (1973). Norcarane [Bicyclo4.1.0. heptane]. *Org. Synth* 5, 855–859.

Smits, T. H. H., Balada, S. B., Witholt, B., and Van Beilen, J. B. (2002). Functional analysis of alkane hydroxylases from gram-negative and gram-positive bacteria. *J. Bacteriol.* 184, 1733–1742.

Smits, T. H. M., Rothlisberger, M., Witholt, B., and Van Beilen, J. B. (1999). Molecular screening for alkane hydroxylase genes in Gram-negative and Gram-positive strains. *Environ. Microbiol.* 1, 307–317.

Sun, M., Luo, Q., Shen, X.-R., Hou, D.-Y., He, Y., Shi, Z., et al. (2012). Isolation and identification of biodegradation ability of alkane-degrading bacteria: molecular detection and analysis of alkane hydroxylase genes. *Afr. J. Microbiol. Res.* 6, 3936–3943.

Tapilatu, Y., Acquaviva, M., Guigue, C., Miralles, G., Bertrand, J.-C., and Cuny, P. (2010). Isolation of alkane-degrading bacteria from deep-sea Mediterranean sediments. *Lett. Appl. Microbiol.* 50, 234–236.

Throne-Holst, M., Wentzel, A., Ellingsen, T. E., Kotlar, H.-K., and Zotchev, S. B. (2007). Identification of novel genes involved in long-chain n-Alkane degradation by acinetobacter sp strain DSN 17874. *Appl. Environ. Microbiol* 73, 3327–3332.

Throne-Holst, M., Markussen, S., Winnberg, A., Ellingsen, T. E., Kotlar, H. K., and Zotchev, S. B. (2006). Utilization of *n*-alkanes by a newly isolated strain of *Acinetobactervenetianus*: the role of two AlkB-type alkane hydroxylases. *Appl. Microbiol. Biotechnol.* 72, 353–360.

Van Beilen, J. B., and Funhoff, E. G. (2007). Alkane hydroxylases involved in microbial alkane degradation. *Appl. Microbiol. Biotechnol.* 74, 13–21.

Van Beilen, J. B., Funhoff, E. G., Van Loon, A., Just, A., Kaysser, L., Bouza, M., et al. (2006). Cytochrome P450 alkane hydroxylases of the CYP153 family are common in alkane-degrading eubacteria lacking integral membrane alkane hydroxylases. *Appl. Environ. Microbiol.* 72, 59–65.

Van Beilen, J. B., Li, Z., Duetz, W. A., Smits, T. H. M., and Witholt, B. (2003). Diversity of alkane hydroxylase systems in the environment. *Oil Gas Sci. Technol.* 58, 427–440.

Van Beilen, J. B., Smits, T. H. M., Roos, F., Brunner, T., Balada, S. B., and Rothlisberger, M. (2005). Identification of an amino acid position that determines the substrate range of integral membrane alkane hydroxylases. *J. Bacteriol.* 187, 85–91.

Van Beilen, J. B. F., and Enrico, G. (2005). Expanding the alkane oxygenase toolbox: new enzymes and applications. *Curr. Opin. Biotech.* 16, 308–314.

Van Dover, C. L. (2000). *The Ecology of Deep-Sea Hydrothermal Vents.* Princeton, NJ: Princeton University Press.

Vetriani, C., Speck, M. D., Ellor, S. V., Lutz, R. A., and Starovoytov, V. (2004). *Thermovibrio ammonificans* sp. nov., a thermophilic, chemolithotrophic, nitrate ammonifying bacterium from deep-sea hydrothermal vents. *Int. J. Syst. Evol. Microbiol.* 54, 175–181.

Viggor, S., Juhanson, J., Joesaar, M., Mitt, M., Truu, J., Vedler, E., et al. (2013). Dynamic changes in the structure of microbial communities in Baltic Sea coastal seawater microcosms modified by crude oil, shale oil or diesel fuel. *Microbiol. Res.* doi: 10.1016/j.micres.2013.02.006. [Epub ahead of print].

Volkman, J. K. (2006). Lipid markers for marine organic matter. *Handb. Environ. Chem.* 2, 27–70.

Wang, B., Lai, Q., Cui, Z., Tan, T., and Shao, Z. (2008). A pyrene-degrading consortium from deep-sea sediment of the West Pacific and its key member *Cycloclasticus* sp. P1. *Environ. Microbiol.* 10, 1948–1963.

Wang, L., Wang, W., Lai, Q., and Shao, A. (2010a). Gene diversity of CYP153A and AlkB alkane hydroxylases in oil-degrading bacteria isolated from the Atlantic Ocean. *Environ. Microbiol.* 12, 1230–1242.

Wang, W., Wang, L., and Shao, Z. (2010b). Diversity and abundance of oil-degrading bacteria and alkane hydroxylase (*alkB*) genes in the subtropical Seawater of Xiamen Island. *Microb. Ecol.* 60, 429–439.

Wang, W., and Shao, Z. (2012a). Diversity of flavin-binding monooxygenase genes (*almA*) in marine bacteria capable of degradation of long-chain alkanes. *FEMS Microbiol. Ecol.* 80, 523–533.

Wang, W., and Shao, Z. (2012b). Genes involved in alkane degradation in the *Alcanovorax hongdenesis* strain A-11–13. *Appl. Microbiol. Biotechnol.* 94, 437–448.

Wankel, S. D., Adams, M. M., Johnston, D. T., Hansel, C. M., Joye, S. B., and Girguis, P. R. (2012). Anaerobic methane oxidation in metalliferous hydrothemal sediments: influence

on carbon flux and decoupling from sulfate reduction. *Environ. Microbiol.* 14, 2726–2740.

Wankel, S. D., Joye, S. B., Samarkin, V. A., Shah, S. R., Friederich, G., Melas-Kyriasi, J., et al. (2010). New constraints on methane fluxes and rates of anaerobic methane oxidation in a Gulf of Mexico brine pool via *in situ* mass spectrometry. *Deep-Sea Res. II* 57, 2022–2029.

Wasmund, K., Burns, K. A., Kurtboke, D. I., and Bourne, D. G. (2009). Novel Alkane Hydroxylase Gene (*alkB*) diversity in sediments associated with hydrocarbon seeps in the timor sea, Australia. *Appl. Environ. Microbiol.* 75, 7391–7398.

Whelan, J. K., and Hunt, J. M. (1983). Volatile C1-C8 organic compounds in sediments from the Peru upwelling region. *Organ. Geochem.* 5, 13–28.

Whelan, J. K., Simoneit, B. R. T., and Tarafa, M. E. (1988). C1-C8 hydrocarbons in sediments from Guaymas Basin, Gulf of California - comparison to Peru Margin, Japan Trench and California Borderlands. *Organ. Geochem.* 12, 171–194.

Whyte, L. G., Smits, T. H., Labbe, D., Witholt, B., Greer, C. W., and Van Beilen, J. B. (2002). Gene cloning and characterization of multiple alkane hydroxylase systems in *Rhodococcus* strains Q15 and NRRL B-16531. *Appl. Environ. Microbiol.* 68, 5933–5942.

Xu, M., Xiao, X., and Wang, F. (2008). Isolation and characterization of alkane hydroxylases from a metagenomic library of Pacific deep-sea sediment. *Extremophiles* 12, 255–262.

Yakimov, M. M., Guiliano, L., Denaro, R., Crisafi, E., Chernikova, T. N., Abraham, W.-R., et al. (2004). *Thalassolituus oleivorans* gen. nov., sp. nov., a novel marine bacterium that obligately utilizes hydrocarbons. *Int. J. Syst. Bacteriol.* 54, 141–148.

Conflict of Interest Statement: The authors declare that the research was conducted in the absence of any commercial or financial relationships that could be construed as a potential conflict of interest.

Received: 07 January 2013; paper pending published: 10 February 2013; accepted: 16 April 2013; published online: 10 May 2013.

*Citation: Bertrand EM, Keddis R, Groves JT, Vetriani C and Austin RN (2013) Identity and mechanisms of alkane-oxidizing metalloenzymes from deep-sea hydrothermal vents. Front. Microbiol. **4**:109. doi: 10.3389/fmicb.2013.00109*

This article was submitted to Frontiers in Microbiological Chemistry, a specialty of Frontiers in Microbiology.